NOTICE

The quality of this microform is heavily dependent upon the quality of the original thesis submitted for microfilming. Every effort has been made to ensure the highest quality of reproduction possible.

If pages are missing, contact the university which granted the degree.

Some pages may have indistinct print especially if the original pages were typed with a poor typewriter ribbon or if the university sent us an inferior photocopy.

Reproduction in full or in part of this microform is governed by the Canadian Copyright Act, R.S.C. 1970, c. C-30, and subsequent amendments.

AVIS

La qualité de cette microforme dépend grandement de la qualité de la thèse soumise au microfilmage. Nous avons tout fait pour assurer une qualité supérieure de reproduction.

S'il manque des pages, veuillez communiquer avec l'université qui a conféré le grade.

La qualité d'impression de certaines pages peut laisser à désirer, surtout si les pages originales ont été dactylographiées à l'aide d'un ruban usé ou si l'université nous a fait parvenir une photocopie de qualité inférieure.

La reproduction, même partielle, de cette microforme est soumise à la Loi canadienne sur le droit d'auteur, SRC 1970, c. C-30, et ses amendements subséquents.

Canada

ARYLDIAZENIDO AND DINITROGEN COMPLEXES OF RHENIUM: INVESTIGATION OF THEIR DYNAMIC BEHAVIOR IN SOLUTION AND THEIR REACTIVITY

by

Antonio Cusanelli

B.Sc. Simon Fraser University (Canada), 1989

A THESIS SUBMITTED IN PARTIAL FULFILLMENT OF
THE REQUIREMENTS FOR THE DEGREE OF
DOCTOR OF PHILOSOPHY
in the Department
of
Chemistry

Simon Fraser University

February 1995

ISBN 0-612-06621-5

Canada

APPROVAL

Name: Antonio Cusanelli

Degree: Ph.D. Chemistry

Title of Thesis: Aryldiazenido and Dinitrogen Complexes of Rhenium: Investigation of their Dynamic Behavior in Solution and their Reactivity

Examining Committee:

Chairperson: S. Holdcroft, Associate Professor

D. Sutton, Senior Supervisor, Professor

I. D. Gay, Professor

R. H. Hill, Associate Professor

F. W. B. Einstein, Professor
Internal Examiner

J. A. Gladysz, Professor
External Examiner,
Department of Chemistry
University of Utah

Date Approved: 22 Feb '95

PARTIAL COPYRIGHT LICENSE

I hereby grant to Simon Fraser University the right to lend my thesis, project or extended essay (the title of which is shown below) to users of the Simon Fraser University Library, and to make partial or single copies only for such users or in response to a request from the library of any other university, or other educational institution, on its own behalf or for one of its users. I further agree that permission for multiple copying of this work for scholarly purposes may be granted by me or the Dean of Graduate Studies. It is understood that copying or publication of this work for financial gain shall not be allowed without my written permission.

Title of Thesis/Project/Extended Essay:

Acylhydrazonic and Dithiocarbazato Complexes of Rhenium: Investigation of their Dynamic Behavior in Solution and their Reactivity

Author:

(signature)

Antonio Cassarelli

(name)

Feb 10, 1995

(date)

ABSTRACT

Interest in transition metal complexes containing dinitrogen itself, diazenido (N_2H), and other reduced forms of the dinitrogen ligand, stems from their potential as models for steps in biological nitrogen fixation and the possibility of designing synthetic nitrogen fixation catalysts. To examine this potential, a series of cationic pentamethylcyclopentadienyl rhenium aryldiazenido complexes of general formula $[Cp^*Re(L_1)(L_2)(p\text{-}N_2C_6H_4OMe)][BF_4]$ ((a) $L_1 = L_2 = CO, PR_3$ and (b) $L_1 = CO$; $L_2 = PR_3$), the bidentate phosphine aryldiazenido complex $[Cp^*Re(dmpe)(p\text{-}N_2C_6H_4OMe)][BF_4]$, and their derivatives were synthesized and fully characterized. These half-sandwich aryldiazenido complexes were examined by X-ray crystallography and variable temperature ^1H, $^{31}P\{^1H\}$, and $^{13}C\{^1H\}$ NMR spectroscopy. The results obtained showed that these complexes have ground state structures in the solid state and in solution in which the aryldiazenido ligand does not orient with the NNC(aryl) plane bisecting the L_1ReL_2 angle, but lies with the aryl substituent oriented closer to one of the ligands L_1 or L_2; furthermore, interconversion between these structures can take place by a conformational isomerization of the aryldiazenido ligand. The barriers to interconversion of the enantiomers in (a) or diastereomers in (b) were measured and the possible mechanisms for the reorientation of the stereochemically non-rigid aryldiazenido ligand in these complexes were discussed.

The aryldiazenido complexes are also important precursors to other rhenium complexes. The reduction of these rhenium aryldiazenido complexes, either chemically or electrochemically, results in the production of the corresponding metal-bound dinitrogen complexes $Cp^*Re(L_1)(L_2)(N_2)$. In a collaborative effort with Professor A. J. Bard the mechanism of this transformation was investigated by cyclic voltammetry (CV), scanning electrochemical microscopy (SECM), and controlled potential electrolysis

(CPE). The results obtained support an electrochemical E_rC_i mechanism for this reduction process.

The rhenium-bound dinitrogen ligand in these newly formed dinitrogen complexes was also shown to undergo an unusual linkage isomerization. A variable temperature and time-dependent ^{15}N NMR study of the $^{15}N_\alpha$ labeled rhenium dinitrogen complexes Cp'Re(CO)(L)($^{15}N^{14}N$) (Cp' = Cp or Cp* and L = CO or PR_3) provided evidence to support an end-to-end rotation process for the coordinated η^1-dinitrogen ligand *via* a side-on (η^2) bonded dinitrogen species. The rates of linkage isomerization of Cp'Re(CO)(L)($^{15}N^{14}N$) to give Cp'Re(CO)(L)($^{14}N^{15}N$) were measured and the barriers for the interconversion were determined.

The dinitrogen complex $Cp^*Re(PMe_3)_2(N_2)$ was shown to be susceptible to protonation. Addition of strong acids, HX (X = CF_3COO^-, BF_4^-, or $CF_3SO_3^-$), to the dinitrogen complex at low temperature resulted in the transfer of a proton to the metal center, with the N_2 ligand remaining intact, giving rise to the cationic hydrido dinitrogen complexes *cis*-$[Cp^*ReH(N_2)(PMe_3)_2][X]$. In all cases, raising the temperature resulted in the formation of the corresponding isomers *trans*-$[Cp^*ReH(N_2)(PMe_3)_2][X]$.

In addition to protonation chemistry, the potential use of dinitrogen complexes in C-H bond activation was also demonstrated by reactions of the rhenium dinitrogen complexes $Cp^*Re(PMe_3)_2(N_2)$ and $Cp^*Re(dmpe)(N_2)$ in saturated and unsaturated hydrocarbons.

DEDICATION

To Debra, Midnite, and *la famiglia.*

ACKNOWLEDGMENTS

I would like to thank my supervisor Dr. Derek Sutton for his patient guidance and assistance and for the freedom and latitude in exploring my ideas and carrying out my research. Our many discussions and the hours he has spent on my behalf are very much appreciated. It has been a pleasure to associate with Drs. I. D. Gay, R. H. Hill, S. Holdcroft, A. J. Bennet, N. L. Lowe, and X. Yan whose expert advice has proven extremely helpful.

I also thank M. M. Tracey for her efficient and friendly service in the course of obtaining several NMR spectra, and for being particularly accommodating in allowing me access to hours of spectrometer time. I thank F. Chin for providing technical assistance, M. Yang for providing the microanalyses, and G. L. Owen for providing the mass spectra. The social and scientific exchanges with the many graduate students, staff, and Faculty of the Chemistry Department and the Institute of Molecular Biology and Biochemistry were enjoyed and will be remembered fondly.

I also thank the members of my examining committee for the time they have taken in appraisal of this thesis.

TABLE OF CONTENTS

Page Number

LIST OF ABBREVIATIONS AND SYMBOLS

acac	acetylacetonato [$CH_3COCH=C(O-)CH_3$]
AgQRE	silver quasi-reversible electrode
Ar	aryl or aromatic
CI	chemical ionization
Cp	cyclopentadienyl (η^5-C_5H_5)
Cp*	pentamethylcyclopentadienyl (η^5-C_5Me_5)
CPE	controlled potential electrolysis
CV	cyclic voltammetry
Cy	cyclohexyl (C_6H_{11})
dmpe	1,2-bis(dimethylphosphino)ethane ($PMe_2CH_2CH_2Me_2P$)
dppe	1,2-bis(diphenylphosphino)ethane ($PPh_2CH_2CH_2Ph_2P$)
dtc	dimethyldithiocarbamate (S_2CNMe_2)
EI	electron impact
Et	ethyl (CH_3CH_2)
FAB	fast atom bombardment
GC	gas chromatography
$HB(pz)_3$	hydrotris(1-pyrazolyl)borato [$HB(C_3N_2H_3)_3$]
HMPA	hexamethylphosphoramide $[(CH_3)_2N]_3PO$
HOMO	highest occupied molecular orbital
IR	infrared
L	monodentate ligand
LUMO	lowest unoccupied molecular orbital
M	central transition metal in complex
Me	methyl (CH_3)

MS	mass spectroscopy
NMR	nuclear magnetic resonance
NOBA	*m*-nitrobenzyl alcohol (*m*-$NO_2C_6H_4CH_2OH$)
NOE	nuclear Overhauser enhancement
OMe	methoxy (OCH_3)
PCage	caged phosphite [$P(OCH_2)_3CMe$]
Ph	phenyl (C_6H_5)
PR_3	tertiary phosphine ligand
R	alkyl
SCE	standard calomel electrode
SECM	scanning electrochemical microscopy
TBA-BF_4	tetrabutylammonium tetrafluoroborate
TEAP	tetraethylammonium perchlorate
THF	tetrahydrofuran (C_4H_8O)
X	halogen
XRF	X-ray fluorescence

LIST OF COMPLEXES

(2.1) $[CpRe(CO)_2(p\text{-}N_2C_6H_4OMe)][BF_4]$

(2.2) $[Cp^*Re(CO)_2(p\text{-}N_2C_6H_4OMe)][BF_4]$

(2.3) $[Cp^*Re(CO)(NCMe)(p\text{-}N_2C_6H_4OMe)][BF_4]$

(2.4) $[Cp^*Re(CO)(PMe_3)(p\text{-}N_2C_6H_4OMe)][BF_4]$

(2.5) $[Cp^*Re(CO)(PEt_3)(p\text{-}N_2C_6H_4OMe)][BF_4]$

(2.6) $[Cp^*Re(CO)(PPh_3)(p\text{-}N_2C_6H_4OMe)][BF_4]$

(2.7) $[Cp^*Re(CO)(PCy_3)(p\text{-}N_2C_6H_4OMe)][BF_4]$

(2.8) $[Cp^*Re(CO)\{P(OMe)_3\}(p\text{-}N_2C_6H_4OMe)][BF_4]$

(2.9) $[Cp^*Re(CO)\{P(OCH_2)_3CMe\}(p\text{-}N_2C_6H_4OMe)][BF_4]$

(2.10) $[Cp^*Re(NCMe)_2(p\text{-}N_2C_6H_4OMe)][BF_4]$

(2.11) $[Cp^*Re(PMe_3)_2(p\text{-}N_2C_6H_4OMe)][BF_4]$

(2.12) $[Cp^*Re(PEt_3)_2(p\text{-}N_2C_6H_4OMe)][BF_4]$

(2.13) $[Cp^*Re(dmpe)(p\text{-}N_2C_6H_4OMe)][BF_4]$

(2.14) $[Cp^*Re\{P(OMe)_3\}_2(p\text{-}N_2C_6H_4OMe)][BF_4]$

(2.15) $[Cp^*Re(CO)_2(N_2C_6H_5)][BF_4]$

(2.16) $[Cp^*Re(NCMe)_2(N_2C_6H_5)][BF_4]$

(2.17) $[Cp^*Re(PMe_3)_2(N_2C_6H_5)][BF_4]$

(2.18) $[Cp^*Re(CO)(THF)(p\text{-}N_2C_6H_4OMe)][BF_4]$

(2.19) $[Cp^*Re(THF)_2(p\text{-}N_2C_6H_4OMe)][BF_4]$

(4.1) $CpRe(CO)_2(N_2)$

(4.2) $Cp^*Re(CO)_2(N_2)$

(4.3) $Cp^*Re(CO)(PMe_3)(N_2)$

(4.4) $Cp^*Re(CO)\{P(OMe)_3\}(N_2)$

(4.5) $Cp^*Re(PMe_3)_2(N_2)$

(4.6) $Cp^*Re(dmpe)(N_2)$

(4.7) $Cp^*Re\{P(OMe)_3\}_2(N_2)$

(4.8) Cp^*ReO_3

(4.9) $Cp^*Re(CO)(COOMe)(p\text{-}N_2C_6H_4OMe)$

(4.10) $Cp^*Re(CO)_2(p\text{-}NHNC_6H_4OMe)$

(4.11) $Cp^*Re(CO)(CONH_2)(p\text{-}N_2C_6H_4OMe)$

(*trans*-4.12) *trans*-$Cp^*Re(PMe_3)_2H_2$

(*cis*-6.1) *cis*-$[Cp^*ReH(N_2)(PMe_3)_2][CF_3COO]$

(*cis*-6.2) *cis*-$[Cp^*ReH(N_2)(PMe_3)_2][BF_4]$

(*cis*-6.3) *cis*-$[Cp^*ReH(N_2)(PMe_3)_2][CF_3SO_3]$

(*trans*-6.1) *trans*-$[Cp^*ReH(N_2)(PMe_3)_2][CF_3COO]$

(*trans*-6.2) *trans*-$[Cp^*ReH(N_2)(PMe_3)_2][BF_4]$

(*trans*-6.3) *trans*-$[Cp^*ReH(N_2)(PMe_3)_2][CF_3SO_3]$

(*trans*-7.1) *trans*-$Cp^*Re(PMe_3)_2(Ph)H$

(*trans*-7.2) *trans*-$Cp^*Re(PMe_3)(\eta^2\text{-}CH_2PMe_2)H$

(*cis*-7.3) *cis*-$Cp^*Re(dmpe)(Ph)H$

(*trans*-7.3) *trans*-$Cp^*Re(dmpe)(Ph)H$

(*trans*-7.4) *trans*-$Cp^*Re(PMe_3)_2(n\text{-}C_6H_{13})H$

(*trans*-7.5) *trans*-$Cp^*Re(PMe_3)_2Cl_2$

LIST OF TABLES

LIST OF FIGURES

Page Number

LIST OF SCHEMES

Page Number

CHAPTER 1

Transition Metal Dinitrogen and Aryldiazenido Complexes and their Relevance to Chemical and Biological Nitrogen Fixation

1.1. Introduction

Nitrogen, or more correctly, dinitrogen gas (N_2), makes up four-fifths of the earth's atmosphere and to the chemist, represents an inexpensive and apparently inexhaustible starting material for the production of important raw materials. Unfortunately, dinitrogen remains a largely untapped resource because of its apparent inertness and reluctance to undergo chemical reaction. In fact, dinitrogen's unreactive nature has been used advantageously by chemical distributors who package their reactive chemicals in an atmosphere of dinitrogen or by laboratory workers who routinely handle these same chemicals using standard Schlenk, drybox, or vacuum line techniques which, in turn, generally use N_2 gas as the inert atmosphere.

The chemical inertness of dinitrogen is not surprising given the great strength of the nitrogen-nitrogen bond which has a very high bond dissociation energy of 945 kJ.[1] It is notably unreactive when compared to other systems which contain triple bonds such as alkynes, nitriles, and isonitriles.[2] This lack of reactivity is attributed to an absence of molecular polarity and an appreciably larger HOMO-LUMO energy difference in N_2 compared to these other systems.[2] Despite dinitrogen's unreactive nature, in 1909, the German scientist Fritz Haber succeeded in activating, or "fixing", dinitrogen into ammonia by reacting dinitrogen and dihydrogen (Equation 1.1)[3] at very high temperatures (673-773 K) and pressures (250 atm).

$$N_2 + 3H_2 \rightleftharpoons 2NH_3 \qquad (1.1)$$

The apparent key to the success of this ammonia synthesis, called the Haber process, is the presence of a special transition metal iron oxide catalyst which apparently binds the dinitrogen molecule, thus providing a site for N_2 activation. Even after nearly 85 years, the Haber process still uses a catalyst which is iron based, and the mechanism of this vitally important transformation is still a matter for discussion.

In stark contrast to the Haber process for ammonia production, with its elevated temperature, pressure, and capital costs, atmospheric nitrogen can be converted to ammonia biologically by soil bacteria and other organisms at ambient temperatures and pressures.[3] The enzyme responsible for this N_2 fixation process is nitrogenase.[3] In 1930, it was demonstrated by Bortels et al. that the transition metals molybdenum, vanadium, and iron were necessary for biological nitrogen fixation by nitrogenase.[4] Once again, as was the case for the Haber process, an important relationship between dinitrogen activation and transition metals was established and an inference was made that the dinitrogen molecule may be activated in this process by binding to the metal(s).

It was this catalytically facile activation of the seemingly inert dinitrogen molecule by nitrogenase which first intrigued scientists to investigate the structure-function relationship in these metalloenzymes, as well as, to gather evidence in support of a plausible mechanism for the fixation pathway.[3] The intent, in the long term, was the eventual design of processes which activate atmospheric dinitrogen under ambient conditions and could be utilized directly in laboratory or industrial scale syntheses of desirable nitrogen-containing products. The mechanism of biological nitrogen fixation remains one of the most challenging problems in chemistry today.

The field of nitrogen fixation has been addressed by biologists and chemists alike. The biological work has concentrated on the investigation of the structure and function of

the metallic center of nitrogenase, i.e., which metal center(s) is involved in dinitrogen binding and reduction and what is its environment(s). The chemical work has focused on elucidating the modes of bonding of both dinitrogen and partially reduced dinitrogen (N_2H_X) ligands to transition metals so as to gather evidence in support of a mechanism for the transition metal-mediated reduction of dinitrogen to ammonia. Scientists of both scientific disciplines have made significant contributions, especially in recent years, to understanding the problem of how nitrogen fixation works. Therefore, to provide a more meaningful introduction and thus familiarize the reader with the chemical importance of my thesis work, it is beneficial that the previous chemical and biological accomplishments be addressed in the subsequent pages. I begin with a historical perspective into how the research area of nitrogen fixation was born, then proceed chronologically documenting and illustrating the major advancements which have taken place in the last 35 years, and finally culminate with a brief description of my contributions to this research area.

1.2. Biological Work

The biological work into the investigation of the structure and function of nitrogenases began with the preparation of the first cell-free extracts of nitrogenase in 1960.[5] The nitrogenases known today can be classified according to the metals they contain as FeMo, FeV, or FeFe nitrogenases. The nitrogenases that have been most thoroughly studied are the FeMo nitrogenases, and for a long time molybdenum was considered an essential metal for nitrogenases.[6] The discovery of FeV nitrogenases, however, showed that the role of molybdenum could possibly be fulfilled by other metals,[7] and the isolation of nitrogenases containing exclusively iron finally ended the belief that two different metals were necessary for the activation and reduction of N_2.[8]

The FeMo nitrogenases consist of two proteins, the Fe protein and the FeMo protein, which can be separated and purified. The Fe protein ($M_r \approx 60\,000$) is a dimer of two identical subunits, bridged by one $[Fe_4S_4]$ cluster (Figure 1.1).[9]

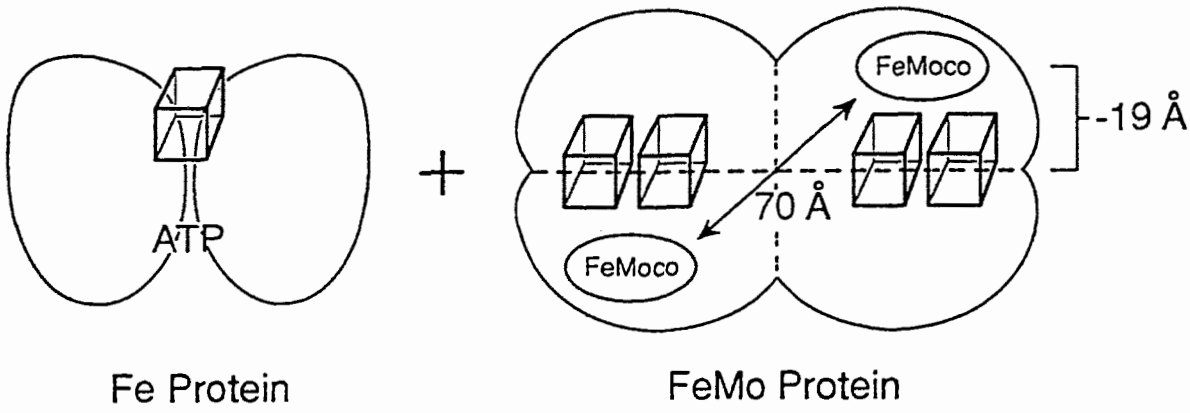

Figure 1.1. Schematic representation of FeMo nitrogenase. Fe and FeMo protein form the complete enzyme. Cube = Fe_4S_4. FeMoco = FeMo cofactor.

The Fe protein functions as a specific one-electron donor for the FeMo protein. Interestingly, no other protein or reducing agent has been able to assume the function of the Fe protein, suggesting that this protein may also cause some unusual conformational change in the FeMo protein upon, or prior to, electron transfer. The FeMo protein ($M_r \approx$ 220, 000) is an $\alpha_2\beta_2$ tetramer containing two Mo centers, 32 ± 3 Fe centers, and 32 ± 3 S units (Figure 1.1).[9]

The FeMo protein contains the FeMo cofactor(s) which is the active center(s) at which bonding, activation, and reduction of the N_2 molecule is believed to occur. Thus, interest was focused on this cofactor(s), since a solution to the "nitrogenase problem" was expected from the elucidation of the composition and structure of this cofactor(s). The separation of the cofactor(s) from the protein was achieved for the first time in 1977.[10] They were found to have a low molecular mass of $M_r \approx 1500$ and were characterized as

cluster(s) with the composition [1 Mo : 6-8 Fe : 8-9 S : 1 homocitrate]. Hence, since the FeMo protein contains two Mo centers and each FeMo cofactor has one Mo center, then *two* such identical FeMo cofactors must be present in the protein (Figure 1.1). The other [FeS] centers in the FeMo protein were believed to contain two $[Fe_4S_4]$ units linked in some manner (Figure 1.1).[11]

A more exact picture of the structural arrangement adopted by these subunits was disclosed by Bolin et al. in 1990[12] after an X-ray structural analysis of crystalline FeMo protein was completed. It was shown that the two FeMo cofactors are located approximately 70 Å apart in two different subunits of the protein (Figure 1.1). Approximately 19 Å from each FeMo cofactor is situated an [FeS] center, which, according to the analytically determined metal content of the FeMo protein, must consist of approximately 8 Fe and 8 S groups (Figure 1.1). An ellipsoid form of the FeMo cofactor could also be deduced from the electron densities; however, due to the low resolution (5 Å), the arrangement of the individual atoms in the cofactor remained open to question. In 1992, a more conclusive structural model for the nitrogenase FeMo cofactor, based on crystallographic analysis of the nitrogenase FeMo protein from *Azotobacter vinelandii*, was proposed by Rees et al.[13] Even this X-ray structure analysis with the best resolution achieved so far (2.7 Å; $R = 0.20$) does not allow the identification of single atoms in the cofactor. However, for the first time, and in a plausible way, most of the analytical, spectroscopic, and chemical findings which had been previously obtained on the nitrogenase FeMo cofactor[14] could be explained by invoking this structural model. The proposed structure of the FeMo cofactor is depicted in Figure 1.2.[13]

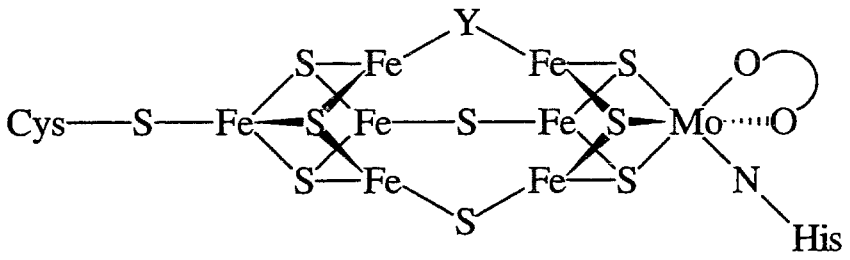

Figure 1.2. Structure of the FeMo cofactor in the FeMo protein of nitrogenase.

The iron-molybdenum cofactor consists of two joined clusters composed of 4 Fe : 3 S and 1 Mo : 3 Fe : 3 S, with three iron atoms from each cluster linked by two S and one "Y" bridge. The nature of the Y bridge cannot yet be determined unambiguously; it has a lower electron density than the two S bridges, and possibly is an NH or O donor. Each cluster is effectively a flattened cubane M_4S_4 with one sulfur removed from a corner, producing a face of three iron atoms linked to the other cluster as described above. The bridged iron atoms in different clusters are about 2.7 Å apart. On the apex of each cluster, remote from the bridged sets of three iron atoms, is the fourth metal atom; an iron in one case and a molybdenum in the other. The extra ligand on this iron is sulfur from a cysteinyl residue. With the exception of this tetrahedrally coordinated iron atom, remarkably all the other six Fe atoms are surrounded by only three donors resulting in a coordination geometry which is approximately trigonal planar. The molybdenum is effectively six-coordinate, being bound to three S ligands within the cluster, a bidentate homocitrate, and a histidinyl residue of the protein.

Having finally established a reasonably accurate structural representation of the active site of nitrogenase, the question which particularly stimulates the imagination of the chemist can now be asked and possibly answered. The question being: at which site on the FeMo cofactor could the N_2 molecule attack to become coordinated, activated, and subsequently reduced?[15] Before attempts are made to answer this question it is worth

noting that the FeMo protein characterized by Rees et al. using X-ray structural analysis was in the "resting state" (no substrate binding). What happens to the cofactor in the "turnover state" of the enzyme is not yet known conclusively. It is almost certain that the embedding protein changes its conformation when going from the resting state to the turnover state. However, since no absolute picture of the turnover state of the nitrogenase enzyme exists, spectroscopically or structurally, our most chemically intuitive predictions on the nature of the substrate binding site(s) must rely on the best factual information attained to date which is arguably the resting state structure proposed by Rees et al. The only clear inference that can be drawn from the resting state structure is that the long-discussed hypothesis that the two Mo centers of the FeMo protein jointly participate in the activation of the N_2 molecule is not valid since the molybdenum atoms are too widely separated (Figure 1.1).

The resting state structure of the FeMo cofactor does not reveal any obvious substrate-binding site, however, some inferences may be drawn. The Mo atom is most likely not predestined for the binding of N_2 because it appears to be coordinatively saturated and has an oxidation state of +IV.[14] The most reasonable substrate-binding site(s) revealed by this resting state structure involves the coordinatively unsaturated iron atom(s) in the opposed faces of the two clusters which appear to be capable of accommodating an N_2 molecule. One proposal is that the dinitrogen molecule binds end-on to a mononuclear site, possibly to an Fe atom.[16] An alternative and more intriguing proposal offered by Orme-Johnson et al. is that the N_2 molecule coordinates side-on to the two Fe atoms, which are linked to one another by the as yet unidentified "Y" bridge (Figure 1.3).[17] The reasons offered for this proposal are as follows: (i) both bridged iron atoms have a vacant site capable of binding an N_2 molecule, (ii) the distance between the two bridged iron atoms is only 2.7 Å and thus, appears to be able to accommodate a side-

on bound N_2 molecule but not an end-on bound N_2 molecule, and (iii) examples of side-on coordination of the N_2 molecule to two metals have been reported.[18]

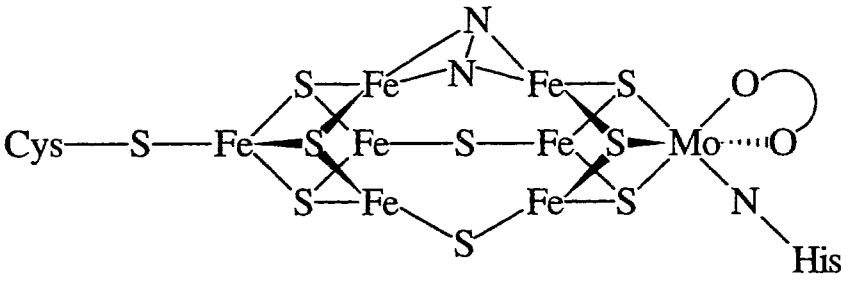

Figure 1.3. Proposal for a model depicting N_2 binding to two Fe atoms of the FeMo cofactor in a side-on fashion.

At present, one can only speculate on the exact substrate-binding site in the cofactor of nitrogenase. However, the combination of biochemical assays with other spectroscopic results, the composition of the isolated FeMo cofactor determined by chemical analysis, and X-ray structural data of model complexes has resulted in a convincing structural representation for the FeMo cofactor.

1.3. Chemical Work

In parallel with the above attempts to define the structure of the metal site(s) in nitrogenase, questions concerning the manner in which the N_2 molecule binds to the nitrogenase cofactors and the mechanism responsible for its subsequent activation and eventual reduction were also addressed. These chemical questions have been answered, if perhaps not conclusively then at least approximately, through the use of transition metal complexes to model the conversion of N_2 to NH_3.

1.3.1. Binding of Dinitrogen to Transition Metals

The recognition that nitrogenases are metalloenzymes reinforced the idea that metal dinitrogen complexes might be involved; this was further reinforced by the belief that since carbon monoxide and dinitrogen are isoelectronic then dinitrogen complexes analogous to metal carbonyls, such as $Ni(CO)_4$, might also exist.[19] A structure for such a complex was first discussed in 1960[20] and an illustration to account for the bonding interaction between the metal and the dinitrogen ligand is presented in Figure 1.4.

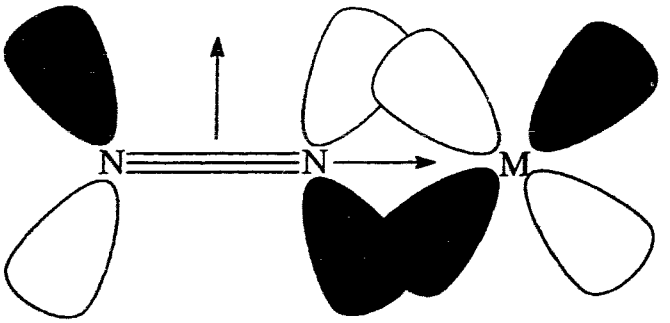

Figure 1.4. Schematic representation of the bonding interaction between the N_2 molecule and the metal atom (M).

The N_2 molecule is believed to donate a lone pair of electrons to the metal atom and receive π-electrons from metal *d*-orbitals into its π-antibonding orbitals. It should be noted that on symmetry grounds a similar interaction with a metal is feasible along the axis represented by the vertical arrow (side-on bonding).

Chemical interest in the study of nitrogen fixation was reawakened in the early 1960's by Vol'pin et al.[21] They were able to show that transition metal compounds and a strong reducing agent in a nonaqueous environment react with N_2 yielding materials which produce ammonia upon hydrolysis. Surprisingly, this work was an example of the highly reduced systems which are currently believed to involve nitrides (resulting from the splitting of the dinitrogen molecule by a metal, giving a formal structure M≡N) rather

than dinitrogen complexes. Ironically, the authors were actually looking for side-on binding of N_2 to metals, as observed for acetylenes in many complexes; simple examples of side-on dinitrogen binding to a single metal atom have as yet to be characterized unequivocally.

The first dinitrogen complex, $[Ru(NH_3)_5(N_2)]^{2+}$, was announced in 1965 by Allen et al.[22] The authors of this seminal communication were actually attempting to synthesize $[Ru(NH_3)_6]^{2+}$ when they realized the novelty of their product. The structure of $[Ru(NH_3)_5(N_2)]^{2+}$ exhibits octahedral geometry about the ruthenium and an end-on coordination mode for the dinitrogen ligand (Figure 1.5).

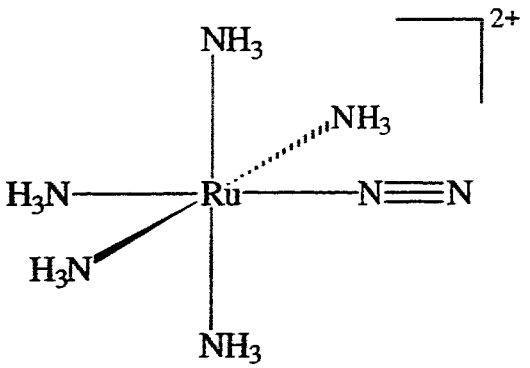

Figure 1.5. Structure of $[Ru(NH_3)_5(N_2)]^{2+}$.

The expectation that the coordination of dinitrogen would lead to a facile activation of this molecule and subsequent conversion to ammonia was not soon realized; however, the discovery itself produced intensive activity aimed at discovering new dinitrogen complexes. Today, hundreds of dinitrogen complexes are known, still far fewer than the number of carbonyls, but with an equally rich variety of structural types.[23] Selected structural varieties of dinitrogen complexes are described in a simplified fashion by the valence bond descriptions (1)-(4) (Figure 1.6).

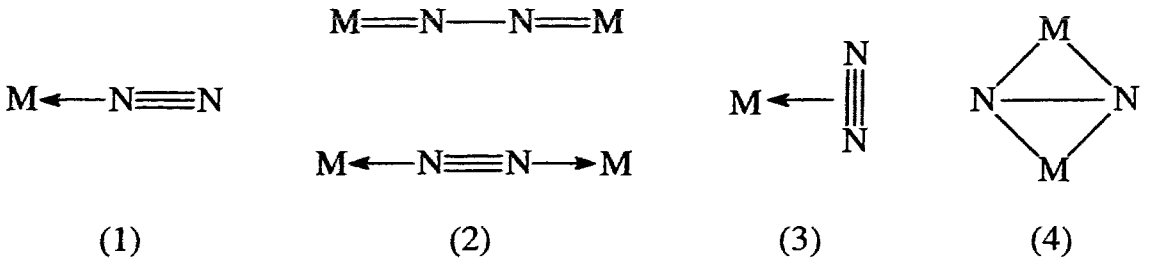

Figure 1.6. Selected structural varieties of dinitrogen complexes.

In terms of the number of spectroscopically or X-ray structurally characterized examples, the terminal end-on bound dinitrogen ligand represented by (1) (Figure 1.6) is by far the most well-established. Examples of these transition metal dinitrogen complexes include the molybdenum complexes *trans*-$Mo(N_2)_2(Et_2PCH_2CH_2PEt_2)$,[24a] *trans*-$Mo(N_2)_2(Ph_2PCH_2CH_2PPh_2)$,[24b] and of course the original ruthenium complex $[Ru(NH_3)_5(N_2)]^{2+}$.[22]

A metal site at which dinitrogen binds in a terminal end-on fashion is believed to be electron rich; characterized by a relatively low formal oxidation state and relative ease of oxidation. A robust co-ligand framework, as provided by tertiary phosphines, aids the stability of these dinitrogen complexes; the maximum number of dinitrogen molecules known to bind to a single metal is three.[25] Although the phosphine co-ligands do not reproduce the sulfur environment found in nitrogenase, they do allow a definitive chemistry of N_2 at metal centers to be developed. Furthermore, the molybdenum complexes of dinitrogen with entirely sulfur-donor co-ligands, which have been synthesized in the last several years, have shown the reactivity of dinitrogen to be very similar to that of the phosphorus-ligated environment.[26] An example of such a complex is the molybdenum dinitrogen complex $Mo(N_2)_2(\text{-}SCH_2C(CH_3)_2CH_2\text{-})_4$ which contains a crown thioether as the sole auxiliary ligand.[27]

Other complexes in which N_2 binds in a terminal fashion include $W(PR_3)_4$ and $ReCl(PR_3)_4$ (PR_3 = tertiary phosphine).[16] These complexes are often used to parallel those of molybdenum because not only do they show similar behavior, as expected from the relationship of their constituent metals to Mo in the periodic table, but they tend to form kinetically stable compounds which allow reaction intermediates to be isolated.

Structure (2) (Figure 1.6), containing the end-on bridging bonding mode for the N_2 ligand, represents the second largest class of dinitrogen compounds. Two representations for the end-on bridging bonding mode for the dinitrogen ligand are given and these are distinguished from one another on the basis of formal assignments of electronic charge. Thus, a M-N_2-M system may be described by the structural representation M-N≡N-M, as is the case for the low oxidation state tungsten (W^0) complex $\{W(N_2)_2(PEt_2Ph)_3\}_2(N_2)$[28] or by M=N-N=M as is ascribed to the high oxidation state tantalum (Ta^{3+}) complex $\{TaCl_3(PEt_3)_2\}_2(N_2)$.[29] Assignment of the structure which is actually adopted is made by consideration of bond lengths; a nitrogen-nitrogen separation of 1.8 Å suggests a structure consisting of an N-N single bond, whereas a separation of 1.1 Å is best represented by a structure containing an N-N triple bond.

Side-on dinitrogen has been discussed in the literature and is suggested to be more reactive than the end-on coordinated species.[30] This particular coordination mode was also postulated by Schrauzer et al.[31] for a large number of fixing systems in which the reacting species had not been absolutely defined. In fact, the only example of the side-on bonded arrangement in (3) (Figure 1.6), namely $ZrCp_2\{CH(SiMe_3)_2\}(N_2)$,[32] relies for its formulation on an EPR spectrum of the $^{15}N_2$ derivative which shows that the two nitrogen atoms are equivalent. Furthermore, only two examples of the double side-on bonded structure represented by (4) (Figure 1.6) are known. However, these have been unequivocally identified by X-ray structure analysis for the samarium dinitrogen

complex $\{SmCp^*_2\}_2(N_2)$[18a] and for the zirconium dinitrogen complex $\{[(Pr^i_2PCH_2SiMe_2)_2N]ZrCl\}_2(N_2)$.[18b]

1.3.2. Reactions of Ligated Dinitrogen

If the binding of dinitrogen to a metal center is regarded as the first step in the reaction sequence of nitrogenase then the next step is conversion of the bound N_2 molecule to ammonia. This has been achieved and studied in detail for mononuclear transition metal complexes, particularly of molybdenum and tungsten.

The best characterized system in which dinitrogen is reduced to ammonia involves low oxidation state complexes of the type $M(N_2)_X(PR_3)_{6-X}$ (M = Mo or W; X = 1, 2 or 3; PR_3 = tertiary phosphine). The dinitrogen ligands in these transition metal complexes are reactive. It is the nature of the binding of dinitrogen, involving synergic "back donation" from the metal to stabilize the metal-N_2 interaction, which confers reactivity on the N_2 ligand.[33] This ligand perturbation on binding is demonstrated by an increase in the nitrogen-nitrogen bond distance, from 1.098(6) Å in free N_2 to approximately 1.12 Å in the terminal end-on dinitrogen complex, although the extent of increase in a particular complex is not a criterion of reactivity.[34] Furthermore, the dinitrogen in these complexes, as a consequence of its binding to the electron rich metal center, is much more nucleophilic than free N_2. It is now sufficiently basic to be attacked by protons from a variety of acids, typically H_2SO_4, HCl, HBr, or p-$CH_3C_6H_4SO_3H$.[35]

It has been postulated by Chatt et al. that protic attack occurs initially at the terminal nitrogen atom (N_β) and continues stepwise as shown in Scheme 1.1.[33] The steps in this cyclic process are based upon isolation and structural characterization of the intermediates shown and/or their reaction behavior in solution, particularly by ^{15}N NMR spectroscopy.[35b, 36]

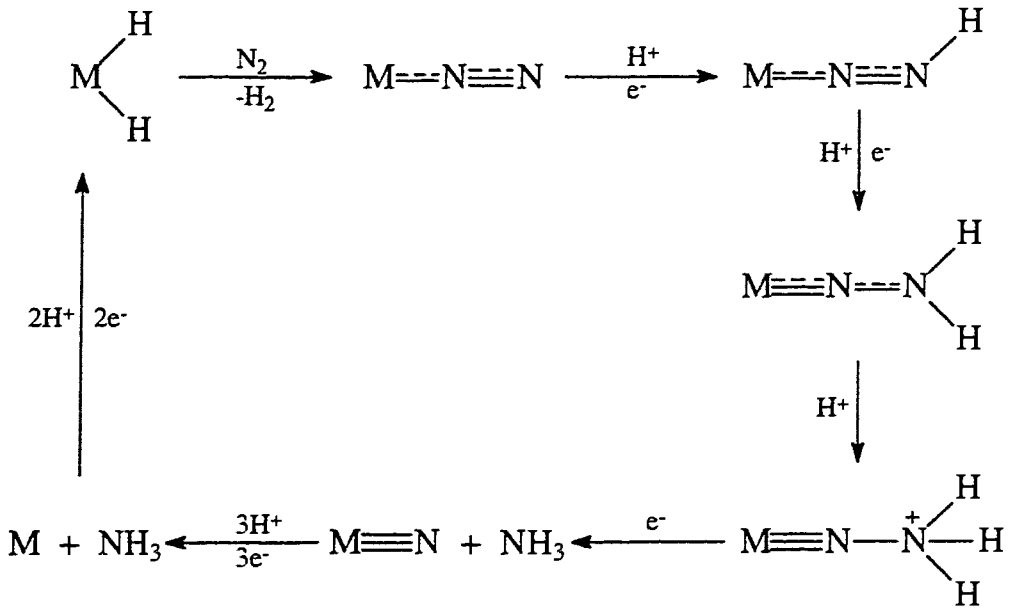

Scheme 1.1. Chatt's proposed mechanism of protonation and subsequent reductive cleavage of metal-bound dinitrogen.

The cycle of Scheme 1.1 includes as a first step the displacement of H_2 from a postulated metal hydrido complex to form the initial dinitrogen complex. There is precedence in the literature to support this type of reaction. For example, the hydride ligands in the molybdenum complex $MoH_4(dppe)_2$ can be displaced by incoming N_2 and, furthermore, this displacement reaction can be accelerated in the presence of protons.[37a] This increase in the substitution rate is generally ascribed to the formation, under the influence of a proton, of a dihydrogen ligand which is more easily displaced by N_2. Thus, for every N_2 bound to Mo one H_2 is displaced, a point which has been incorporated into the first step of the reaction mechanism given in Scheme 1.1. More importantly, this initial step is necessary to account for the reduction of protons to hydrogen which always accompanies biological N_2 fixation. Thus, the overall stoichiometry represented by this cyclic process is exactly that of the nitrogenase enzyme process (Equation 1.2).[14, 33]

$$N_2 + 8H^+ + 8e^- \longrightarrow 2NH_3 + H_2 \qquad (1.2)$$

A key intermediate in the cyclic process shown in Scheme 1.1 is the metal diazenido complex (MNNH) since this is the product of initial protonation of metal coordinated N_2. The diazenido moiety (NNH) has been identified in only a few complexes, an example being the tungsten complex *trans*-$W(N_2H)X(dppe)_2$ (X = F, Cl, Br, or I),[37b] thus little is known about the chemistry exhibited by this ligand.[38] In fact, no X-ray structures of these diazenido complexes have yet been obtained and as a result their characterization is based primarily on ^{15}N NMR spectroscopy.[39-41]

Examples of metal dinitrogen ligand complexes formed after attack of the first two protons, i.e., the metal hydrazido complex ($MNNH_2$), have been known for some time. The hydrazido stage gives particularly stable compounds which have been studied in detail and shown to give hydrazine, when treated with acid or base under certain conditions.[36a, 42] This behavior mimics that shown by nitrogenase, which also gives hydrazine rather than ammonia when quenched by acid or base at an early stage in its reduction cycle.[43]

The hydrazidium ligand (NNH_3), which represents the next stage of the reduction process, has only recently been isolated and characterized for the transition metal complex $[WCl(NNH_3)(PMe_3)_4][Cl]_2$.[36c] The confirmation of this hydrazidium moiety was of utmost importance for the N_2 reduction process proposed by Chatt, since it represented the key intermediate from which it was postulated that cleavage of the nitrogen-nitrogen bond was to occur. The surprising stability of this tungsten hydrazidium complex in the solid state is attributed to extensive hydrogen bonding between the NNH_3 ligand protons and the chloride ions. Extensive hydrogen bonding of this type also occurs in solid complexes of the NNH_2 ligand and raises the question of

whether such interactions could play a role in the enzymic mechanism by aiding the formation of intermediates in the reduction process.[44] In the chemical reactions which form the basis of the cyclic process illustrated in Scheme 1.1, the electrons necessary for conversion of N_2 to NH_3 are supplied by the single low oxidation state transition metal center.

To summarize, few details are known conclusively about the manner in which the N-N bond of dinitrogen is cleaved to give ammonia. Synthetic and mechanistic studies on low oxidation state "Chatt-type" complexes $M(N_2)_2(L)_4$ (M = Mo or W; L = PR_3) and related derivatives suggest that: (i) dinitrogen can be stoichiometrically reduced to ammonia at a single metal center if an open coordination site is available, (ii) the hydrazido complex ($MNNH_2$) is an important intermediate in the metal-mediated reduction since it indicates that the all important second proton also attacks the terminal nitrogen atom (N_β) and not the metal-bound nitrogen atom (N_α), and (iii) cleavage of the N-N bond most likely results from the key hydrazidium ($MNNH_3$) intermediate to give the nitrido species (M≡N). Taken together, these results are the basis for the simplified reduction cycle shown in Scheme 1.1, which remains the best characterized description of N_2 reduction to ammonia at a metal site.

Some other systems have been developed which have claimed to reduce dinitrogen *via* mononuclear dinitrogen complexes of molybdenum. Typically, these systems are prepared by reducing a molybdate salt with borohydride in a borate buffer, under dinitrogen and in the presence of potential co-ligands such as cysteine, cyanide ion, or bovine serum albumin.[31] Yields of ammonia in the last case, although low in absolute terms, are apparently as high as 70 mol NH_3 per mol Mo atom. It was originally proposed by Schrauzer et al. that these reductions proceed through an intermediate, having dinitrogen bound side-on to Mo.[31] As mentioned earlier, this mode of binding is rare, and no direct evidence for such an intermediate, or any other, has been obtained.[45]

Recent work by Schrock et al. has shown that the N-N bond in the transition metal complexes $Cp^*MMe_3(\eta^1\text{-}NNH_2)$ or $[Cp^*MMe_3(\eta^2\text{-}NH_2NH_2)]^+$ (M = Mo or W) can be cleaved efficiently to give ammonia in the presence of protons and electrons.[46] Schrock's investigations into the chemistry displayed by these high oxidation state complexes have resurrected the notion that side-on bonded nitrogenous ligands, of the form N_2H_X, may be involved as intermediates in the mechanistic pathway for the activation of dinitrogen to ammonia.[47] There are several interesting features of this chemistry that differ significantly from Chatt's hydrazido chemistry of metals in low oxidation states and supports a scheme for dinitrogen reduction (Scheme 1.2) that differs in several important details from previously proposed schemes.[48]

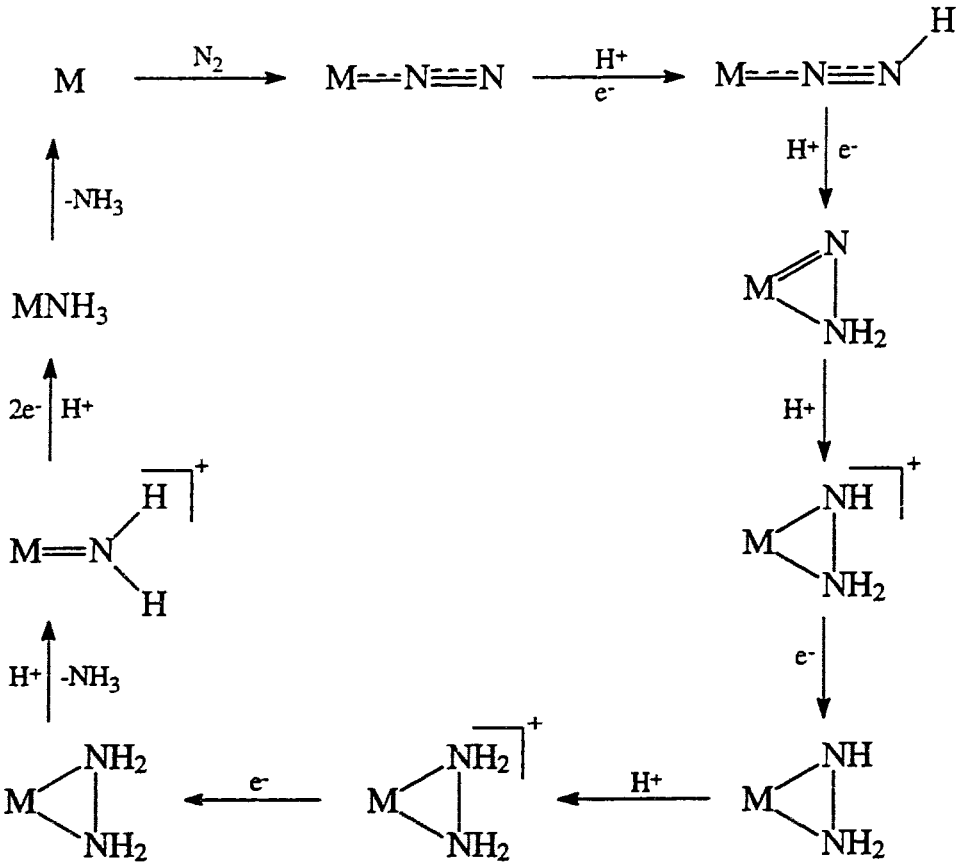

Scheme 1.2. Schrock's proposed mechanism of protonation and subsequent reductive cleavage of metal-bound dinitrogen.

First, it was mentioned previously that ammonia can be generated from low oxidation state metal dinitrogen complexes by adding only protons; the transition metal serves as the source of electrons. However, analogous reactions at high oxidation state metal centers require an external source of electrons to obtain yields of ammonia. Second, a potentially important feature of Cp^*MMe_3 hydrazine and hydrazido chemistry is the confirmation of a side-on bonding mode for these N_2H_X substituents. The metal complexes $Cp^*MMe_3(\eta^2\text{-}NNH_2)$, $[Cp^*MMe_3(\eta^2\text{-}NHNH_2)]^+$, $Cp^*MMe_3(\eta^2\text{-}NHNH_2)$, and $[Cp^*MMe_3(\eta^2\text{-}NH_2NH_2)]^+$ (M = Mo or W) have all been isolated and characterized and support the cyclic reduction process illustrated in Scheme 1.2.[47, 48] While this research does not yield evidence to prove that η^2-bonding is required for a controlled N-N bond cleavage, it strongly suggests that η^2-bonding yields more stable intermediates in a sequence of steps leading to cleavage of the N-N bond. Finally, the most important feature of the Cp^*MMe_3 system is that the metal-bound hydrazine $M(\eta^2\text{-}NH_2NH_2)$ is believed to lie on the pathway to ammonia (Scheme 1.2) and that it is the key intermediate from which cleavage of the N-N bond results; it is not the product of a side reaction, a view that appears to prevail in the chemistry of lower oxidation state complexes.

In summary, inorganic chemists have demonstrated that the reduction of dinitrogen can be achieved under ambient conditions of temperature and pressure in the laboratory. The mechanisms which are believed to account for this conversion are derived from the belief that cleavage of the N-N bond in dinitrogen can only be achieved by stepwise erosion of the nitrogen-nitrogen bond order. This is accomplished by specifically tailoring a transition metal complex to bind the dinitrogen molecule and "activate" it, thus rendering the N-N bond susceptible to attack by protons resulting in eventual cleavage of the N-N bond. However, it is clear that there is no single

mechanism of protonation to account for the stepwise conversion of dinitrogen to ammonia.

The route taken in any particular case is sure to depend upon the ancillary ligands, solvent, and acid as well as upon the metal and its particular oxidation state. Nevertheless, two plausible mechanisms for the cyclic reduction of N_2 to NH_3 or other nitrogenous products have been described. Given the fact that both mechanisms are based on two very different transition metal model systems (Chatt's mechanism is derived from work on low oxidation state octahedral complexes whereas Schrock's mechanism is based on research on high oxidation state half-sandwich piano-stool type complexes), it is not surprising that they differ significantly. However, of utmost importance to the contents of this thesis is the fact that the initial steps of both mechanisms are identical; that is, the binding of the N_2 molecule to a transition metal center and its subsequent protonation to give the metal diazenido (MNNH) and metal hydrazido ($MNNH_2$) complexes respectively, are common to both mechanisms.

As alluded to previously in this introduction, the hydrazido intermediate has been studied in detail, whereas little is known about the chemistry of the elusive diazenido ligand, presumably because of its lack of stability, and it thus warrants further investigation.

1.4. Chemical Background and Previous Work

The inter-relationship of metal-bound N_2 and N_2H is particularly important to understand if, indeed, the first stage of activation of dinitrogen is the formal addition of a single hydrogen atom to a coordinated N_2 molecule. Thus far, reactions in which the N_2H ligand is believed to have been formed are quite rare, and its characterization is far from complete.[38-41] To address these concerns, a route to stable analogs of these compounds, pioneered at our research laboratory, utilizing transition metals in

combination with aryldiazonium ligands (NNAr) was developed.[49] Following this protocol, numerous *metal aryldiazenido* complexes (MNNAr) were synthesized and their properties studied.[50] From these studies, it was concluded that the aryldiazonium ligand is easily stabilized by coordination to a rhenium metal center and as a result, an extensive investigation of the chemistry displayed by rhenium aryldiazenido complexes was undertaken by our research group.

Work on these complexes has shown that the aryldiazenido ligand (NNAr) in rhenium complex cations of composition $[CpRe(CO)_2(N_2Ar)]^+$ is capable of transformation to give, initially, aryldiazene (NHNAr) or substituted arylhydrazido(2-) (NNHAr) intermediates and, subsequently, the substituted arylhydrazido(1-) (NHNHAr) derivatives.[51] This transformation is notable since it models a possible sequence of steps $MNNH \rightarrow MNNH_2 \rightarrow MNHNH_2$ for the reduction and protonation of dinitrogen bound to a transition metal, M. Therefore, it is reasonable to suggest that characterization of the structure and dynamics of the model intermediate MNNAr can potentially provide information to evaluate the chemistry of metal-bound NNH.

1.5. Thesis

Stimulated initially by the biological studies of nitrogenase, and employing what our laboratory and other research groups had learned over the years about the types of metal-ligand environment which can be used to activate dinitrogen and the mechanisms involved, I sought to develop an alternative transition metal model for investigating the *first step* of nitrogen fixation. My approach involved the design and synthesis of specific aryldiazenido and dinitrogen complexes of rhenium utilizing the $Cp'Re(L_1)(L_2)$ (Cp' = Cp or Cp*) framework where L_1 and L_2 are formally 2-electron donor ligands such as CO or PR_3. By using a series of ligands with differing electronic and steric properties for L_1 and L_2, the chemistry of the ligated aryldiazenido and dinitrogen in these types of

complexes was studied. These complexes were prepared initially as synthetic models to elucidate mechanistic information; specifically, the chemistry associated with the metal dinitrogen complex (MNN), the metal diazenido complex (MNNH) as modeled by its aryldiazenido analog (MNNAr), and their interconversion. However, during the course of this investigation into the "nitrogenase problem", other unexpected and exciting chemistry was also discovered and explored. Thus, taken together, these results which are described in the following paragraphs constitute my contributions to the research area of nitrogen fixation, or more generally, to the field of organometallic chemistry.

In Chapter 2 of this thesis, the preparation and characterization of a series of cationic carbonyl phosphine and phosphite rhenium aryldiazenido complexes of the type $[Cp^*Re(CO)(PR_3)(p\text{-}N_2C_6H_4CMe)][BF_4]$ is described. In addition, the synthesis and characterization of a series of cationic bis(phosphorus-ligand) aryldiazenido complexes of general formula $[Cp^*Re(PR_3)_2(N_2Ar)][BF_4]$ (Ar = p-C_6H_4OMe or C_6H_5) along with the cationic bidentate phosphine aryldiazenido complex $[Cp^*Re(dmpe)(p\text{-}N_2C_6H_4OMe)][BF_4]$ are also presented.

Over the years, research in the field of transition metal aryldiazenido chemistry has been dominated by synthesis and product characterization.[52] Despite the large number of structurally characterized examples, there has been little attempt to review and to discuss the specific orientations adopted by these aryldiazenido ligands. The results of an investigation directed at acquiring information about the specific orientation adopted by the aryldiazenido substituent in selected rhenium aryldiazenido complexes and how it is affected by the electronic and steric properties of the ancillary ligands in these complexes are described in Chapter 3. To this end, I report the results of an X-ray structural and variable temperature solution ^1H, $^{13}C\{^1H\}$, and $^{31}P\{^1H\}$ NMR study of the half-sandwich complexes $[Cp^*Re(L_1)(L_2)(p\text{-}N_2C_6H_4OMe)][BF_4]$ ((a) $L_1 = L_2 = CO$ or PR_3 and (b) $L_1 = CO$; $L_2 = PR_3$).

The chemistry associated with the conversion of the metal aryldiazenido complex (MNNAr) to the metal dinitrogen complex (MNN) is addressed in Chapter 4. Chemical or electrochemical reduction of the cationic aryldiazenido complexes of the type $[Cp^*Re(L_1)(L_2)(N_2Ar)][BF_4]$ ((a) $L_1 = L_2 = CO$ or PR_3; Ar = *p*-C_6H_4OMe or C_6H_5 and (b) $L_1 = CO$; $L_2 = PR_3$; Ar = *p*-C_6H_4OMe) or $[Cp^*Re(dmpe)(p\text{-}N_2C_6H_4OMe)][BF_4]$ affords the respective neutral dinitrogen complexes $Cp^*Re(L_1)(L_2)(N_2)$ and $Cp^*Re(dmpe)(N_2)$ cleanly, quickly, and in high yield. The details of this transformation, together with the complete characterization of the products, are also presented in this chapter. Furthermore, in a collaborative effort with Professor A. J. Bard, the mechanism of this conversion was investigated by cyclic voltammetry, scanning electrochemical microscopy, and controlled potential electrolysis. These findings are given in Chapter 4 as well.

Dinitrogen universally occurs as an end-on (η^1) bonded ligand in all the known isolable mononuclear complexes to date, with one possible exception.[32] However, as was mentioned earlier in this introduction, recent developments in the research area of nitrogen fixation (Orme-Johnson proposal for how N_2 binds to nitrogenase[17] based on the X-ray structure of Rees et al.,[13] and chemical work by Schrauzer[31, 45] and Shrock[46-48]) have generated interest into the accessibility of the side-on (η^2) bonded form of dinitrogen, either in stable complexes or as a reactive intermediate. Evidence to support the occurrence of an η^2-bonded dinitrogen species was obtained from a variable temperature and time-dependent ^{15}N NMR study of the rhenium η^1-dinitrogen complexes $Cp'Re(CO)(L)(^{15}N^{14}N)$ (Cp' = Cp or Cp* and L = CO or PR_3) which were specifically labeled at the rhenium-bound nitrogen atom with ^{15}N. The coordinated η^1-dinitrogen ligand was shown to undergo an end-to-end rotation process *via* an η^2-bonded dinitrogen species. This work is described in Chapter 5.

To investigate the reactivity of metal-bound dinitrogen and potentially the chemistry of the elusive diazenido moiety (ReNNH), a protonation study of the corresponding rhenium dinitrogen complex (ReNN) was undertaken. Based on the criteria derived by Chatt et al.,[33, 35] the N_2 ligand in metal dinitrogen complexes could be made more susceptible to protic attack by using highly electron-releasing co-ligands. As a consequence, the dinitrogen complex $Cp^*Re(PMe_3)_2(N_2)$ was chosen and the results of this study are detailed in Chapter 6.

In addition to investigating the rhenium dinitrogen complexes for their susceptibility to protonation, the reactivity of the rhenium-bound dinitrogen ligand was further explored. The rhenium dinitrogen complex $Cp^*Re(PMe_3)_2(N_2)$ was found to be substitutionally inert in N_2-saturated organic solvents at ambient temperatures as judged from the IR and ^{15}N NMR spectra of ^{15}N-enriched samples. Nevertheless, under UV irradiation or heating, this rhenium dinitrogen complex readily loses the N_2 ligand to produce the respective 16-electron intermediate "$Cp^*Re(PMe_3)_2$", which in turn, reacts with C-H bonds. A description of this chemistry is presented in Chapter 7.

In an interview after he was awarded the Priestley Medal by the American Chemical Society in 1985, Henry Taube commented that one of the most valuable lessons he learned as a graduate student was "to slow down and observe carefully; to make capital not only out of what happens, but what doesn't happen". I believe that what Professor Taube was referring to was the ideal that when one investigates a particular piece of chemistry, one should always be aware of potentially more exciting chemistry which may arise as an indirect result of some preconceived chemical strategy. This thesis serves as a testament to his words, since during the course of this investigation into the "nitrogenase problem", other stimulating chemistry was discovered, explored, and brought to fruition as described in the pages which follow.

CHAPTER 2

Aryldiazenido Complexes of Rhenium

2.1. Introduction

With the synthesis of $CpMo(CO)_2(N_2Ph)$[53] in 1964 and $PtCl(N_2Ph)(PEt_3)_2$[54] in 1965, the field of organodiazenido (NNR) chemistry was born. Although these complexes were initially considered as novelties, the subsequent synthesis of a wide range of organodiazenido complexes for the majority of the transition metals and the continued investigation of their structural and chemical properties have well-established the versatility of organodiazenido ligands in transition metal chemistry.[49, 52, 55] Because of the ready availability of stable aryldiazonium salts as reagents, aryldiazenido (NNAr) complexes represent the major class of known organodiazenido complexes.

The $CpM(CO)_2$ fragment and its methylated analog have figured prominently in the organometallic aryldiazenido chemistry of rhenium. Previous publications from our laboratory have detailed the synthesis of the cationic aryldiazenido complexes $[CpRe(CO)_2(N_2Ar)]^+$ and $[Cp^*Re(CO)_2(N_2Ar)]^+$ by treatment of the corresponding neutral intermediates $CpRe(CO)_2(THF)$ and $Cp^*Re(CO)_2(THF)$ with the appropriate aryldiazonium salt $[N_2Ar][BF_4]$.[56, 57] Elsewhere, the synthesis of the cationic acetonitrile-substituted aryldiazenido complexes $[Cp'Re(CO)(NCMe)(N_2Ar)]^+$ (Cp' = Cp or Cp*) by decarbonylation of the corresponding dicarbonyl complex with PhIO in neat acetonitrile was described.[58] These acetonitrile complexes readily undergo substitution of the acetonitrile by a variety of ligands. In this chapter, I describe a series of cationic carbonyl phosphine and phosphite aryldiazenido complexes of the type $[Cp^*Re(CO)(PR_3)(p\text{-}N_2C_6H_4OMe)][BF_4]$ ($PR_3 = PMe_3$ **(2.4)**, PEt_3 **(2.5)**, PPh_3 **(2.6)**, PCy_3 **(2.7)**, $P(OMe)_3$ **(2.8)**, or PCage **(2.9)**) synthesized in this way (Scheme 2.1).

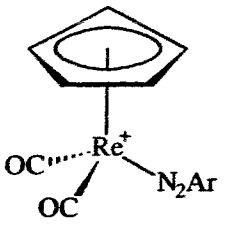

2.1

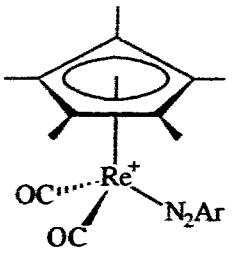

2.2 and 2.15

	Ar
2.2	*p*-C_6H_4OMe
2.15	C_6H_5

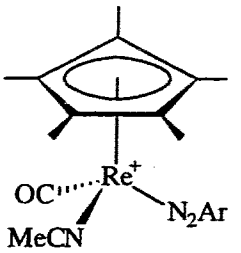

2.3

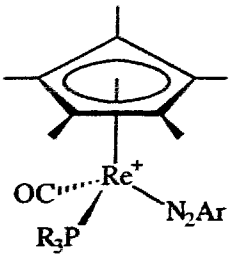

2.4-2.9

	PR_3
2.4	PMe_3
2.5	PEt_3
2.6	PPh_3
2.7	PCy_3
2.8	$P(OMe)_3$
2.9	PCage

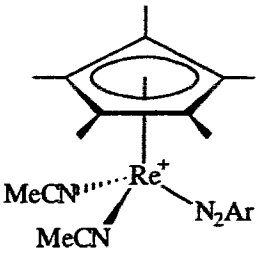

2.10 and 2.16

	Ar
2.10	*p*-C_6H_4OMe
2.16	C_6H_5

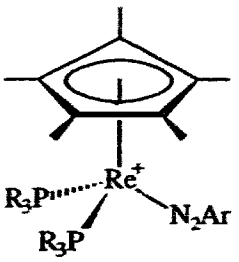

2.11-2.14 and 2.17

	PR_3	Ar
2.11	PMe_3	*p*-C_6H_4OMe
2.12	PEt_3	*p*-C_6H_4OMe
2.13	dmpe	*p*-C_6H_4OMe
2.14	$P(OMe)_3$	*p*-C_6H_4OMe
2.17	PMe_3	C_6H_5

Scheme 2.1. Structures of **2.1-2.17** (Ar = *p*-C_6H_4OMe unless stated otherwise).

Using Me_3NO instead of PhIO in acetonitrile leads to the complete decarbonylation of the dicarbonyl complexes $[Cp^*Re(CO)_2(N_2Ar)][BF_4]$ (Ar = *p*-C_6H_4OMe (**2.2**) or C_6H_5 (**2.15**)) and the formation of the corresponding cationic bis-acetonitrile aryldiazenido complexes $[Cp^*Re(NCMe)_2(N_2Ar)][BF_4]$ (Ar = *p*-C_6H_4OMe (**2.10**) or C_6H_5 (**2.16**)) (Scheme 2.1). Subsequent substitution of both acetonitrile ligands by a series of PR_3 ligands or by the bidentate phosphine ligand $PMe_2CH_2CH_2Me_2P$ (dmpe) affords the complexes $[Cp^*Re(PR_3)_2(p\text{-}N_2C_6H_4OMe)][BF_4]$ (PR_3 = PMe_3 (**2.11**), PEt_3 (**2.12**), or $P(OMe)_3$ (**2.14**)), $[Cp^*Re(PMe_3)_2(N_2C_6H_5)][BF_4]$ (**2.17**), and $[Cp^*Re(dmpe)(p\text{-}N_2C_6H_4OMe)][BF_4]$ (**2.13**) respectively (Scheme 2.1). These synthetic results along with their complete characterization are also presented in this chapter.

2.2. Results

2.2.1. Synthesis and Characterization of Acetonitrile Complexes

One of the carbonyl groups in $[Cp^*Re(CO)_2(p\text{-}N_2C_6H_4OMe)][BF_4]$ (**2.2**) can be oxidatively removed by reaction with iodosobenzene (PhIO) in the presence of acetonitrile as a solvent to give the mono-substituted acetonitrile complex $[Cp^*Re(CO)(NCMe)(p\text{-}N_2C_6H_4OMe)][BF_4]$ (**2.3**) in good yield. This method of synthesis was first reported from our laboratory some years ago[59] and follows closely the corresponding chemistry of the nitrosyls $[Cp'Re(CO)_2(NO)]^+$ (Cp' = Cp or Cp*) reported by Gladysz et al.[60] The reaction works equally well with the corresponding Cp aryldiazenido complex **2.1**.[58] Previously, no success was achieved by using trimethylamine *N*-oxide (Me_3NO) instead of PhIO.[59] However, I now find that **2.3** can also be made by using a stoichiometric amount of Me_3NO. More importantly, I find that the addition of two equivalents of Me_3NO to **2.2** or the dicarbonyl complex $[Cp^*Re(CO)_2(N_2C_6H_5)][BF_4]$ (**2.15**) results in the oxidative removal of both carbonyl

groups to give the new bis-acetonitrile complexes [Cp*Re(NCMe)$_2$(*p*-$N_2C_6H_4OMe$)][BF_4] (**2.10**) and [Cp*Re(NCMe)$_2$($N_2C_6H_5$)][BF_4] (**2.16**) respectively, in moderate yield.

As ionic species, the orange and red-orange complexes **2.3**, **2.10**, and **2.16** are insoluble in hexane or diethyl ether but dissolve in CH_2Cl_2 and acetone. As solids, they can be exposed to air for short periods of time without appreciable deterioration. However, in solution exposure to air results in decomposition.

In the IR spectrum of **2.3**, recorded in CH_2Cl_2, ν(CO) appeared as a broad, very strong absorption at 1959 cm^{-1} and ν(NN) as a broad, moderately intense absorption at 1658 cm^{-1}. The assignment of ν(NN) was confirmed by ^{15}N isotopic substitution at the rhenium-bound nitrogen atom (N_α) of the aryldiazenido ligand in the acetonitrile complex [Cp*Re(CO)(NCMe)(*p*-$^{15}N^{14}NC_6H_4OMe$)][BF_4] (**2.3-$^{15}N_\alpha$**). A shift to lower wavenumber by 21 cm^{-1} was then observed. The IR spectrum of **2.10**, recorded in CH_2Cl_2, displayed a broad, moderately intense absorption at 1618 cm^{-1} which was assigned to ν(NN + CC). This assignment was also confirmed by ^{15}N isotopic substitution at N_α of the aryldiazenido ligand in the bis-acetonitrile complex [Cp*Re(NCMe)$_2$(*p*-$^{15}N^{14}NC_6H_4OMe$)][BF_4] (**2.10-$^{15}N_\alpha$**). A significant shift to lower wavenumber by 11 cm^{-1} was observed. The IR spectrum of **2.16**, recorded in CH_2Cl_2, displayed a broad, moderately intense absorption at 1562 cm^{-1} which was also assigned to ν(NN + CC). This assignment was confirmed by ^{15}N isotopic substitution at the terminal nitrogen atom (N_β) of the aryldiazenido ligand in the bis-acetonitrile complex [Cp*Re(NCMe)$_2$($^{14}N^{15}NC_6H_5$)][BF_4] (**2.16-$^{15}N_\beta$**). Once again, a significant shift to lower wavenumber was observed (14 cm^{-1}). Notably, ν(CN) for the acetonitrile ligand, usually expected to occur quite strongly near 2300 cm^{-1} in the IR spectrum of η^1-bonded acetonitrile complexes, could not be observed in spectra obtained for CH_2Cl_2 solutions or KBr discs for **2.3**, **2.10**, or **2.16**.

In addition to the typical resonances for the Cp* and aryldiazenido groups, the presence of one acetonitrile ligand in **2.3** and two acetonitrile ligands in **2.10** and **2.16** were clearly indicated in the ^{1}H NMR spectra of these complexes, which exhibited a singlet for the respective methyl resonances at δ 3.13, 3.15, and 3.29 integrating to 3, 6, and 6 protons respectively. In the case of **2.10** and **2.16** this indicates that the two MeCN ligands are equivalent on the ^{1}H NMR timescale at room temperature. Evidence for coordinated acetonitrile was also provided by ^{13}C{^{1}H} NMR spectroscopy. The ^{13}C{^{1}H} NMR chemical shift for the CN carbon(s) of **2.3**, **2.10**, and **2.16** occurred at δ 143.94, 139.65, and 140.07 respectively. The relevant IR and NMR results are summarized in Table 2.1.

Table 2.1. IR, ^{1}H, and ^{13}C{^{1}H} NMR Data for the Acetonitrile Aryldiazenido Complexes

Complex	IR (cm^{-1})[a]	^{1}H NMR δ(MeCN)[b]	^{13}C{^{1}H} NMR δ(MeCN)[b]
	1959 ν(CO), 1658 ν(NN)	3.13	143.94
2.3-^{15}N$_\alpha$	1959 ν(CO), 1637 ν(NN)		
2.10	1618 ν(NN + CC)	3.15	139.65
2.10-^{15}N$_\alpha$	1607 ν(NN + CC)		
2.16	1562 ν(NN + CC)	3.29	140.07
2.16-^{15}N$_\beta$	1548 ν(NN + CC)		

[a] In CH_2Cl_2.

[b] In acetone-d_6; referenced to TMS; δ given in ppm.

The FAB mass spectra showed the unfragmented cations as molecular ions M^+, and in each case a fragment corresponding to the loss of the acetonitrile ligand (M^+ - MeCN) was noted. No fragments were observed corresponding to the loss of CO or the loss of CO and MeCN from **2.3** or the loss of two MeCN from **2.10** or **2.16**.

2.2.2. Synthesis and Characterization of Carbonyl Phosphine and Phosphite Complexes

The cationic carbonyl phosphine and phosphite aryldiazenido complexes of the type $[Cp^*Re(CO)(PR_3)(p\text{-}N_2C_6H_4OMe)][BF_4]$ (PR_3 = PMe_3 (**2.4**), PEt_3 (**2.5**), PPh_3 (**2.6**), PCy_3 (**2.7**), $P(OMe)_3$ (**2.8**), or PCage (**2.9**))[59] were obtained in good yield by direct addition of the neat phosphine or phosphite to a stirred solution of **2.3** in acetone at room temperature.

In all cases, the complexes were isolated as orange-brown solids, soluble in polar solvents such as acetone and CH_2Cl_2 but insoluble in hexane or diethyl ether. As solids, these complexes can be exposed to air for short periods of time without appreciable deterioration and can be stored indefinitely at low temperature (263 K) under an atmosphere of N_2. However, in solution they are more sensitive to air and prolonged exposure results in decomposition.

The IR spectra of complexes **2.4-2.9**, recorded in CH_2Cl_2, exhibited a broad, very strong terminal ν(CO) band in the region 1982-1925 cm^{-1} and a broad, strong band in the 1701-1626 cm^{-1} region assigned to ν(NN) (Table 2.2). The assignment of ν(NN) for complexes **2.4** and **2.8** was confirmed by ^{15}N isotopic substitution at N_α of the aryldiazenido ligand. An isotopic shift in ν(NN) of 35 cm^{-1} was observed in going from **2.4** to **2.4-$^{15}N_\alpha$** and an isotopic shift of 43 cm^{-1} was noted in going from **2.8** to **2.8-$^{15}N_\alpha$** (Table 2.2).

Table 2.2. IR, $^{31}P\{^1H\}$, and $^{13}C\{^1H\}$ NMR Data for the Carbonyl Phosphine and Phosphite Aryldiazenido Complexes

Complex	IR (cm^{-1})[a]	$^{31}P\{^1H\}$ NMR[b]	$^{13}C\{^1H\}$ NMR δ(CO)[c]
2.2[d]	2054, 1998 ν(CO); 1732 ν(NN)		190.22
2.4	1950 ν(CO), 1678 ν(NN)	-28.23	202.59
2.4-$^{15}N_\alpha$	1950 ν(CO), 1643 ν(NN)		
2.5	1948 ν(CO), 1680 ν(NN)	6.60	203.32
2.6	1956 ν(CO), 1682 ν(NN)	16.22	202.67
2.7	1925 ν(CO), 1626 ν(NN)	23.23	203.62
2.8	1966 ν(CO), 1691 ν(NN)	110.35	201.08
2.8-$^{15}N_\alpha$	1966 ν(CO), 1648 ν(NN)		
2.9	1982 ν(CO), 1701 ν(NN)	104.40	198.10

[a] In CH_2Cl_2.
[b] In acetone-d_6; referenced to 85% H_3PO_4; δ given in ppm.
[c] In acetone-d_6; referenced to TMS; δ given in ppm.
[d] Included as a reference for comparison with the IR and $^{13}C\{^1H\}$ NMR data obtained for complexes **2.4-2.9**.

The ^1H NMR spectra exhibited the typical resonances expected for the Cp*, aryldiazenido, and phosphorus groups. The only observation of note was that the Cp* resonances in **2.4**, **2.8**, and **2.9** were in each case split into a doublet with J_{H-P} couplings of 0.5, 0.7, and 0.9 Hz respectively, further substantiating the presence of one phosphorus ligand in the respective complexes. In complexes **2.5**, **2.6**, and **2.7** the Cp* resonance remained a singlet; the expected J_{H-P} couplings are believed to be too small to

be observed. The $^{31}P\{^1H\}$ NMR spectra of **2.4-2.9**, in each case, showed a singlet at room temperature in the normal region for a coordinated phosphine or phosphite (Table 2.2). The $^{13}C\{^1H\}$ NMR spectra were recorded for all the complexes **2.4-2.9**. It was observed from $^{13}C\{^1H\}$ NMR spectra that replacement of one carbonyl ligand in $[Cp^*Re(CO)_2(p\text{-}N_2C_6H_4OMe)][BF_4]$ (**2.2**) by either a phosphine or a phosphite group causes an appreciable downfield shift of the carbonyl carbon resonance; the magnitude of the shift is of the order of 13 ppm (Table 2.2). However, within the phosphorus containing complexes only a small deviation in the chemical shift of the carbonyl resonance was observed; the δ(CO) for complexes **2.4-2.9** was located between a chemical shift range of 198.10-203.62 ppm with no apparent order which can be unambiguously assigned to the properties of the phosphorus ligand. To lend further evidence to phosphorus coordination in these complexes, the $^{13}C\{^1H\}$ NMR spectra also showed that the carbonyl resonance was in each case split into a doublet with a $J_{C\text{-}P}$ coupling of 7-12 Hz for the phosphine complexes **2.4-2.7** and a $J_{C\text{-}P}$ coupling of 17 and 21 Hz respectively for the phosphite complexes **2.8** and **2.9**. The parent dicarbonyl complex **2.2** exhibited only a singlet for δ(CO) indicating that the CO groups were presumably symmetry-equivalent.[61]

FAB mass spectra showed the unfragmented cation as the molecular peak for complexes **2.4-2.9**. No fragments corresponding to loss of CO or PR_3 were observed. However, an $M^+\text{-}N_2C_6H_4OMe$ fragment was noted for the PMe_3 complex **2.4**.

2.2.3. Synthesis and Characterization of Bis(phosphorus-ligand) Complexes

Addition of a 10-fold stoichiometric excess of neat phosphine or phosphite directly to a stirred solution of the bis-acetonitrile complexes **2.10** or **2.16** in acetone at room temperature affords the corresponding cationic bis(phosphorus-ligand) aryldiazenido complexes $[Cp^*Re(PR_3)_2(p\text{-}N_2C_6H_4OMe)][BF_4]$ (PR_3 = PMe_3 (**2.11**), PEt_3

(**2.12**), or $P(OMe)_3$ (**2.14**)), $[Cp^*Re(dmpe)(p\text{-}N_2C_6H_4OMe)][BF_4]$ (**2.13**), and $[Cp^*Re(PMe_3)_2(N_2C_6H_5)][BF_4]$ (**2.17**) in moderate yield.

All complexes were isolated as red-orange solids that are soluble in polar solvents such as acetone and CH_2Cl_2 but insoluble in hexane or diethyl ether. For these complexes exposure to air, as solids or in solution, results in decomposition. However, they can be stored at low temperature (263 K) under N_2 for short periods of time without appreciable decomposition.

The IR spectra of complexes **2.11-2.14** and **2.17**, recorded in CH_2Cl_2, displayed a broad, moderately intense band in the 1640-1566 cm^{-1} region assigned to ν(NN + CC) (Table 2.3). This assignment was confirmed by ^{15}N isotopic substitution either at N_α of the aryldiazenido ligand (**2.11** and **2.14**) or at N_β of the aryldiazenido group (**2.17**). Significant shifts to lower wavenumbers were observed for **2.11** [Δν(NN + CC) = 13 cm^{-1}], **2.14** [Δν(NN + CC) = 16 cm^{-1}], and **2.17** [Δν(NN + CC) = 9 cm^{-1}] in going from the unlabeled to the ^{15}N labeled complexes (Table 2.3).

From the ^1H NMR spectra, the Cp* resonance for **2.11-2.14** and **2.17** appeared as a singlet rather than the expected triplet if the Cp* methyls are observably coupled to two equivalent phosphorus ligands. In the complexes **2.4**, **2.8**, and **2.9** these $J_{H\text{-}P}$ couplings were typically of the order of 0.9 Hz or less, and are believed to be too small to be observed here (as was also the case for complexes **2.5**, **2.6**, and **2.7**). The ^1H NMR spectra of complexes **2.12-2.14** and **2.17** exhibited the typical resonances expected for the aryldiazenido group. However, in **2.11** the ^1H NMR spectrum (acetone-d_6) showed only a singlet for the four protons of the aryldiazenido substituent owing presumably to a coincidental chemical shift. Notably, the ^1H NMR spectrum of **2.11** recorded in $CDCl_3$ exhibited a doublet for the four protons of the aryldiazenido moiety (Figure 2.1). In **2.11** the ^1H resonance at δ 1.77 assigned to the PMe_3 ligands was observed to be a virtual doublet integrating to 18 protons (Table 2.3) (Figure 2.1).

Table 2.3. IR, ^1H, and $^{31}P\{^1H\}$ NMR Data for the Bis(phosphorus-ligand) Aryldiazenido Complexes

Complex	IR (cm^{-1})[a]	^1H NMR $\delta(PR_3)$[b]	$^{31}P\{^1H\}$ NMR[c]
2.11	1624 ν(NN + CC)	1.77, virtual d, J = 9.0	-43.28
2.11-$^{15}N_\alpha$	1611 ν(NN + CC)		
2.12	1620 ν(NN + CC)		-7.68
2.13	1622 ν(NN + CC)		-46.76
2.14	1640 ν(NN + CC)	3.80, virtual t, J = 11.6	113.63
2.14-$^{15}N_\alpha$	1624 ν(NN + CC)		
2.17	1566 ν(NN + CC)	1.78, virtual d, J = 9.6	-42.41
2.17-$^{15}N_\beta$	1557 ν(NN + CC)		

[a] In CH_2Cl_2.

[b] In acetone-d_6; referenced to TMS; J given in Hz and δ given in ppm for only those complexes exhibiting virtual coupling.

[c] In acetone-d_6; referenced to 85% H_3PO_4; δ given in ppm.

The apparent coupling constant ($^2J_{H\text{-}P} + {}^4J_{H\text{-}P}$), given by the separation between the two outside peaks, was 9.0 Hz. Further evidence to support virtual coupling in complex **2.11** comes from the $^{13}C\{^1H\}$ NMR spectrum where the carbon resonance of the PMe_3 ligands also appears as a virtual doublet with a coupling constant ($^1J_{C\text{-}P} + {}^3J_{C\text{-}P}$) of 37 Hz.

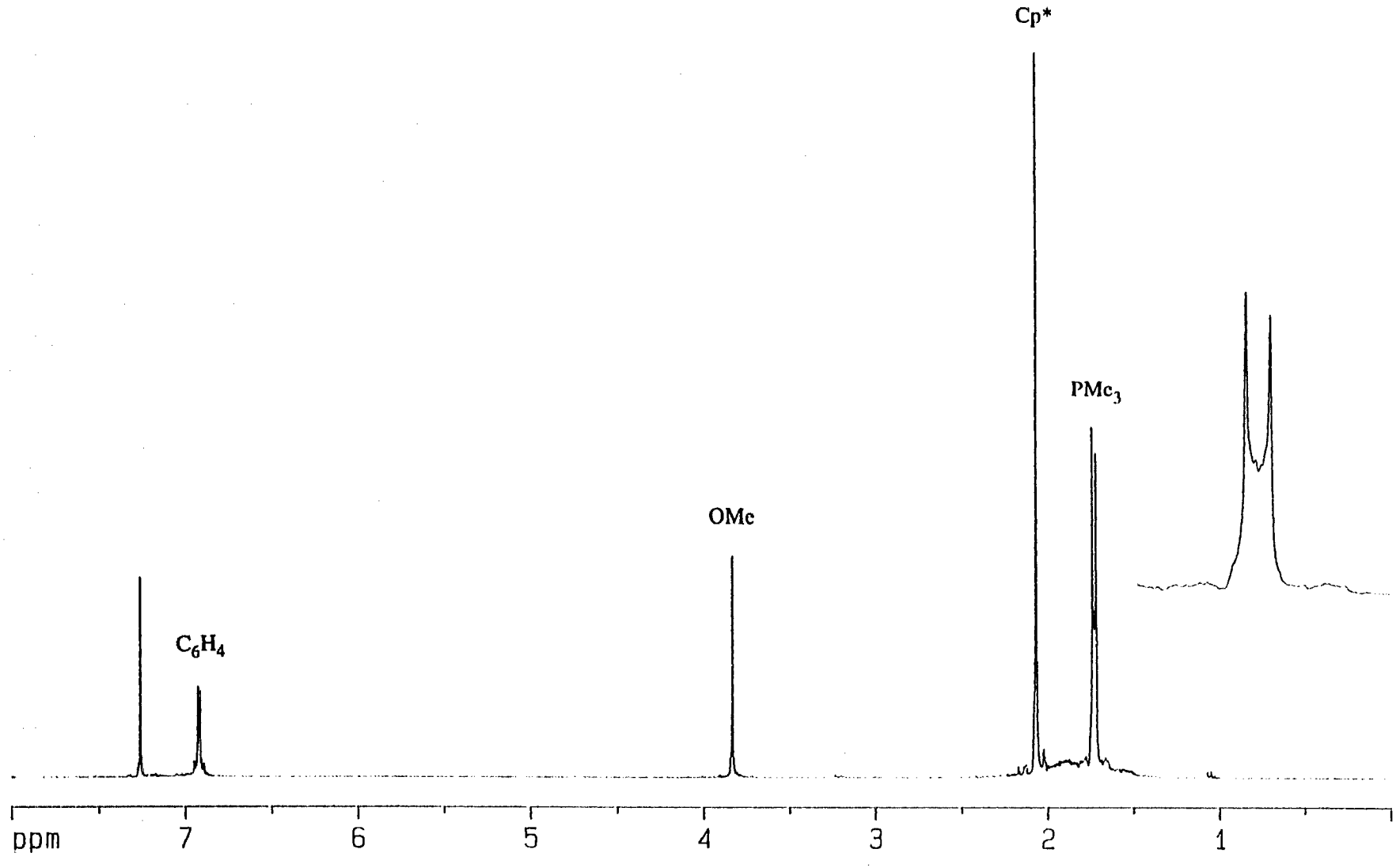

Figure 2.1. ^{1}H NMR spectrum (400 MHz) of [Cp*Re(PMe_3)$_2$(p-$N_2C_6H_4OMe$)][BF_4] (**2.11**) in $CDCl_3$. Virtual doublet has been expanded for clarity.

In **2.17** the ^1H NMR resonance at δ 1.78 assigned to the PMe_3 ligands was also observed to be a virtual doublet integrating to 18 protons with an apparent coupling constant ($^2J_{H-P} + {}^4J_{H-P}$) of 9.6 Hz (Table 2.3). In **2.14** the ^1H NMR resonance at δ 3.80 assigned to the $P(OMe)_3$ ligands was observed to be a virtual triplet integrating to 18 protons with a coupling constant ($^3J_{H-P} + {}^5J_{H-P}$) of 11.6 Hz (Table 2.3) (Figure 2.2). This result was also corroborated by $^{13}C\{^1H\}$ NMR spectroscopy where the spectrum of **2.14** exhibited a virtual triplet for the carbon resonance of the $P(OMe)_3$ ligands with a coupling constant ($^2J_{C-P} + {}^4J_{C-P}$) of 41 Hz. For complexes **2.12** and **2.13**, the ^1H NMR spectra exhibited the typical resonances expected for the respective phosphine ligand.

For the bis(phosphorus-ligand) aryldiazenido complexes **2.11-2.14** and **2.17** the $^{31}P\{^1H\}$ NMR spectra displayed a singlet at room temperature in the normal region for a coordinated phosphine or phosphite (Table 2.3). Other than the virtual couplings for the phosphorus ligands already mentioned, the $^{13}C\{^1H\}$ NMR spectra recorded for **2.11-2.14** showed no atypical resonances.

FAB mass spectra showed the unfragmented cation as the molecular peak for all the bis(phosphorus-ligand) complexes. A fragment corresponding to loss of one PMe_3 ligand was observed for **2.11** and **2.17** and a fragment corresponding to loss of one PEt_3 was observed for **2.12**. No fragments were observed for **2.13** and **2.14**.

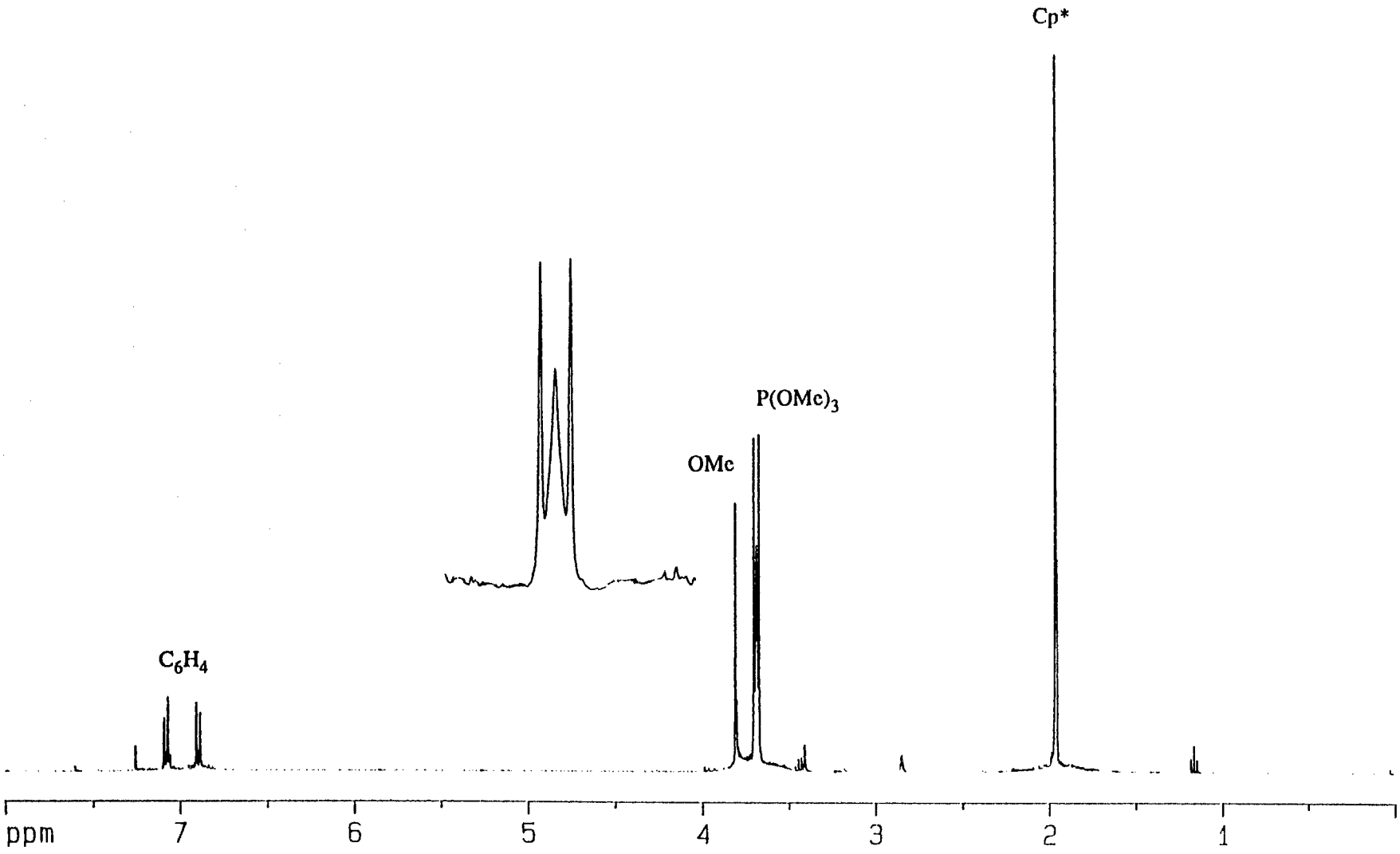

Figure 2.2. ^{1}H NMR spectrum (400 MHz) of $[Cp^*Re\{P(OMe)_3\}_2(p\text{-}N_2C_6H_4OMe)][BF_4]$ (**2.14**) in $CDCl_3$. Virtual triplet has been expanded for clarity.

2.3. Discussion

2.3.1. Acetonitrile Complexes

Oxidative removal of coordinated CO using iodosobenzene (PhIO) was first reported by Gladysz et al., who found that the reaction of the dicarbonyl nitrosyl cation $[CpRe(CO)_2(NO)]^+$ in acetonitrile with PhIO resulted in the formation of the acetonitrile-substituted complex $[CpRe(CO)(NCMe)(NO)]^+$ in good yield.[60b] Subsequently, the synthesis of the Cp* analog $[Cp^*Re(CO)(NCMe)(NO)]^+$ was reported by the same group.[60a] Using a similar procedure, the substitution of a CO group in the dicarbonyl complex **2.2** by acetonitrile to give $[Cp^*Re(CO)(NCMe)(p\text{-}N_2C_6H_4OMe)][BF_4]$ **(2.3)** was also achieved in reasonable yield. However, iodosobenzene was incapable of removing both carbonyl ligands, regardless of the amount added. In fact, addition of a large excess of iodosobenzene lead to decomposition of the mono-substituted acetonitrile complex **2.3** once it was formed.

Complex **2.3** can also be made in good yield by using a stoichiometric amount of trimethylamine *N*-oxide (Me_3NO) in acetonitrile (Scheme 2.2).

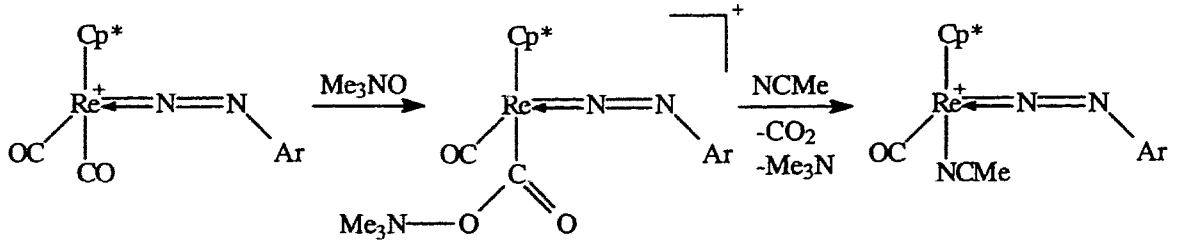

Scheme 2.2. Oxidative removal of coordinated CO using Me_3NO.

It is believed that this reaction is initiated by nucleophilic attack of Me_3NO at the carbonyl carbon atom followed by liberation of CO_2 and coordination of an acetonitrile

molecule from the solvent. A similar reaction pathway was proposed in reactions of $Re_2(CO)_{10}$ with Me_3NO in acetonitrile to give $Re_2(CO)_9(NCMe)$.[62]

In contrast to PhIO, Me_3NO can also oxidatively remove both coordinated CO groups in the presence of acetonitrile as a solvent to give the bis-acetonitrile substituted complexes **2.10** and **2.16** in reasonable yield. This is feasible since trimethylamine *N*-oxide is a stronger oxidizing agent than iodosobenzene and is soluble in the coordinating solvent acetonitrile, whereas iodosobenzene is only sparingly soluble.

There is also evidence to suggest that addition of one or two equivalents of Me_3NO to the dicarbonyl complex **2.2** in THF results in the oxidative removal of one or two CO groups to give the THF-substituted complexes [Cp*Re(CO)(THF)(*p*-$N_2C_6H_4OMe$)][BF_4] (**2.18**) and [Cp*Re(THF)$_2$(*p*-$N_2C_6H_4OMe$)][BF_4] (**2.19**) respectively. An IR spectrum, recorded immediately after the addition of one equivalent of Me_3NO to **2.2** in THF, showed a broad, very strong absorption at 1921 cm^{-1} assigned to ν(CO), and a broad, moderately intense absorption at 1618 cm^{-1} assigned to ν(NN). The addition of a second equivalent of Me_3NO resulted in the disappearance of these two absorptions and the appearance of a new broad, moderately intense absorption at 1576 cm^{-1}, once again assigned to ν(NN). Furthermore, the addition of excess PMe_3 directly to the THF solutions, after either one equivalent or two equivalents of Me_3NO had been added, gave the PMe_3-substituted complexes [Cp*Re(CO)(PMe_3)(*p*-$N_2C_6H_4OMe$)][BF_4] (**2.4**) and [Cp*Re(PMe_3)$_2$(*p*-$N_2C_6H_4OMe$)][BF_4] (**2.11**) respectively as characterized by IR and ^1H NMR spectroscopy. Although I was unable to isolate and fully characterize the THF-substituted complexes, these findings support the presence of these reactive species.

The assignment of ν(NN) in the IR spectra recorded for the acetonitrile complexes was confirmed by ^{15}N isotopic substitution at N_α of the aryldiazenido ligand in **2.3** and **2.10**, and at N_β of the aryldiazenido substituent in **2.16**. From Table 2.1, it is

clear that the magnitude of the shift due to isotopic labeling was significantly smaller for the bis-acetonitrile complexes **2.10** [$\Delta\nu$ = 11 cm^{-1}] and **2.16** [$\Delta\nu$ = 14 cm^{-1}] (regardless of whether the ^{15}N label was at N_α or N_β of the aryldiazenido ligand) as compared to the mono-acetonitrile complex **2.3** [$\Delta\nu$ = 21 cm^{-1}]. This result can be accounted for by observing ν(NN) and ν(CC) (aromatic ring stretch) for **2.3**, **2.10**, and **2.16** for both the isotopically labeled and unlabeled complexes. For unlabeled **2.3**, ν(NN) and ν(CC) are 1658 and 1590 cm^{-1} respectively. The labeled complex exhibited an isotopic shift to 1637 cm^{-1} for ν(NN) but no appreciable shift for ν(CC). For unlabeled **2.10**, ν(NN) and ν(CC) are 1618 and 1588 cm^{-1} respectively. The labeled complex exhibited an isotopic shift to 1607 cm^{-1} for ν(NN) and a shift to 1578 cm^{-1} for ν(CC). A similar isotopic shift was observed for **2.16** in going from the unlabeled [ν(NN) and ν(CC) are 1562 and 1485 cm^{-1} respectively] to the ^{15}N labeled [ν(NN) and ν(CC) are 1548 and 1472 cm^{-1} respectively] complex. These results are consistent with assignment of the 1658 cm^{-1} band in **2.3** as essentially pure ν(NN). However, the IR absorptions in **2.10** (1618 cm^{-1} and 1588 cm^{-1}) and **2.16** (1562 cm^{-1} and 1485 cm^{-1}) are not pure ν(NN) and ν(CC) but are coupled because of their close proximity.

The methyl proton resonance of the acetonitrile ligand in **2.3** (δ 3.13 in acetone-d_6) is in good agreement with that reported for the nitrosyl analog $[Cp^*Re(CO)(NCMe)(NO)]^+$ (δ 3.05 in acetone-d_6).[60a] The ^{13}C NMR spectrum of the nitrosyl complex was also comparable to the $^{13}C\{^1H\}$ NMR spectrum obtained for **2.3**, particularly the resonances corresponding to the carbon nuclei of the acetonitrile ligand. For the nitrosyl complex δ(MeCN) is 4.70 and δ(MeCN) is 139.30 in acetone-d_6. Similarly, for complex **2.3** δ(MeCN) is 5.02 and δ(MeCN) is 143.94 in the same deuterated solvent. These values are also in agreement with the general region for $^{13}C\{^1H\}$ NMR resonances for comparable cationic MeCN complexes such as $[Re(CO)_5(NCMe)]^+$[63] and $[CpFe(CO)(NCMe)_2]^+$[64, 65] which have IR spectra with ν(CN)

≈ 2300 cm^{-1} in accordance with η^1-NCMe groups. The failure to observe ν(CN) in the acetonitrile-substituted complexes **2.3**, **2.10**, and **2.16** is believed to be indicative of a weak absorption band. Other examples of η^1-bonded nitrile complexes with weak or unobserved ν(CN) absorptions have been documented.[66]

Interestingly, IR spectra obtained during the synthesis of the acetonitrile aryldiazenido complexes, recorded immediately after the addition of Me_3NO, exhibited a weak band at 2341 cm^{-1}. However, this band was assigned not to the coordinated MeCN but to the antisymmetric stretch of carbon dioxide formed during the synthesis, since Me_3NO acts as a decarbonylating agent and removes CO from the rhenium complex as CO_2. This assignment was confirmed by bubbling CO_2(g) through acetonitrile for 5 min and then recording an IR spectrum of the resulting solution.

2.3.2. Carbonyl Phosphine and Phosphite Complexes

The mono-acetonitrile complex has proven to be a useful precursor to derivatives where the acetonitrile is substituted by another ligand. For example, MeLi reacts with **2.3** to give the neutral methyl complex Cp*Re(CO)(CH_3)(*p*-$N_2C_6H_4OMe$).[61] In much the same manner, phosphines or phosphites displace the acetonitrile ligand to give the corresponding cationic complexes of formula [Cp*Re(CO)(PR_3)(*p*-$N_2C_6H_4OMe$)][BF_4] **(2.4-2.9)** (Equation 2.1) which are otherwise inaccessible from the dicarbonyl cation **2.2** directly.

$$[Cp^*Re(CO)(NCMe)(p\text{-}N_2C_6H_4OMe)][BF_4] \xrightarrow[\text{-NCMe}]{PR_3} [Cp^*Re(CO)(PR_3)(p\text{-}N_2C_6H_4OMe)][BF_4] \qquad (2.1)$$

For example, an attempt to synthesize the triphenylphosphine complex **2.6** by direct reaction of **2.2** with an excess of PPh_3 in acetone was unsuccessful.[61] The only

organometallic product isolated was the dicarbonyl triphenylphosphine complex $Cp^*Re(CO)_2(PPh_3)$.[67] This result suggests that an ancillary ligand, such as MeCN or THF, which is more labile than the aryldiazenido substituent, is necessary to obtain the phosphine or phosphite complexes **2.4-2.9**. Without such a labile ligand, addition of PPh_3 to the dicarbonyl complex **2.2** results not in the labilization of a CO group to give **2.6** but the labilization of the aryldiazenido ligand and the subsequent formation of $Cp^*Re(CO)_2(PPh_3)$. Furthermore, the addition of PMe_3 to a solution of **2.2** in acetone did not give the desired trimethylphosphine complex **2.4**, nor the dicarbonyl trimethylphosphine complex $Cp^*Re(CO)_2(PMe_3)$ (based on the previous reaction using PPh_3) but instead the dicarbonyl dinitrogen complex $Cp^*Re(CO)_2(N)_2$ (**4.2**) was produced (see Chapter 4 Experimental).

In the syntheses conducted for the present study the time required for substitution of the acetonitrile by the respective phosphine or phosphite differed appreciably, with PMe_3 requiring less than an hour to complete the reaction, PEt_3 less than two hours, $P(OMe)_3$, PCage, and PCy_3 4 hours and PPh_3 24 hours. In all cases a 10-fold stoichiometric excess of the phosphorus group was added and the reaction was monitored by IR spectroscopy. While no detailed kinetic analysis has been undertaken, this dependence on the phosphine argues against a dissociative mechanism. (Note: this phosphine dependence is also consistent with an in solvent cage dissociative mechanism). More probably, the substitution reaction may proceed in a concerted fashion, where the Re-P bond is made as the Re-NCMe bond is broken, resulting in a crowded intermediate. If one considers the electronic and steric properties of these phosphorus ligands, as quantified by Tolman,[68] the time required to complete these substitution reactions can be understood. That is, PMe_3 is a very good nucleophile and has a relatively small cone angle (small steric effect) and thus substitution of the acetonitrile ligand proceeds rapidly; PEt_3 is an equally good nucleophile but has a larger cone angle and thus the

substitution reaction is slower; $P(OMe)_3$ and PCage are the poorest nucleophiles but have the smallest cone angles while PCy_3 is the best nucleophile but has the largest cone angle and this competing subtle interplay of electronic and steric effects results in an overall longer time to complete the substitution reaction. The substitution reaction is slowest for the PPh_3 ligand since it is a moderate nucleophile but it has a large cone angle.

The relative electronic properties of the phosphorus ligands (σ-donor or π-acceptor abilities) are revealed by changes in ν(CO) (Table 2.2). The greater the σ-donor (or poorer the π-acceptor) ability of the phosphorus ligand, the higher the degree of charge delocalization into the carbonyl antibonding orbitals and the lower the ν(CO). For example, the values for ν(CO) follow the order PCage > $P(OMe)_3$ > PPh_3 > $PMe_3 \approx PEt_3$ > PCy_3 which correlates with increasing σ-donor ability of the phosphorus ligand. The values for ν(NN) (Table 2.2) follow a similar order to those for ν(CO) but are not as pronounced owing to the better π-acceptor properties of the CO group compared with the aryldiazenido substituent.[49a] These results corroborate the electronic properties assigned to these ligands by Tolman[68] and also support the discussion presented previously dealing with the rate of acetonitrile substitution by these phosphorus groups.

The downfield shift of the carbonyl carbon resonance when one of the carbonyl ligands in $[Cp^*Re(CO)_2(p\text{-}N_2C_6H_4OMe)][BF_4]$ **(2.2)** was replaced by either a phosphine or a phosphite group is once again attributed to the electronic properties of these phosphorus ligands. An increase in the electron donating ability of a ligand, as is achieved by substituting a CO group with PR_3, causes an increase of electron density at the metal center which in turn leads to greater metal d-π^*(CO) backbonding. It was rationalized that this effect then results in a decrease in the magnitude of the separation (ΔE) between the electronic ground state and the lowest lying excited state, leading to an increase in the local paramagnetic term (σ_p) which, in turn, increases the deshielding

contribution to the chemical shift. In the case of ^{13}C nuclei, σ_p is believed to be the major contributor to the chemical shift.[69, 70]

2.3.3. Bis(phosphorus-ligand) Complexes

The bis-acetonitrile complexes are valuable for the synthesis of derivatives in which both acetonitrile ligands are substituted by other ligands. The cationic bis(phosphorus-ligand) complexes $[Cp^*Re(PR_3)_2(p\text{-}N_2C_6H_4OMe)][BF_4]$ ($PR_3 = PMe_3$ (**2.11**), PEt_3 (**2.12**), or $P(OMe)_3$ (**2.14**)), $[Cp^*Re(PMe_3)_2(N_2C_6H_5)][BF_4]$ (**2.17**), and the bidentate phosphine complex $[Cp^*Re(dmpe)(p\text{-}N_2C_6H_4OMe)][BF_4]$ (**2.13**) were prepared at room temperature by addition of a 10-fold stoichiometric excess of the corresponding phosphine or phosphite group directly to a solution of **2.10** or **2.16** (Equation 2.2).

$$[Cp^*Re(NCMe)_2(N_2Ar)][BF_4] \xrightarrow[-2NCMe]{2PR_3 \text{ or dmpe}} [Cp^*Re(PR_3)_2(N_2Ar)][BF_4] \text{ or } [Cp^*Re(dmpe)(N_2Ar)][BF_4] \qquad (2.2)$$

$Ar = p\text{-}C_6H_4OMe$ or C_6H_5

Attempts to synthesize other bis-phosphine complexes (i.e., where $PR_3 = PPh_3$ or PCy_3) by using the same method were not successful. It is believed that this lack of success may be attributed to the large cone angles of these phosphine ligands which make coordination of both phosphines not sterically feasible. Purification of complexes **2.11-2.14** and **2.17** proved to be very difficult due to their tendency to oil out of solution upon attempted recrystallization. This problem was eventually overcome by slow recrystallization by layering diethyl ether over a solution of the particular complex in a minimum amount of acetone at low temperature (*ca.* 263 K).

The time required for substitution of both acetonitrile ligands by the phosphorus ligands differed greatly, with PMe_3 and dmpe requiring less than 24 hours to complete the reaction, whereas PEt_3 required 48 hours and $P(OMe)_3$ needed nearly 72 hours. These results further corroborate the discussion presented in the previous section for the carbonyl phosphine and phosphite complexes, which inferred that the rate of acetonitrile substitution by these phosphorus ligands was dependent on their electronic and steric properties. IR spectra obtained during the synthesis of **2.11** and **2.14** showed a direct conversion from the bis-acetonitrile complex **2.10** to the corresponding bis(phosphorus-ligand) complexes as evidenced by the loss of ν(NN + CC) for **2.10** and the concomitant growth of the corresponding ν(NN + CC) for **2.11** or **2.14**. No IR absorption corresponding to the formation of an observable reaction intermediate such as $[Cp^*Re(PR_3)(NCMe)(p\text{-}N_2C_6H_4OMe)][BF_4]$ was found. Attempts to shorten these reaction times by employing higher temperatures (i.e., refluxing in acetone) were not successful but instead lead to the decomposition of **2.10** with no formation of **2.11** or **2.14**.

As with the bis-acetonitrile complexes **2.10** and **2.16**, the magnitude of the shifts due to ^{15}N isotopic labeling in **2.11**, **2.14**, and **2.17** were smaller than expected (Table 2.3). The reason once again manifests itself in the IR bands assigned to ν(CC) of the aromatic ring of the aryldiazenido ligand. For unlabeled **2.11**, ν(NN) is 1624 cm^{-1} and ν(CC) are 1591 and 1570 cm^{-1} respectively. The labeled complex exhibited an isotopic shift to 1611 cm^{-1} for ν(NN) and a shift to 1580 and 1559 cm^{-1} for ν(CC). Similar isotopic shifts for ν(NN) and ν(CC) were observed for **2.14** and **2.17** in going from the unlabeled to the ^{15}N labeled complex, regardless of whether the ^{15}N label was at N_α or N_β of the aryldiazenido ligand. These results are again consistent with significant coupling of the ν(NN) and ν(CC) vibrations in **2.11**, **2.14**, and **2.17**.

The concept of virtual coupling has been well documented in the literature for square planar complexes containing two phosphine ligands.[71] Thus, it is chemically intuitive that virtual couplings should also manifest themselves in bis(phosphorus-ligand) complexes having a half-sandwich piano-stool type geometry. This has been shown to be the case, for example, for $Cp^*Ru(PMe_3)_2Cl$[72] and for *trans*-$CpRe(PMe_3)_2(Ph)H$.[73] For the former complex, the ^1H and $^{13}C\{^1H\}$ NMR spectra show a virtual triplet while a virtual doublet is seen for the latter complex for the PMe_3 protons or carbons respectively.

It was first shown by Musher and Corey[74] that the virtual coupling pattern is dependent on the strength of the phosphorus-phosphorus coupling. That is, a small P-P coupling gives rise to a virtual doublet while a large P-P coupling results in a virtual triplet. Using a square planar complex of palladium, *trans*-$PdI_2(PMe_2Ph)_2$, Jenkins and Shaw[75] showed that the methyl resonance appeared as a virtual triplet while in the *cis* complex the methyl resonance was observed as a virtual doublet. It was suggested that these results were obtained because $J_{P\text{-}P}$ (*trans*) > $J_{P\text{-}P}$ (*cis*).[76] It is of interest to note that complexes **2.11**, **2.14**, and **2.17** give rise to both extremes of virtual coupling. Complexes **2.11** and **2.17** exhibit an NMR resonance which is a virtual doublet for the PMe_3 ligands while complex **2.14** shows a virtual triplet for $P(OMe)_3$. As follows from the preceding discussion, this result suggests that the P-P coupling between the two $P(OMe)_3$ ligands is larger than the P-P coupling between the two PMe_3 ligands. Without any structural information, and thus with caution, I suggest that this result may provide stereochemical information with respect to the relative orientations of the phosphorus ligands. Thus, it is suggested that the P-Re-P bond angle in **2.11** and **2.17** approaches 90° (corresponding to the phosphorus arrangement in Jenkins and Shaw's *cis* square planar complex) while the P-Re-P bond angle in **2.14** may open up to an angle significantly larger than 90°.

2.4. Conclusion

In this chapter, a series of cationic carbonyl phosphine and phosphite aryldiazenido complexes of the type [Cp*Re(CO)(PR_3)(*p*-$N_2C_6H_4OMe$)][BF_4] (PR_3 = PMe_3 (**2.4**), PEt_3 (**2.5**), PPh_3 (**2.6**), PCy_3 (**2.7**), $P(OMe)_3$ (**2.8**), or PCage (**2.9**)) were synthesized from the cationic acetonitrile complex [Cp*Re(CO)(NCMe)(*p*-$N_2C_6H_4OMe$)][BF_4] (**2.3**) and the appropriate phosphine or phosphite group. Furthermore, the cationic bis(phosphorus-ligand) aryldiazenido complexes [Cp*Re(PR_3)$_2$(N_2Ar)][BF_4] ((a) Ar = *p*-C_6H_4OMe; PR_3 = PMe_3 (**2.11**), PEt_3 (**2.12**), or $P(OMe)_3$ (**2.14**) and (b) Ar = C_6H_5; PR_3 = PMe_3 (**2.17**)) and the cationic bidentate phosphine aryldiazenido complex [Cp*Re(dmpe)(*p*-$N_2C_6H_4OMe$)][BF_4] (**2.13**) were also prepared from the corresponding bis-acetonitrile complexes [Cp*Re(NCMe)$_2$(N_2Ar)][BF_4] (Ar = *p*-C_6H_4OMe (**2.10**) or C_6H_5 (**2.16**)). In all cases, these complexes were spectroscopically and analytically characterized and their chemical properties were also described.

2.5. Experimental

2.5.1. General Methods

All manipulations were performed under nitrogen or argon by using standard Schlenk, drybox, or vacuum line techniques unless stated otherwise. Drybox manipulations were carried out in a nitrogen filled Vacuum Atmospheres HE-493 Dri-Lab with attached Dri-Train.

Acetone-d_6 (Isotec Inc.) and $CDCl_3$ (Isotec) were used as solvents for the NMR work. All NMR data were recorded at ambient temperatures on a Bruker AMX 400 instrument at an operating frequency of 400, 162, and 100 MHz for ^{1}H, ^{31}P, and ^{13}C nuclei respectively. ^{1}H and ^{13}C NMR chemical shifts are reported in ppm downfield

(positive) of tetramethylsilane. ^{31}P NMR chemical shifts are referenced to external 85% H_3PO_4. The terms "virtual doublet" or "virtual triplet" refer to the non-first-order multiplets which are seen in some of the ^1H and $^{13}C\{^1H\}$ NMR spectra; the apparent coupling constant is given by the separation between the two outside peaks.

Infrared spectra were measured by using a Bomem Michelson model 120 FT-IR instrument, usually as solutions in CaF_2 cells (0.1 mm). The IR spectra of the ^{15}N labeled complexes were obtained for 99% ^{15}N isotopically enriched samples.

Photochemical reactions of $CpRe(CO)_3$ and $Cp^*Re(CO)_3$ were carried out in a quartz vessel (100 mL) at atmospheric pressure and a temperature of 273 K. A 200 watt Hanovia high pressure mercury lamp was used as the UV source. Nitrogen was passed through the reaction vessel prior to the introduction of the solvent and starting materials, and slow passage of nitrogen was maintained during the photolysis. All solutions were subjected to a freeze-pump-thaw cycle (2 times) prior to photolysis.

Melting points were determined with a Fisher-Johns melting point apparatus and are uncorrected. Mass spectra were obtained with a Hewlett-Packard Model 5985 mass spectrometer equipped with a fast atom bombardment source (FAB; Phrasor Scientific Inc. accessory, *m*-nitrobenzyl alcohol, xenon). Masses are quoted for the ^{187}Re isotope. Microanalyses were performed by the Simon Fraser University Microanalytical Laboratory.

Tetrahydrofuran and diethyl ether were distilled from sodium benzophenone ketyl. Hexane was distilled from sodium wire. Acetone was distilled from calcium sulfate. Dichloromethane and acetonitrile were distilled from calcium hydride. All solvents were distilled under nitrogen and used immediately.

Trimethylphosphine (Strem Chemical Co.), triethylphosphine (Aldrich Chemical Co.), triphenylphosphine (BDH Chemicals Ltd.), tricyclohexylphosphine (Strem), 1,2-bis(dimethylphosphino)ethane (Strem), and trimethylphosphite (Alfa Products, Ventron

Division) were used as purchased and were stored under nitrogen and in the dark. The caged phosphite $P(OCH_2)_3CMe$ (PCage) was synthesized by the published method[77] and sublimed twice at room temperature immediately before use. Iodosobenzene was prepared from iodosobenzenediacetate (Aldrich) by the published method[78] and was stored in the refrigerator. Trimethylamine *N*-oxide (Aldrich) was used as purchased and was stored under nitrogen. $CpRe(CO)_3$ was synthesized by the published method.[79] $Cp^*Re(CO)_3$ was synthesized from $Re_2(CO)_{10}$ (Strem) by reaction with pentamethylcyclopentadiene (Strem) directly.[60a] The diazonium salts, $[N_\alpha N_\beta Ar][BF_4]$ were prepared by diazotization of aniline (Aldrich) or *p*-anisidine (Fisher Scientific Co.) with $NaNO_2$ (BDH)[80] and were recrystallized from acetone-diethyl ether. The ^{15}N isotopic label was introduced at N_α using $Na^{15}NO_2$ (99% ^{15}N; MSD Isotopes Inc.) or at N_β using $^{15}NH_2C_6H_5$ (99% ^{15}N; Stohler Isotopes Inc.).

2.5.2. Syntheses

Details have been given in previous publications of the preparation and characterization of $[Cp'Re(CO)_2(p\text{-}N_2C_6H_4OMe)][BF_4]$ (Cp' = Cp **(2.1)**[56, 81] or Cp* **(2.2)**[57]) and the acetonitrile complex $[Cp^*Re(CO)(NCMe)(p\text{-}N_2C_6H_4OMe)][BF_4]$ **(2.3)**.[58, 59] The methods used to prepare these materials in this study were modified. The characterizing spectroscopic data obtained were essentially identical, and additional data have been obtained for some of the complexes. Details for these complexes are included in this chapter for completeness, and as a reference for the new chemistry exhibited by these complexes, which is presented in the following chapters.

The reasons for the preparation of the bis-trimethylphosphine complex **2.17**, along with its precursors the dicarbonyl complex **2.15** and the bis-acetonitrile complex **2.16**, were twofold: (i) to compare their chemistry to their *p*-OMe substituted analogs and (ii) more importantly, to develop a method by which the ^{15}N isotopic label could be

introduced at the terminal nitrogen atom (N_β) of the aryldiazenido complex. The importance of the ^{15}N isotopic label at N_β is demonstrated in Chapter 6.

Preparation of [CpRe(CO)$_2$(*p*-N$_2$C$_6$H$_4$OMe)][BF$_4$] (2.1) and (2.1-^{15}N$_\alpha$). A solution of $CpRe(CO)_3$ (200 mg, 0.597 mmol) in freshly distilled THF (100 mL) was irradiated for 45 min to give a yellow-brown solution. After this time, an IR spectrum of the solution showed a conversion to the THF complex $CpRe(CO)_2(THF)$ in excess of 80%. This solution was then added directly to a stirred solution of [*p*-$N_2C_6H_4OMe$][BF_4] or [*p*-$^{15}N^{14}NC_6H_4OMe$][BF_4] (105 mg, 0.475 mmol) in acetone (5 mL). The resulting orange-brown solution was then stirred for an additional 30 min. The solution was then concentrated to *ca.* 10 mL by rotary evaporation and excess diethyl ether (60 mL) was added to precipitate the dicarbonyl complex. Supernatant solvent was removed by pipet and the remaining solid was washed with diethyl ether (3 times). Recrystallization from acetone-ether gave **2.1** or **2.1-$^{15}N_\alpha$** as a salmon colored microcrystalline solid in 68% yield (214 mg, 0.406 mmol) based on the original $CpRe(CO)_3$. M.p.: 387-388 K. IR (CH_2Cl_2): 2067, 2008 cm^{-1} ν(CO); 1767 cm^{-1} ν(NN) (1738 cm^{-1} for $^{15}N_\alpha$ labeled complex). ^1H NMR (acetone-d_6): δ 3.81 (s, 3H, OMe), 6.52 (s, 5H, Cp), 7.11 (d, 2H, C_6H_4), 7.40 (d, 2H, C_6H_4). $^{13}C\{^1H\}$ NMR (acetone-d_6): δ 56.61 (s, OMe), 96.26 (s, Cp), 116.24, 117.18, 126.92, 164.88 (s, C_6H_4), 188.09 (s, CO). M.S. (FAB, *m*-nitrobenzyl alcohol, xenon): m/z 443 (M^+ of cation), 359 (M^+ - 2CO - N_2). Anal. Calcd: C, 31.76; H, 2.27; N, 5.29. Found: C, 31.94; H, 2.30; N, 5.44.

Preparation of [Cp*Re(CO)$_2$(*p*-N$_2$C$_6$H$_4$OMe)][BF$_4$] (2.2) and (2.2-^{15}N$_\alpha$). A solution of $Cp^*Re(CO)_3$ (200 mg, 0.494 mmol) in freshly distilled THF (100 mL) was irradiated for 90 min to give a yellow-brown solution. An IR spectrum of this solution showed a conversion to the THF complex $Cp^*Re(CO)_2(THF)$ in excess of 60%. This solution was then added directly to a stirred solution of [*p*-$N_2C_6H_4OMe$][BF_4] or

[*p*-$^{15}N^{14}NC_6H_4OMe$][BF_4] (65 mg, 0.29 mmol) in acetone (5 mL). The resulting red-brown solution was then stirred for an additional 30 min. The solution was then purified following a similar procedure to that used for complex **2.1**. Recrystallization from acetone-ether gave **2.2** or **2.2-$^{15}N_\alpha$** as a maroon colored microcrystalline solid in 56% yield (166 mg, 0.277 mmol) based on the original Cp*Re$(CO)_3$. M.p.: 407-409 K. IR (CH_2Cl_2): 2054, 1998 cm^{-1} ν(CO); 1732 cm^{-1} ν(NN) (1708 cm^{-1} for $^{15}N_\alpha$ labeled complex). ^1H NMR (acetone-d_6): δ 2.37 (s, 15H, Cp*), 3.84 (s, 3H, OMe), 7.15 (d, 2H, C_6H_4), 7.50 (d, 2H, C_6H_4). $^{13}C\{^1H\}$ NMR (acetone-d_6): δ 10.32 (s, $C_5\underline{Me}_5$), 56.32 (s, OMe), 109.47 (s, $\underline{C}_5Me_5$), 116.10, 116.81, 126.09, 164.12 (s, C_6H_4), 190.22 (s, CO). M.S. (FAB, *m*-nitrobenzyl alcohol, xenon): m/z 513 (M^+ of cation), 429 (M^+ - 2CO - N_2), 378 (M^+ - $N_2C_6H_4OMe$). Anal. Calcd: C, 38.06; H, 3.67; N, 4.67. Found: C, 37.93; H, 3.80; N, 4.84.

Preparation of [Cp*Re(CO)(NCMe)(*p*-$N_2C_6H_4OMe$)][BF_4] (2.3) and (2.3-$^{15}N_\alpha$). An approximate 20% stoichiometric excess of iodosobenzene (or a stoichiometric amount of trimethylamine *N*-oxide) was added as a solid to a stirred solution of **2.2** or **2.2-$^{15}N_\alpha$** (100 mg, 0.167 mmol) in freshly distilled MeCN (5 mL). (Note: avoid adding a large excess of iodosobenzene since this leads to decomposition of the acetonitrile complex once it is formed). After 30 min all the dicarbonyl complex had reacted to produce the acetonitrile complex as monitored by IR spectroscopy. The solution was then filtered through Celite to remove the undissolved iodosobenzene. Removal of solvent under vacuum gave a red, oily product which was washed with diethyl ether (3 times). Recrystallization from acetone-ether gave **2.3** or **2.3-$^{15}N_\alpha$** as an orange microcrystalline solid in 88% yield (90 mg, 0.15 mmol). M.p.: 338-340 K with decomposition. IR (CH_2Cl_2): 1959 cm^{-1} ν(CO); 1658 cm^{-1} ν(NN) (1637 cm^{-1} for $^{15}N_\alpha$ labeled complex). ^1H NMR (acetone-d_6): δ 2.15 (s, 15H, Cp*), 3.13 (s, 3H, MeCN), 3.88 (s, 3H, OMe), 7.09 (d, 2H, C_6H_4), 7.26 (d, 2H, C_6H_4). $^{13}C\{^1H\}$ NMR (acetone-d_6):

δ 5.02 (s, MeCN), 10.17 (s, C_5Me_5), 56.18 (s, OMe), 106.85 (s, C_5Me_5), 116.43, 122.17, 123.28, 161.82 (s, C_6H_4), 143.94 (s, MeCN), 196.39 (s, CO). M.S. (FAB, *m*-nitrobenzyl alcohol, xenon): m/z 526 (M^+ of cation), 485 (M^+ - MeCN). Anal. Calcd: C, 39.22; H, 4.11; N, 6.86. Found: C, 38.96; H, 3.92; N, 6.77.

Preparation of [Cp*Re(CO)(PMe_3)(*p*-$N_2C_6H_4OMe$)][BF_4] (2.4) and (2.4-$^{15}N_\alpha$). A 10-fold stoichiometric excess of PMe_3 was added by syringe to a stirred solution of the acetonitrile complex **2.3** or **2.3-$^{15}N_\alpha$** (100 mg, 0.163 mmol) in acetone (5 mL). An IR spectrum recorded after 1 h indicated that the reaction was complete. No apparent color change was noted. The solvent was removed by vacuum and the remaining oily, orange product was solidified by washing with diethyl ether (3 times). Recrystallization from acetone-ether gave **2.4** or **2.4-$^{15}N_\alpha$** as a orange-brown solid in 80% yield (84 mg, 0.13 mmol). M.p.: 442-444 K. IR (CH_2Cl_2): 1950 cm^{-1} ν(CO); 1678 cm^{-1} ν(NN) (1643 cm^{-1} for $^{15}N_\alpha$ labeled complex). ^1H NMR (acetone-d_6): δ 1.97 (d, 9H, PMe_3, J_{H-P} = 10.6 Hz), 2.28 (d, 15H, Cp*, J_{H-P} = 0.5 Hz), 3.88 (s, 3H, OMe), 7.16 (d, 2H, C_6H_4), 7.35 (d, 2H, C_6H_4). $^{13}C\{^1H\}$ NMR (acetone-d_6): δ 10.83 (s, C_5Me_5), 18.48 (d, PMe_3, J_{C-P} = 39 Hz), 56.02 (s, OMe), 106.71 (s, C_5Me_5), 116.63, 120.09, 122.91, 162.32 (s, C_6H_4), 202.59 (d, CO, J_{C-P} = 12 Hz). $^{31}P\{^1H\}$ NMR (acetone-d_6): δ -28.23 (s, PMe_3). M.S. (FAB, *m*-nitrobenzyl alcohol, xenon): m/z 561 (M^+ of cation), 426 (M^+ - $N_2C_6H_4OMe$). Anal. Calcd: C, 38.95; H, 4.79; N, 4.33. Found: C, 39.04; H, 4.94; N, 4.30.

Preparation of [Cp*Re(CO)(PEt_3)(*p*-$N_2C_6H_4OMe$)][BF_4] (2.5). This complex was prepared in a similar manner to that of complex **2.4**. The only change made to the procedure was that upon addition of excess PEt_3, by syringe, the solution was stirred for 2 h in order to complete the reaction. After recrystallization from acetone-ether, the phosphine complex **2.5** was obtained in 83% yield (93 mg, 0.14 mmol) as an orange-brown solid. M.p.: 421-423 K. IR (CH_2Cl_2): 1948 cm^{-1} ν(CO); 1680 cm^{-1} ν(NN). ^1H

NMR (acetone-d_6): δ 1.16 (dt, 9H, $P(CH_2C\underline{H}_3)_3$, J_{H-H} = 17.6 Hz, J_{H-P} = 7.6 Hz), 2.19 (m, 6H, $P(C\underline{H}_2CH_3)_3$), 2.27 (s, 15H, Cp*), 3.88 (s, 3H, OMe), 7.18 (d, 2H, C_6H_4), 7.36 (d, 2H, C_6H_4). $^{13}C\{^1H\}$ NMR (acetone-d_6): δ 7.98 (s, $P(CH_2\underline{C}H_3)_3$), 10.70 (s, $C_5\underline{Me}_5$), 19.75 (d, $P(\underline{C}H_2CH_3)_3$, J_{C-P} = 35 Hz), 56.04 (s, OMe), 106.92 (s, $\underline{C}_5Me_5$), 116.24, 120.10, 123.32, 162.80 (s, C_6H_4), 203.32 (d, CO, J_{C-P} = 11 Hz). $^{31}P\{^1H\}$ NMR (acetone-d_6): δ 6.60 (s, PEt_3). M.S. (FAB, *m*-nitrobenzyl alcohol, xenon): m/z 603 (M^+ of cation). Anal. Calcd: C, 41.80; H, 5.41; N, 4.06. Found: C, 41.51; H, 5.55; N, 3.77.

Preparation of [Cp*Re(CO)(PPh_3)(*p*-$N_2C_6H_4OMe$)][BF_4] (2.6). This complex was prepared in a similar manner to that of complex **2.4**. The only change made to the procedure was that upon addition of excess PPh_3, as a solid, the solution was stirred for 24 h in order to complete the reaction. After recrystallization from acetone-ether, the phosphine complex **2.6** was obtained in 74% yield (100 mg, 0.121 mmol) as an orange-brown solid. M.p.: 489-491 K. IR (CH_2Cl_2): 1956 cm^{-1} ν(CO); 1682 cm^{-1} ν(NN). ^1H NMR (acetone-d_6): δ 2.03 (s, 15H, Cp*), 3.87 (s, 3H, OMe), 7.11 (d, 2H, C_6H_4), 7.25 (d, 2H, C_6H_4), 7.42-7.53 (m, 15H, PPh_3). $^{13}C\{^1H\}$ NMR (acetone-d_6): δ 10.04 (s, $C_5\underline{Me}_5$), 56.02 (s, OMe), 107.30 (s, $\underline{C}_5Me_5$), 116.07, 119.22, 123.89, 162.75 (s, C_6H_4), 128.71 (d, PPh_3, J_{C-P} = 12 Hz), 129.41 (d, PPh_3, J_{C-P} = 11 Hz), 132.16 (s, PPh_3), 133.85 (d, PPh_3, J_{C-P} = 24 Hz), 202.67 (d, CO, J_{C-P} = 9 Hz). $^{31}P\{^1H\}$ NMR (acetone-d_6): δ 16.22 (s, PPh_3). M.S. (FAB, *m*-nitrobenzyl alcohol, xenon): m/z 747 (M^+ of cation). Anal. Calcd: C, 51.87; H, 4.47; N, 3.36. Found: C, 51.42; H, 4.19; N, 3.44.

Preparation of [Cp*Re(CO)(PCy_3)(*p*-$N_2C_6H_4OMe$)][BF_4] (2.7). This complex was prepared in a similar manner to that of complex **2.4**. The only change made to the procedure was that upon addition of excess PCy_3, as a solid, the solution was stirred for 4 h in order to complete the reaction. After recrystallization from acetone-ether, the phosphine complex **2.7** was obtained in 69% yield (96 mg, 0.11 mmol) as an orange-brown solid. M.p.: 384-386 K. IR (CH_2Cl_2): 1925 cm^{-1} ν(CO); 1626 cm^{-1} ν(NN). ^1H

NMR (acetone-d_6): δ 1.41 and 1.84 (both multiplets, 33H, PCy_3), 2.24 (s, 15H, Cp*), 3.89 (s, 3H, OMe), 7.19 (d, 2H, C_6H_4), 7.34 (d, 2H, C_6H_4). $^{13}C\{^1H\}$ NMR (acetone-d_6): δ 10.78 (s, $C_5\underline{Me}_5$), 26.62 (s, PCy_3), 27.51 (d, PCy_3, J_{C-P} = 10 Hz), 31.43 (d, PCy_3, J_{C-P} = 3 Hz), 32.33 (d, PCy_3, J_{C-P} = 21 Hz), 56.09 (s, OMe), 107.02 (s, $\underline{C}_5Me_5$), 116.29, 120.24, 123.57, 162.87 (s, C_6H_4), 203.62 (d, CO, J_{C-P} = 7 Hz). $^{31}P\{^1H\}$ NMR (acetone-d_6): δ 23.23 (s, PCy_3). M.S. (FAB, *m*-nitrobenzyl alcohol, xenon): m/z 765 (M^+ of cation). Anal. Calcd: C, 50.76; H, 6.51; N, 3.29. Found: C, 50.49; H, 6.47; N, 3.19.

Preparation of [Cp*Re(CO){P(OMe)$_3$}(*p*-N$_2$C$_6$H$_4$OMe)][BF$_4$] (2.8) and (2.8-$^{15}N_\alpha$). This complex was prepared in a similar manner to that of complex **2.4**. The only change made to the procedure was that upon addition of excess $P(OMe)_3$, by syringe, the solution was stirred for 4 h in order to complete the reaction. After recrystallization from acetone-ether, the phosphite complex **2.8** or **2.8**-$^{15}N_\alpha$ was obtained in 73% yield (83 mg, 0.12 mmol) as an orange-brown solid. M.p.: 377-379 K. IR (CH_2Cl_2): 1966 cm^{-1} ν(CO); 1691 cm^{-1} ν(NN) (1648 cm^{-1} for $^{15}N_\alpha$ labeled complex). ^1H NMR (acetone-d_6): δ 2.27 (d, 15H, Cp*, J_{H-P} = 0.7 Hz), 3.89 (d, 9H, $P(OMe)_3$, J_{H-P} = 12.1 Hz), 3.89 (s, 3H, OMe), 7.18 (d, 2H, C_6H_4), 7.40 (d, 2H, C_6H_4). $^{13}C\{^1H\}$ NMR (acetone-d_6): δ 12.17 (s, $C_5\underline{Me}_5$), 56.50 (d, $P(OMe)_3$, J_{C-P} = 6 Hz), 57.81 (s, OMe), 108.80 (s, $\underline{C}_5Me_5$), 117.57, 120.54, 125.26, 164.40 (s, C_6H_4), 201.08 (d, CO, J_{C-P} = 17 Hz). $^{31}P\{^1H\}$ NMR (acetone-d_6): δ 110.35 (s, $P(OMe)_3$). M.S. (FAB, *m*-nitrobenzyl alcohol, xenon): m/z 609 (M^+ of cation). Anal. Calcd: C, 36.26; H, 4.46; N, 4.03. Found: C, 36.20; H, 4.66; N, 3.86.

Preparation of [Cp*Re(CO){P(OCH$_2$)$_3$CMe}(*p*-N$_2$C$_6$H$_4$OMe)][BF$_4$] (2.9). This complex was prepared in a similar manner to that of complex **2.4**. The only change made to the procedure was that upon addition of excess $P(OCH_2)_3CMe$, as a solid, the solution was stirred for 4 h in order to complete the reaction. After recrystallization from acetone-ether, the phosphite complex **2.9** was obtained in 76% yield (89 mg, 0.12 mmol)

as an orange-brown solid. M.p.: 430-432 K. IR (CH_2Cl_2): 1982 cm^{-1} ν(CO); 1701 cm^{-1} ν(NN). ^1H NMR (acetone-d_6): δ 0.94 (s, 3H, $P(OCH_2)_3C\underline{Me}$), 2.27 (d, 15H, Cp*, J_{H-P} = 0.9 Hz), 3.89 (s, 3H, OMe), 4.65 (d, 6H, $P(O\underline{CH_2})_3CMe$, J_{H-P} = 5.0 Hz), 7.17 (d, 2H, C_6H_4), 7.42 (d, 2H, C_6H_4). $^{13}C\{^1H\}$ NMR (acetone-d_6): δ 10.29 (s, $C_5\underline{Me_5}$), 14.62 (s, $P(OCH_2)_3C\underline{Me}$), 33.94 (s, $P(OCH_2)_3\underline{C}Me$), 56.14 (s, OMe), 78.37 (d, $P(O\underline{C}H_2)_3CMe$, J_{C-P} = 6 Hz), 107.75 (s, $\underline{C}_5Me_5$), 116.43, 118.92, 124.58, 163.19 (s, C_6H_4), 198.10 (d, CO, J_{C-P} = 21 Hz). $^{31}P\{^1H\}$ NMR (acetone-d_6): δ 104.40 (s, $P(OCH_2)_3CMe$). M.S. (FAB, *m*-nitrobenzyl alcohol, xenon): m/z 633 (M^+ of cation). Anal. Calcd: C, 38.40; H, 4.34; N, 3.89. Found: C, 38.11; H, 4.25; N, 3.61.

Preparation of [Cp*Re(NCMe)$_2$(*p*-$N_2C_6H_4OMe$)][BF_4] (2.10) and (2.10-$^{15}N_\alpha$). Twice the stoichiometric amount of trimethylamine *N*-oxide was added as a solid to a stirred solution of **2.2** or **2.2-$^{15}N_\alpha$** (100 mg, 0.167 mmol) in freshly distilled MeCN (5 mL). (Note: avoid adding a large excess of trimethylamine *N*-oxide since this leads to decomposition of the bis-acetonitrile complex once it is formed). After 30 min all the dicarbonyl complex had reacted to produce the bis-acetonitrile complex as monitored by IR spectroscopy. Removal of solvent under vacuum gave a red, oily product which was solidified by washing with diethyl ether (3 times) and dried under vacuum for two days to give **2.10** or **2.10-$^{15}N_\alpha$** as a red-orange solid in 78% yield (81 mg, 0.13 mmol). M.p.: 334-336 K with decomposition. IR (CH_2Cl_2): 1618, 1588 cm^{-1} ν(NN + CC) (1607, 1578 cm^{-1} for $^{15}N_\alpha$ labeled complex). ^1H NMR (acetone-d_6): δ 1.94 (s, 15H, Cp*), 3.15 (s, 6H, MeCN), 3.83 (s, 3H, OMe), 6.91 (d, 2H, C_6H_4), 7.07 (d, 2H, C_6H_4). $^{13}C\{^1H\}$ NMR (acetone-d_6): δ 4.34 (s, $\underline{Me}CN$), 9.28 (s, $C_5\underline{Me_5}$), 55.53 (s, OMe), 102.86 (s, $\underline{C}_5Me_5$), 114.46, 120.39, 123.73, 159.11 (s, C_6H_4), 139.65 (s, $Me\underline{C}N$). M.S. (FAB, *m*-nitrobenzyl alcohol, xenon): m/z 539 (M^+ of cation), 498 (M^+ - MeCN). Anal. Calcd: C, 40.33; H, 4.51; N, 8.96. Found: C, 39.84; H, 4.55; N, 8.77.

Preparation of $[Cp^*Re(PMe_3)_2(p\text{-}N_2C_6H_4OMe)][BF_4]$ (2.11) and (2.11-$^{15}N_\alpha$). A 10-fold stoichiometric excess of PMe_3 was added by syringe to a stirred solution of the bis-acetonitrile complex **2.10** or **2.10-$^{15}N_\alpha$** (100 mg, 0.160 mmol) in acetone (5 mL). An IR spectrum recorded after 24 h indicated that the reaction was complete. No apparent color change was noted. The solvent was removed by vacuum and the remaining oily, red-orange product was solidified by washing with diethyl ether (3 times). Recrystallization from acetone-ether gave **2.11** or **2.11-$^{15}N_\alpha$** as a red-orange solid in 72% yield (80 mg, 0.12 mmol). M.p.: 414-416 K. IR (CH_2Cl_2): 1624, 1591, 1570 cm^{-1} ν(NN + CC) (1611, 1580, 1559 cm^{-1} for $^{15}N_\alpha$ labeled complex). ^1H NMR (acetone-d_6): δ 1.77 (virtual doublet, 18H, PMe_3, J_{app} = 9.0 Hz), 2.11 (s, 15H, Cp*), 3.79 (s, 3H, OMe), 7.03 (s, 4H, C_6H_4). ^1H NMR ($CDCl_3$): δ 1.73 (virtual doublet, 18H, PMe_3, J_{app} = 9.0 Hz), 2.06 (s, 15H, Cp*), 3.83 (s, 3H, OMe), 6.92 (d, 4H, C_6H_4). $^{13}C\{^1H\}$ NMR (acetone-d_6): δ 11.65 (s, $C_5\underline{Me}_5$), 21.66 (virtual doublet, PMe_3, J_{app} = 37 Hz), 55.98 (s, OMe), 102.81 (s, $\underline{C}_5Me_5$), 115.10, 119.54, 122.83, 159.52 (s, C_6H_4). $^{31}P\{^1H\}$ NMR (acetone-d_6): δ -43.28 (s, PMe_3). M.S. (FAB, *m*-nitrobenzyl alcohol, xenon): m/z 609 (M^+ of cation), 533 (M^+ - PMe_3). Anal. Calcd: C, 39.72; H, 5.80; N, 4.03. Found: C, 39.56; H, 5.62; N, 4.09.

Preparation of $[Cp^*Re(PEt_3)_2(p\text{-}N_2C_6H_4OMe)][BF_4]$ (2.12). This complex was prepared in a similar manner to complex **2.11**. The only change made to the procedure was that upon addition of excess PEt_3, by syringe, the solution was stirred for 48 h in order to complete the reaction. After recrystallization from acetone-ether complex **2.12** was obtained in 73% yield (91 mg, 0.12 mmol) as a red-orange solid. M.p.: 421-422 K. IR (CH_2Cl_2): 1620 cm^{-1} ν(NN + CC). ^1H NMR (acetone-d_6): δ 1.09 (m, 18H, $P(CH_2C\underline{H}_3)_3$), 1.33 (m, 12H, $P(C\underline{H}_2CH_3)_3$), 2.03 (s, 15H, Cp*), 3.81 (s, 3H, OMe), 6.99 (d, 2H, C_6H_4), 7.17 (d, 2H, C_6H_4). $^{13}C\{^1H\}$ NMR (acetone-d_6): δ 10.88

(s, $P(CH_2\underline{C}H_3)_3$), 11.51 (s, $C_5\underline{Me}_5$), 22.15 (d, $P(\underline{C}H_2CH_3)_3$, $J_{C\text{-}P}$ = 33 Hz), 56.01 (s, OMe), 103.27 (s, $\underline{C}_5Me_5$), 114.93, 119.38, 122.91, 160.09 (s, C_6H_4). $^{31}P\{^1H\}$ NMR (acetone-d_6): δ -7.68 (s, PEt_3). M.S. (FAB, *m*-nitrobenzyl alcohol, xenon): m/z 693 (M^+ of cation), 575 (M^+ - PEt_3). Anal. Calcd: C, 44.67; H, 6.68; N, 3.59. Found: C, 44.48; H, 6.63; N, 3.71.

Preparation of [Cp*Re(dmpe)(*p*-$N_2C_6H_4OMe$)][BF_4] (2.13). This complex was prepared analogously to complex **2.11**. Upon addition of excess dmpe, by syringe, the solution was stirred for 24 h in order to complete the reaction. After recrystallization from acetone-ether complex **2.13** was obtained in 77% yield (85 mg, 0.12 mmol) as a red-orange solid. M.p.: 417-418 K. IR (CH_2Cl_2): 1622 cm^{-1} ν(NN + CC). ^1H NMR (acetone-d_6): δ 1.65 (d, 6H, $P\underline{Me}_2CH_2CH_2\underline{Me}_2P$, $J_{H\text{-}P}$ = 10.1 Hz), 1.78 (m, 4H, $PMe_2C\underline{H}_2C\underline{H}_2Me_2P$), 1.88 (d, 6H, $P\underline{Me}_2CH_2CH_2\underline{Me}_2P$, $J_{H\text{-}P}$ = 10.5 Hz), 2.15 (s, 15H, Cp*), 3.78 (s, 3H, OMe), 6.98 (d, 2H, C_6H_4), 7.04 (d, 2H, C_6H_4). $^{13}C\{^1H\}$ NMR (acetone-d_6): δ 11.58 (s, $C_5\underline{Me}_5$), 15.54 (d, $P\underline{Me}_2CH_2CH_2\underline{Me}_2P$, $J_{C\text{-}P}$ = 37 Hz), 20.57 (d, $P\underline{Me}_2CH_2CH_2\underline{Me}_2P$, $J_{C\text{-}P}$ = 37 Hz), 33.16 (d, $PMe_2\underline{C}H_2\underline{C}H_2Me_2P$, $J_{C\text{-}P}$ = 35 Hz), 56.37 (s, OMe), 103.46 (s, $\underline{C}_5Me_5$), 115.59, 116.08, 122.68, 160.34 (s, C_6H_4). $^{31}P\{^1H\}$ NMR (acetone-d_6): δ -46.76 (s, dmpe). M.S. (FAB, *m*-nitrobenzyl alcohol, xenon): m/z 607 (M^+ of cation). Anal. Calcd: C, 39.83; H, 5.48; N, 4.04. Found: C, 39.52; H, 5.44; N, 4.19.

Preparation of [Cp*Re{$P(OMe)_3$}$_2$(*p*-$N_2C_6H_4OMe$)][BF_4] (2.14) and (2.14-$^{15}N_\alpha$). This complex was prepared in a similar manner to complex **2.11**. The only change made to the procedure was that upon addition of excess $P(OMe)_3$, by syringe, the solution was stirred for 72 h in order to complete the reaction. After recrystallization from acetone-ether complex **2.14** or **2.14-$^{15}N_\alpha$** was obtained in 69% yield (87 mg, 0.11 mmol) as a red-orange solid. M.p.: 386-388 K. IR (CH_2Cl_2): 1640, 1593, 1572 cm^{-1} ν(NN + CC) (1624, 1587, 1566 cm^{-1} for $^{15}N_\alpha$ labeled complex). ^1H NMR

(acetone-d_6): δ 2.06 (s, 15H, Cp*), 3.80 (virtual triplet, 18H, $P(OMe)_3$, J_{app} = 11.6 Hz), 3.84 (s, 3H, OMe), 7.07 (d, 2H, C_6H_4), 7.24 (d, 2H, C_6H_4). ^1H NMR ($CDCl_3$): δ 1.96 (s, 15H, Cp*), 3.69 (virtual triplet, 18H, $P(OMe)_3$, J_{app} = 11.6 Hz), 3.81 (s, 3H, OMe), 6.89 (d, 2H, C_6H_4), 7.08 (d, 2H, C_6H_4). $^{13}C\{^1H\}$ NMR (acetone-d_6): δ 11.67 (s, $C_5\underline{Me}_5$), 54.34 (virtual triplet, $P(OMe)_3$, J_{app} = 41 Hz), 55.93 (s, OMe), 109.34 (s, $\underline{C}_5Me_5$), 118.32, 120.79, 126.31, 163.34 (s, C_6H_4). $^{31}P\{^1H\}$ NMR (acetone-d_6): δ 113.63 (s, $P(OMe)_3$). M.S. (FAB, *m*-nitrobenzyl alcohol, xenon): m/z 705 (M^+ of cation). Anal. Calcd: C, 34.90; H, 5.09; N, 3.54. Found: C, 34.81; H, 5.01; N, 3.47.

Preparation of $[Cp^*Re(CO)_2(N_2C_6H_5)][BF_4]$ (2.15) and (2.15-$^{15}N_\beta$). This complex was prepared in a similar manner to complex **2.2**. The only change made to the procedure was that $[N_2C_6H_5][BF_4]$ or $[^{14}N^{15}NC_6H_5][BF_4]$ (56 mg, 0.29 mmol) were used instead of the *p*-OMe diazonium salts. Recrystallization from acetone-ether gave **2.15** or **2.15-$^{15}N_\beta$** as an orange colored microcrystalline solid in 59% yield (166 mg, 0.29 mmol) based on the original $Cp^*Re(CO)_3$. M.p.: 425-427 K. IR (CH_2Cl_2): 2056, 2000 cm^{-1} ν(CO); 1736 cm^{-1} ν(NN) (1716 cm^{-1} for $^{15}N_\beta$ labeled complex). ^1H NMR (acetone-d_6): δ 2.48 (s, 15H, Cp*), 7.48 (m, 2H, C_6H_5), 7.59 (m, 1H, C_6H_5), 7.71 (m, 2H, C_6H_5). $^{13}C\{^1H\}$ NMR (acetone-d_6): δ 10.27 (s, $C_5\underline{Me}_5$), 109.69 (s, $\underline{C}_5Me_5$), 124.47, 126.13, 132.01, 134.32 (s, C_6H_5), 189.62 (s, CO). M.S. (FAB, *m*-nitrobenzyl alcohol, xenon): m/z 483 (M^+ of cation), 455 (M^+ - CO), 427 (M^+ - 2CO). Anal. Calcd: C, 37.96; H, 3.51; N, 4.92. Found: C, 37.69; H, 3.43; N, 5.03.

Preparation of $[Cp^*Re(NCMe)_2(N_2C_6H_5)][BF_4]$ (2.16) and (2.16-$^{15}N_\beta$). Twice the stoichiometric amount of trimethylamine *N*-oxide was added as a solid to a stirred solution of **2.15** or **2.15-$^{15}N_\beta$** (100 mg, 0.176 mmol) in freshly distilled MeCN (5 mL). (Note: avoid adding a large excess of trimethylamine *N*-oxide since this leads to decomposition of the bis-acetonitrile complex once it is formed). After 60 min all the dicarbonyl complex had reacted to produce the bis-acetonitrile complex as monitored by

IR spectroscopy. Removal of solvent under vacuum gave a red, oily product which was solidified by washing with diethyl ether (3 times) and dried under vacuum for one day to give **2.16** or **2.16-$^{15}N_{\beta}$** as a red-orange solid in 73% yield (76 mg, 0.13 mmol). M.p.: 331-332 K with decomposition. IR (CH_2Cl_2): 1562, 1485 cm^{-1} ν(NN + CC) (1548, 1472 cm^{-1} for $^{15}N_{\beta}$ labeled complex). ^1H NMR (acetone-d_6): δ 1.97 (s, 15H, Cp*), 3.29 (s, 6H, MeCN), 7.10 (m, 2H, C_6H_5), 7.23 (m, 1H, C_6H_5), 7.37 (m, 2H, C_6H_5). $^{13}C\{^1H\}$ NMR (acetone-d_6): δ 4.21 (s, MeCN), 9.22 (s, C_5Me_5), 102.98 (s, C_5Me_5), 122.67, 124.33, 130.14, 132.47 (s, C_6H_5), 140.07 (s, MeCN). M.S. (FAB, *m*-nitrobenzyl alcohol, xenon): m/z 509 (M^+ of cation), 468 (M^+ - MeCN). Anal. Calcd: C, 40.34; H, 4.37; N, 9.41. Found: C, 39.89; H, 4.70; N, 9.48.

Preparation of [Cp*Re(PMe_3)$_2$($N_2C_6H_5$)][BF_4] (2.17) and (2.17-$^{15}N_{\beta}$). A 10-fold stoichiometric excess of PMe_3 was added by syringe to a stirred solution of the bis-acetonitrile complex **2.16** or **2.16-$^{15}N_{\beta}$** (100 mg, 0.168 mmol) in acetone (5 mL). An IR spectrum recorded after 24 h indicated that the reaction was complete. No apparent color change was noted. The solvent was removed by vacuum and the remaining oily, red-orange product was solidified by washing with diethyl ether (3 times). Recrystallization from acetone-ether gave **2.17** or **2.17-$^{15}N_{\beta}$** as a red-orange solid in 78% yield (87 mg, 0.13 mmol). M.p.: 410-411 K. IR (CH_2Cl_2): 1566, 1485 cm^{-1} ν(NN + CC) (1557, 1476 cm^{-1} for $^{15}N_{\beta}$ labeled complex). ^1H NMR (acetone-d_6): δ 1.78 (virtual doublet, 18H, PMe_3, J_{app} = 9.6 Hz), 2.12 (s, 15H, Cp*), 7.08 (m, 2H, C_6H_4), 7.13 (m, 1H, C_6H_4), 7.47 (m, 2H, C_6H_4). $^{31}P\{^1H\}$ NMR (acetone-d_6): δ -42.41 (s, PMe_3). M.S. (FAB, *m*-nitrobenzyl alcohol, xenon): m/z 579 (M^+ of cation), 503 (M^+ - PMe_3). Anal. Calcd: C, 39.70; H, 5.71; N, 4.21. Found: C, 39.38; H, 5.61; N, 4.31.

Reaction of [Cp*Re(CO)$_2$(*p*-$N_2C_6H_4$OMe)][BF_4] (2.2) with Me_3NO in THF. A stoichiometric amount of trimethylamine *N*-oxide was added as a solid to a stirred solution of **2.2** in freshly distilled THF (10 mL). An IR spectrum, recorded immediately

after the addition, showed the complete disappearance of **2.2** and the presence of a broad, very strong absorption at 1921 cm^{-1} and a broad, moderately intense absorption at 1618 cm^{-1} assigned to the THF complex [Cp*Re(CO)(THF)(*p*-$N_2C_6H_4OMe$)][BF_4] (**2.18**). All attempts to isolate **2.18** were not successful. However, the addition of excess PMe_3 directly to the THF solution gave the PMe_3 complex [Cp*Re(CO)(PMe_3)(*p*-$N_2C_6H_4OMe$)][BF_4] (**2.4**) as characterized by IR and ^1H NMR spectroscopy, corroborating the assignment of **2.18**. IR (THF): 1921 cm^{-1} ν(CO); 1618 cm^{-1} ν(NN). Furthermore, an IR spectrum recorded immediately after the addition of two equivalents of Me_3NO to a THF solution (10 mL) of the dicarbonyl complex **2.2** showed the total disappearance of **2.2** and the presence of a single, broad, moderately intense absorption at 1576 cm^{-1} assigned to the bis-THF complex [Cp*Re$(THF)_2$(*p*-$N_2C_6H_4OMe$)][BF_4] (**2.19**). Complex **2.19** did not survive purification. However, the addition of excess PMe_3 directly to the THF solution gave the bis-PMe_3 complex [Cp*Re$(PMe_3)_2$(*p*-$N_2C_6H_4OMe$)][BF_4] (**2.11**) as characterized by IR and ^1H NMR spectroscopy, supporting the assignment of **2.19**. IR (THF): 1576 cm^{-1} ν(NN).

CHAPTER 3

Investigation of Stereochemical Non-rigidity of a Singly-bent Aryldiazenido Ligand

3.1. Introduction

Exploratory synthesis and product characterization have dominated the first quarter-century of research in transition metal aryldiazenido (MNNAr) chemistry in order to establish not only the possible geometric and electronic features of these ligands, but also the metal and co-ligand requirements for forming stable isolable products. A variety of possible electronic structures and geometries can be visualized for the terminal NNAr ligand in a neutral MNNAr situation, and these are described in a simplified fashion by the valence bond descriptions (1)-(4) (Scheme 3.1).

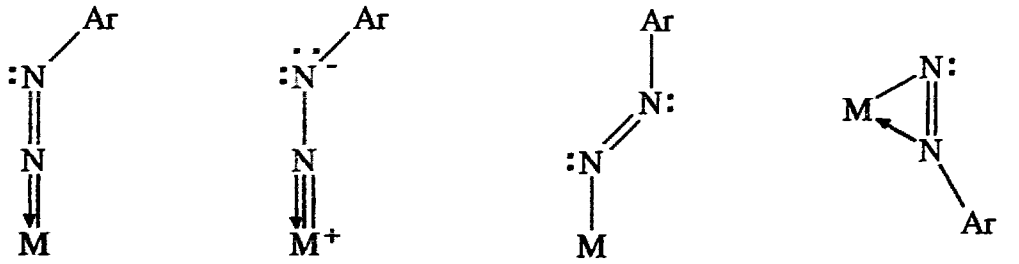

Scheme 3.1. Valence bond descriptions for MNNAr.

In terms of the number of spectroscopically or X-ray structurally characterized examples, the singly-bent terminal aryldiazenido ligand represented by (1) is by far the most common and well-established for both alkyl (R), and aryl (Ar) substituents. All the rhenium aryldiazenido complexes presented in this chapter, and for that matter in this

thesis, belong to this structural class. There is little evidence for examples approximating the electron distribution represented by the zwitterion (2). Much less common in transition metal chemistry is the doubly-bent structure (3) even though this is the configuration prevalent in purely organic diazenes such as azobenzene. Currently, (3) is known to be adopted in the X-ray structures of $PtCl(p\text{-}N_2C_6H_4F)(PEt_3)_2$,[82] $IrCl_2(o\text{-}N_2C_6H_4NO_2)(CO)(PPh_3)_2$,[83] and $[RhCl(triphos)(N_2Ph)]^+$ (triphos = $PhP(CH_2PPh_2)_2$).[84] Finally, only a single example of the side-on bonded arrangement (4) is known, namely $CpTiCl_2(N_2Ph)$.[85]

It is worth noting that, despite the large number of structurally characterized examples, there has been little attempt to review and discuss the specific orientations adopted by these aryldiazenido ligands. For example, in the case of (1), what is the favored orientation of the NNC (aryl) plane of the singly-bent aryldiazenido ligand relative to the other co-ligands or the coordinate axes and is the geometry of the complex influenced by the nature of the co-ligands? Answers to these questions would provide insight into the conformational behavior exhibited by the aryldiazenido ligand (NNAr), and may in turn, infer information regarding the specific orientation adopted by the hydrogen atom of its diazenido analog (NNH).

In this chapter, I report the results of an X-ray structural and variable temperature solution ^1H, $^{31}P\{^1H\}$, and $^{13}C\{^1H\}$ NMR study of the half-sandwich complexes $[Cp^*Re(L_1)(L_2)(p\text{-}N_2C_6H_4OMe)][BF_4]$ ((a) $L_1 = L_2 = CO$ **(2.2)**, PMe_3 **(2.11)**, or $P(OMe)_3$ **(2.14)** and (b) $L_1 = CO$; $L_2 = PMe_3$ **(2.4)**, PEt_3 **(2.5)**, PPh_3 **(2.6)**, PCy_3 **(2.7)**, $P(OMe)_3$ **(2.8)**, or PCage **(2.9)**) (Scheme 3.2).

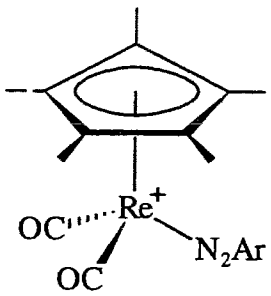

2.2

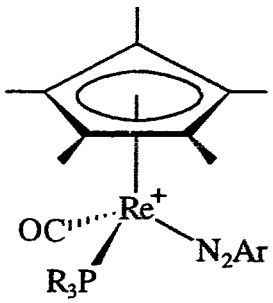

2.4-2.9

	PR_3
2.4	PMe_3
2.5	PEt_3
2.6	PPh_3
2.7	PCy_3
2.8	$P(OMe)_3$
2.9	PCage

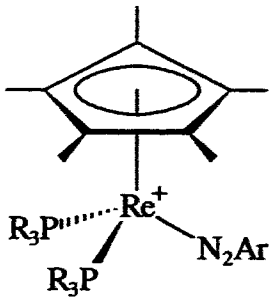

2.11 and 2.14

	PR_3
2.11	PMe_3
2.14	$P(OMe)_3$

Scheme 3.2. Structures of **2.2**, **2.4-2.9**, **2.11**, and **2.14** (Ar = *p*-C_6H_4OMe).

I show that these complexes have ground state structures in the solid state and in solution in which the aryldiazenido ligand does not orient with the NNC(aryl) plane bisecting the L_1ReL_2 angle, but lies with the aryl substituent oriented closer to one of the ligands L_1 or L_2; furthermore, interconversion between these structures can take place by a conformational isomerization of the aryldiazenido ligand illustrated schematically in Figure 3.1.

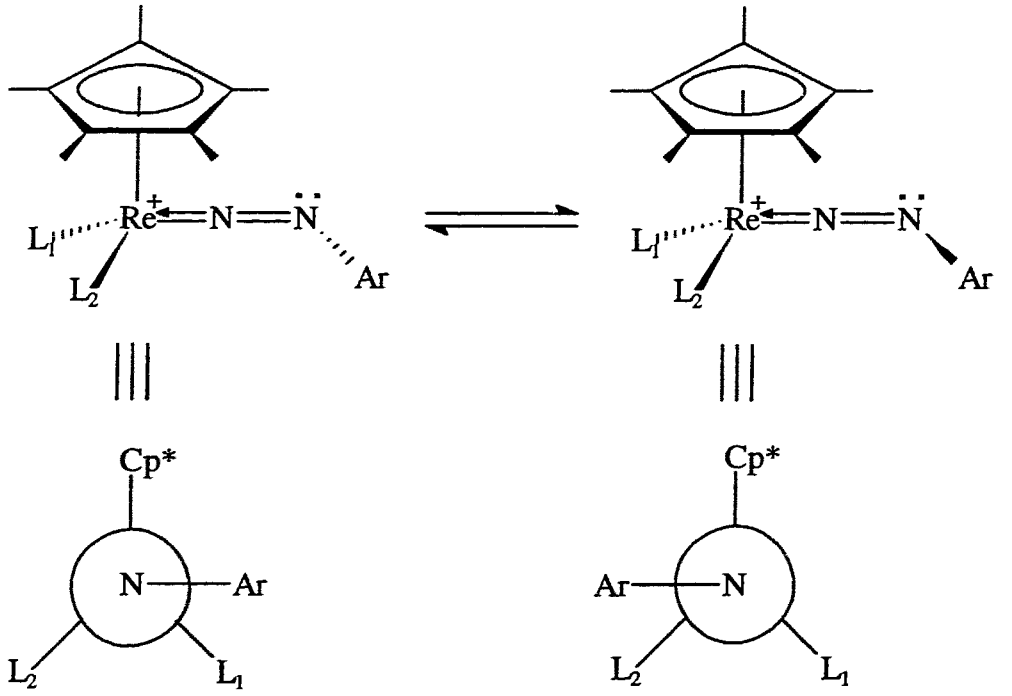

Figure 3.1. Newman projections of the idealized conformations of the complexes $[Cp^*Re(L_1)(L_2)(N_2Ar)]^+$ (Ar = *p*-C_6H_4OMe).

Thus, complexes of type (a), where $L_1 = L_2$, are 1:1 mixtures of the two possible enantiomers while those of type (b), where $L_1 \neq L_2$, are in principle mixtures of the two possible diastereomers along with their corresponding enantiomers arising from chirality at Re. The barriers to interconversion of the enantiomers in (a) or diastereomers in (b)

have been measured and the possible mechanisms for the reorientation of the stereochemically non-rigid aryldiazenido ligand in these complexes are discussed.

3.2. Results

3.2.1. X-ray Structure of [Cp*Re(CO)(PMe_3)(*p*-$N_2C_6H_4OMe$)][BF_4] (2.4)

The structure was solved with the intention of determining (i) how the geometrical details of this structure compare to previously determined rhenium aryldiazenido structures[86, 87] and (ii) the specific orientation or conformation adopted by the aryldiazenido ligand for a comparison with the solution behavior to be discussed, where chemically distinguishable structures are observed at low temperature.

The results of the X-ray structural analysis indicated disorder of the expected anion BF_4^- as well as a large excess of residual electron density at the boron atom site(s). This can be most reasonably explained by partial substitution of the BF_4^- ion with another anion such as I^- or perhaps ReO_4^-. Iodide was identified as the most reasonable anionic impurity, since it probably arises from PhIO used in the method of preparation and iodine was detected qualitatively by an X-ray fluorescence (XRF) analysis. Using a crystallographic model, the I^- occupancy was determined to be 5%.

The X-ray structure contains discrete molecular ions [Cp*Re(CO)(PMe_3)(*p*-$N_2C_6H_4OMe$)]$^+$ and BF_4^-/I^- (95/5). There are no interionic separations significantly less than the sums of the appropriate pairs of van der Waals radii. A perspective view of the cation is shown in Figure 3.2. The important geometrical details of the structure are given in Tables 3.1 and 3.2. As a point of interest, a pair of BF_4^- and I^- salts of the rhenium complex [Cp*Re$(CO)_2$(NO)]$^+$ were recently reported and their structures were also determined by X-ray crystallography.[88]

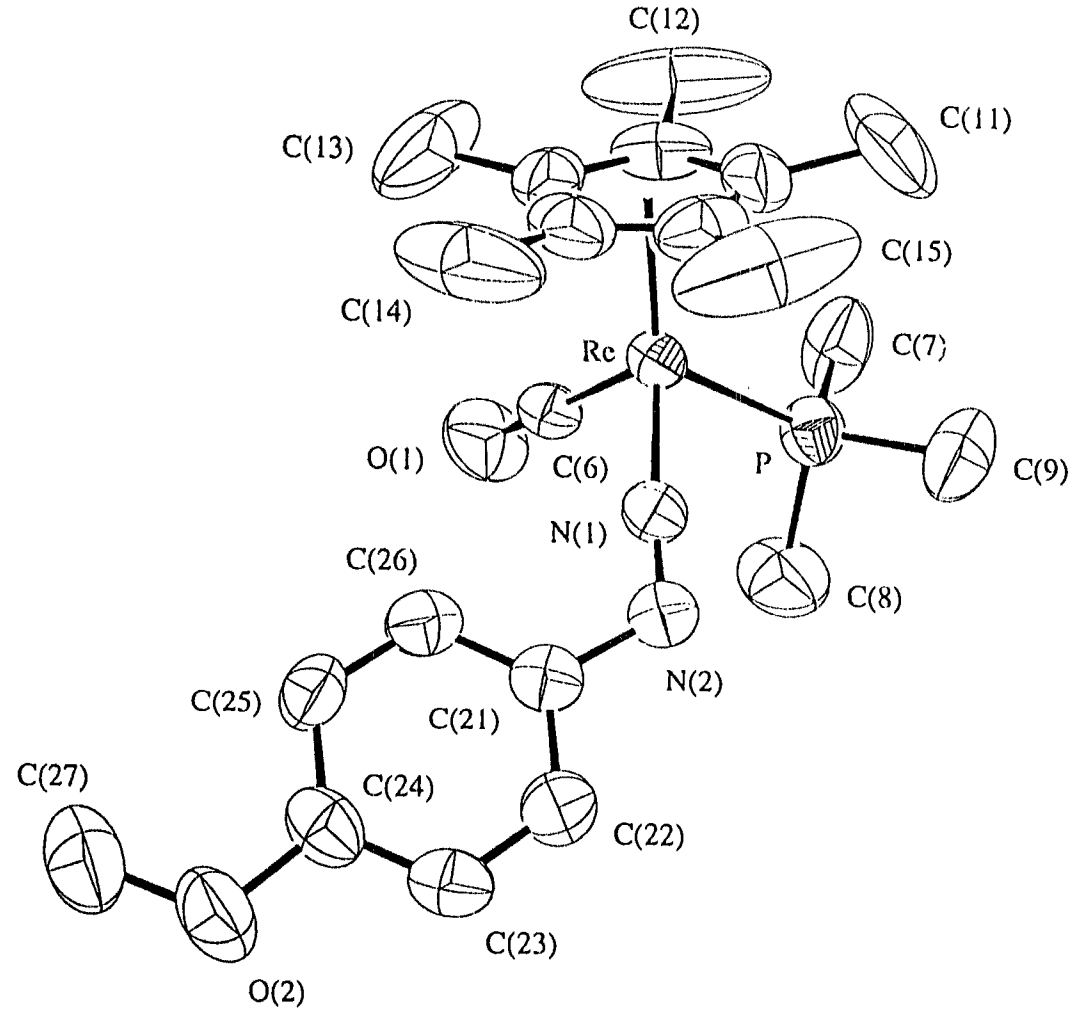

Figure 3.2. A perspective view of the structure of the cation $[Cp^*Re(CO)(PMe_3)(p\text{-}N_2C_6H_4OMe)]^+$ in **2.4**. Vibrational ellipsoids are drawn at the 50% probability level.

Table 3.1. Selected Geometrical Details for $[Cp^*Re(CO)(PMe_3)(p\text{-}N_2C_6H_4OMe)]^+$

Distances (Å)			
Re - P	2.388(2)	Re - C(5)	2.283(9)
Re - N(1)	1.816(6)	Re - Cp*	1.956
Re - C(1)	2.304(9)	Re - C(6)	1.912(9)
Re - C(2)	2.286(8)	P - C(7)	1.810(12)
Re - C(3)	2.281(8)	P - C(8)	1.805(11)
Re - C(4)	2.293(10)	P - C(9)	1.792(10)
O(1) - C(6)	1.154(10)	C(3) - C(4)	1.407(13)
O(2) - C(24)	1.376(9)	C(3) - C(13)	1.497(15)
O(2) - C(27)	1.412(13)	C(4) - C(5)	1.355(15)
N(i) - N(2)	1.209(8)	C(4) - C(14)	1.491(15)
N(2) - C(21)	1.443(10)	C(5) - C(15)	1.468(14)
C(1) - C(2)	1.409(14)	C(21) - C(22)	1.394(10)
C(1) - C(5)	1.412(16)	C(21) - C(26)	1.394(11)
C(1) - C(11)	1.501(15)	C(22) - C(23)	1.329(11)
C(2) - C(3)	1.412(14)	C(23) - C(24)	1.374(13)
C(2) - C(12)	1.515(12)	C(24) - C(25)	1.401(11)
		C(25) - C(26)	1.375(12)

Cp* denotes the center of mass of the five carbon atoms of the ring.

Table 3.2. Selected Geometrical Details for $[Cp^*Re(CO)(PMe_3)(p\text{-}N_2C_6H_4OMe)]^+$

Angles (°)			
N(1) - Re - P	90.3(2)	Cp* - Re - P	125.4
C(6) - Re - P	86.7(3)	Cp* - Re - N(1)	126.9
C(6) - Re - N(1)	93.3(3)	Cp* - Re - C(6)	123.0
C(7) - P - Re	117.5(4)	C(9) - P - Re	115.3(4)
C(8) - P - Re	111.6(4)	C(9) - P - C(7)	105.1(5)
C(8) - P - C(7)	105.5(7)	C(9) - P - C(8)	100.0(6)
C(27) - O(2) - C(24)	118.5(8)	C(4) - C(5) - C(1)	108.7(9)
N(2) - N(1) - Re	174.7(6)	C(15) - C(5) - C(1)	128.3(13)
C(21) - N(2) - N(1)	119.1(7)	C(15) - C(5) - C(4)	122.6(14)
C(5) - C(1) - C(2)	108.5(9)	O(1) - C(6) - Re	177.4(9)
C(11) - C(1) - C(2)	125.0(15)	C(22) - C(21) - N(2)	117.2(7)
C(11) - C(1) - C(5)	126.1(14)	C(26) - C(21) - N(2)	123.8(7)
C(3) - C(2) - C(1)	105.5(8)	C(26) - C(21) - C(22)	119.0(8)
C(12) - C(2) - C(1)	125.7(14)	C(23) - C(22) - C(21)	120.7(8)
C(12) - C(2) - C(3)	127.0(14)	C(24) - C(23) - C(22)	121.3(8)
C(4) - C(3) - C(2)	109.0(9)	C(23) - C(24) - O(2)	116.6(7)
C(13) - C(3) - C(2)	123.6(14)	C(25) - C(24) - O(2)	123.8(8)
C(13) - C(3) - C(4)	127.1(14)	C(25) - C(24) - C(23)	119.6(8)
C(5) - C(4) - C(3)	108.1(9)	C(26) - C(25) - C(24)	119.2(8)
C(14) - C(4) - C(3)	125.9(14)	C(25) - C(26) - C(21)	120.0(7)
C(14) - C(4) - C(5)	125.8(14)		

Cp* denotes the center of mass of the five carbon atoms of the ring.

The (*p*-methoxyphenyl)diazenido ligand in **2.4** adopts the singly-bent structure expected to be present from the ν(NN) value of 1678 cm^{-1} in the infrared spectrum and has reasonable values for the dimensions Re-N [1.816(6) Å], N-N [1.209(8) Å], Re-N-N [174.7(6)°], and N-N-C(aryl) [119.1(7)°]. These values are comparable to those determined for other singly-bent rhenium aryldiazenido structures already published. For example, $ReCl_2(N_2Ph)(PMe_2Ph)_3$[86a] has the dimensions Re-N [1.77(2) Å], N-N [1.23(2) Å], Re-N-N [173(2)°], and N-N-C(aryl) [119(2)°] and $ReBr_2(N_2Ph)(N_2HPh)(PPh_3)_2$[86b] has the geometrical details Re-N [1.793(11) Å], N-N [1.212(16) Å], Re-N-N [172.4(10)°], and N-N-C(aryl) [120.2(11)°]. Furthermore, the half-sandwich complex $CpRe(CO)(p\text{-}N_2C_6H_4Me)(AuPPh_3)$, the only other structurally determined example of a singly-bent rhenium aryldiazenido complex from our laboratory, has the following geometrical values:[87] Re-N [1.78(2) Å], N-N [1.27(2) Å], Re-N-N [171(1)°], and N-N-C(aryl) [119(1)°] and a ν(NN) value of 1612 cm^{-1}. These values are also comparable to the those obtained for structure **2.4**. The N-N bond length in complex **2.4** (1.209 Å) is much shorter than typical values of N-N single bonds, which are near 1.43 Å, and thus indicates the retention of significant multiple bond character in this bond. The short Re-N bond length in complex **2.4** (1.816 Å) indicates that this bond has some multiple bond character as well.

The most important piece of information provided by the X-ray structure of **2.4** is the specific orientation of the aryldiazenido ligand relative to the other co-ligands. From Figure 3.2 it is clear that complex **2.4** has a structure in which the aryldiazenido ligand does not orient "symmetrically", i.e., with the NNC (aryl) plane bisecting the L_1ReL_2 angle, but lies "unsymmetrically" with the aryl substituent oriented towards the carbonyl ligand. This is dramatically illustrated in Figure 3.3 which shows a view of the cation down the NNRe direction, i.e., essentially the view of a Newman projection in this direction.

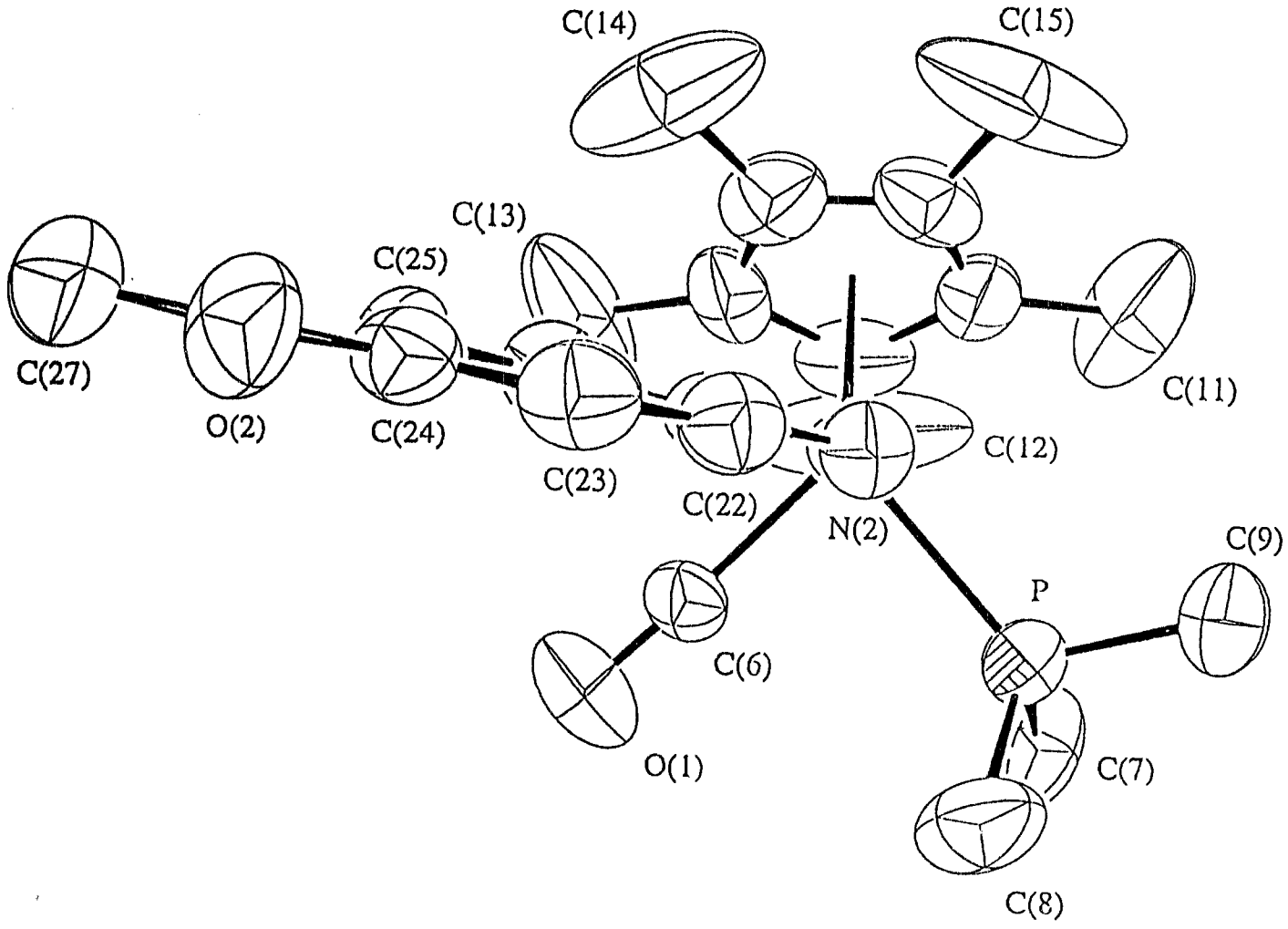

Figure 3.3. A view of the cation $[Cp^*Re(CO)(PMe_3)(p\text{-}N_2C_6H_4OMe)]^+$ in **2.4** down the NNRe direction, showing the orientation of the aryl ring.

In fact, the torsion angle with respect to the carbonyl co-ligand, defined by C(6)-Re-N(2)-C(21), is -56.0(4)° while the torsion angle with respect to the trimethylphosphine co-ligand represented by P-Re-N(2)-C(21) is -142.6(5)°. In addition, both the Re-N-N and the O-C(methoxy) fragments are approximately coplanar with the aryl ring, which suggests a degree of charge delocalization into this ring.

3.2.2. Dynamic NMR Spectroscopy of Bis(phosphorus-ligand) Complexes

The room temperature $^{31}P\{^{1}H\}$ NMR spectrum of $[Cp^*Re(PMe_3)_2(p\text{-}N_2C_6H_4OMe)][BF_4]$ (**2.11**) exhibited a single trimethylphosphine resonance at δ -43.28. However, a variable temperature $^{31}P\{^{1}H\}$ NMR study of **2.11** revealed that as the temperature was lowered the single resonance began to broaden, decoalesced (192 K), and then sharpened again at 183 K into two equal intensity resonances separated by a chemical shift difference (δν) of 217 Hz (Figure 3.4). The spectrum recorded at 183 K exhibited no apparent phosphorus-phosphorus coupling. This is the expected result if each signal results from different species, each of which possesses two magnetically equivalent phosphines, but it could also be consistent with a single species with magnetically inequivalent phosphine ligands, provided that $J_{P\text{-}P}$ is too small to be observed. The linewidth at half-peak-height for each of the ^{31}P resonances of **2.11** at 183 K is 69 Hz, therefore the magnitude of $J_{P\text{-}P}$ must be significantly smaller than this value. This is consistent with the literature[89] and with an example from our laboratory where phosphorus-phosphorus coupling has been observed for the cationic complex *cis*-$[Cp^*ReH(N_2)(PMe_3)_2][CF_3COO]$ which has a $J_{P\text{-}P}$ value of 48.6 Hz (see Chapter 6). The ^{1}H NMR spectrum of **2.11** showed no broadening of any of the proton resonances down to a temperature of 190 K.

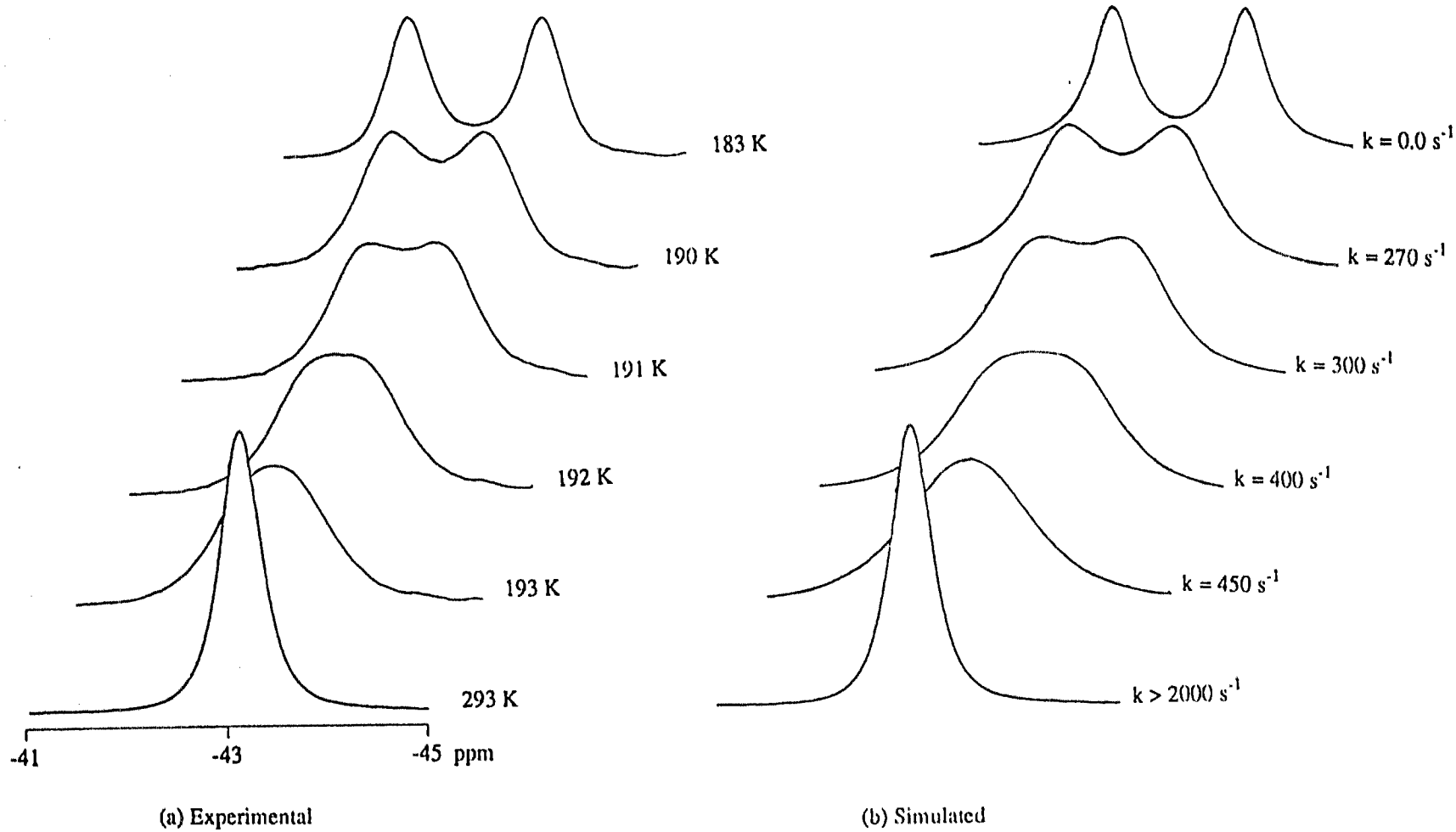

Figure 3.4. (a) Variable temperature $^{31}P\{^{1}H\}$ NMR spectra (162 MHz) of $[Cp^*Re(PMe_3)_2(p\text{-}N_2C_6H_4OMe)][BF_4]$ (**2.11**) in acetone-d_6. (b) Simulated spectra.

The bis-trimethylphosphite complex $[Cp^*Re\{P(OMe)_3\}_2(p\text{-}N_2C_6H_4OMe)][BF_4]$ **(2.14)** was also investigated by variable temperature $^{31}P\{^1H\}$ NMR spectroscopy and results similar to **2.11** were obtained. A room temperature $^{31}P\{^1H\}$ NMR spectrum of **2.14** showed a single resonance at δ 113.63. This began to broaden as the temperature was lowered, decoalesced at 180 K, and then separated into two equal intensity broad resonances at 173 K with a chemical shift difference (δν) of 1124 Hz. As was the case for **2.11**, the low temperature limit spectrum of **2.14** exhibited no phosphorus-phosphorus coupling. For **2.11** and **2.14**, a significant temperature-dependence of the chemical shifts was observed, and the dynamic NMR processes were confirmed to be reversible for both complexes. Attempts to collect spectra below 173 K were not successful because the NMR solvent (acetone-d_6) froze at this temperature. Attempts to use a solvent of lower freezing point suitable for NMR spectroscopy such as $CDFCl_2$ also proved unsuccessful since this solvent was unable to solubilize the cationic complexes.

3.2.3. Dynamic NMR Spectroscopy of Carbonyl Phosphine and Phosphite Complexes

The room temperature $^{31}P\{^1H\}$ NMR spectrum of $[Cp^*Re(CO)(PMe_3)(p\text{-}N_2C_6H_4OMe)][BF_4]$ **(2.4)** exhibited a single trimethylphosphine resonance at δ -28.23. As the temperature was lowered the single resonance began to broaden until the signal decoalesced into two unequally populated resonances at 185 K (Figure 3.5) which must be assigned to the presence of two stereoisomers (δ -27.01 for the major isomer and δ -27.77 for the minor isomer). Integration of both resonances at the low temperature limit gave a population of 95% for the major isomer and 5% for the minor isomer.

Similar results were also obtained for the phosphite complexes, $[Cp^*Re(CO)\{P(OMe)_3\}(p\text{-}N_2C_6H_4OMe)][BF_4]$ **(2.8)** and $[Cp^*Re(CO)\{P(OCH_2)_3CMe\}(p\text{-}N_2C_6H_4OMe)][BF_4]$ **(2.9)**.

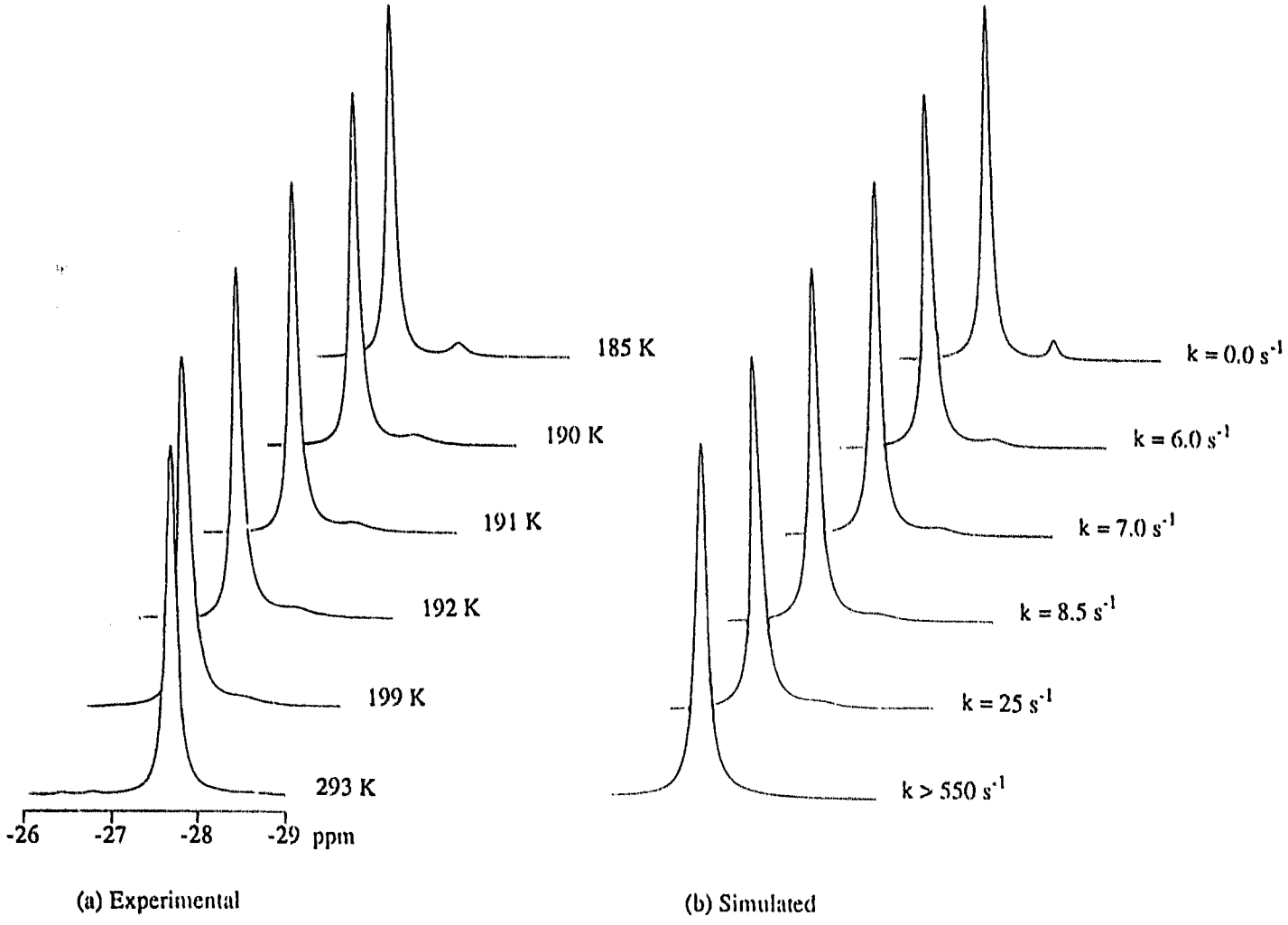

Figure 3.5. (a) Variable temperature $^{31}P\{^{1}H\}$ NMR spectra (162 MHz) of $[Cp^*Re(CO)(PMe_3)(p\text{-}N_2C_6H_4OMe)][BF_4]$ (**2.4**) in acetone-d_6. (b) Simulated spectra. Rates are reported for the isomerization process from the more populated to the less populated conformer.

A room temperature $^{31}P\{^{1}H\}$ NMR spectrum of **2.8** showed a single resonance at δ 110.35. This resonance began to broaden as the temperature was lowered, decoalesced, and then sharpened again into two unequal intensity resonances at 183 K assignable to two stereoisomers (δ 114.99 for the major isomer and δ 116.93 for the minor isomer). Integration of both resonances at the low temperature limit gave a population of 86% for the major isomer and 14% for the minor isomer. A room temperature $^{31}P\{^{1}H\}$ NMR spectrum of **2.9** also exhibited a single resonance at δ 104.40. The resonance began to broaden as the temperature was lowered, decoalesced, and then sharpened again into two unequal intensity resonances at 183 K assignable to two stereoisomers (δ 103.40 for the major isomer and δ 106.79 for the minor isomer). Integration of both resonances at the low temperature limit gave a population of 59% for the major isomer and 41% for the minor isomer. Once again, for **2.4**, **2.8**, and **2.9** a significant variation of the chemical shifts with temperature was observed, and the dynamic NMR processes were confirmed to be reversible.

Comparing the low temperature $^{31}P\{^{1}H\}$ spectra of complexes **2.4**, **2.8**, and **2.9**, it is clear that in **2.4** the major isomer is deshielded relative to the minor isomer whereas in **2.8** and **2.9** the major isomer is shielded with respect to the minor isomer. This result is most likely due to the paramagnetic component (σ_p) of the shielding constant which is the dominant term influencing changes in chemical shift for heavier nuclei such as phosphorus. Unfortunately, a complete understanding of how σ_p contributes to the ^{31}P NMR chemical shift of phosphorus nuclei in metal-phosphorus-ligand complexes has not yet been achieved.[90] Furthermore, the ratio of minor:major isomers for the complexes **2.4**, **2.8**, and **2.9**, as obtained from their respective low temperature $^{31}P\{^{1}H\}$ spectra, are 1:19, 1:6.1, and 1:1.4 respectively.

A room temperature $^{13}C\{^{1}H\}$ NMR spectrum of **2.8** also exhibited a single resonance for the carbon of the CO ligand. This single resonance also began to broaden

as the temperature was lowered and began to decoalesce at 185 K. Unfortunately, we were unable to decrease the temperature further to allow complete decoalescence to occur since the solution froze at 185 K. Although this experiment suggests that $^{13}C\{^1H\}$ NMR spectroscopy may be used to probe the isomerization process, $^{31}P\{^1H\}$ NMR spectroscopy is a better choice because ^{31}P is a more NMR sensitive nucleus, it can be used to monitor the isomerization process for both the carbonyl phosphorus-ligand complexes and bis(phosphorus-ligand) complexes, and complete decoalescence was attained within the low temperature limit of the NMR solvent (acetone-d_6).

In contrast with these results, the $^{31}P\{^1H\}$ NMR spectra of complexes **2.5-2.7**, where the phosphorus ligand is PEt_3, PPh_3, and PCy_3 respectively, showed the presence of only a single phosphine resonance in each case, with no evidence of broadening down to 185 K.

3.2.4. Determination of Rate Constants and Activation Parameters

The rate constants (k_c) for the conformational isomerization of the aryldiazenido ligand in the bis(phosphorus-ligand) complexes **2.11** and **2.14** were determined from the variable temperature $^{31}P\{^1H\}$ NMR studies. The k_c values for the interconversion in these uncoupled, equally populated, two-site systems were calculated using two different methods.

Using Equation 3.1 (generally referred to as the coalescence expression),[91] an approximate value for k_c (Table 3.3) was obtained for **2.11** and **2.14** at their respective temperatures of coalescence (T_c).

$$k_c = (\pi/2^{1/2})(\delta\nu) \qquad (3.1)$$

Table 3.3. Rate Constants (k_c) for Conformational Isomerization of the Aryldiazenido Ligand

Complex	Temperature (K)[a]	k_c (s^{-1})[b, c]	k_c (s^{-1})[d, e]
2.4	190	6.0 ± 0.2	115 ± 5
	191	7.0 ± 0.2	125 ± 5
	192	8.5 ± 0.5	145 ± 10
	193	10.0 ± 0.5	170 ± 10
	199	25 ± 1	410 ± 25
	210	110 ± 5	1475 ± 75
	223	550 ± 25	5875 ± 300
2.8	185	9.0 ± 0.5	61.0 ± 2.5
	190	19 ± 1	115 ± 5
	195	38 ± 2	225 ± 10
	197	55 ± 4	340 ± 20
	199	75 ± 5	470 ± 20
	210	325 ± 25	1525 ± 75
	223	1400 ± 100	7100 ± 400
2.9	188	45.0 ± 2.5	70 ± 5
	190	66 ± 4	95 ± 5
	193	90 ± 5	130 ± 10
	198	250 ± 20	330 ± 30
	203	500 ± 25	670 ± 50
	208	750 ± 50	1100 ± 100
	223	4000 ± 400	5800 ± 500
2.11	186	135 ± 5	
	190	270 ± 15	
	191	300 ± 20	
	T_c = 192	400 ± 25	482 ± 60
	193	450 ± 25	
	195	580 ± 30	
	198	860 ± 50	
	203	2000 ± 150	
2.14	175	975 ± 50	
	T_c = 180	2200 ± 100	2497 ± 200
	185	5100 ± 300	
	190	10000 ± 500	
	195	19000 ± 1000	
	200	30000 ± 2000	

[a] All errors in temperature are ± 1 K.

[b] Calculated from lineshape analysis for the isomerization process from the more populated to the less populated conformer for complexes **2.4**, **2.8**, and **2.9**.

[c] Calculated from lineshape analysis for **2.11** and **2.14**.

[d] Calculated from lineshape analysis for the isomerization process from the less populated to the more populated conformer for complexes **2.4**, **2.8**, and **2.9**.

[e] Calculated at T_c using Equation 3.1 for **2.11** and **2.14**.

This equation relates the rate constant to the difference in ^{31}P NMR peak separations ($\delta\nu$); the parameter $\delta\nu$ is generally extracted from the low temperature spectrum. The errors in the rate constant derived from k_c were determined from the errors associated with determining $\delta\nu$. An obvious disadvantage of Equation 3.1 is that the rate constant is obtained at only one temperature and thus kinetic comparisons between related complexes such as **2.11** and **2.14** are not meaningful unless the two complexes have the same temperature of coalescence; this is not the case for complexes **2.11** and **2.14**.

To overcome the shortcomings of Equation 3.1, rigorous lineshape analyses of the variable temperature $^{31}P\{^1H\}$ NMR spectra obtained for **2.11** and **2.14** were performed using the program *DNMR3*.[92] Rate constants were obtained for a number of temperatures (Table 3.3) by visual comparison of the experimental spectra with those calculated by *DNMR3* for various rates; the errors were considered to be the ranges in rates over which it was impossible to distinguish between the experimental and calculated spectra.

The rate constants for the conformational isomerization of the aryldiazenido group in the carbonyl phosphine and phosphite complexes **2.4**, **2.8**, and **2.9** were also determined from their variable temperature $^{31}P\{^1H\}$ NMR spectra using *DNMR3*. Because the interconversion in these complexes was between two unequally populated sites, k_c values were extracted for the isomerization process from the more populated to the less populated conformer as well as the reverse isomerization process (Table 3.3).

From the rate constants (k_c), activation parameters were calculated for complexes **2.4**, **2.8**, **2.9**, **2.11**, and **2.14** (Table 3.4). Values for the free energy of activation ($\Delta G^{\neq}$) were determined from the Eyring equation (Equation 3.2)[93] assuming a transmission coefficient of 1.

$$k_c = \kappa(K_B T/h)e^{(-\Delta G^{\neq})/RT} \qquad (3.2)$$

where κ = transmission coefficient

K_B = Boltzmann constant

h = Planck constant

R = Gas constant

T = Temperature

Table 3.4. Activation Parameters for Isomerization of the Aryldiazenido Ligand

Complex	$\Delta G^{\neq}$ (kJ/mol)	$\Delta H^{\neq}$ (kJ/mol)	$\Delta S^{\neq}$ (J/mol·K)	E_a (kJ/mol)	A ($x10^{13}$) (s^{-1})
2.4[a, c]	43.0 ± 0.4	46.5 ± 0.6	18.5 ± 2.8	48.2 ± 0.6	11.0 ± 8.0
2.4[b, c]	38.4 ± 0.4	40.7 ± 1.0	12.5 ± 4.6	42.4 ± 0.8	5.3 ± 2.6
2.8[a, c]	41.2 ± 0.4	44.3 ± 1.0	16.7 ± 5.6	46.0 ± 1.2	8.5 ± 4.8
2.8[b, c]	38.3 ± 0.4	41.4 ± 2.0	16.6 ± 10.2	43.0 ± 2.0	8.4 ± 8.0
2.9[a, c]	39.2 ± 0.6	43.8 ± 2.3	24.4 ± 11.8	46.5 ± 2.4	40.0 ± 31.0
2.9[b, c]	38.6 ± 0.6	43.0 ± 1.5	23.1 ± 7.4	44.7 ± 1.5	19.0 ± 8.0
2.11[c]	37.0 ± 0.6	47.3 ± 2.2	54.1 ± 18.0	48.9 ± 2.2	730 ± 720
2.11[d]	36.5 ± 0.4				
2.14[c]	31.4 ± 0.4	39.4 ± 2.4	42.3 ± 16.2	41.0 ± 2.4	180 ± 200
2.14[d]	31.6 ± 0.4				

[a] For the isomerization process from the more populated to the less populated conformer.

[b] For the isomerization process from the less populated to the more populated conformer.

[c] Values for $\Delta G^{\neq}$ are given for a temperature of 190 K.

[d] Values for $\Delta G^{\neq}$ are given for the respective coalescence temperatures, which are 192 K for **2.11** and 180 K for **2.14**.

Errors in the $\Delta G^{\neq}$ values were obtained by use of Equation 3.3 for the linearized relative statistical error.[94]

$$(\sigma\Delta G^{\neq}/\Delta G^{\neq})^2 = [\ln(k_BT/hk)]^{-2}(\sigma_k/k)^2 + \{1 + [\ln(k_BT/hk)]^{-1}\}^2(\sigma_T/T)^2 \qquad (3.3)$$

Values for the enthalpy of activation ($\Delta H^{\neq}$) and for the entropy of activation ($\Delta S^{\neq}$) were calculated from Equation 3.2 (substituting $\Delta H^{\neq} - T\Delta S^{\neq}$ for $\Delta G^{\neq}$), expressed as an equation of the form $y = a + bx$, by plotting a graph of $\ln(k_c/T)$ versus $1/T$ using a linear least-squares program.[95] An example of such a plot is shown in Figure 3.6 for complex **2.4**. Values for the activation energy (E_a) and the frequency factor (A) were determined from the Arrhenius equation (Equation 3.4)[93] by following the previous protocol and thus plotting a graph of $\ln k_c$ versus $1/T$ utilizing a linear least-squares program.[95] An example of the graphic application of the Arrhenius equation is presented in Figure 3.7 for complex **2.11**.

$$k_c = A*e^{(-E_a)/RT} \qquad (3.4)$$

where R = Gas constant

T = Temperature

Errors in $\Delta H^{\neq}$, $\Delta S^{\neq}$, E_a, and A were obtained from the standard deviations derived from the Eyring and Arrhenius plots multiplied by the appropriate statistical factor.[94]

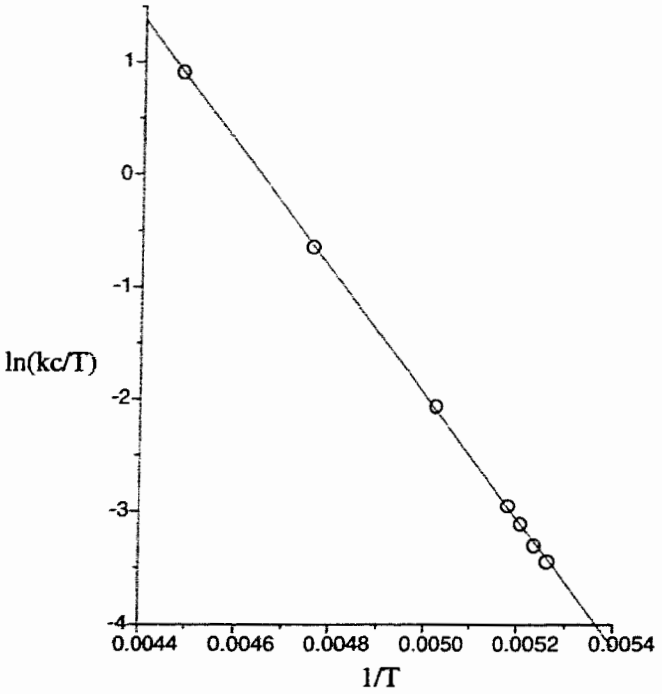

Figure 3.6. Eyring plot for the conformational isomerization of the aryldiazenido ligand in [Cp*Re(CO)(PMe_3)(*p*-$N_2C_6H_4OMe$)][BF_4] (**2.4**).

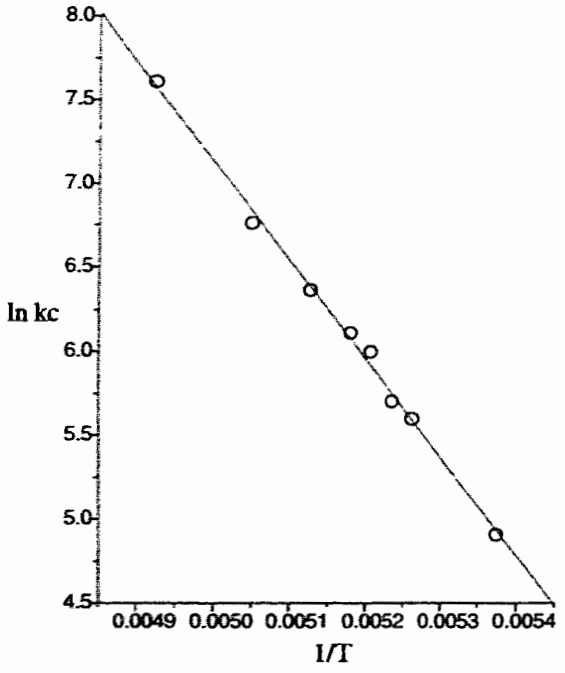

Figure 3.7. Arrhenius plot for the conformational isomerization of the aryldiazenido ligand in [Cp*Re(PMe_3)$_2$(*p*-$N_2C_6H_4OMe$)][BF_4] (**2.11**).

3.3. Discussion

3.3.1. The Aryldiazenido Ligand: Conformational Preference

Although there have been numerous X-ray structure determinations of complexes with singly-bent aryldiazenido ligands,[96] rather scant attention has been paid to evaluating the conformational preference adopted by this ligand with respect to the co-ligands. The X-ray structure of the carbonyl phosphine complex **2.4** is consistent with the suggestion that the steric properties of the ancillary ligands Cp*, CO, and PMe_3 contribute to the orientation of the rhenium aryldiazenido fragment. The aryl ring is virtually coplanar with the NNRe backbone, and is situated as shown in the Newman projection in Figure 3.3. The conformer observed is represented by structure **3.1**, which is sterically less congested than the conformer depicted by structure **3.2** (which places the aryl ring adjacent to the sterically larger PMe_3 ligand) (Scheme 3.3). The observed dihedral angle, as defined by Cp*(centroid)-Re-N(2)-C(21), is 82°. An inspection of the stereochemistry of the aryldiazenido ligand as revealed by the X-ray structures of other 3-legged piano-stool complexes related to **2.4** indicates that this type of unsymmetrical orientation of the aryldiazenido ligand commonly prevails. Examples include $CpMo(CO)(PPh_3)(p\text{-}N_2C_6H_4Me)$,[97] $[CpMo(NO)(PPh_3)(p\text{-}N_2C_6H_4F)]^+$,[97] and $CpRe(CO)(AuPPh_3)(p\text{-}N_2C_6H_4OMe)$.[87]

To gain a better understanding into the conformational preference adopted by the aryldiazenido ligand in the complexes mentioned above, the X-ray structures of half-sandwich aryldiazenido complexes containing two identical co-ligands were examined. It was of interest to see what orientation the aryldiazenido ligand would adopt in complexes which were not sterically predisposed as a result of the different co-ligands (as was perhaps the case in the carbonyl phosphine complex **2.4**).

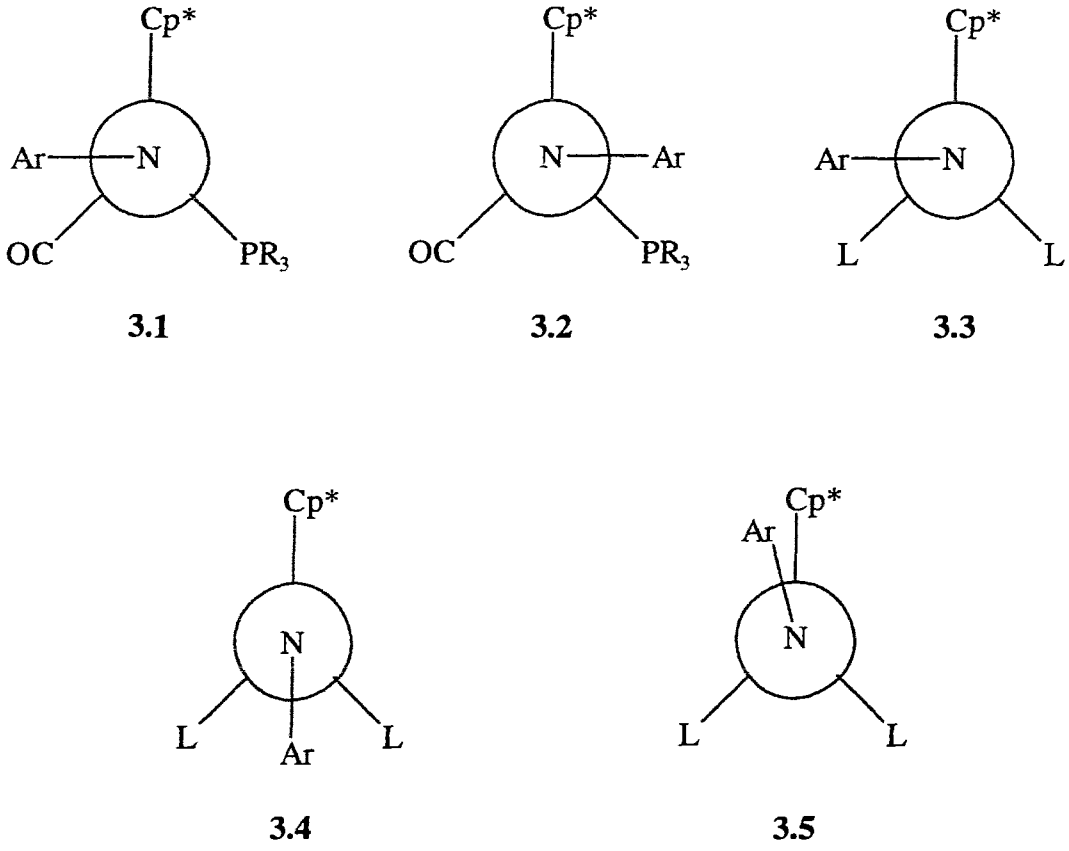

Scheme 3.3. Structural representations of the plausible conformers resulting from the orientation adopted by the aryldiazenido ligand.

Although no X-ray structures were obtained for the dicarbonyl or the bis(phosphorus-ligand) rhenium complexes $[Cp^*Re(L_1)(L_2)(p\text{-}N_2C_6H_4OMe)]^+$ ($L_1 = L_2 = CO$ or PR_3), the structure[98] of the manganese complex $[(\eta^5\text{-}C_5H_4Me)Mn(CO)_2(o\text{-}N_2C_6H_4CF_3)][BF_4]$ has been reported. The Newman projection viewed down the MnNN axis (Figure 3.8) clearly shows that the aryl ring of the aryldiazenido ligand is coplanar with the NNMn backbone (as was also the case for complex **2.4**) as depicted by structure **3.3** (Scheme 3.3). The observed dihedral angle, as defined by MeCp(centroid)-Mn-N-N-C(aryl), is 95°. Similar results were found for the related molybdenum dicarbonyl complex $HB(pz)_3Mo(CO)_2(N_2Ph)$.[99]

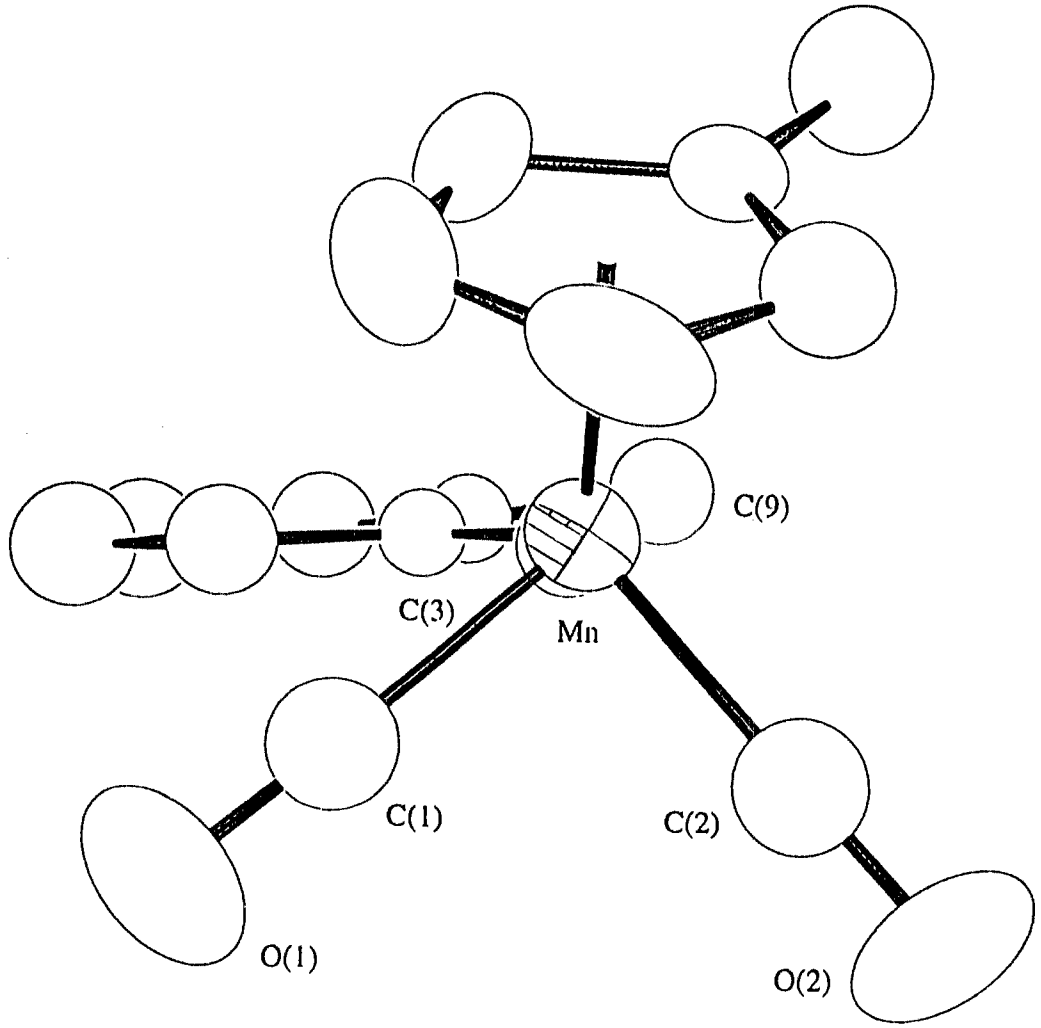

Figure 3.8. A view of the cation $[(\eta^5\text{-}C_5H_4Me)Mn(CO)_2(o\text{-}N_2C_6H_4CF_3)]^+$ down the NNMn direction, showing the orientation of the aryl ring. Vibrational ellipsoids are drawn at the 50% probability level.

These observations infer that the stereochemistry of the aryldiazenido ligand in these complexes may be influenced by electronic, as well as steric factors. Furthermore, that there is a stereoelectronic preference is vividly illustrated by the X-ray structure of $[Cp^*Ir(C_2H_4)(N_2Ar)]^+$ (Ar = *p*-C_6H_4OMe), where the IrNN(aryl) plane does not lie in the plane defined by the iridium and centroids of the Cp* and C_2H_4 ligands, but bisects it and thus destroys the mirror symmetry. As a consequence, the aryl group makes a closer approach to one ethylene carbon than the other.[100]

To summarize, examination of the X-ray structures of numerous metal aryldiazenido complexes, in all cases, show a ground state structure in which the aryl ring of the aryldiazenido group lies unsymmetrically, as shown in structures **3.1** or **3.3** (Scheme 3.3), with the plane of the aryl ring approximately coplanar with the NNM backbone. In addition, this stereochemical preference appears to be electronically as well as sterically driven.

3.3.2. Temperature-dependence of the $^{31}P\{^1H\}$ NMR Spectra for the Aryldiazenido Complexes

As described previously, the room temperature $^{31}P\{^1H\}$ NMR spectrum of the symmetrically phosphorus-substituted complex $[Cp^*Re(PMe_3)_2(p\text{-}N_2C_6H_4OMe)][BF_4]$ **(2.11)** exhibited only a single phosphorus resonance. The trimethylphosphite complex **2.14** behaved similarly. One possible explanation for this would be a ground state structure **3.4** in which the PR_3 ligands are made equivalent by virtue of the aryldiazenido ligand adopting a position on the mirror plane containing the Cp* centroid and Re, and bisecting the angle subtended by the two PR_3 ligands (Scheme 3.3). However, this possibility contradicts the observed X-ray structure for **2.4** as well as the X-ray structures of related complexes just presented, and is not consistent with the variable temperature $^{31}P\{^1H\}$ NMR spectra.

An alternative explanation which I believe to be correct is that the room temperature spectrum arises from a fast interconversion of the unsymmetrical structure illustrated in **3.3** with its enantiomer, as was shown in Figure 1. This readily explains the variable temperature $^{31}P\{^{1}H\}$ NMR spectra, where, at the low temperature limit two equal intensity ^{31}P resonances were observed and subsequently assigned to the inequivalent phosphine or phosphite groups in configuration **3.3** (L = PMe_3 or $P(OMe)_3$). However, each ^{31}P resonance should have appeared as one half of an AB quartet. It was mentioned in the Results section that at the lowest temperature achieved, the expected $J_{P\text{-}P}$ coupling was not observed (perhaps being obscured, since the resonances were still exchange broadened). The expected AB quartet has been observed in comparable examples, such as a related iron vinylidene complex for which $J_{P\text{-}P}$ had the value 42 Hz.[89]

There are other possibilities to consider. One is interconversion of **3.3** with the symmetrical conformer **3.4**. This cannot alone be responsible for the observed temperature-dependence for two reasons. First, the pathways from **3.4** to both **3.3** and its enantiomer are equivalent, so that if **3.4** equilibrates with **3.3** it also must have an equal probability of equilibrating with the enantiomer of **3.3** and therefore these enantiomers are themselves interconverting. Second, **3.4** cannot be significantly populated at the low temperature, otherwise a separate resonance for the equivalent PMe_3 ligands of **3.4** should be observed in addition to the two equal intensity resonances for **3.3**. Thus, while the interconversion of **3.3** and its enantiomer may possibly proceed by way of rotamer **3.4** (see discussion of possible mechanisms below) it is not plausible to account for the NMR behavior simply by interconversion of rotamers **3.3** and **3.4**. A second possibility (that also would readily account for the absence of P-P coupling) is that the low temperature resonances arise from the two conformers where the plane of the aryldiazenido group lies in the mirror plane of the Cp^*ReL_2 fragment and the aryl ring is either down, as illustrated by structure **3.4**, or up as depicted by structure **3.5** (Scheme

3.3). I consider this implausible for two reasons. First, it would be highly unlikely that these two conformers would be equally populated and give rise to the observed equal intensity resonances; second, molecular modelling calculations using *PCMODEL*[101] show that eclipsed conformations such as **3.5** do not correspond to minima.

To gain further insight into the isomerization process which had been established with the bis(phosphorus-ligand) complexes, the investigation was extended to include the carbonyl phosphorus-ligand complexes **2.4-2.9**. In the case of the mono-substituted complexes [Cp*Re(CO)(PMe_3)(*p*-$N_2C_6H_4OMe$)][BF_4] (**2.4**), [Cp*Re(CO){$P(OMe)_3$}(*p*-$N_2C_6H_4OMe$)][BF_4] (**2.8**), and [Cp*Re(CO){$P(OCH_2)_3CMe$}(*p*-$N_2C_6H_4OMe$)][BF_4] (**2.9**) again a single $^{31}P\{^1H\}$ NMR resonance was observed at room temperature, but the low temperature spectrum consisted of two resonances that differed considerably in intensity (Figure 3.5). Precedents in the literature suggests that if there is a strong preference for one conformer in solution, the molecular conformation observed in the crystal usually dominates in solution.[102] Thus, using the carbonyl trimethylphosphine complex **2.4** as an example, it is reasonable to assign the major resonance at 185 K to conformer **3.1**, i.e., the conformer observed in the X-ray structure. The minor conformer cannot be assigned unambiguously. It could be the rotamer **3.4**, but since we have argued above that, for the bis-PMe_3 complex **2.11** this conformer cannot be significantly populated, this possibility is unlikely. More probable is that the minor resonance arises from conformer **3.2** where the aryl ring of the aryldiazenido ligand occupies the sterically less favorable position adjacent to the PMe_3 group. The single ^{31}P resonance observed at room temperature then results from rapid interconversion of diastereomers **3.1** and **3.2**. Analogous conformers are proposed for two *isolable* geometric isomers in the case of the related vinylidene complex [CpRe(NO)(PPh_3)(=C=CHPh)]$^+$, which are present at equilibrium in solution in a 4:1 ratio.[103] Notably, as with the bis(phosphorus-ligand) complexes, the conformations where the aryldiazenido ligand eclipses either the Cp*,

CO, or the PR_3 co-ligands are rejected, since they do not correspond to minima, as indicated by molecular modelling calculations using *PCMODEL*.[101]

Furthermore, and of utmost importance, the differences in the minor:major isomer ratios for complexes **2.4**, **2.8**, and **2.9** are seen to reflect the differing steric demand of the phosphorus ligands and support assigning the minor and major isomers to **3.2** and **3.1** respectively. The ratio was found to be 1:19 for the PMe_3 complex **2.4**, 1:6.1 for the $P(OMe)_3$ derivative **2.8**, and 1:1.4 for the PCage derivative **2.9**. The larger conformational preference shown for **2.4** is reduced when PMe_3 is replaced by the less sterically demanding ligand $P(OMe)_3$ and reduced further when PMe_3 is substituted by PCage (the cone angles of PMe_3, $P(OMe)_3$, and PCage are 118°, 107°, and 101° respectively)[68] and as a result the population of the minor conformer is increased for **2.8** and is greatest for **2.9**.

In principle, ^1H Nuclear Overhauser Enhancement (NOE) spectroscopy might be considered as a suitable technique to assign the major and minor conformers in complexes **2.4**, **2.8**, and **2.9**. However, it is not feasible since variable temperature ^1H NMR spectroscopy indicated no apparent decoalescence of the aryl ring or ligand proton resonances into the necessary unique sets.

If interconverting diastereomers **3.1** and **3.2** are present in solution for **2.4** (and similarly for **2.8**, and **2.9**), it might be possible to detect these by IR spectroscopy in view of its shorter timescale when compared to NMR spectroscopy. We carefully examined the ν(CO) and ν(NN) absorptions for **2.4**, **2.8**, and **2.9** both for solution (CH_2Cl_2) and solid state (KBr) room temperature spectra, but in all cases these appeared to be single absorptions. Reasons for this could be the preponderance of one diastereomer, or small and unresolvable differences in the ν(CO) and ν(NN) values for each diastereomer.

It should be noted that the results from the dynamic $^{31}P\{^1H\}$ NMR study of **2.4**, **2.8**, and **2.9** indicate the presence of two diastereomers, where each diastereomer is

responsible for one ^{31}P resonance at 185 K. Each diastereomer is actually comprised of two enantiomers, arising from chirality at Re, which are indistinguishable from each other by NMR spectroscopy. Formation of the enantiomers arises from the method of synthesis, i.e., there is equal probability of removing either one of the two carbonyl co-ligands in complex **2.2** during the synthesis of complexes **2.4-2.9**.

The triethylphosphine (carbonyl), triphenylphosphine (carbonyl) and tricyclohexylphosphine (carbonyl) complexes **2.5**, **2.6**, and **2.7** respectively, were also investigated by variable temperature $^{31}P\{^1H\}$ NMR spectroscopy. Complexes **2.5**, **2.6**, and **2.7** were chosen because triethylphosphine (cone angle = 132°),[68] triphenylphosphine (cone angle = 145°),[68] and tricyclohexylphosphine (cone angle = 170°)[68] are sterically larger ligands than PMe_3, $P(OMe)_3$, or PCage, and PEt_3 and PCy_3 have similar electronic properties to PMe_3 but varying size. Variable temperature $^{31}P\{^1H\}$ NMR spectra of **2.5**, **2.6**, and **2.7** indicated no decoalescence of the single phosphorus resonance observed at room temperature even down to *ca.* 183 K.

To summarize, the bis(phosphorus-ligand) complexes $[Cp^*Re(PR_3)_2(p\text{-}N_2C_6H_4OMe)][BF_4]$ ($PR_3 = PMe_3$ (**2.11**) and $P(OMe)_3$ (**2.14**)) exhibited a single ^{31}P resonance at room temperature which decoalesced into two equally populated resonances at low temperature. The carbonyl phosphorus-ligand complexes $[Cp^*Re(CO)(PR_3)(p\text{-}N_2C_6H_4OMe)][BF_4]$ ($PR_3 = PMe_3$ (**2.4**), PEt_3 (**2.5**), PPh_3 (**2.6**), PCy_3 (**2.7**), $P(OMe)_3$ (**2.8**), and PCage (**2.9**)), in all cases, exhibited a single ^{31}P resonance at room temperature, but only for the ones with the smallest cone angle, i.e., **2.4**, **2.8**, and **2.9**, could separate low temperature resonances for the major and minor stereoisomers be observed. The failure to observe this in the case of the remainder could possibly be due to a lower temperature of decoalescence in these cases. However, as is clearly illustrated by the minor:major isomer ratios from the low temperature $^{31}P\{^1H\}$ NMR spectra for **2.4**, **2.8**, and **2.9**, the population of the minor conformer decreases as

the cone angle of the phosphorus ligand increases on going from PCage to $P(OMe)_3$ to PMe_3. Therefore, it is more likely that in **2.5-2.7** the crowded conformer **3.2** is not significantly populated and the observed resonance is essentially that of the uncrowded conformer **3.1**.

Interestingly, the variable temperature $^{13}C\{^1H\}$ NMR spectrum of the dicarbonyl complex $[Cp^*Re(CO)_2(p\text{-}N_2C_6H_4OMe)][BF_4]$ (**2.2**), which exhibited a single carbonyl resonance at room temperature, showed no decoalescence of the carbonyl signal even down to a temperature of 173 K. Unlike complexes **2.4-2.9** which have a sterically demanding phosphorus co-ligand, the two carbonyl co-ligands of complex **2.2** offer little if any steric contribution to the orientation of the aryldiazenido substituent. Although no X-ray structure of **2.2** has been obtained, it was pointed out in the previous section that the structure of the related Mn complex $[(\eta^5\text{-}C_5H_4Me)Mn(CO)_2(o\text{-}N_2C_6H_4CF_3)][BF_4]$ shows that the two CO groups are indeed inequivalent as a result of the unsymmetrical orientation of the aryldiazenido group (Figure 3.8).[98] The rhenium complex **2.2** is expected to be entirely similar. Furthermore, as will be addressed in the discussion which follows, the energies of activation for conformational isomerization of the aryldiazenido ligand are larger for complexes whose ligands are good σ-electron donors and poor π-electron acceptors (i.e., **2.11** > **2.14** and **2.4** > **2.8** or **2.9**). With this in mind it is reasoned that the room temperature $^{13}C\{^1H\}$ NMR spectrum of **2.2** arises from a fast interconversion (Figure 3.1) of the unsymmetrical structure illustrated in **3.3** (L = CO) with its enantiomer (as was postulated for complexes **2.11** and **2.14**) and that the static spectrum is not achieved even at 173 K perhaps because of a small ^{13}C chemical shift difference in the individual CO resonances, or, more likely as a result of a very low activation barrier. A similar explanation would account for the apparently equivalent MeCN ligands in the ^1H and $^{13}C\{^1H\}$ NMR spectra of the bis-acetonitrile complexes **2.10** and **2.16** (see Chapter 2). Furthermore, this explanation is also in keeping with the

findings reported for the related methyldiazenido complex $CpW(CO)_2(N_2Me)$ where it was observed that the CO groups, which were shown to be inequivalent in the X-ray structure, exhibited only a single CO resonance in the ambient temperature ^{13}C NMR spectrum.[104]

3.3.3. Activation Parameters for Conformational Isomerization of the Aryldiazenido Ligand

From the dynamic $^{31}P\{^1H\}$ NMR investigation, the activation parameters for the isomerization of the aryldiazenido ligand in complexes **2.4**, **2.8**, **2.9**, **2.11**, and **2.14** were determined and are summarized in Table 3.4. Values of $\Delta G^{\neq}$ for the bis(phosphorus-ligand) complexes **2.11** and **2.14** were determined initially at their respective coalescence temperatures. For the bis-PMe_3 complex **2.11**, $\Delta G^{\neq}_{Tc}$ was calculated to be 36.5 ± 0.4 kJ/mole at 192 K while a value for $\Delta G^{\neq}_{Tc}$ of 31.6 ± 0.4 kJ/mole at 180 K was determined for the bis-$P(OMe)_3$ complex **2.14**. These results indicate that the energy of activation for the isomerization of the aryldiazenido ligand is raised when the co-ligands are both trimethylphosphine instead of trimethylphosphite. This statement is made with caution since it is recognized that the $\Delta G^{\neq}_{Tc}$ values for complexes **2.11** and **2.14** were calculated at different coalescence temperatures. However, these energy of activation values for **2.11** and **2.14** are sufficiently different that a qualitative comparison is still likely to be meaningful.[94a] The lineshape analysis substantiates this. The observed and simulated spectra for **2.11** are shown in Figure 3.4. For the bis-PMe_3 complex **2.11**, $\Delta G^{\neq}_{190}$ was calculated to be 37.0 ± 0.6 kJ/mole, whereas for the bis-$P(OMe)_3$ complex **2.14**, $\Delta G^{\neq}_{190}$ was 31.4 ± 0.4 kJ/mole. These values are consistent, within experimental error, with the energies of activation calculated for **2.11** and **2.14** using the temperature of coalescence approximation, and taken together these results indicate that the energy of activation is raised by *ca.* 5 kJ upon substituting $P(OMe)_3$ by PMe_3.

For complexes **2.4**, **2.8**, and **2.9**, where the interconverting diastereomers have unequal populations, the rate constants were determined from the lineshape analysis for the interconversion from the more populated conformer to the less populated conformer, and for the reverse direction (Table 3.3). The observed and simulated spectra for **2.4** are shown in Figure 3.5. The values of $\Delta G^{\neq}$ for the isomerization process (major isomer to minor isomer) for the carbonyl phosphine and phosphite complexes **2.4**, **2.8**, and **2.9** were found to be 43.0 ± 0.4, 41.2 ± 0.4, and 39.2 ± 0.6 kJ/mole respectively at 190 K. The trimethylphosphine ligand again evidently causes a small increase in the energy of activation compared with either phosphite, but less than the *ca.* 5 kJ difference observed for the bis-trimethylphosphine and bis-trimethylphosphite complexes **2.11** and **2.14** at the same temperature. The data, though limited, indicate a higher energy of activation for the better σ-donor (and poorer π-acceptor) PMe_3 ligand.

The two unequally populated ground state conformers in **2.4**, **2.8**, or **2.9** give rise to two different values of $\Delta G^{\neq}$ for the interconversion processes which correspond to the kinetic energy of activation for conversion of major to minor isomer and for minor to major isomer. The difference in $\Delta G^{\neq}$ for these forward and reverse interconversions equals $\Delta G°$. The $\Delta G°$ value obtained in this fashion was then compared to the $\Delta G°$ value determined from the relative populations of the major and minor isomers at the low temperature limit and these were found to be in complete agreement within experimental error (Table 3.5). (Note: this comparison was done as a check to assure that the program *DNMR3* was being used correctly).

Table 3.5. Comparison of $\Delta G°$ Values Determined from Lineshape Analysis and from Equilibrium Populations

Complex	Temperature (K)	$\Delta G°$ (kJ/mol)
2.4	190	4.6 ± 0.8^a
2.4	190	4.7 ± 0.8^b
2.8	190	2.9 ± 0.8^a
2.8	190	2.9 ± 0.8^b
2.9	190	0.6 ± 1.2^a
2.9	190	0.6 ± 1.2^b

[a] From lineshape analysis.
[b] From equilibrium populations.

It is apparent that the entropy of activation terms ($\Delta S^{\neq}$) for the interconversion process are of comparable magnitudes, and are small positive values, indicative of an intramolecular exchange (Table 3.4).[105] Several reliable examples of positive values for $\Delta S^{\neq}$ have been reported in the literature for intramolecular processes in organometallic complexes.[106] It is believed that different interactions with the solvent in the ground and excited states is responsible for these positive entropy of activation values.[93, 107] If the transition state is significantly less polar than the ground state then interactions with polar solvent molecules will be diminished, resulting in a decreased order in the solvent cage around the molecule in the transition state and thus an appreciable positive value for $\Delta S^{\neq}$.

The variation of the $^{31}P\{^1H\}$ NMR chemical shift with temperature for complexes **2.4**, **2.8**, **2.9**, **2.11**, and **2.14** was mentioned previously. The temperature-dependence of chemical shifts in the literature has been explained in terms of changes in fast rotamer equilibria and in solute-solute and/or solute-solvent interactions.[108] The positive values

for $\Delta S^{\neq}$ and the considerable temperature-dependence observed here are therefore consistent with solvent (acetone-d_6) interactions with these complexes and the positive $\Delta S^{\neq}$ values are indicative of fewer solvent-complex interactions in the transition state. To justify this explanation for positive $\Delta S^{\neq}$ values requires the solvent-dependence exhibited by the variable temperature $^{31}P\{^1H\}$ NMR spectra to be studied, especially using a nonpolar solvent. Unfortunately, these are all cationic complexes and are not soluble in nonpolar solvents. To conclude, although the $\Delta S^{\neq}$ values support an intramolecular exchange process, they do not distinguish between different possible intramolecular mechanisms for isomerization.

Further support for an intramolecular isomerization process is provided by a series of competition experiments. The carbonyl trimethylphosphine complex $[Cp^*Re(CO)(PMe_3)(p\text{-}N_2C_6H_4OMe)][BF_4]$ (**2.4**) was examined in acetone-d_6 for dissociative exchange in the presence of excess $P(OMe)_3$ by ^1H NMR. A spectrum of this solution acquired after 24 h indicated no substitution of PMe_3 in **2.4** by $P(OMe)_3$. Furthermore, the ^1H NMR spectrum obtained after this solution was refluxed for 4 h, also showed only the resonances corresponding to complex **2.4** and excess trimethylphosphite. Analogous results were obtained when this procedure was repeated for $[Cp^*Re(CO)\{P(OMe)_3\}(p\text{-}N_2C_6H_4OMe)][BF_4]$ (**2.8**) in the presence of excess PMe_3.

3.3.4. Conformational Isomerization of the Aryldiazenido Ligand

Despite the numerous singly-bent aryldiazenido complexes that have been synthesized and characterized, there has been remarkably little note taken of whether the aryldiazenido ligand adopts a rigid structure and orientation with respect to the co-ligands, or whether it readily undergoes some kind of rearrangement. Indeed, there are very few cases where the reported data allow examination of this feature. For example, it has been mentioned that the CO groups are inequivalent in the X-ray structure of

$[(\eta^5\text{-}C_5H_4Me)Mn(CO)_2(o\text{-}N_2C_6H_4CF_3)]^+$ as a result of the orientation of the aryldiazenido ligand, yet whether or not the expected two CO resonances occur is not known since the ^{13}C NMR spectrum has not been reported.[98] Furthermore, the bis(phenyldiazenido) complex $[(acac)Mo(OCH_3)(N_2Ph)_2]_2$ has been isolated and crystallographically characterized in two isomeric forms in which two of the N_2Ph ligands are mutually either *syn* or *anti*. These isomers interconvert in solution, and a conformational isomerization of the phenyldiazenido ligand was suggested to be responsible.[109] A variable temperature ^1H NMR study resulted in a value of $\Delta G^{\neq} = 57 \pm 1$ kJ/mole (at $T_c = 280$ K) for the energy of activation. It was suggested that this value was in the region of the energy of activation for restricted rotation about a partial double bond. Isomers resulting from bis(aryldiazenido) ligands have been discussed in other cases.[110] Instances where stereochemical non-rigidity of the angular singly-bent aryldiazenido ligand seems to have been automatically assumed (though not commented upon) in interpreting solution NMR data have also been found. In one example, there are more equivalent Mo and oxo sites by ^{95}Mo and ^{17}O NMR spectroscopy in $[Mo_6O_{18}(NNPh)]^{3-}$ than the static structure would predict.[111] In another, although there is no plane of symmetry equating equatorial dimethyldithiocarbamate (dtc) ligands in the X-ray structure of $[Mo(dtc)_3(N_2Ph)]$, nevertheless these methyl groups are pairwise equivalent in the room temperature NMR spectrum.[112] For the complexes in this study, we have been able to obtain direct NMR evidence for the stereochemical non-rigidity of the aryldiazenido group and have been able to observe the slowed-exchange conditions in particular examples.

The two possible mechanisms that must be considered for the conformational isomerization of the aryldiazenido ligand are (i) an sp^2 nitrogen inversion at N_β, sometimes called a lateral shift mechanism, or (ii) a restricted rotation around the Re-N-N axis. These are illustrated in Scheme 3.4.

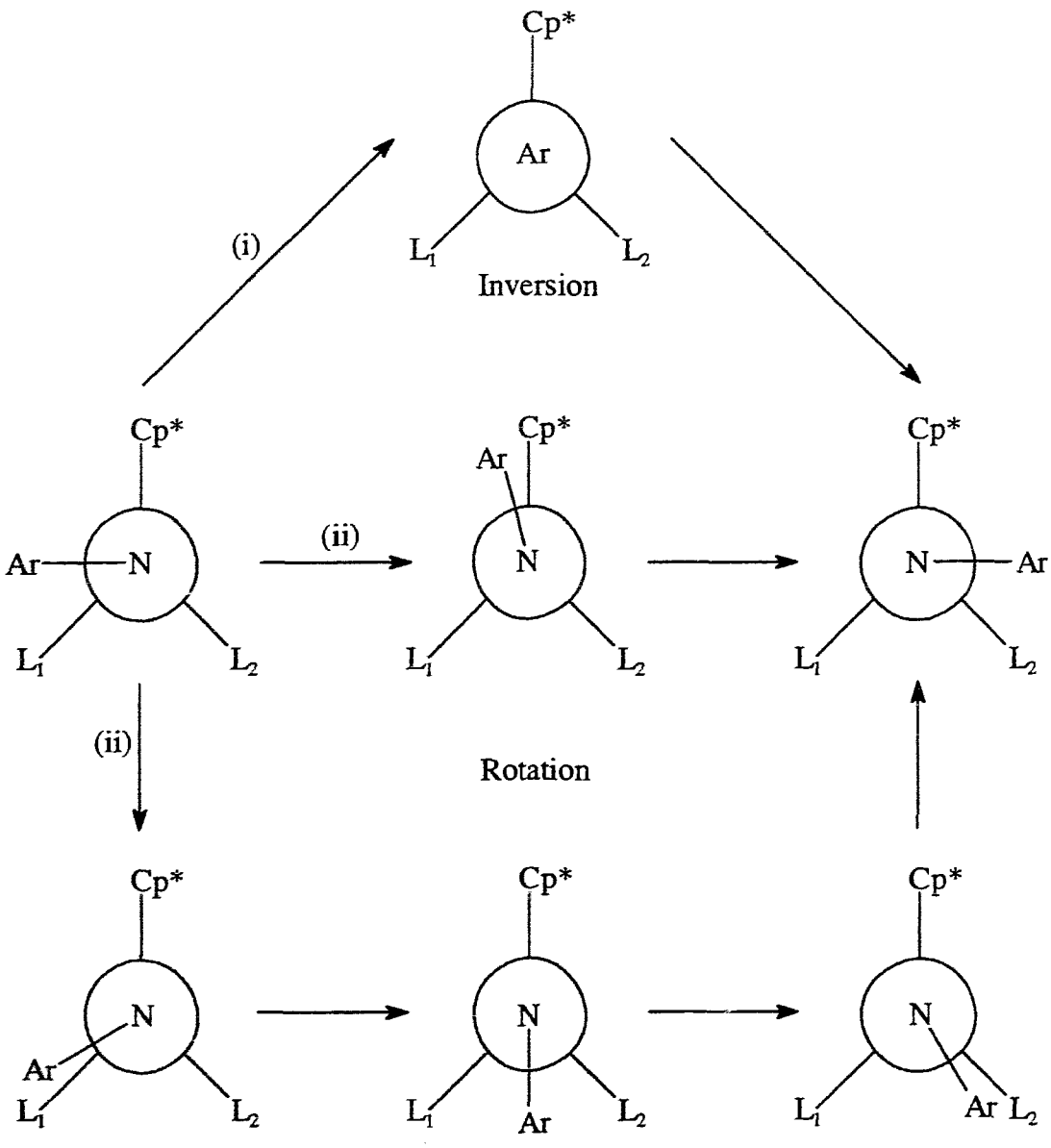

Scheme 3.4. Plausible mechanistic pathways for the conformational isomerization of the aryldiazenido ligand: (i) sp^2 nitrogen inversion at N_β or (ii) restricted rotation around the Re-N-N axis.

Even in the evidently much simpler cases of organic Schiff bases or imines (R_2C=NPh) the prevailing mechanism of isomerization has been much debated.[113] For an unactivated imine such as Me_2C=NPh, $\Delta G^{\neq}$ is approximately 88 kJ/mole.[114] This corresponds reasonably well to the calculated energy of activation for a lateral shift mechanism, whereas that for rotation about the C=N double bond is about twice as large.[115] It therefore seems to be generally thought that the lateral shift mechanism operates in simple unactivated imines. However, the presence of substituent heteroatoms on the imino carbon atom can lower the energy of activation dramatically, and rotation about the C=N bond (of reduced bond order) becomes dominant.[113] Conversely, the presence of a phenyl group on the imino nitrogen is expected to act to stabilize the transition state for the lateral shift mechanism.[113]

Phenyl-substituted vinylidene (M=C=CHPh) and linear azavinylidene (M=N=CHPh) ligands are interesting systems with which to compare the energy of activation for the singly-bent phenyldiazenido ligand (M=N=NPh). In these, of course, it would appear that rotation is the only possible isomerization mechanism (but see subsequent discussion of azavinylidene). The energy of activation in the Gladysz et al. rhenium vinylidene complex $[CpRe(NO)(PPh_3)(=C=CHPh)]^+$ ($\Delta G^{\neq}$ = 92 kJ/mole at 298 K) is very similar to that for the corresponding alkylidene complex $[CpRe(NO)(PPh_3)(=CHPh)]^+$ despite the expectation that steric hindrance to rotation of the more remote phenyl group in the former might be significantly less.[103] To the best of my knowledge, this is the only vinylidene system for which geometric isomers have been isolated. Energies of activation for rotation are generally much lower in other vinylidene complexes. For example, $\Delta G^{\neq}$ = 38-42 kJ/mole has been estimated for [CpFe(diphosphine)(=C=CHPh)]$^+$.[89] Turning to the azavinylidene ligand, the energy of activation has been measured recently for some tungsten hydridotris(3,5-dimethylpyrazolylborate) (Tp') complexes of the type $Tp'W(CO)_2$(=N=CHR).[116] For R =

n-Pr, a value of $\Delta G^{\neq} = 40.2$ kJ/mole at 193 K was obtained, but for the complex with R = Ph the energy of activation is presumably smaller since, while spectral broadening was observed, decoalescence could not be achieved down to 168 K. A low energy of activation, and consequently only averaged NMR spectra have been reported for other azavinylidene complexes.[117, 118] It has been suggested that low energies of activation may be the result of isomerization of the azavinylidene ligand to a nonlinear structure in which the nitrogen is sp^2-hybridized.[117] However, the energy of activation in $Cp_2ZrCl(=N=CHPh)$ may be very high, since geometric isomerization could not be achieved thermally or photochemically.[117]

It is clear from the above comparisons that even the rotational energies of activation for linear metallocumulene ligands of this type can cover a wide range, and show significant dependence on such variables as the metal, its *d*-electron configuration and row in the periodic table, the number and nature of the co-ligands, and the geometry of the complex. Therefore, with only the limited data that we have presently accumulated in this study for the much more complex case of the aryldiazenido ligand, it would be premature to venture an opinion at this time as to whether this ligand isomerizes by way of rotation or inversion in these rhenium complexes. Nevertheless, it is notable that the energies of activation we observe are extremely low in comparison to the closest analog presently available, i.e., the *rotation* energy of activation for the Gladysz et al. rhenium nitrosyl vinylidene complex[103] and thus the suggestion that the more facile *inversion* process may be the operative mechanism is an intriguing one.

3.4. Conclusion

In this chapter we have demonstrated that the rhenium half-sandwich complexes $[Cp^*Re(L_1)(L_2)(p\text{-}N_2C_6H_4OMe)][BF_4]$ ((a) $L_1 = L_2 = CO$ (**2.2**), PMe_3 (**2.11**), or $P(OMe)_3$ (**2.14**) and (b) $L_1 = CO$; $L_2 = PMe_3$ (**2.4**), PEt_3 (**2.5**), PPh_3 (**2.6**), PCy_3 (**2.7**), $P(OMe)_3$

(**2.8**), or PCage (**2.9**)) have ground state structures in which the aryl ring of the singly-bent aryldiazenido ligand orients with its molecular plane orthogonal to the plane bisecting the L_1ReL_2 angle. This conformational preference adopted by the aryldiazenido ligand is based on the results of a variable temperature ^1H, $^{31}P\{^1H\}$, and $^{13}C\{^1H\}$ NMR study of complexes **2.2**, **2.4-2.9**, **2.11**, and **2.14** as well as on X-ray structural analyses of complex **2.4** and related complexes. Furthermore, the aryldiazenido ligand is capable of undergoing a conformational isomerization which interconverts the conformer in which the aryl group is oriented towards L_1 with its enantiomer (or diastereomer) in which it is oriented towards L_2. The relative populations of the two conformers were examined in selected examples, and the barriers to isomerization were measured.

3.5. Experimental

3.5.1. General Methods and Syntheses

Manipulations, solvent purification, and routine spectroscopic measurements were carried out as described in Chapter 2. The cationic rhenium aryldiazenido complexes which were investigated in this chapter were prepared and purified following the procedures detailed in Chapter 2.

The deuterated solvents used for NMR spectroscopy were degassed prior to use to remove any residual oxygen. ^{31}P NMR chemical shifts are referenced to external 85% H_3PO_4.

X-ray fluorescence (XRF) spectroscopy was accomplished with a Kevex Corporation system utilizing a molybdenum secondary target.

Hexane and dichloromethane, which were used to grow X-ray quality crystals of complex **2.4**, were purified and dried by conventional methods, distilled under nitrogen, and used immediately.

3.5.2. X-ray Structure of [Cp*Re(CO)(PMe_3)(*p*-$N_2C_6H_4OMe$)][BF_4] (2.4)

X-ray quality crystals of **2.4** proved difficult to grow initially as the complex had a tendency to oil out of solution. This problem was overcome by dissolving **2.4** in a minimum amount of CH_2Cl_2; the solution was then cooled to 195 K and an excess of hexane was then slowly layered over the CH_2Cl_2 to achieve a distinct solution-solvent interface. The solution was warmed to 263 K and allowed to intermix for 24 h. At the end of this time, block-like red crystals of **2.4** suitable for X-ray crystallography had formed.

The crystal structure analysis of **2.4** reported in this chapter was determined by Professor F. W. B. Einstein and Dr. R. J. Batchelor at Simon Fraser University.

3.5.3. Variable Temperature NMR and Lineshape Analysis

The variable temperature ^1H, $^{31}P\{^1H\}$, and $^{13}C\{^1H\}$ NMR spectra of complexes **2.2**, **2.4-2.9**, **2.11**, and **2.14** were recorded at 400, 162, and 100 MHz respectively on a Bruker AMX 400 instrument equipped with a B-VT 1000 variable temperature unit. A cooling unit containing liquid nitrogen and a heater coil was attached to the NMR probe and was used to attain the desired temperature. The NMR sample, in a 5 mm tube, was allowed to equilibrate for 30 min at the desired temperature prior to acquisition of the spectra. A Bruker single frequency probe was used to obtain the ^1H and $^{13}C\{^1H\}$ spectra. A Bruker tunable broad band probe was used to acquire the $^{31}P\{^1H\}$ spectra. Acetone-d_6 (Isotec Inc.) was used as the solvent for all the low temperature NMR work and spectra were obtained at decreasing temperatures until the solution froze.

Temperatures, which were obtained directly from the VT unit, were checked by measuring peak separations for a standard Bruker sealed sample of methanol and converting these into temperature values using the quadratic equation of Van Geet[119] for methanol. Temperature gradients within the sample region of the AMX 400 spectrometer are considered to be negligible because of the large distance between the cooling unit and the probe; temperatures are accurate to ±1 K. Chemical shifts in the exchange-broadened region were derived from a linear extrapolation[95] of the values obtained at the higher temperatures; this procedure resulted in excellent matching of the experimental and calculated chemical shifts. Linewidths were found to be unchanged at the slow and fast exchange limits and were assumed to be temperature invariant. Calculation of simulated lineshapes was performed by use of a slightly modified version of the program *DNMR3*.[92]

CHAPTER 4

Investigation of the Formation of Ligated Dinitrogen from Rhenium-bound Aryldiazenido

4.1. Introduction

The first examples of rhenium dinitrogen complexes were reported in 1969 by Chatt et al.[120] These octahedral rhenium (I) dinitrogen complexes *trans*-$ReCl(N_2)(dppe)_2$, *trans*-$ReCl(N_2)(PMe_2Ph)_4$, and *trans*-$ReCl(N_2)(PPh_3)_2(PF_3)_2$ were prepared by the degradation of the chelated benzoyldiazenido complex $ReCl_2(PPh_3)_2(N_2COPh)$ (Scheme 4.1).

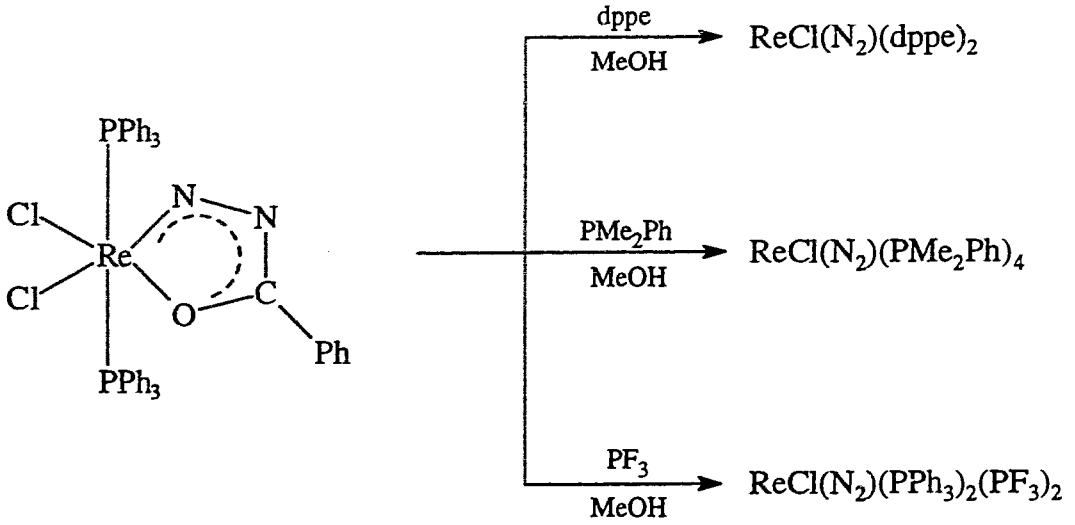

Scheme 4.1. Synthetic route to rhenium dinitrogen complexes developed by Chatt et al.[120]

The production of methylbenzoate in the reactions illustrated in Scheme 4.1 suggested that nucleophilic attack of methanol or methoxide ion on the carbonyl carbon atom may

be involved in the production of the dinitrogen complexes.[121] Unfortunately, the mechanistic details have as yet to be ascertained.

Since the initial discovery by Chatt et al., numerous dinitrogen complexes of rhenium have been prepared *via* many different routes. For example, the rhenium hydrido dinitrogen complex $ReH(N_2)(dppe)_2$ resulted from the reaction of the ammonium salt $[NH_4]_2[ReH_9]$ with two equivalents of dppe in 2-propanol under an atmosphere of dinitrogen.[122] Furthermore, the half-sandwich rhenium dinitrogen complex $CpRe(CO)_2(N_2)$ was synthesized by controlled oxidation of the corresponding hydrazine complex $CpRe(CO)_2(N_2H_4)$ with H_2O_2 in the presence of copper (II) salts[123] or by displacement of the labile THF ligand in $CpRe(CO)_2(THF)$ by dinitrogen under high pressure.[124]

Despite these synthetic accomplishments the original Chatt synthesis remained, for more than a decade, the only example in which an organodiazenido ligand was transformed into a dinitrogen ligand. However, it was observed several years ago by co-workers in our laboratory that the aryldiazenido ligand in the cationic manganese complex $[(\eta^5\text{-}C_5H_4Me)Mn(CO)_2(N_2Ar)]^+$ was converted into ligated dinitrogen by I^-, Br^-, or Cl^- to yield the neutral complex $(\eta^5\text{-}C_5H_4Me)Mn(CO)_2(N_2)$;[98] the only other product formed during the reaction was the respective substituted arene IAr, BrAr, and ClAr. The limited available experimental evidence obtained for these reactions was consistent with a nucleophilic displacement mechanism.

Interestingly, identical results were not obtained when these nucleophilic addition reactions were repeated with the analogous cationic aryldiazenido complexes of rhenium. For example, reaction of the rhenium aryldiazenido complex $[CpRe(CO)_2(p\text{-}N_2C_6H_4OMe)]^+$ with I^- gave not only the expected dinitrogen complex $CpRe(CO)_2(N_2)$, but the known diiodo complex $CpRe(CO)_2I_2$ as well.[125] Treatment of the rhenium aryldiazenido complex with Br^- yielded the dinitrogen complex, the corresponding

dibromo complex $CpRe(CO)_2Br_2$,[126] and the carbonyl substituted complex $CpReBr(CO)(p\text{-}N_2C_6H_4OMe)$. GC-MS analysis of the reaction mixtures resulting from these halide ion additions showed in each case the presence of the respective iodo and bromo arene compounds (IC_6H_4OMe or BrC_6H_4OMe) as well as the formation of anisole (C_6H_5OMe). Using Cl^- as the reagent produced only the carbonyl substituted complex $CpReCl(CO)(p\text{-}N_2C_6H_4OMe)$; the dichloro derivative $CpRe(CO)_2Cl_2$ and the dinitrogen complex were not formed. Furthermore, the reaction of the halide ion X^- ($X^- = I^-$, Br^-, or Cl^-) with the pentamethylcyclopentadienyl analog $[Cp^*Re(CO)_2(p\text{-}N_2C_6H_4OMe)]^+$ yielded in all cases the respective carbonyl substituted complex $Cp^*ReX(CO)(p\text{-}N_2C_6H_4OMe)$ exclusively with no production of the expected dinitrogen complex.[57] These results, unlike those obtained for the related manganese complexes, could not be explained by invoking solely a nucleophilic displacement mechanism, but instead were suggestive of a competitive radical process.

It was clear from the synthetic results just presented that the chemistry associated with the conversion of the aryldiazenido ligand to the dinitrogen ligand, especially at a rhenium metal center, was complex and warranted further investigation. Subsequently, a novel general route to a wide variety of rhenium dinitrogen complexes has now been developed, the details of which are described in this chapter. It is shown that chemical or electrochemical reduction of the cationic rhenium arydiazenido complexes generates the corresponding neutral dinitrogen complexes of the type $Cp'Re(L_1)(L_2)(N_2)$ ((a) Cp' = Cp; $L_1 = L_2 = CO$ **(4.1)**,[123, 124] (b) Cp' = Cp*; $L_1 = CO$; $L_2 = PMe_3$ **(4.3)**[59] or $P(OMe)_3$ **(4.4)**,[59] and (c) Cp' = Cp*; $L_1 = L_2 = CO$ **(4.2)**,[59] PMe_3 **(4.5)**, dmpe **(4.6)**, or $P(OMe)_3$ **(4.7)**) (Scheme 4.2) cleanly, quickly, and in high yield. Furthermore, the mechanism of this conversion was investigated by cyclic voltammetry, scanning electrochemical microscopy, and controlled potential electrolysis. These findings are also given in this chapter.

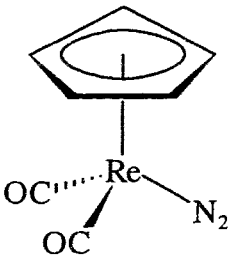

4.1

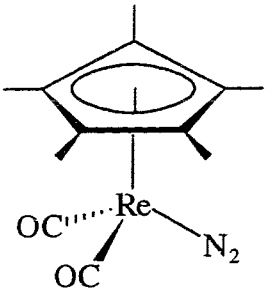

4.2

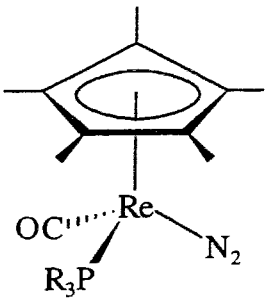

4.3 and **4.4**

	PR_3
4.3	PMe_3
4.4	$P(OMe)_3$

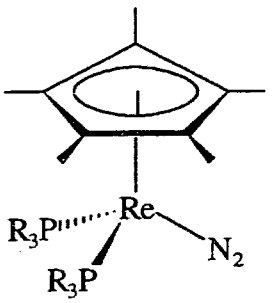

4.5 and **4.7**

	PR_3
4.5	PMe_3
4.7	$P(OMe)_3$

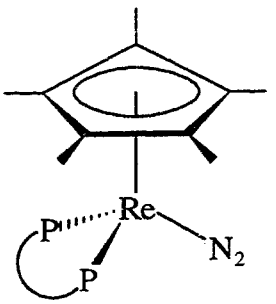

4.6

Scheme 4.2. Structures of **4.1-4.7**.

4.2. Results

4.2.1. Synthesis and Characterization of Dinitrogen Complexes

The dinitrogen complexes of general formula $Cp'Re(L_1)(L_2)(N_2)$ ((a) Cp' = Cp; $L_1 = L_2 = CO$ (**4.1**),[123, 124] (b) Cp' = Cp*; L_1 = CO; $L_2 = PMe_3$ (**4.3**)[59] or $P(OMe)_3$ (**4.4**),[59] and (c) Cp' = Cp*; $L_1 = L_2 = CO$ (**4.2**),[59] PMe_3 (**4.5**), dmpe (**4.6**), or $P(OMe)_3$ (**4.7**)) (Scheme 4.2) were synthesized by reacting the respective cationic aryldiazenido complex with a variety of reagents. For example, addition of excess $NaBH_4$ as a solid to a solution of the cationic dicarbonyl aryldiazenido complex $[Cp^*Re(CO)_2(p\text{-}N_2C_6H_4OMe)][BF_4]$ (**2.2**) in methanol or acetone resulted in the immediate formation of a deep red solution. After several minutes the color of the solution changed from red to yellow and this color change was accompanied by the production of the dinitrogen complex **4.2**. Reactions of **2.2** with hexamethylphosphoramide (HMPA), trimethylphosphine, or sodium metal also afforded the dinitrogen complex **4.2**.

The cationic dicarbonyl aryldiazenido complexes $[Cp'Re(CO)_2(p\text{-}N_2C_6H_4OMe)][BF_4]$ (Cp' = Cp (**2.1**) or Cp* (**2.2**)) were also converted to the corresponding neutral dinitrogen complexes **4.1** and **4.2** at room temperature by reaction with a THF solution containing an excess of the triphenylmethyl radical ($Ph_3C\cdot$) or with an acetone solution containing excess cobaltocene (Cp_2Co). The Cp_2Co reactions resulted in the instantaneous formation of the respective dinitrogen complexes in excellent yield. Furthermore, the neutral carbonyl trimethylphosphite dinitrogen complex $Cp^*Re(CO)\{P(OMe)_3\}(N_2)$ (**4.4**) was also synthesized from the corresponding cationic aryldiazenido complex **2.8** by reaction with excess Cp_2Co in acetone at room temperature. However, none of the reagents previously mentioned, including Cp_2Co, were capable of converting the cationic aryldiazenido complexes $[Cp^*Re(CO)(PMe_3)(p\text{-}N_2C_6H_4OMe)][BF_4]$ (**2.4**), $[Cp^*Re(PR_3)_2(p\text{-}N_2C_6H_4OMe)][BF_4]$ ($PR_3 = PMe_3$ (**2.11**) or

$P(OMe)_3$ (**2.14**)), or [Cp*Re(dmpe)(*p*-$N_2C_6H_4OMe$)][BF_4] (**2.13**) to their respective neutral dinitrogen complexes **4.3** and **4.5-4.7**. Instead, these dinitrogen complexes were synthesized by treatment of a solution of the corresponding aryldiazenido complex in THF with sodium amalgam at room temperature.

The dinitrogen complexes **4.1-4.7** were obtained as pale yellow solids analytically and spectroscopically pure, and were very soluble in the majority of organic solvents.

From the IR spectra of the dinitrogen complexes **4.1-4.7**, recorded in hexane, ν(NN) was observed as a strong absorption in the 2145-1975 cm^{-1} region (Table 4.1). The assignment of ν(NN) was confirmed by ^{15}N isotopic substitution at the rhenium-bound nitrogen atom (N_α) in **4.1-4.5**. In all cases an isotopic shift to lower wavenumber by *ca.* 33 cm^{-1} was observed for ν(NN). This ^{15}N isotopic shift is similar to that observed for the rhodium dinitrogen complex $RhCl(P^iPr_3)_2(N_2)$ [$\Delta\nu(NN) = 35\ cm^{-1}$].[127]

The dicarbonyl dinitrogen complexes **4.1** and **4.2** each exhibit two very strong ν(CO) absorptions, as expected, at 1973, 1919 and 1954, 1902 cm^{-1} respectively in hexane (Table 4.1). The IR spectra of the carbonyl phosphine and phosphite complexes **4.3** and **4.4**, recorded in hexane, showed a single, very strong absorption at 1865 and 1877 cm^{-1} respectively for ν(CO) (Table 4.1).

The ^1H NMR spectra for complexes **4.1-4.4** exhibited the typical resonances expected for the Cp, Cp*, and phosphorus groups. The only observation of note was that the Cp* resonance in the carbonyl phosphine and phosphite complexes **4.3** and **4.4** was split into a doublet with $J_{H\text{-}P}$ couplings of 0.7 and 0.8 Hz respectively, which supports the presence of a single phosphorus ligand in these complexes (Table 4.1). For complexes **4.5-4.7**, the ^1H NMR spectra showed some notable features. The Cp* resonance for both the bis-trimethylphosphine dinitrogen complex **4.5** and for the bis-trimethylphosphite dinitrogen complex **4.7** appeared as a triplet indicating that the Cp* methyls were observably coupled to two equivalent phosphorus ligands (Table 4.1).

Table 4.1. IR, ^{1}H, $^{31}P\{^{1}H\}$, and $^{13}C\{^{1}H\}$ NMR Data for the Dinitrogen Complexes

Complex	IR (cm^{-1})[a]	^{1}H NMR δ(Cp*)[b]	$^{31}P\{^{1}H\}$ NMR[c]	$^{13}C\{^{1}H\}$ NMR δ(CO)[b]
4.1	2145 ν(NN); 1973, 1919 ν(CO)	5.23 s		195.79 s
4.1-$^{15}N_{\alpha}$	2110 ν(NN); 1973, 1919 ν(CO)			
4.2	2125 ν(NN); 1954, 1902 ν(CO)	2.09 s		200.09 s
4.2-$^{15}N_{\alpha}$	2092 ν(NN); 1954, 1902 ν(CO)			
4.3	2044 ν(NN); 1865 ν(CO)	2.00 d (J = 0.7)	-29.86	207.18 d (J = 7)
4.3-$^{15}N_{\alpha}$	2011 ν(NN); 1865 ν(CO)			
4.4	2078, 2066 ν(NN); 1877 ν(CO)	2.04 d (J = 0.8)	139.12	204.96 d (J = 12)
4.4-$^{15}N_{\alpha}$	2045, 2033 ν(NN); 1877 ν(CO)			
4.5	1975 ν(NN)	1.88 t (J = 0.7)	-35.31	
4.5-$^{15}N_{\alpha}$	1943 ν(NN)			
4.5-$^{15}N_{\beta}$	1943 ν(NN)			
4.6	1977 ν(NN)	1.92 s	-16.88	
4.7	2014 ν(NN)	1.87 t (J = 0.8)	138.80	

[a] In hexane.
[b] In $CDCl_3$ for **4.1-4.4** and acetone-d_6 for **4.5-4.7**; referenced to TMS; J given in Hz; δ given in ppm.
[c] In $CDCl_3$ for **4.1-4.4** and acetone-d_6 for **4.5-4.7**; referenced to 85% H_3PO_4; δ given in ppm.

Interestingly, for the bidentate phosphine dinitrogen complex **4.6** only a singlet Cp* resonance was observed from the ^1H NMR spectra (Table 4.1). In **4.5** and **4.7** the J_{H-P} couplings were determined to be 0.7 and 0.8 Hz respectively, and may be too small to be observed for **4.6**. Furthermore, the ^1H NMR spectrum of **4.6** exhibited the typical resonances expected for the bidentate dmpe ligand. However, in **4.5** the ^1H resonance at δ 1.48 assigned to the PMe_3 ligands was observed to be a virtual doublet integrating to 18 protons. The apparent coupling constant ($^2J_{H-P} + {}^4J_{H-P}$), given by the separation between the two outside peaks, was 7.4 Hz. In **4.7** the ^1H resonance at δ 3.45 assigned to the $P(OMe)_3$ ligands was also observed to be a virtual doublet integrating to 18 protons with a coupling constant ($^3J_{H-P} + {}^5J_{H-P}$) of 11.5 Hz.

The $^{31}P\{^1H\}$ NMR spectra of complexes **4.3-4.7**, in each case, displayed a single resonance in the normal region for a coordinated phosphine or phosphite (Table 4.1). These results are also in agreement with the suggestion made previously from the ^1H NMR spectra of **4.5** and **4.7** that the phosphorus ligand in these bis(phosphorus-ligand) complexes are equivalent by symmetry. The $^{13}C\{^1H\}$ NMR spectra of complexes **4.1-4.4** showed a carbonyl carbon resonance in the region 195.79-207.18 ppm; a singlet was observed for **4.1** and **4.2** whereas the resonance was split into a doublet for the phosphorus-ligand complexes **4.3** and **4.4** with a J_{C-P} coupling of 7 and 12 Hz respectively (Table 4.1). The single resonance observed for δ(CO) for the dicarbonyl dinitrogen complexes **4.1** and **4.2** indicates that these two CO ligands are also symmetry-equivalent.

Further characterization for the dinitrogen complexes **4.1-4.7** was provided by mass spectroscopy. In all cases the molecular ion M^+ was observed as a weak peak and was always accompanied by a fragment corresponding to loss of the dinitrogen ligand ($M^+ - N_2$).

4.2.2. Electrochemical Methods

4.2.2.1. Cyclic Voltammetry and Scanning Electrochemical Microscopy

Cyclic voltammetry (CV) of the cationic aryldiazenido complexes **2.1**, **2.2**, **2.4**, **2.8**, **2.11**, **2.13**, and **2.14** was carried out at a stationary platinum electrode in an acetonitrile solution containing tetraethylammonium perchlorate (TEAP, 0.2 M) as the supporting electrolyte. The cyclic voltammograms of these complexes, recorded at a scan rate of 0.2 V/s, displayed in each case a single cathodic wave between -0.46 V and -1.89 V vs SCE but no observable return oxidative wave, representative of a chemically irreversible process. The CV data are summarized in Table 4.2.

Table 4.2. Cyclic Voltammetric Cathodic Peak Potentials for Complexes **2.1**, **2.2**, **2.4**, **2.8**, **2.11**, **2.13**, and **2.14**.[a]

Complex	E_p^c (V)
$[CpRe(CO)_2(p\text{-}N_2C_6H_4OMe)][BF_4]$ (**2.1**)	-0. 46
$[Cp^*Re(CO)_2(p\text{-}N_2C_6H_4OMe)][BF_4]$ (**2.2**)	-0.62
$[Cp^*Re(CO)(PMe_3)(p\text{-}N_2C_6H_4OMe)][BF_4]$ (**2.4**)	-1.24
$[Cp^*Re(CO)\{P(OMe)_3\}(p\text{-}N_2C_6H_4OMe)][BF_4]$ (**2.8**)	-0.98
$[Cp^*Re(PMe_3)_2(p\text{-}N_2C_6H_4OMe)][BF_4]$ (**2.11**)	-1.89
$[Cp^*Re(dmpe)(p\text{-}N_2C_6H_4OMe)][BF_4]$ (**2.13**)	-1.74
$[Cp^*Re\{P(OMe)_3\}_2(p\text{-}N_2C_6H_4OMe)][BF_4]$ (**2.14**)	-1.41

[a] Recorded for 1.0 mM solutions of the complexes in acetonitrile at a Pt electrode with 0.2 M TEAP as the supporting electrolyte; scan rate 0.2 V/s; potentials are vs SCE.

The cyclic voltammograms of complexes **2.1**, **2.2**, **2.11**, **2.13**, and **2.14** showed no signs of approaching electrochemical reversibility as the scan rate was increased to 1.0 V/s as evidenced by those recorded for the cationic dicarbonyl aryldiazenido complexes **2.1** and **2.2** (Figures 4.1 and 4.2). However, at this scan rate a return anodic wave was clearly resolved for the cationic carbonyl phosphine and phosphite complexes **2.4** and **2.8** (Figures 4.3 and 4.4). Unfortunately, a well-defined reversible wave form could not be achieved for **2.4**, **2.8**, or any of the other cationic complexes by employing scan rates faster than 1.0 V/s because of limitations in the electrochemical equipment.

To overcome these limitations a collaborative effort with Bard and co-workers was undertaken. Bard et al. successfully employed fast scan rate cyclic voltammetry and scanning electrochemical microscopy (SECM) to examine the electrochemical behavior of the cationic dicarbonyl aryldiazenido complex $[Cp^*Re(CO)_2(p\text{-}N_2C_6H_4OMe)][BF_4]$ (**2.2**).[128] Cyclic voltammetry of a solution of **2.2** in acetonitrile with tetrabutylammonium tetrafluoroborate (TBA-BF_4, 0.1 M) as the supporting electrolyte was conducted at a 25-μm-diameter Pt electrode (Figure 4.5). The cyclic voltammogram of **2.2** exhibited a reversible wave with a cathodic peak potential of -0.66 V with respect to AgQRE at a scan rate of 10 V/s. The anodic wave was first resolved at this scan rate and became well-defined at 50 V/s. Digital simulation[129] of these cyclic voltammograms assuming an electrochemical E_rC_i mechanism afforded a rate constant $k_c = 145 \pm 10\ s^{-1}$ for the decomposition of the reduced species to products (Figure 4.5). The error in k_c was considered to be the range in rates over which it was impossible to distinguish between the experimental and simulated CV spectra. The validity of this rate constant was substantiated by SECM[130-136] which also produced a value of 145 s^{-1} for k_c.

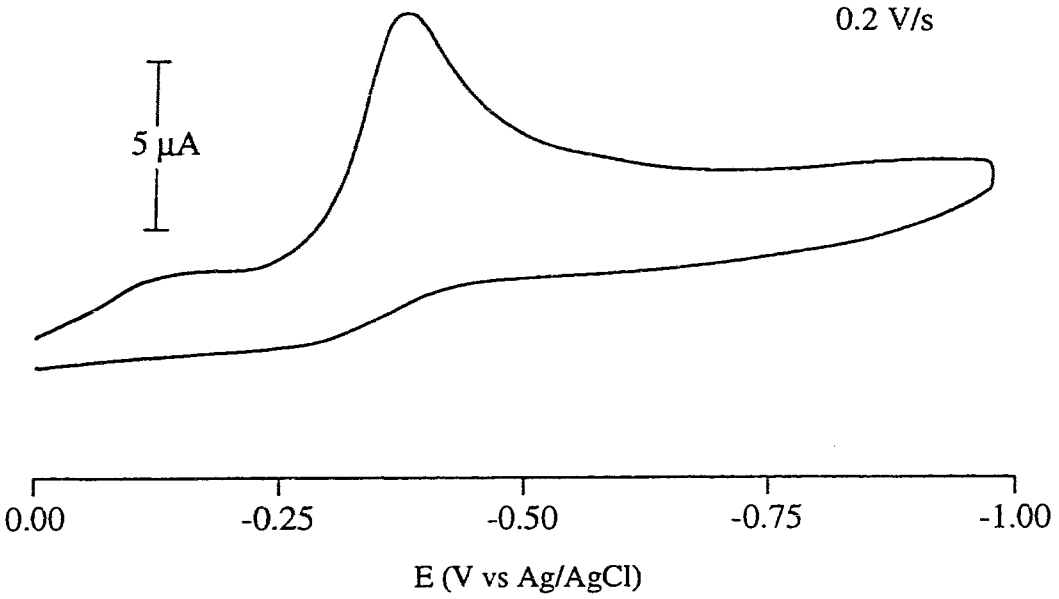

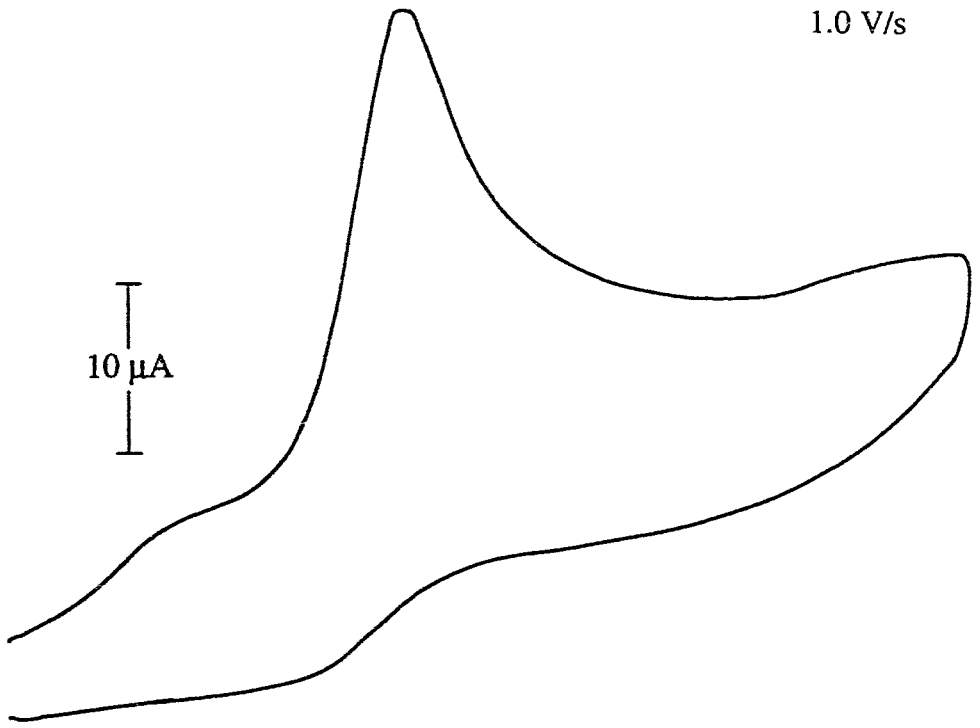

Figure 4.1. Cyclic voltammogram of **2.1** (1.0 mM MeCN solution); 0.2 M TEAP; Pt working electrode.

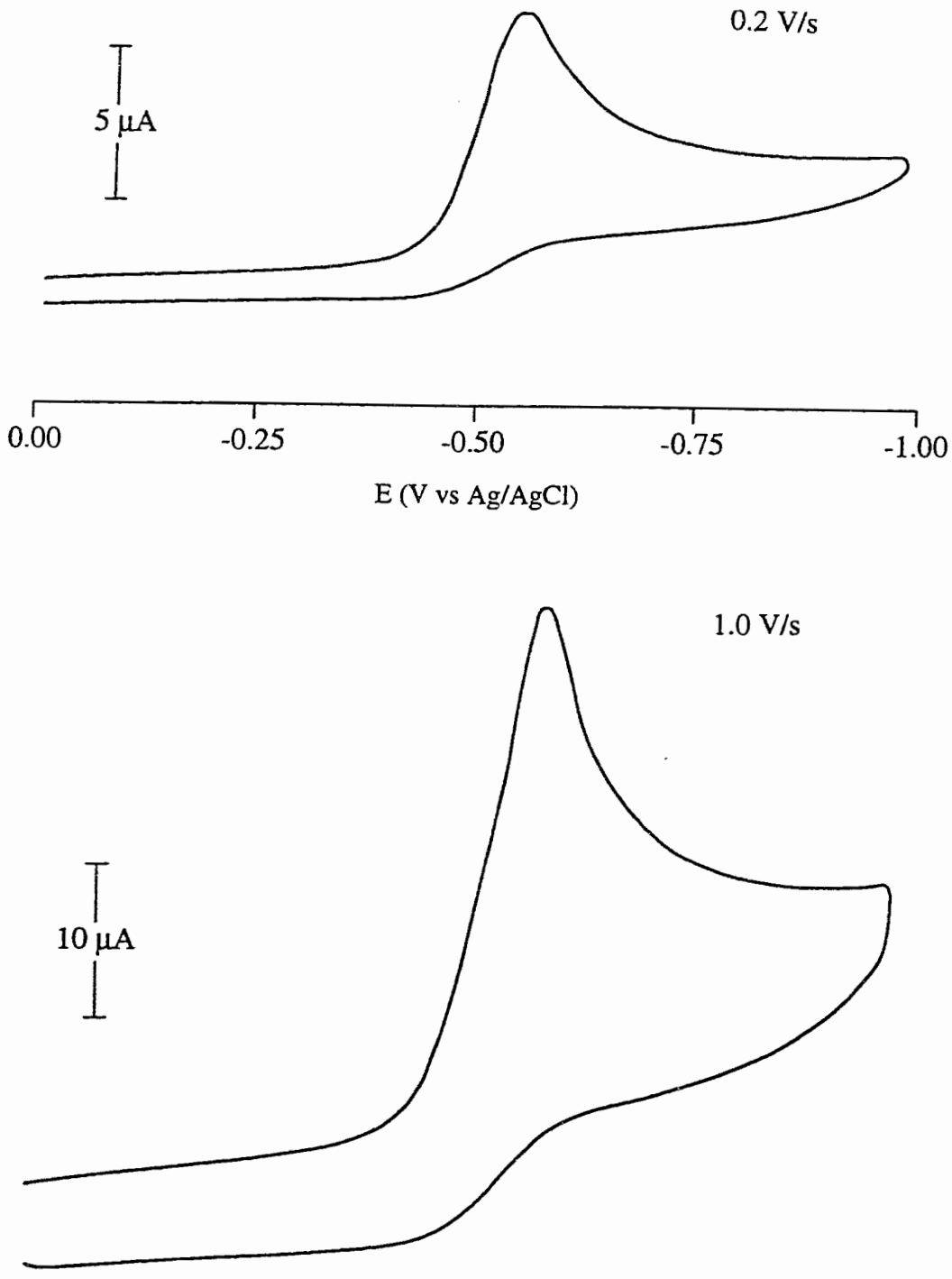

Figure 4.2. Cyclic voltammogram of **2.2** (1.0 mM MeCN solution); 0.2 M TEAP; Pt working electrode.

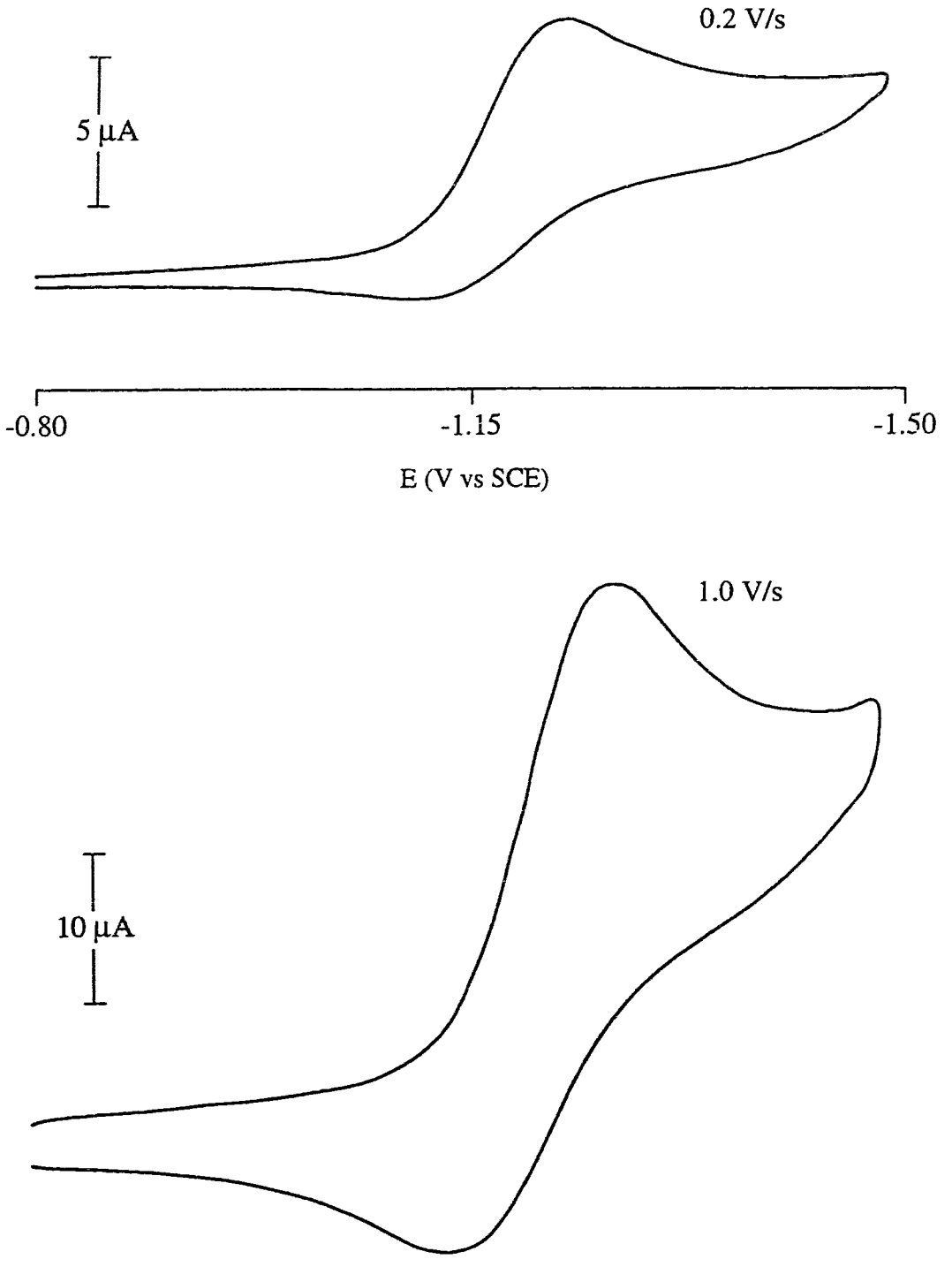

Figure 4.3. Cyclic voltammogram of **2.4** (1.0 mM MeCN solution); 0.2 M TEAP; Pt working electrode.

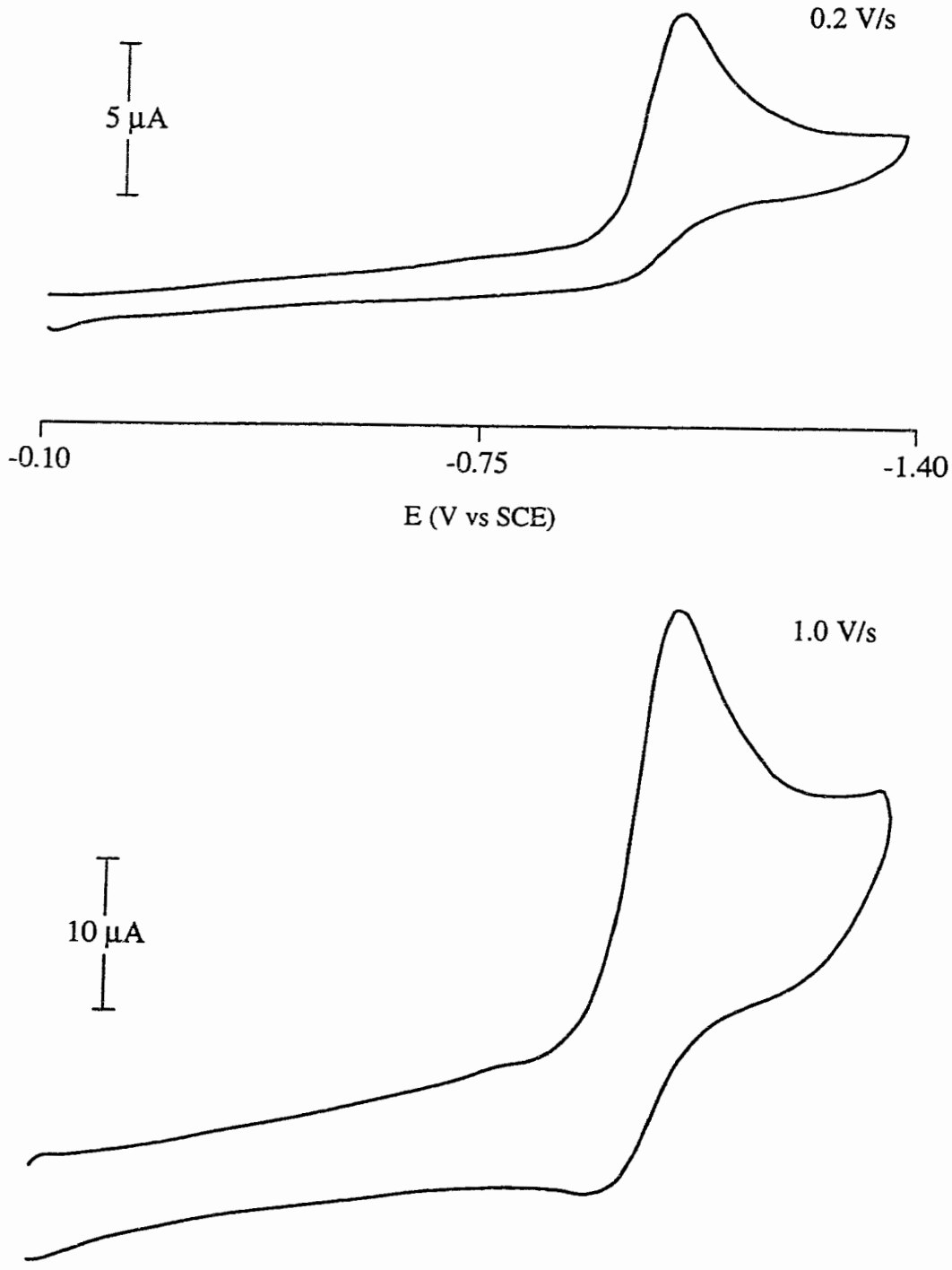

Figure 4.4. Cyclic voltammogram of **2.8** (1.0 mM MeCN solution); 0.2 M TEAP; Pt working electrode.

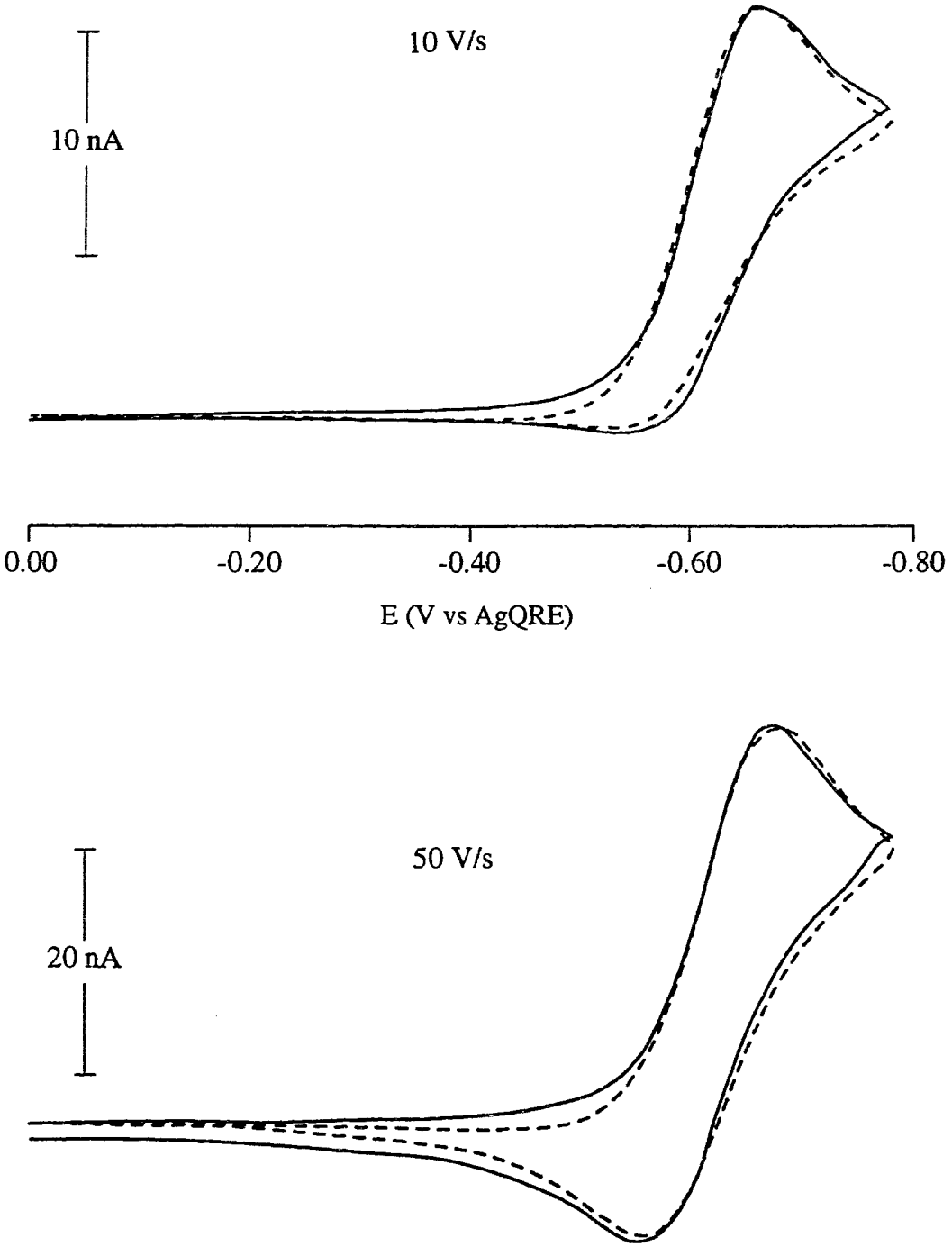

Figure 4.5. Experimental (solid lines) and simulated (dashed lines) cyclic voltammograms of **2.2** (1.1 mM MeCN solution); 0.1 M TBA-BF_4; 25-μm-diameter Pt working electrode.

4.2.2.2. Controlled Potential Electrolysis

The controlled potential electrolysis (CPE) of solutions of the cationic aryldiazenido complexes **2.1**, **2.2**, **2.4**, and **2.11** in acetonitrile (5 mM) were performed at a large Pt gauze electrode with tetraethylammonium perchlorate (TEAP, 0.2 M) as the supporting electrolyte. From Equation 4.1,[137] and by monitoring the amount of charge consumed at the end of the CPE experiment, a value for the number of electron(s) involved in the overall reduction reaction was determined for **2.1**, **2.2**, and **2.4**.

$$n = q_{\infty}/FcV \qquad (4.1)$$

where q_{∞} = total charge consumed at the end of the experiment

F = Faraday constant

c = the concentration of the particular cationic aryldiazenido reactant

V = volume of solution in the working electrode compartment

Exhaustive CPE of **2.1**, **2.2**, and **2.4** (60 min) at a potential sufficiently larger (higher negative number) than their respective cathodic peak potentials vs SCE (Table 4.2) indicated the consumption of 1 equivalent of electrons in all cases.

Monitoring the progress of the electrolysis of **2.1**, **2.2**, and **2.4** by IR spectroscopy showed the clean production of the corresponding neutral dinitrogen complexes **4.1**, **4.2**, and **4.3** respectively, in good yield; an example of the electrochemical reduction is illustrated in Figure 4.6 for the cationic dicarbonyl aryldiazenido complex **2.2**. The results from the CPE studies of the cationic bis-trimethylphosphine aryldiazenido complex **2.11** were inconclusive since **2.11** proved to be very air-sensitive and was easily oxidized to the known trioxo complex Cp^*ReO_3 (**4.8**)[138] prior to or during the CPE measurements despite all efforts to maintain an inert atmosphere in the CPE cell.

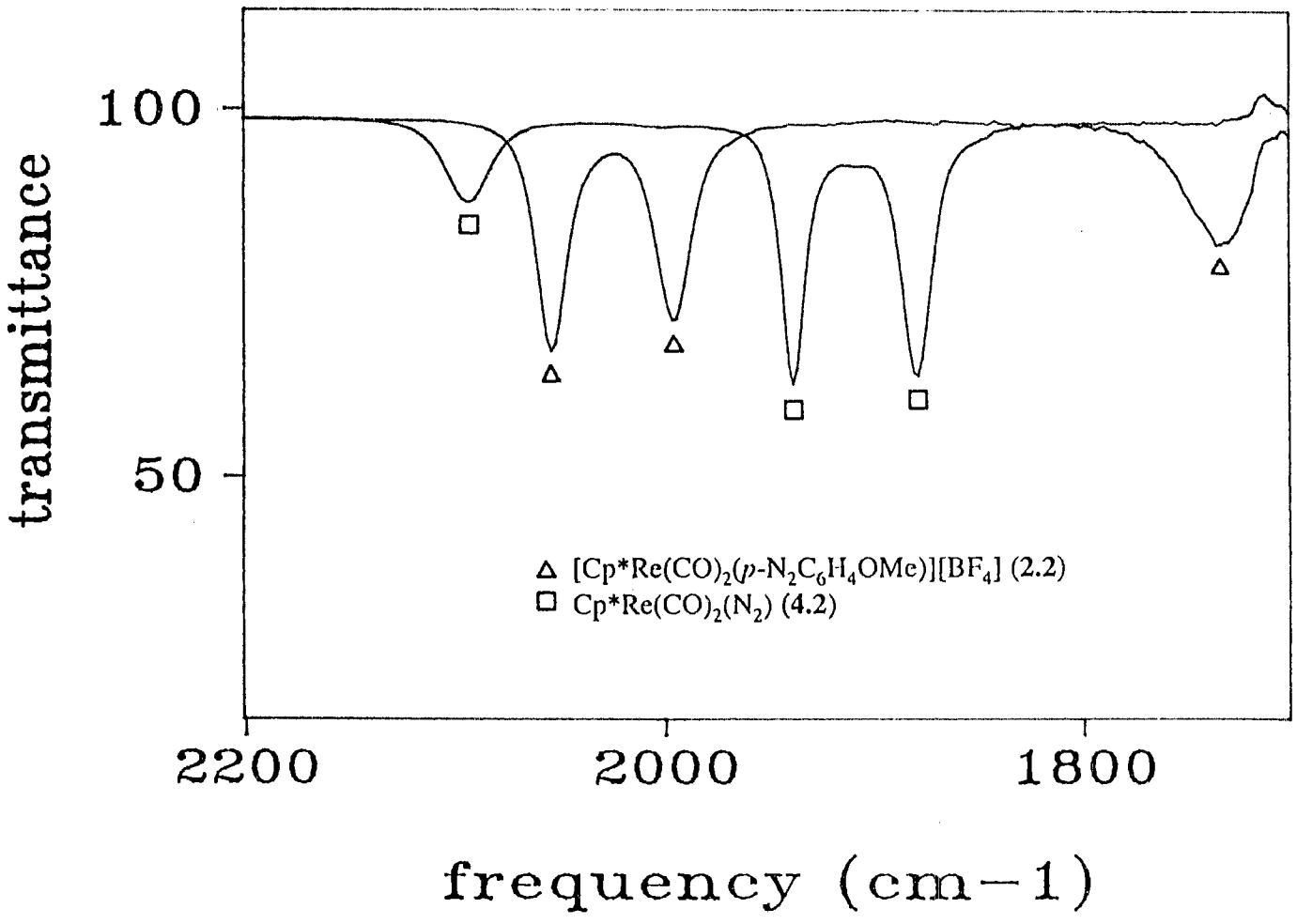

Figure 4.6. IR spectra obtained before and after the CPE of **2.2** (5.0 mM MeCN solution) at a reduction potential of -0.66 V vs Ag/AgCl; 0.2 M TEAP; Pt gauze working electrode. $[Cp^*Re(CO)_2(p\text{-}N_2C_6H_4OMe)][BF_4]$ (**2.2**): 2054, 1995 cm^{-1} ν(CO); 1732 cm^{-1} ν(NN). $Cp^*Re(CO)_2(N_2)$ (**4.2**): 2121 cm^{-1} ν(NN); 1939, 1879 cm^{-1} ν(CO).

4.3. Discussion

4.3.1. Synthesis and Characterization of Dinitrogen Complexes

A wide variety of Cp and Cp* rhenium aryldiazenido complexes have been converted to the corresponding dinitrogen complexes of general formula $Cp'Re(L_1)(L_2)(N_2)$ ((a) Cp' = Cp; $L_1 = L_2 = CO$ (**4.1**),[123, 124] (b) Cp' = Cp*; $L_1 = CO$; $L_2 = PMe_3$ (**4.3**)[59] or $P(OMe)_3$ (**4.4**),[59] and (c) Cp' = Cp*; $L_1 = L_2 = CO$ (**4.2**),[59] PMe_3 (**4.5**), dmpe (**4.6**), or $P(OMe)_3$ (**4.7**)) (Scheme 4.2) by the use of $NaBH_4$, $Ph_3C\cdot$, Cp_2Co, or Na/Hg. The synthesis of the phosphorus-ligand substituted dinitrogen complexes **4.3-4.7** by this method is of utmost importance since these types of dinitrogen complexes could not be prepared from $Cp^*Re(CO)_2(N_2)$ (**4.2**) by conventional carbonyl substitution under thermal or photochemical conditions; instead, employing these conditions results in thermal or photoextrusion of the N_2 ligand. Furthermore, attempts to synthesize **4.3-4.7** by oxidative removal of the carbonyl ligand in **4.2** with PhIO or Me_3NO in a coordinating solvent such as MeCN, and then subsequent substitution of the ligated solvent by phosphine or phosphite were also not successful (this procedure was successful for the analogous aryldiazenido complexes described in Chapter 2).

As solids, complexes **4.1-4.4** can be exposed to air for short periods of time without appreciable deterioration and can be stored indefinitely at low temperature (263 K) under an atmosphere of N_2; solutions are more sensitive to air. The bis(phosphorus-ligand) dinitrogen complexes **4.5** and **4.7**, and the bidentate phosphine dinitrogen complex **4.6**, either in solution or as solids, are very air-sensitive and exposure to air for even short periods of time results in the oxidation of these complexes to the known trioxo complex of rhenium, Cp^*ReO_3 (**4.8**).[138] In fact, even exposure of complexes **4.5-4.7** to nondegassed solvents affords **4.8**. Confirmation of the trioxo complex was achieved by bubbling $O_2(g)$ through a solution of the dinitrogen complexes **4.5-4.7** in hexane for 5

min and then analyzing the product formed by ^{1}H NMR and mass spectroscopy. The mechanism for this conversion is not known, and is currently under investigation in our laboratory.

In the IR spectra of complexes **4.1-4.7**, ν(NN) was observed as a strong absorption in the 2145-1975 cm^{-1} region. This region is typical for ν(NN) of terminal dinitrogen complexes where the N_2 ligand is coordinated in an end-on (η^1) fashion.[23, 33] For complexes **4.1-4.7** the relative electronic properties of the Cp, Cp*, or phosphorus ligands are borne out by changes in ν(CO), or more dramatically, by changes in ν(NN) (Table 4.1). The greater the σ-donor (or poorer the π-acceptor) ability of these ligands, the higher the degree of charge delocalization into the carbonyl or dinitrogen antibonding orbitals and the lower ν(CO) or ν(NN). For example, the IR spectrum of the Cp dicarbonyl dinitrogen complex **4.1** exhibited absorptions for ν(NN) that are substantially higher than those observed for the methylated analogue **4.2**; the same trend was observed for ν(CO). This result is in agreement with the general view that Cp* is a better electron donating ligand than Cp and these findings are similar to those reported for the chromium dicarbonyl dinitrogen complexes (η-aryl)Cr(CO)$_2$(N_2) (aryl = C_6H_6, $C_6H_3Me_3$, or C_6Me_6).[139] Furthermore, values for ν(NN) and where applicable ν(CO), follow the order of the co-ligands (CO){P(OMe)$_3$} (**4.4**) > (CO)(PMe_3) (**4.3**) > {P(OMe)$_3$}$_2$ (**4.7**) > dmpe (**4.6**) ≈ (PMe_3)$_2$ (**4.5**) which correlates with increasing σ-donor ability (or decreasing π-acceptor ability) of the phosphorus ligand. Taken together, these results suggest that PMe_3 is a significantly better electron donating ligand [Δν(NN) = 81 cm^{-1} on going from **4.2** to **4.3**] than P(OMe)$_3$ [Δν(NN) = *ca.* 53 cm^{-1} on going from **4.2** to **4.4**], and both these phosphorus ligands are dramatically better electron donors than Cp* [Δν(NN) = 20 cm^{-1} on going from **4.1** to **4.2**].

It should be noted here that the two resolved ν(NN) absorptions reported for the carbonyl trimethylphosphite dinitrogen complex **4.4** (Table 4.1) were investigated by co-

workers in our laboratory and as a result these absorptions have been accounted for by the presence of conformational isomers brought about by the specific orientation of the Me group of the $P(OMe)_3$ ligand.[59] In contrast to this result, the bis-trimethylphosphite dinitrogen complex **4.7** exhibited only a single IR absorption for ν(NN) (Table 4.1).

The concept of virtual coupling was addressed in Chapter 2 where it was first observed for the bis(phosphorus-ligand) aryldiazenido complexes **2.11** and **2.14**. The ^1H NMR spectrum obtained for the bis-PMe_3 aryldiazenido complex **2.11** exhibited a virtual doublet for the resonance assigned to the PMe_3 ligand whereas a virtual triplet was observed for the $P(OMe)_3$ ligand of the bis-$P(OMe)_3$ aryldiazenido complex **2.14**. Interestingly, the ^1H NMR spectra of the corresponding dinitrogen complexes **4.5** and **4.7** exhibited in both cases a virtual doublet for the resonances assigned to the respective phosphorus ligands. The concept of virtual coupling was developed from studies involving metal complexes which adopt a square planar geometry. Therefore, an understanding of how these virtual couplings arise and what information they may convey to the particular orientation of the phosphorus ligands is still not clear in the case of the half-sandwich piano-stool type complexes such as **4.5** or **4.7**. Before an understanding can be reached, more examples of such complexes must be examined.

From the $^{13}C\{^1H\}$ NMR spectra of complexes **4.1-4.4**, it was observed that the values for δ(CO) follow the order of the co-ligands $Cp^*(CO)(PMe_3)$ > $Cp^*(CO)\{P(OMe)_3\}$ > $Cp^*(CO)_2$ > $Cp(CO)_2$ which also correlates with increasing electron donating ability of the co-ligands. This trend and the rationale for it is similar to that mentioned previously in Chapter 2 for the corresponding aryldiazenido precursors.

4.3.1.1. Reactions Involving Hydride (H^-) Sources

Studies conducted on the cationic manganese complex $[(\eta^5\text{-}C_5H_4Me)Mn(CO)_2(N_2Ar)]^+$ by previous co-workers suggested that the conversion

of the Mn-bound aryldiazenido group to the dinitrogen ligand may proceed by a nucleophilic displacement mechanism.[98] In order to investigate the validity of this suggestion, the hydride sources $LiAlH_4$ and $NaBH_4$ were reacted with the cationic rhenium aryldiazenido complexes $[Cp^*Re(CO)_2(p\text{-}N_2C_6H_4OMe)][BF_4]$ (**2.2**) and $[Cp^*Re(PMe_3)_2(p\text{-}N_2C_6H_4OMe)][BF_4]$ (**2.11**) and the products were examined.

Treatment of a solution of **2.11** in methanol with either $LiAlH_4$ or $NaBH_4$ produced no reaction at all even after a large excess of the hydride sources were added and the solutions were allowed to stir for several hours. In contrast, treatment of a solution of the cationic dicarbonyl aryldiazenido complex **2.2** in methanol with excess solid $LiAlH_4$ afforded the known methoxycarbonyl complex $Cp^*Re(CO)(COOMe)(p\text{-}N_2C_6H_4OMe)$ (**4.9**)[61] as characterized by IR and ^1H NMR spectroscopy. Complex **4.9** was most likely formed *via* attack of the carbonyl carbon atom in **2.2** by methoxide ion (MeO^-) which was generated "in situ" from the reaction of $LiAlH_4$ with methanol. In support of this suggestion it was shown that **4.9** can also be synthesized quantitatively by addition of NaOMe to a solution of **2.2** in methanol. Furthermore, the evolution of gas which was noted upon addition of $LiAlH_4$ to the methanol solution is consistent with the abstraction of a proton from the solvent which in turn would yield MeO^- and H_2. The desired dinitrogen complex **4.2** was not formed in this reaction. However, addition of excess $NaBH_4$, as a solid, to a solution of **2.2** in methanol at room temperature did not produce **4.9** but instead resulted in the initial formation of a deep red colored solution. The reaction then progressed further, with loss of the red color and formation of a yellow colored solution containing the dinitrogen complex **4.2** (Equation 4.2). Similar results were obtained when this reaction was repeated using acetone as a solvent (Equation 4.2).

$$[Cp^*Re(CO)_2(p\text{-}N_2C_6H_4OMe)][BF_4] \xrightarrow[\text{MeOH or acetone}]{NaBH_4} Cp^*Re(CO)_2(N_2) + C_6H_5OMe \qquad (4.2)$$

GC analysis of this reaction mixture indicated that anisole (C_6H_5OMe) was also a product of this reaction (Equation 4.2).

The results obtained for the reaction between the cationic dicarbonyl aryldiazenido complex **2.2** and $NaBH_4$ suggest that a thermally unstable intermediate (red colored solution) may lie on the path toward the dinitrogen complex **4.2**. If that is the case, the reaction of H^- with this complex can, in principle, be visualized to occur by initial nucleophilic attack at several sites on the metal complex followed by some type of rearrangement to give the dinitrogen complex **4.2** and anisole (Scheme 4.3).
In (i), attack at the carbon atom of the CO group produces a formyl complex whereas in (ii) attack at the metal center, with substitution of a carbonyl ligand, forms a monocarbonyl hydrido complex. Alternatively, if attack occurs at the aryldiazenido group, there are three potential sites for nucleophilic attack: (iii) at the ipso carbon of the aromatic ring to give directly the dinitrogen complex **4.2** and anisole; (iv) at the rhenium-bound nitrogen atom (N_α) to yield the aryldiazene complex or (v) at the terminal nitrogen atom (N_β) to form the arylhydrazido complex.

An IR spectrum, recorded of the red colored solution which was formed immediately after the addition of $NaBH_4$ to a solution of **2.2,** in acetone at room temperature showed the complete disappearance of **2.2** and the presence of two new strong absorptions of similar intensity at 1917 and 1852 cm^{-1} assigned to the intermediate species. The position and the intensity of these IR absorptions are consistent with their assignment as two terminal ν(CO) bands. IR spectra acquired every 5 min showed that the absorptions corresponding to the intermediate species smoothly disappeared as the bands due to the dinitrogen complex **4.2** gradually appeared. Complex **4.2** was the final product.

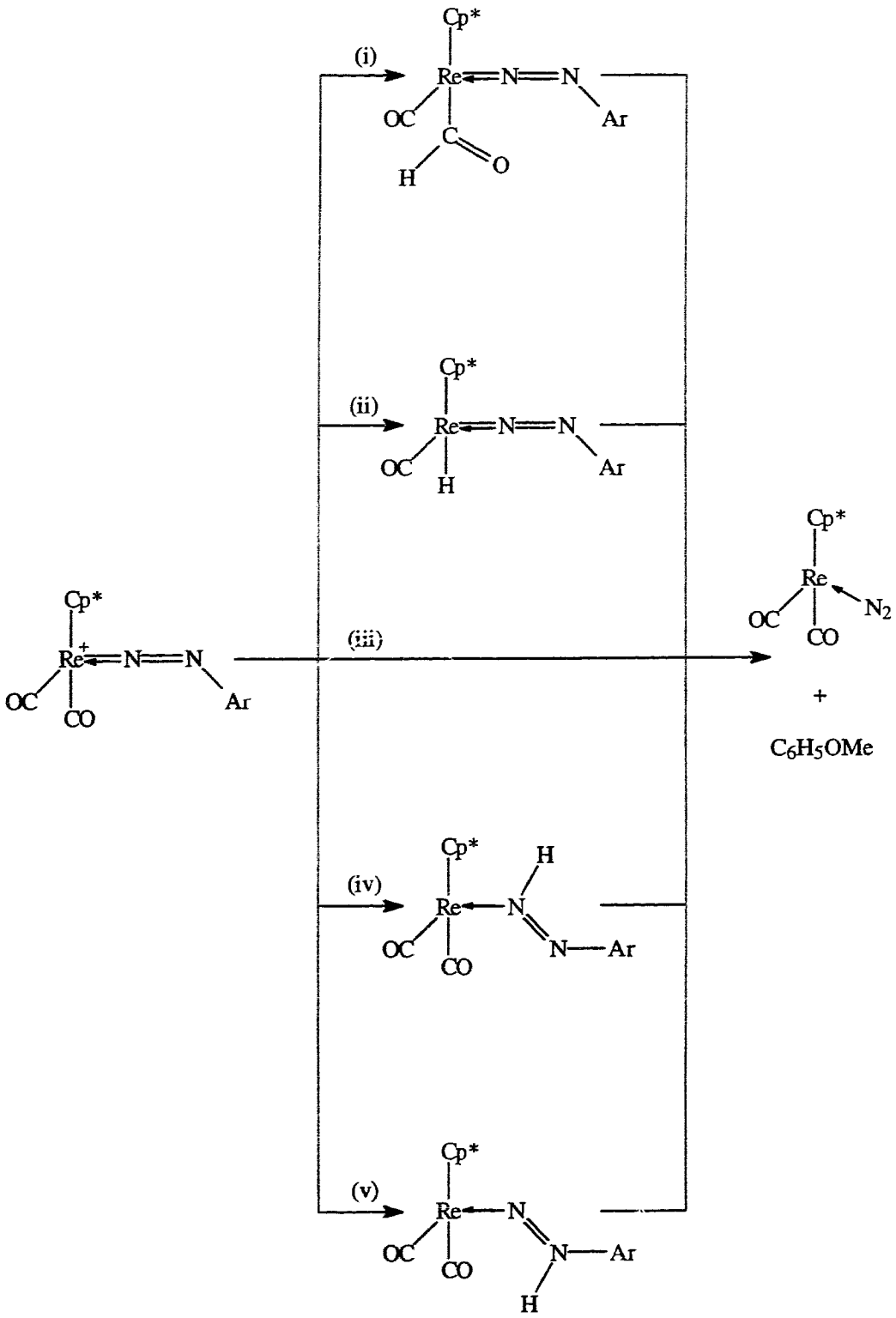

Scheme 4.3. Proposed possible hydride addition pathways to the dinitrogen complex $Cp^*Re(CO)_2(N_2)$ **(4.2)** from the aryldiazenido complex $[Cp^*Re(CO)_2(N_2Ar)][BF_4]$ **(2.2)** (Ar = *p*-C_6H_4OMe).

The synthesis of the red colored solution was repeated at 195 K using acetone-d_6 as the solvent. A ^{1}H NMR spectrum of this solution acquired at 233 K demonstrated the disappearance of **2.2** and the presence of resonances attributable to a Cp* and an aryldiazenido group common to all the intermediates shown in Scheme 4.3. Most notably, however, the ^{1}H spectrum also exhibited a broad singlet at δ 15.68 integrating to one proton. No signal upfield from TMS was observed.

The presence of two terminal ν(CO) bands in the IR spectrum and the lack of a rhenium hydrido signal in the ^{1}H NMR spectrum (expected to be upfield of TMS) eliminates the metal hydrido derivative [pathway (ii)] as a possible intermediate. Furthermore, the fact that the IR and ^{1}H NMR results establish the presence of an intermediate is not in agreement with pathway (iii) since no spectroscopically observable intermediate is expected from direct nucleophilic attack of H^- at the ipso carbon of the aromatic ring.

The downfield broad proton signal at δ 15.68 could correspond to the hydrogen atom of a formyl (M-HCO) ligand since this is the typical region where these formyl resonances are found.[140] However, the presence of two terminal ν(CO) absorptions in the IR spectrum at 1917 and 1852 cm^{-1} is not consistent with a monocarbonyl species [pathway (i)]; ν(CO) for the formyl ligand is typically found at *ca.* 1650 cm^{-1}.[140]

The two remaining pathways [(iv) and (v)] are both consistent with all the spectroscopic data obtained thus far. To differentiate between these two pathways the intermediate species was once again prepared at 195 K by adding $NaBH_4$ to an acetone-d_6 solution of the dicarbonyl aryldiazenido complex which was specifically labeled at the rhenium-bound nitrogen atom (N_α) with ^{15}N (**2.2-$^{15}N_\alpha$**) (Figure 4.7a). A ^{1}H NMR spectrum of this solution acquired at 233 K exhibited, in addition to the typical resonances expected for the Cp* and the aryldiazenido group, a *doublet* at δ 15.68 ($J_{H\text{-}N}$ = 69 Hz) integrating to one proton (Figure 4.7b).

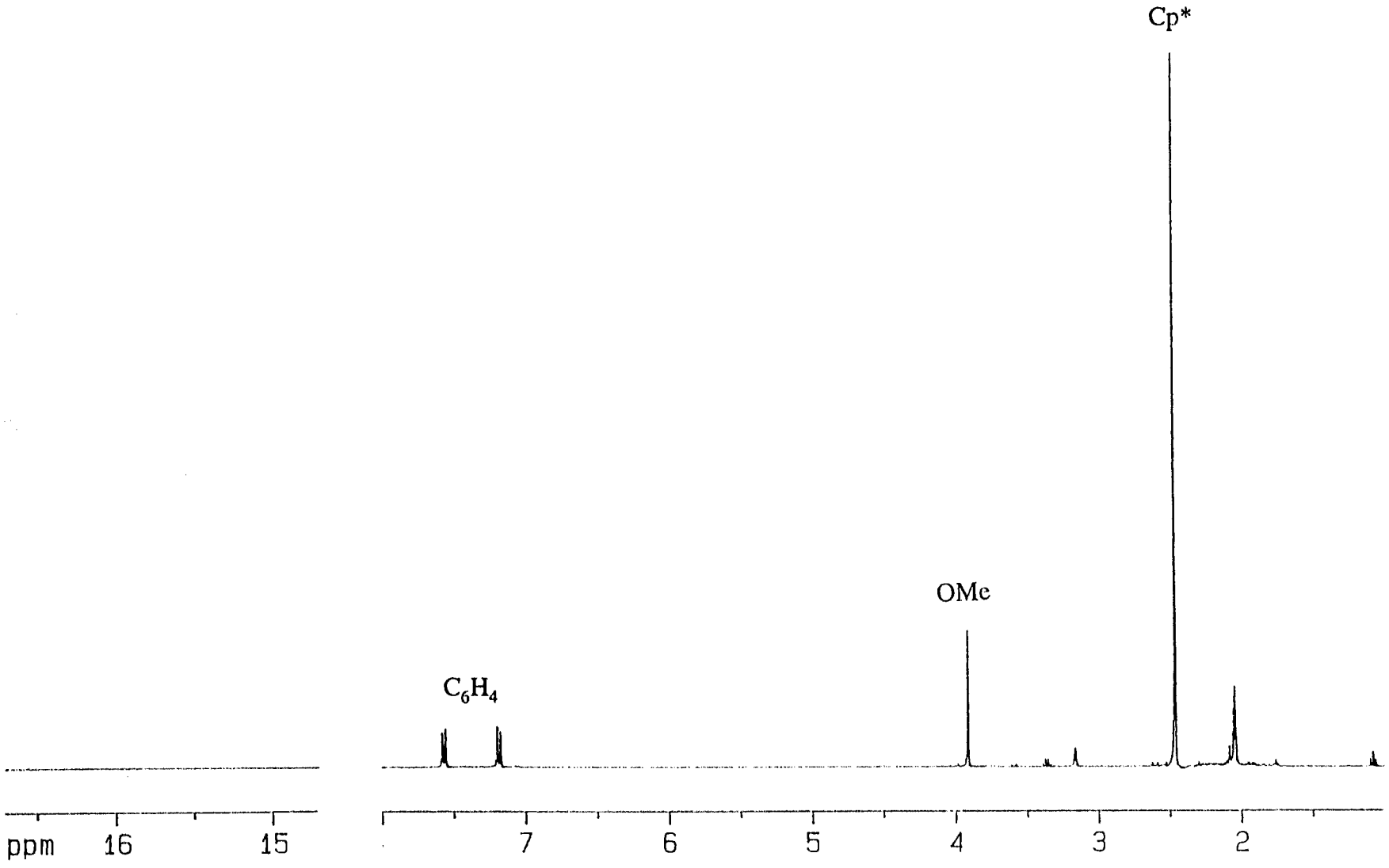

Figure 4.7a. ^{1}H NMR spectrum (400 MHz) of $[Cp^*Re(CO)_2(p\text{-}^{15}N^{14}NC_6H_4OMe)][BF_4]$ (**2.2-$^{15}N_\alpha$**) in acetone-d_6 at 233 K.

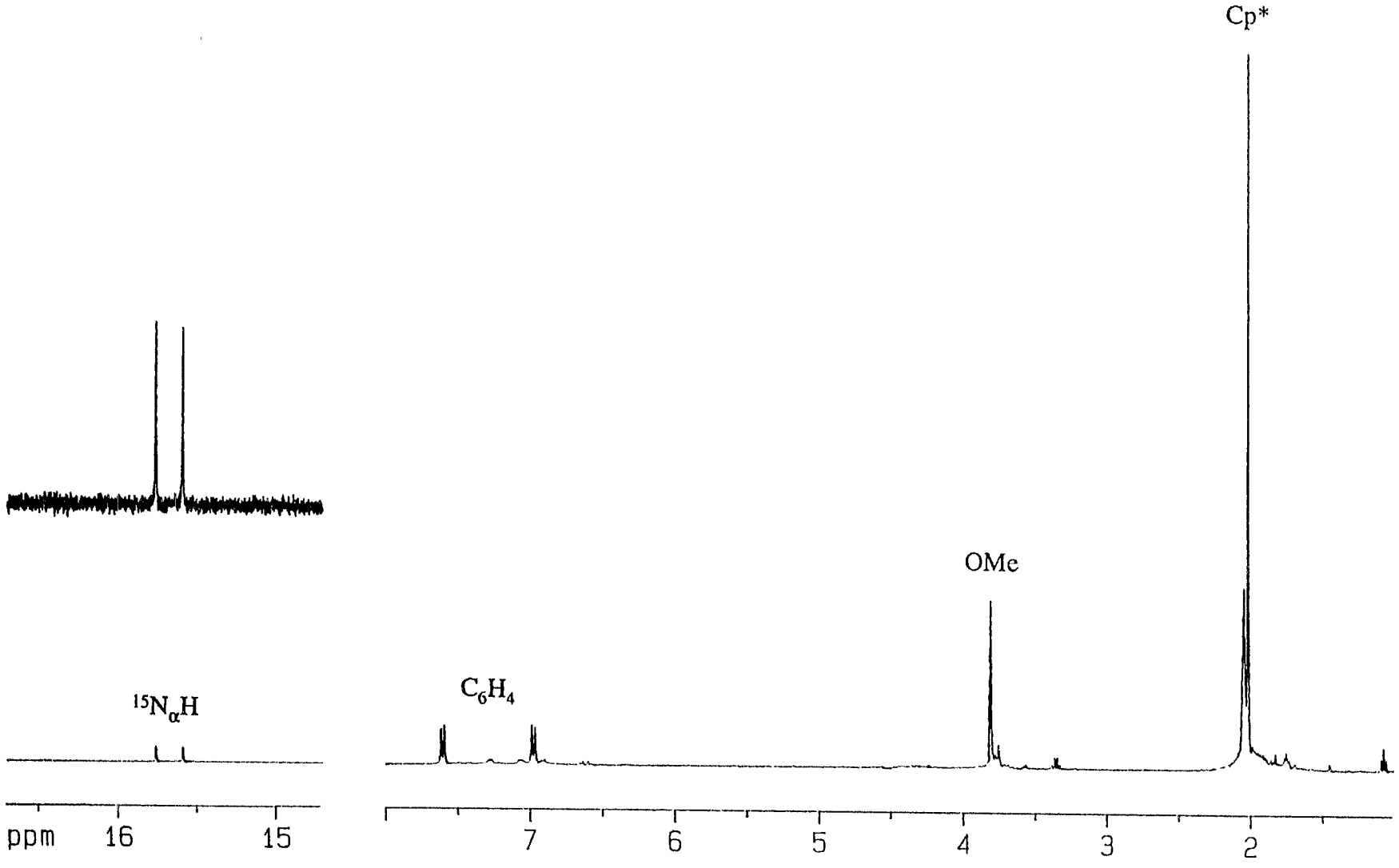

Figure 4.7b. ^1H NMR spectrum (400 MHz) of the reaction between $[Cp^*Re(CO)_2(p\text{-}^{15}N^{14}NC_6H_4OMe)][BF_4]$ (**2.2-$^{15}N_\alpha$**) and $NaBH_4$ in acetone-d_6 at 233 K. Downfield doublet has been expanded for clarity.

Furthermore, a ^{15}N NMR spectrum obtained of this solution at this temperature also showed a *doublet* at δ -46.7 with the same coupling constant (J_{N-H} = 69 Hz) (Figure 4.8). The NMR solution was then allowed to warm to room temperature. Purification of this solution afforded exclusively the dinitrogen complex **4.2**. GC analysis of the solvent remains confirmed the presence of anisole.

The downfield doublet at δ 15.68 (J_{H-N} = 69 Hz) observed in the low temperature ^1H NMR spectrum and the doublet at δ -46.7 (J_{N-H} = 69 Hz) detected in the low temperature ^{15}N spectrum are confirmation of a ^{15}N-H coupling. Therefore, since the ^{15}N label was introduced at the rhenium-bound nitrogen atom (N_α) exclusively, the intermediate was unambiguously assigned as the aryldiazene complex $Cp^*Re(CO)_2(p\text{-}^{15}NH^{14}NC_6H_4OMe)$ (**4.10-$^{15}N_\alpha$**). Thus, the hydrazido species can be ruled out as an observable precursor to the dinitrogen complex in this reaction.

To summarize, the evidence clearly demonstrates that the reaction between $NaBH_4$ and the cationic dicarbonyl aryldiazenido complex **2.2** proceeds by initial H^- attack at the rhenium-bound nitrogen atom (N_α) to give the neutral aryldiazene complex **4.10**, which then eliminates anisole resulting in the formation of the respective neutral dinitrogen complex **4.2**. Thus, the mechanism which best describes this conversion is pathway (iv) (Scheme 4.3).

The IR spectra of the aryldiazene complex **4.10** showed two ν(CO) absorptions (1917 and 1852 cm^{-1} in acetone), which were lowered substantially from the corresponding positions in the aryldiazenido complex **2.2** (2054 and 1995 cm^{-1} in acetone). The ν(NN) band for the aryldiazene complex **4.10** was not observed, nor was the absorption due to ν(NH). Notably, even ^{15}N isotopic substitution of the rhenium-bound nitrogen atom (N_α) in the aryldiazene complex $Cp^*Re(CO)_2(p\text{-}^{15}NH^{14}NC_6H_4OMe)$ (**4.10-$^{15}N_\alpha$**) did not lead to the assignment of ν(NN) or ν(NH).

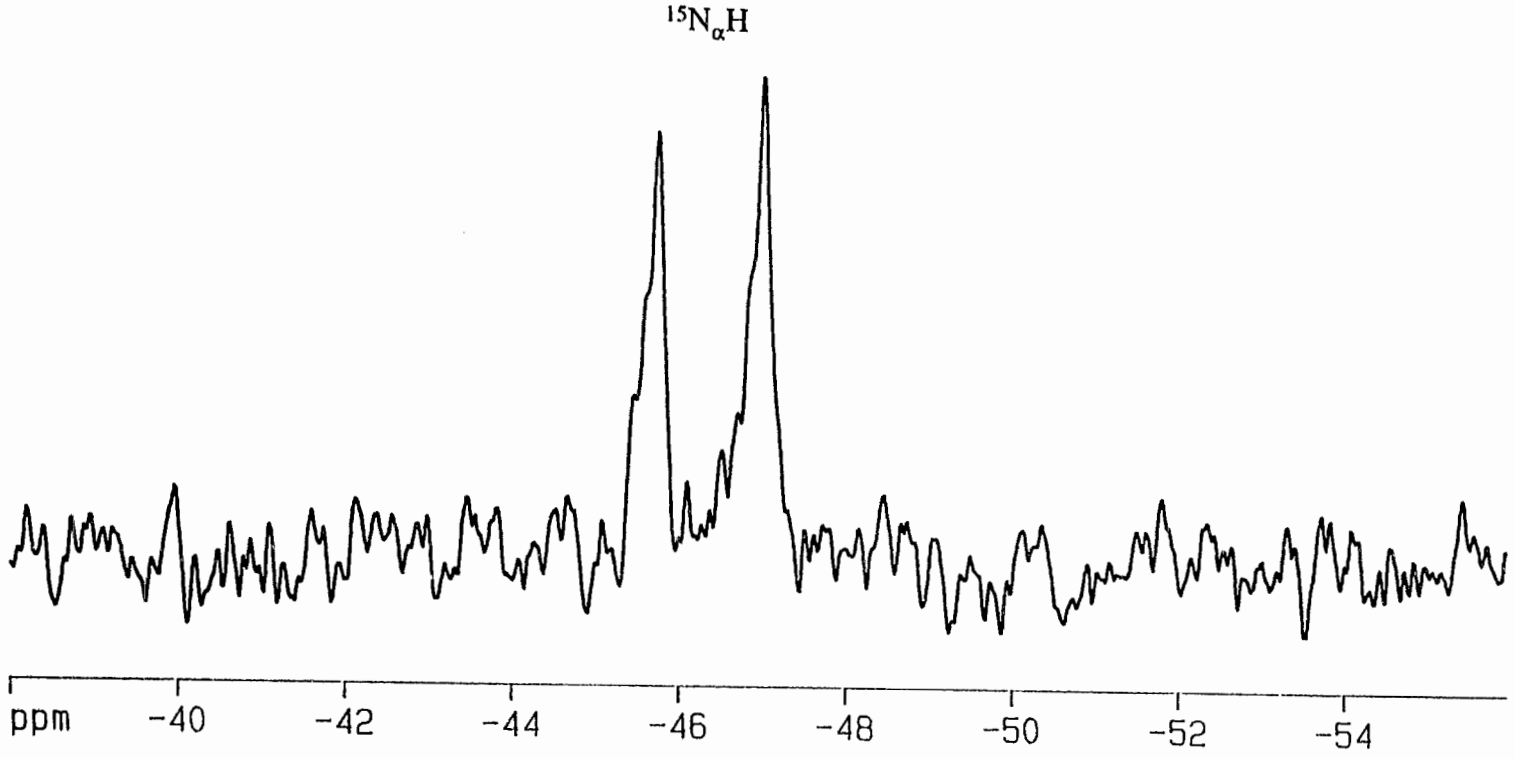

Figure 4.8. ^{15}N NMR spectrum (40.6 MHz) of the reaction between $[Cp^*Re(CO)_2(p\text{-}^{15}N^{14}NC_6H_4OMe)][BF_4]$ (**2.2-$^{15}N_{\alpha}$**) and $NaBH_4$ in acetone-d_6 at 233 K.

The ^{1}H NMR spectrum of **4.10** demonstrated that the NH resonance occurs well downfield (δ 15.68), at the lower end of the range (*ca.* δ 11-15) observed for many other aryldiazenes,[141-143] and the resonance was split into a sharp doublet [J(H-^{15}N) = 69 Hz] in the spectrum of the $^{15}N_\alpha$ derivative Cp*Re(CO)$_2$(*p*-^{15}NH^{14}NC$_6$H$_4$OMe) (**4.10**-$^{15}N_\alpha$). This coupling constant is in agreement with J(H-^{15}N) values reported for other aryldiazene complexes, such as [PtCl(PEt$_3$)$_2$(*p*-^{15}NH^{14}NC$_6$H$_4$F)][BF$_4$] [J(H-^{15}N) = 77 Hz],[141] [RuCl(^{15}NH^{14}NPh)(CO)$_2$(PPh$_3$)$_2$][ClO$_4$] [J(H-^{15}N) = 65 Hz],[142] and [W(CO)$_2$(NO)(PPh$_3$)$_2$(^{15}NH^{14}NPh)][PF$_6$] [J(H-^{15}N) = 63 Hz].[143]

The spectroscopic evidence clearly supports the formulation of **4.10** as an aryldiazene complex, but the actual bonding mode of the ligand (i.e., end-on (η^1) or side-on (η^2) bonded) could not be deduced from these data (Figure 4.9).

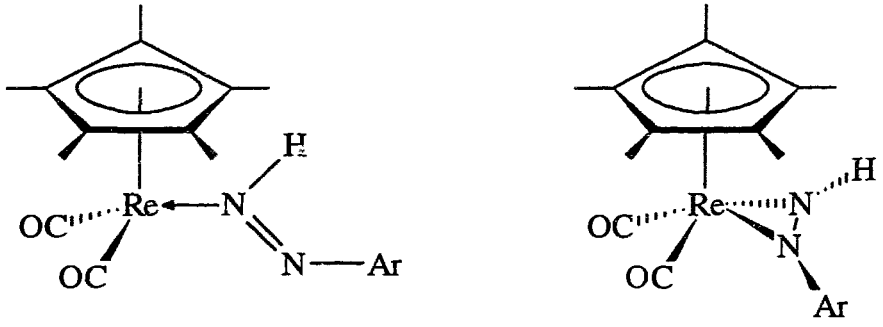

η^1-aryldiazene η^2-aryldiazene

Figure 4.9. Structures illustrating the end-on (η^1) and side-on (η^2) bonding modes for the aryldiazene ligand.

To gain some insight on the bonding mode adopted by the aryldiazene ligand, complex **4.10** was examined by low temperature ^{13}C{^{1}H} NMR spectroscopy. A ^{13}C{^{1}H} NMR spectrum of this complex recorded at 233 K in acetone-d$_6$ exhibited, in addition to the typical resonances for the Cp* and aryldiazene groups, a single resonance in the carbonyl region at δ 208.32 indicative of two symmetry-equivalent CO ligands (Figure 4.10).

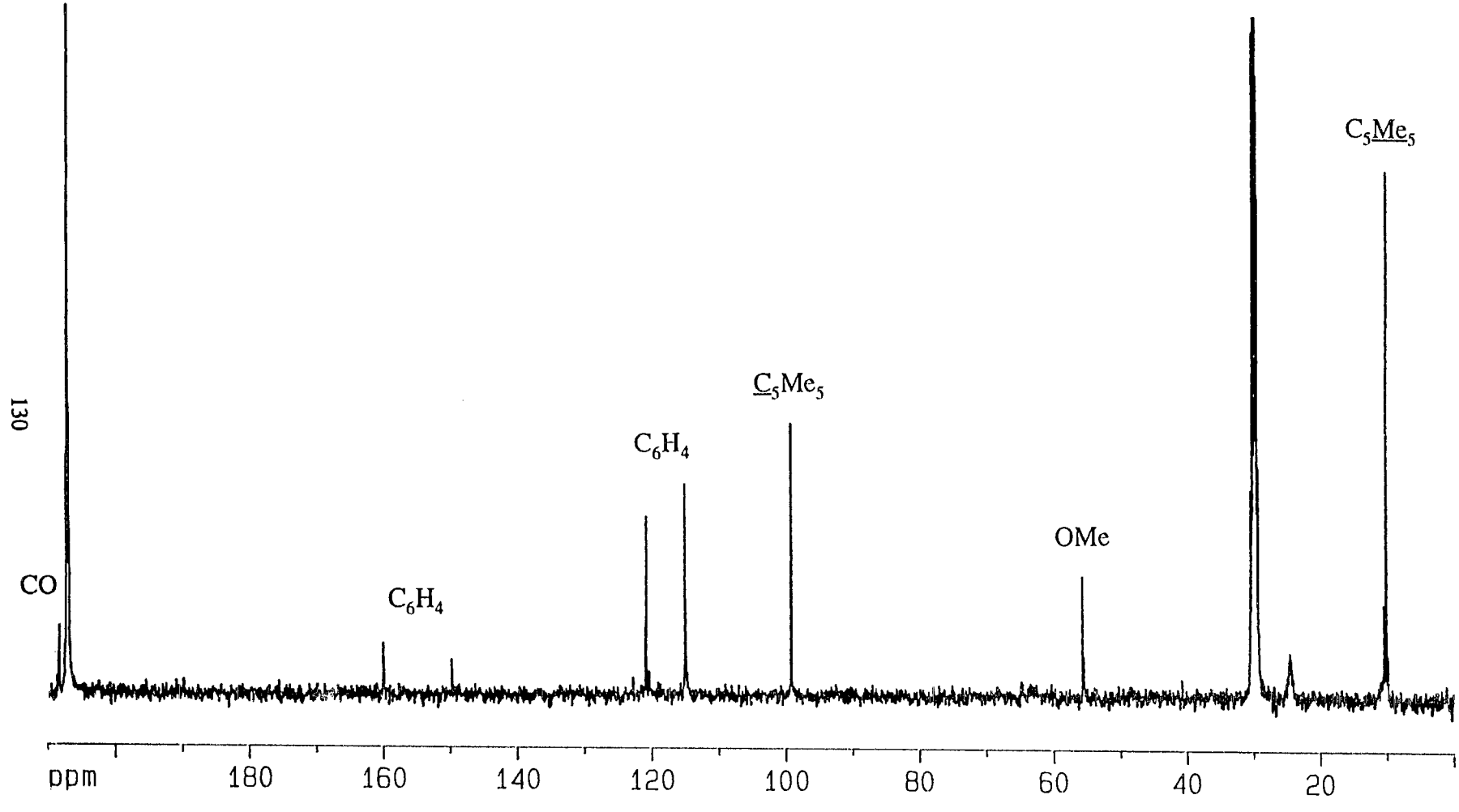

Figure 4.10. $^{13}C\{^{1}H\}$ NMR spectrum (100 MHz) of $Cp^*Re(CO)_2(p\text{-}NHNC_6H_4OMe)$ (**4.10**) in acetone-d_6 at 233 K.

To verify that a second resonance was not hidden under the solvent resonance, the $^{13}C\{^1H\}$ NMR spectrum of **4.10** was reacquired at 233 K in methanol-d_4; the resultant spectrum was identical to that obtained previously using acetone-d_6. The observed single carbonyl resonance is consistent with a structure in which the CO ligands are made equivalent by virtue of the aryldiazene ligand adopting a position on the mirror plane containing the Cp* centroid and Re, and bisecting the angle subtended by the two CO ligands. This criterion strongly infers that the aryldiazene ligand is bound in an η^1 manner to the Re metal since a complex containing a rigid η^2-bound aryldiazene ligand (but not a fluxional one) is expected to adopt a pseudo four-legged piano-stool type geometry, thereby making the CO ligands inequivalent (Figure 4.9). This particular geometry was shown by crystal structure to be adopted for the related η^2-bonded diphenyldiazene complex $CpRe(CO)_2(N_2Ph_2)$.[144] Furthermore, to date, all previously reported aryldiazene complexes have been shown, or are believed to be, η^1-bonded to the metal center.

Surprisingly, the dicarbonyl and bis-trimethylphosphine aryldiazenido cations, **2.2** and **2.11** respectively, showed no evidence of undergoing reactions analogous to those of the closely related nitrosyl complex $[CpRe(CO)_2(NO)]^+$ with $NaBH_4$. The nitrosyl complex is capable of stepwise reduction of the CO group by $NaBH_4$ to HCO, CH_2OH, and CH_3 ligands.[145] Furthermore, precedence in the literature suggests that reactions of aryldiazenido complexes with borohydride typically give products arising from attack at the metal center (i.e., metal hydrido complex)[146] or attack at an ancillary ligand.[147] In contrast, the results just presented illustrate that H^- from the $NaBH_4$ reagent attacks the aryldiazenido complex **2.2** exclusively at the rhenium-bound nitrogen atom resulting in the novel conversion of the aryldiazenido complex to the identifiable aryldiazene complex **4.10**.[56] Remarkably, the replacement of both CO ligands by PMe_3 appears to block this reaction, as neither the corresponding aryldiazene nor the dinitrogen

complex was observed. Instead, the treatment of the bis-trimethylphosphine complex **2.11** with $NaBH_4$ resulted in no reaction at all. The differences in reactivity toward $NaBH_4$ shown by **2.2** and **2.11** are attributed to the relative electronic properties of the ancillary ligands (σ-donor or π-acceptor abilities). An increase in the electron donating ability of a ligand, as is achieved by substituting a CO group with PMe_3, causes an increase of electron density at the metal center which in turn leads to greater metal *d*-π*(NNAr) backbonding. The end result is that the rhenium center and the rhenium-bound nitrogen atom are made less susceptible to nucleophilic attack by H^-.

4.3.1.2. Reactions Involving the Triphenylmethyl Radical ($Ph_3C\cdot$)

Investigations conducted several years ago by co-workers in our laboratory on the cationic rhenium complex $[CpRe(CO)_2(N_2Ar)]^+$ suggested that the conversion of the rhenium-bound aryldiazenido group to ligated dinitrogen may follow a radical mechanism.[59, 61] To test the validity of this suggestion, a variety of cationic rhenium aryldiazenido complexes were treated with the triphenylmethyl radical ($Ph_3C\cdot$) and the products arising from these reactions were examined.

Addition of excess $Ph_3C\cdot$, formed from the reduction of Ph_3CCl with zinc dust in THF, to a solution of the cationic dicarbonyl aryldiazenido complexes **2.1** or **2.2** in CH_2Cl_2 at room temperature afforded the corresponding neutral dinitrogen complexes **4.1** and **4.2** respectively in moderate yield (Equation 4.3).

$$[Cp'Re(CO)_2(p\text{-}N_2C_6H_4OMe)][BF_4] \xrightarrow[CH_2Cl_2]{Ph_3C\cdot\ /\ THF} Cp'Re(CO)_2(N_2) + C_6H_5OMe \qquad (4.3)$$

Cp' = Cp or Cp*

In both cases the production of the dinitrogen complex was accompanied by the formation of a white precipitate. The precipitate was identified by melting point, ^1H NMR spectroscopy, and elemental analysis as the peroxide $Ph_3COOCPh_3$ which was formed from the oxidation of the $Ph_3C\cdot$ radical. Using freshly distilled and degassed solvents and high purity Ar as the inert atmosphere for the radical reactions prevented the formation of this peroxide.

A gas chromatogram of the solvent, which was removed under vacuum and condensed into a liquid nitrogen trap prior to the purification of the dinitrogen complexes **4.1** or **4.2**, indicated the presence of anisole (Equation 4.3). Notably, no evidence to support the formation of the radical addition product $Ph_3CC_6H_4OMe$ or Ph_3CCPh_3 was obtained. However, ^1H NMR spectroscopy and elemental analysis confirmed the presence of $[Ph_3C][BF_4]$. The formation of anisole and $[Ph_3C][BF_4]$ is consistent with an electron transfer mechanism for the conversion of the cationic dicarbonyl aryldiazenido complexes **2.1** or **2.2** to their respective neutral dinitrogen derivatives. The mechanism is believed to proceed by electron transfer from the triphenylmethyl radical ($Ph_3C\cdot$) to the metal complex, resulting in the formation of the stable triphenylmethyl cation Ph_3C^+ and an organometallic radical of the type Re-NNAr·. The organometallic species could then decompose to give the desired dinitrogen complex Re-NN and Ar·, and in turn, the organic radical could then abstract a hydrogen atom from the solvent to give anisole.

To confirm the existence of the organometallic radical Re-NNAr· the reaction between the triphenylmethyl radical and the aryldiazenido complex **2.2** was monitored by electron spin resonance (ESR) spectroscopy. However, no ESR signal was obtained when this reaction was carried out at ambient temperature or at low temperature (195 K). These results were not conclusive since these experiments would not detect radical species with very short lifetimes.

Interestingly, the addition of a large excess of the triphenylmethyl radical to a solution of the cationic carbonyl phosphine or phosphite aryldiazenido complexes **2.4** or **2.8** in CH_2Cl_2 did not yield the desired dinitrogen complexes **4.3** and **4.4** respectively, nor any other product. In fact, the starting aryldiazenido complexes **2.4** or **2.8** were recovered quantitatively even after the mixtures were allowed to stir for 24 h. Identical results were obtained for the bis(phosphorus-ligand) complexes **2.11**, **2.13**, and **2.14**.

4.3.1.3. Reactions Involving a One-electron Chemical Reduction

The results obtained from reactions between the cationic aryldiazenido complexes and the triphenylmethyl radical showed that $Ph_3C\cdot$ was particularly effective in converting the dicarbonyl aryldiazenido complexes **2.1** and **2.2** to their corresponding neutral dinitrogen complexes, but was completely ineffective in the analogous conversion of the phosphorus-substituted aryldiazenido complexes **2.4**, **2.8**, **2.11**, **2.13**, and **2.14** to their respective dinitrogen derivatives. To clarify these results, a systematic study involving the treatment of these cationic aryldiazenido complexes with a number of one-electron reducing agents was carried out.

Addition of excess cobaltocene (Cp_2Co) to a solution of the dicarbonyl aryldiazenido complexes **2.1** and **2.2** in acetone at room temperature gave the corresponding neutral dinitrogen complexes **4.1** and **4.2** in excellent yield (Equation 4.4).

$$[Cp'Re(CO)(L)(p\text{-}N_2C_6H_4OMe)][BF_4] \xrightarrow[\text{acetone}]{Cp_2Co} Cp'Re(CO)(L)(N_2) + C_6H_5OMe \qquad (4.4)$$

Cp' = Cp or Cp*
L = CO, $P(OMe)_3$

Unlike the triphenylmethyl radical chemistry mentioned previously, Cp_2Co was also effective in reducing the cationic carbonyl trimethylphosphite aryldiazenido complex **2.8** to its respective neutral dinitrogen complex **4.4** in good yield (Equation 4.4). Furthermore, anisole, confirmed by gas chromatography, was also formed in each of these reduction reactions (Equation 4.4). The salt $[Cp_2Co][BF_4]$ was also detected by ^1H NMR spectroscopy as a byproduct in these reduction reactions. Notably, when this reduction procedure was repeated for the carbonyl trimethylphosphine or bis(phosphorus-ligand) aryldiazenido complexes **2.4**, **2.11**, **2.13**, or **2.14**, the corresponding dinitrogen complexes were not produced. The fact that no reaction occurred at all inferred that the reduction potential of Cp_2Co was not sufficiently large enough to reduce these aryldiazenido complexes to their corresponding dinitrogen derivatives **4.3**, **4.5-4.7**. As a consequence, stronger reducing agents such as sodium metal were investigated as possible candidates for the production of the dinitrogen complexes **4.3**, **4.5-4.7** from their aryldiazenido precursors.

The effectiveness of sodium metal as a reducing agent was initially tested using the cationic dicarbonyl aryldiazenido complex **2.2** since the reduction of this complex to **4.2** had already been established. Treatment of a solution of **2.2** in liquid ammonia/THF with sodium metal did not give the desired dinitrogen complex **4.2** but instead the known neutral carbamoyl complex $Cp^*Re(CO)(CONH_2)(p\text{-}N_2C_6H_4OMe)$ **(4.11)** was produced,[61] and subsequently identified by IR and ^1H NMR spectroscopy. Complex **4.11** was also synthesized in the absence of Na by direct addition of **2.2**, as a solid, to liquid NH_3. The latter result strongly suggests that the ammonia, which was chosen as a solvent for the reduction reaction because it is capable of solubilizing the sodium metal, is responsible for the formation of the carbamoyl complex **4.11** prior to the addition of the reducing agent. Presumably the production of **4.11** results from nucleophilic attack of the amide ion NH_2^-, which is in equilibrium with NH_3, on the relatively electrophilic carbonyl

carbon atom in **2.2**. It is worth mentioning that repeating the Na/NH_3 reduction with a cationic aryldiazenido complex where the carbonyl ligands are replaced by PMe_3, such as **2.11**, did not yield the desired dinitrogen complex **4.3** either; instead, the dihydride complex *trans*-$Cp^*Re(PMe_3)_2H_2$ (***trans*-4.12**) was produced as characterized by ^1H and $^{31}P\{^1H\}$ NMR spectroscopy.

To prevent the formation of the carbamoyl complex **4.11** and thus allow complex **2.2** to react with the sodium metal and not the liquid ammonia, the reduction reaction was repeated using only THF as the solvent. Sonication of a mixture of sodium metal and **2.2** in THF afforded the dinitrogen complex **4.2** in poor yield. The production of **4.2**, even though the yield was low, suggested that the dinitrogen complex could be synthesized by sodium reduction of its aryldiazenido derivative. In an effort to increase the efficiency of the sodium reduction, the reactive surface area of the sodium was increased by preparing a sodium amalgam. Addition of a solution of **2.2** in THF to Na/Hg at room temperature gave exclusively the dinitrogen complex **4.2** in excellent yield. More importantly, treatment of the cationic carbonyl trimethylphosphine **2.4** or the bis(phosphorus-ligand) aryldiazenido complexes **2.11**, **2.13**, or **2.14** with Na/Hg afforded the neutral dinitrogen complexes **4.3**, **4.5-4.7** respectively in good yield (Equation 4.5).

$$[Cp^*Re(L_1)(L_2)(p\text{-}N_2C_6H_4OMe)][BF_4] \xrightarrow[THF]{Na/Hg} Cp^*Re(L_1)(L_2)(N_2) + C_6H_5OMe \qquad (4.5)$$

$L_1 = CO, L_2 = PMe_3$
$L_1 = L_2 = PMe_3$, dmpe, or $P(OMe)_3$

Once again, anisole was determined by gas chromatography to accompany the production of the dinitrogen complexes **4.3**, **4.5-4.7** (Equation 4.5). Notably, treatment of **2.1**, **2.2**, and **2.8** with Na/Hg also gave the corresponding dinitrogen complexes **4.1**, **4.2**, and **4.4**.

To summarize, the cationic rhenium aryldiazenido complexes **2.1**, **2.2**, **2.4**, **2.8**, **2.11**, **2.13**, or **2.14** were all converted to the corresponding neutral dinitrogen complexes **4.1-4.7** and anisole cleanly and efficiently at room temperature by using the appropriate one-electron reducing agent. The mechanism believed to be responsible for this conversion is illustrated in Scheme 4.4.

$$[Cp'Re(L_1)(L_2)(N_2Ar)]^+ \xrightarrow{e^-} Cp'Re(L_1)(L_2)(N_2Ar)$$

$$\longrightarrow Cp'Re(L_1)(L_2)(N_2) + Ar\cdot$$

$$\xrightarrow{\text{solvent}} ArH$$

Scheme 4.4. Proposed mechanism for the conversion of rhenium-bound aryldiazenido to ligated dinitrogen (Ar = *p*-C_6H_4OMe).

The initial step in this mechanism is the transfer of one-electron from the reducing agent (i.e., Cp_2Co, Na/Hg, or as described in the previous section $Ph_3C\cdot$) to the cationic aryldiazenido complex to give the neutral 19-electron intermediate. Once formed this unstable intermediate then decomposes to produce the desired dinitrogen complex and the *p*-methoxyphenyl radical. The organic radical then abstracts a hydrogen from the solvent to give anisole. IR or NMR spectroscopy, used to monitor these reduction reactions, provided no evidence to confirm the existence of the proposed 19-electron intermediate.

4.3.1.4. Reactions Involving a One-electron Electrochemical Reduction

The suggestion that a one-electron chemical reduction was responsible for the conversion of the cationic aryldiazenido ligand to the neutral dinitrogen moiety was quantitatively corroborated by electrochemical measurements conducted on the complexes **2.1**, **2.2**, **2.4**, **2.8**, **2.11**, **2.13**, and **2.14**. The cyclic voltammograms of these complexes displayed in each case a single irreversible cathodic wave which was representative of the reduction potential required to convert the aryldiazenido complexes to their corresponding neutral aryldiazenido complexes (Table 4.2).

For these complexes the relative electronic properties of the Cp, Cp*, or phosphorus ligands were revealed by differences in the reduction potentials which were obtained. For example, the Cp dicarbonyl aryldiazenido complex **2.1** was found to have a smaller negative value for the reduction potential (-0.46 V) than its methylated analogue **2.2** (-0.62 V). Furthermore, the reduction potentials for the remaining aryldiazenido complexes follow the order of the co-ligands $(PMe_3)_2$ (**2.11**, -1.89 V) > dmpe (**2.13**, -1.74 V) > $\{P(OMe)_3\}_2$ (**2.14**, -1.41 V) > $(CO)(PMe_3)$ (**2.4**, -1.24 V) > $(CO)\{P(OMe)_3\}$ (**2.8**, -0.98 V). Taken together, these results suggest that an increase in the σ-donor ability (or decrease in the π-acceptor ability) of an ancillary ligand leads to an increase in the magnitude of the reduction potential. Thus, substituting Cp by Cp* (**2.1** $\rightarrow$ **2.2**) or a CO ligand by PMe_3 (**2.2** $\rightarrow$ **2.4**) leads to a significant increase in the reduction potential and as a result the *chemical* reduction of these aryldiazenido complexes to the corresponding dinitrogen complexes becomes dependent on the reduction potential of the chemical reagent which is used. For example, it was previously demonstrated that Cp_2Co was capable of reducing the aryldiazenido complexes **2.1**, **2.2**, and **2.8** to their respective dinitrogen complexes **4.1**, **4.2**, and **4.4** but was incapable of reducing the remaining aryldiazenido complexes. These results are in agreement with the reduction potential of Cp_2Co, which was reported to be *ca.* -0.9 V vs

SCE in CH_2Cl_2.[148] Similarly, the reduction potential of sodium is *ca.* -3.0 V vs SCE,[130b] and therefore it is not surprising that Na/Hg was shown to be capable of reducing all the aryldiazenido complexes to the corresponding dinitrogen derivatives. More importantly, the CV data also clarifies the inconsistency provided by the results obtained previously for the reactions involving the cationic aryldiazenido complexes and the triphenylmethyl radical ($Ph_3C\cdot$). Specifically, the fact that $Ph_3C\cdot$ was capable of reducing the dicarbonyl complexes **2.1** and **2.2** but not the phosphorus-substituted complexes **2.4**, **2.8**, **2.11**, **2.13**, and **2.14** to their corresponding nitrogen derivatives suggests that the reduction capacity of $Ph_3C\cdot$ is of the order of the reduction potential determined for the Cp* dicarbonyl aryldiazenido complex **2.2** (-0.62 V). The reduction potential of $Ph_3C\cdot$, to the best of our knowledge, has not been reported in the literature.

Further evidence to support an electron transfer mechanism for the observed transformation of the aryldiazenido moiety to the respective dinitrogen derivative was provided by the application of fast scan rate cyclic voltammetry (CV), scanning electrochemical microscopy (SECM), and controlled potential electrolysis (CPE) to the cationic aryldiazenido complex $[Cp^*Re(CO)_2(p\text{-}N_2C_6H_4OMe)][BF_4]$ (**2.2**). The fast scan rate CV and SECM analyses reported in this chapter were conducted by Professor Allen J. Bard and Dr. Thomas C. Richards at the University of Texas at Austin (see Experimental section of this chapter).

Assuming that **2.2** is reduced to the neutral 19-electron complex $Cp^*Re(CO)_2(p\text{-}N_2C_6H_4OMe)$ which then decomposes to give products (Equation 4.6) allows treatment as an electrochemical E_rC_i mechanism[149] following Equations 4.7 and 4.8 wherein O and R correspond to the cationic and neutral forms of the rhenium complex respectively and P designates products. Both fast scan rate CV and SECM are useful techniques for studying the kinetics of chemical reactions coupled to electron transfer[132, 133] and can be

used to determine the rate constant (k_c) for the decomposition of the neutral 19-electron complex (R) to products (P).

$$[Cp^*Re(CO)_2(p\text{-}N_2C_6H_4OMe)]^+ \xrightarrow{e^-} Cp^*Re(CO)_2(p\text{-}N_2C_6H_4OMe)$$

$$\longrightarrow Cp^*Re(CO)_2(N_2) \qquad (4.6)$$

$$O + e^- \longrightarrow R \qquad (4.7)$$

$$R \xrightarrow{k_c} P \qquad (4.8)$$

The cyclic voltammogram of **2.2** exhibited a reversible one-electron wave with a cathodic peak potential of -0.66 V corresponding to the reduction of **2.2** to the neutral 19-electron complex $Cp^*Re(CO)_2(p\text{-}N_2C_6H_4OMe)$ (Figure 4.5). A return wave for the oxidation of the neutral 19-electron complex was first resolved at 10 V/s and became well-defined at 50 V/s. CV spectra were obtained at fast enough scan rates such that the cathodic and anodic peak potentials were independent of the scan rate, and their peak-to-peak separation approached a value of 60 mV expected for a one-electron reversible process. Digital simulation[129] of these cyclic voltammograms assuming an electrochemical E_rC_i mechanism afforded a rate constant (k_c) of 145 ± 10 s^{-1} for the decomposition of the neutral 19-electron complex (R) to products (P) (Figure 4.5). The validity of this rate constant was supported by SECM[130-136] which also gave a value of 145 s^{-1} for k_c.

The CPE study lends further support to the electrochemical E_rC_i mechanism. Exhaustive controlled potential electrolysis of **2.2** (60 min.) at -0.62 V versus SCE indicated the consumption of one equivalent of electrons. This result is obviously consistent with the production of the neutral 19-electron complex (Equation 4.6) and its

subsequent decomposition. Notably, exhaustive CPE of the Cp dicarbonyl (**2.1**) and the carbonyl trimethylphosphine (**2.4**) aryldiazenido complexes also established these reactions to be clean one-electron processes.

Monitoring the progress of the electrolysis for **2.2** by IR spectroscopy showed the production of the neutral dinitrogen complex $Cp^*Re(CO)_2(N_2)$ (**4.2**) which was accompanied by the complete disappearance of **2.2** (Figure 4.6). Upon completion of the electrolysis, the solvent and volatiles were removed by vacuum and a gas chromatogram of the condensate confirmed the presence of anisole, as expected to result from hydrogen abstraction from the solvent by the *p*-methoxyphenyl radical formed in the irreversible chemical step. Once again, similar results were observed for the aryldiazenido complexes **2.1** and **2.4**. These electrochemical results firmly establish the existence of the 19-electron intermediate which was proposed previously but never detected spectroscopically by IR, NMR, or ESR because of its short lifetime.

4.3.2. Mechanism of Formation of Ligated Dinitrogen from Rhenium-bound Aryldiazenido

The chemistry displayed by rhenium aryldiazenido complexes, in particular, the unique transformation by which they proceed to ligated dinitrogen was found to be dependent on the particular chemical reagent used. The cationic dicarbonyl aryldiazenido complex **2.2** can be converted to the corresponding dinitrogen complex **4.2** by reaction with $NaBH_4$. The mechanism for this conversion involves initial H^- attack at the rhenium-bound nitrogen atom to give the neutral aryldiazene complex $Cp^*Re(CO)_2(p\text{-}NHNC_6H_4OMe)$ (**4.10**), which then eliminates anisole resulting in the formation of the respective neutral dinitrogen complex **4.2**. This mechanism appears to be dependent on the electronic properties of the ancillary ligands in complex **2.2**; ligands such as CO which remove electron density from the metal center and to some degree the

metal-bound nitrogen are believed to facilitate this mechanism whereas ligands such as PMe_3 which have the opposite electronic properties do not. Thus, treatment of the bis-PMe_3 aryldiazenido complex **2.11** with $NaBH_4$ does not afford the respective dinitrogen complex nor any product at all. However, complex **2.2** as well as all the other cationic aryldiazenido complexes which were investigated (**2.1**, **2.4**, **2.8**, **2.11**, **2.13**, and **2.14**) can be converted to their corresponding dinitrogen complexes by reaction with a suitable one-electron reducing agent. The initial step in this mechanism is the transfer of one-electron from the reducing agent to the cationic aryldiazenido complex to give the neutral 19-electron intermediate. Once formed this unstable intermediate then decomposes to produce the desired dinitrogen complex and the *p*-methoxyphenyl radical. The organic radical then abstracts a hydrogen from the solvent to give anisole. This mechanism appears to be independent of the electronic properties of the ancillary ligands in the respective aryldiazenido complexes. Although these properties influence the particular reduction potential required for conversion to the corresponding dinitrogen derivatives, their influence can be compensated for by selecting a suitable reducing agent and thus the mechanism remains unaffected.

As alluded to in the Introduction to this chapter, investigations conducted several years ago by co-workers in our laboratory on the cationic manganese complexes $[(\eta^5\text{-}C_5H_4Me)Mn(CO)_2(N_2Ar)]^+$ suggested that the conversion of the metal-bound aryldiazenido group to the corresponding neutral ligated dinitrogen complex by reaction with a halide ion X^- ($X^- = I^-$, Br^-, or Cl^-) was consistent with a nucleophilic displacement mechanism. Indeed, this type of mechanism was suggested by Chatt et al. to occur in the only other example that we know of, in which an organodiazenido ligand is transformed into ligated dinitrogen.[120, 121] This is the reaction of the benzoyldiazenido complex $ReCl_2(PPh_3)_2(N_2COPh)$ with phosphines in methanol, previously illustrated in Scheme 4.1. It was suggested that this reaction is initiated by nucleophilic attack of

methanol or methoxide ion on the carbonyl carbon since methylbenzoate was also produced. My investigations into the conversion of the aryldiazenido group to the corresponding ligated dinitrogen at a rhenium metal center by using the reagents presented here have yielded no evidence in support of a nucleophilic displacement mechanism.

4.4. Conclusion

In this chapter, a series of neutral dinitrogen complexes of the type $Cp'Re(L_1)(L_2)(N_2)$ ((a) Cp' = Cp; $L_1 = L_2 = CO$ (**4.1**),[123, 124] (b) Cp' = Cp*; L_1 = CO; $L_2 = PMe_3$ (**4.3**)[59] or $P(OMe)_3$ (**4.4**),[59] and (c) Cp' = Cp*; $L_1 = L_2 = CO$ (**4.2**),[59] PMe_3 (**4.5**), dmpe (**4.6**), or $P(OMe)_3$ (**4.7**)) were synthesized cleanly, quickly, and in high yield from the corresponding cationic aryldiazenido complexes. This conversion was shown to be consistent with two different mechanisms. First, reaction of the cationic dicarbonyl aryldiazenido complex **2.2** with $NaBH_4$ results in initial H^- attack at the rhenium-bound nitrogen atom to give the neutral aryldiazene complex $Cp^*Re(CO)_2(p\text{-}NHNC_6H_4OMe)$ (**4.10**), which then eliminates anisole resulting in the formation of the respective neutral dinitrogen complex **4.2**. Second, treatment of any of the cationic aryldiazenido complexes **2.1**, **2.2**, **2.4**, **2.8**, **2.11**, **2.13**, and **2.14** with a suitable one-electron reducing agent leads to the initial transfer of one-electron from the reducing agent to the cationic aryldiazenido complex to give a neutral 19-electron intermediate. Once formed this unstable intermediate then decomposes to produce the desired dinitrogen complex and the *p*-methoxyphenyl radical which then abstracts a hydrogen from the solvent to give anisole. This one-electron reduction mechanism was corroborated by cyclic voltammetry (CV), scanning electrochemical microscopy (SECM), and controlled potential electrolysis (CPE).

4.5. Experimental

4.5.1. General Methods

Manipulations, solvent purification, and spectroscopic measurements were carried out as described in Chapter 2. Acetone-d_6, $CDCl_3$, CD_3CN, and benzene-d_6 were used as the solvents for all the NMR spectra recorded at ambient temperatures. All NMR data were recorded on a Bruker AMX 400 instrument at an operating frequency of 400, 162, 100, 40.6, and 28.9 MHz for ^1H, ^{31}P, ^{13}C, ^{15}N, and ^{14}N nuclei respectively. The term "virtual doublet" refers to the non-first-order multiplet which is seen in some of the ^1H NMR spectra; the apparent coupling constant is given by the separation between the two outside peaks. Electron spin resonance (ESR) spectra were recorded both at room temperature and at low temperature on a Varian E-4 instrument. Gas chromatography of the solutions after chemical and electrochemical reductions were complete was performed on a Hewlett-Packard 5890 A Series gas chromatograph containing a DB-1 capillary column and equipped with a Hewlett-Packard 3392 A integrator. Identification of the chromatographic peak for anisole was made by comparison with that of the authentic compound.

The cationic rhenium aryldiazenido complexes used in this chapter were prepared and purified following the protocol established in Chapter 2. Methanol was distilled from calcium sulfate under nitrogen and used immediately. Hexamethylphosphoramide (HMPA) (Aldrich Chemical Co.) was distilled from calcium hydride and stored over 4A molecular sieve, which had been activated by drying under vacuum at 573 K for several days.

Anisole (Fisher Scientific Co.) was used as received. Sodium metal (BDH Chemicals Ltd.) was washed with hexane prior to use and was cut from a piece prior to use to ensure an unhydrolysed surface. Mercury (Aldrich) was cleaned by filtration

through fine filter paper and then distilled under vacuum. Ammonia gas (Linde Union Carbide) was used as purchased. Sodium borohydride (BDH) and lithium aluminum hydride (Alfa Products, Ventron Division) were used as purchased and were stored under nitrogen. The triphenylmethyl radical ($Ph_3C\cdot$) was synthesized by zinc (Aldrich) reduction of triphenylchloromethane (Ph_3CCl)[150] which was prepared initially by reaction of triphenylmethanol (Ph_3COH) (Aldrich) with acetyl chloride (Fisher Scientific Co.).[151] Cobaltocene (Cp_2Co) was prepared by reaction of anhydrous cobalt (II) chloride (Alfa) with sodium cyclopentadienide prepared from sodium and dicyclopentadiene (Aldrich)[152] and was sublimed under vacuum onto a dry ice-cooled cold-finger before use.

^1H and ^{13}C NMR chemical shifts are reported in ppm downfield (positive) of tetramethylsilane. ^{31}P NMR chemical shifts are referenced to 85% H_3PO_4. ^{14}N and ^{15}N NMR chemical shifts are referenced to external nitromethane ($MeNO_2$). The low temperature ^1H, ^{13}C, and ^{15}N NMR spectra of complex **4.10** were obtained in a similar manner to that outlined in Chapter 3. Acetone-d_6 (Isotec Inc.) and methanol-d_4 (Isotec) were used as solvents for all the low temperature NMR work.

4.5.2. Syntheses

The bis-trimethylphosphine dinitrogen complex **4.5** was prepared with the ^{15}N isotopic label at either the rhenium-bound nitrogen atom (N_α) or at the terminal nitrogen atom (N_β). The importance of the ^{15}N isotopic label being introduced exclusively at either N_α or N_β is demonstrated in this chapter and in Chapters 5 and 6 as well. ^{14}N and ^{15}N NMR data are given in this chapter as characterization for complexes **4.1-4.5** but will be discussed in detail in Chapter 5.

Preparation of $CpRe(CO)_2(N_2)$ (4.1) and (4.1-$^{15}N_\alpha$). A 5-fold stoichiometric excess of Cp_2Co was dissolved in a minimum amount of acetone (5 mL) and then added

via syringe to a solution of the cationic dicarbonyl complex **2.1** or **2.1-$^{15}N_{\alpha}$** (100 mg, 0.189 mmol) in acetone (10 mL) at room temperature. The IR spectrum of this mixture recorded immediately after the cobaltocene addition showed the total disappearance of the cationic complex and only the presence of absorptions due to the dinitrogen complex **4.1** or **4.1-$^{15}N_{\alpha}$**. Diethyl ether (20 mL) was added to precipitate the cobaltocenium cation (Cp_2Co^+) and the solution was stirred for 30 min. The solution was then filtered through a short column of Celite and the solvent was removed under vacuum to give a pale brown oil. The oil was then absorbed by a small amount of neutral alumina, dried under vacuum, and the mixture was then added to the top of a neutral alumina column and then chromatographed. Elution with hexane afforded **4.1** or **4.1-$^{15}N_{\alpha}$** as a pale yellow colored microcrystalline solid in 87% yield (55 mg, 0.16 mmol). IR (hexane): 2145 cm^{-1} ν(NN) (2110 cm^{-1} for $^{15}N_{\alpha}$ labeled complex); 1973, 1919 cm^{-1} ν(CO). ^1H NMR ($CDCl_3$): δ 5.23 (s, 5H, Cp). $^{13}C\{^1H\}$ NMR ($CDCl_3$): δ 93.72 (s, Cp), 195.79 (s, CO). ^{15}N NMR (acetone-d_6): δ -120.9 (s, $^{15}N_{\alpha}$). ^{14}N NMR (acetone-d_6): δ -120 (s, $^{14}N_{\alpha}$), -26 (s, $^{14}N_{\beta}$). M.S. (EI): m/z 336 (337 in **4.1-$^{15}N_{\alpha}$**) (M^+), 308 ($M^+ - N_2$). Anal. Calcd: C, 25.06; H, 1.49; N, 8.35. Found: C, 24.97; H, 1.71; N, 8.43.

Preparation of Cp*Re(CO)$_2$(N$_2$) (4.2) and (4.2-$^{15}N_{\alpha}$). A 5-fold stoichiometric excess of Cp_2Co was dissolved in a minimum amount of acetone (5 mL) and then added *via* syringe to a solution of the cationic dicarbonyl complex **2.2** or **2.2-$^{15}N_{\alpha}$** (100 mg, 0.167 mmol) in acetone (10 mL) at room temperature. The IR spectrum of this mixture recorded immediately after the cobaltocene addition showed the total disappearance of the cationic complex and only the presence of absorptions corresponding to the dinitrogen complex **4.2** or **4.2-$^{15}N_{\alpha}$**. Purification following the procedure used for complex **4.1** gave **4.2** or **4.2-$^{15}N_{\alpha}$** as a pale yellow colored microcrystalline solid in 89% yield (60 mg, 0.15 mmol). IR (hexane): 2125 cm^{-1} ν(NN) (2092 cm^{-1} for $^{15}N_{\alpha}$ labeled complex); 1954, 1902 cm^{-1} ν(CO). ^1H NMR ($CDCl_3$): δ 2.09 (s, 15H, Cp*). $^{13}C\{^1H\}$

NMR ($CDCl_3$): δ 10.38 (s, $C_5\underline{Me}_5$), 96.27 (s, $\underline{C}_5Me_5$), 200.09 (s, CO). ^{15}N NMR (acetone-d_6): δ -110.8 (s, $^{15}N_\alpha$). ^{14}N NMR (acetone-d_6): δ -110 (s, $^{14}N_\alpha$), -26 (s, $^{14}N_\beta$). M.S. (EI): m/z 406 (407 in **4.2-$^{15}N_\alpha$**) (M^+), 378 ($M^+ - N_2$). Anal. Calcd: C, 35.55; H, 3.70; N, 6.91. Found: C, 35.52; H, 3.74; N, 6.98.

Preparation of Cp*Re(CO)(PMe_3)(N_2) (4.3) and (4.3-$^{15}N_\alpha$). A sodium amalgam was prepared by adding small freshly cut pieces of sodium metal (5-fold stoichiometric excess) to a pool of mercury (5 mL) under argon; with gentle stirring the sodium pieces were taken up by the mercury. The orange-brown solution of the cationic carbonyl phosphine complex **2.4** or **2.4-$^{15}N_\alpha$** (100 mg, 0.155 mmol) in THF (10 mL) was then added *via* syringe to the sodium amalgam at room temperature and the mixture was vigorously stirred for 30 min. An IR spectrum of the resulting yellow-brown solution recorded at this time showed the total disappearance of the cationic complex and only the presence of absorptions corresponding to the dinitrogen complex **4.3** or **4.3-$^{15}N_\alpha$**. The solution was then filtered through a short column of Celite and the solvent was removed under vacuum to give a pale brown oil. The oil was then absorbed by a small amount of neutral alumina, dried under vacuum, and the mixture was then added to the top of a neutral alumina column and then chromatographed. Elution with hexane afforded **4.3** or **4.3-$^{15}N_\alpha$** as a pale yellow colored microcrystalline solid in 82% yield (58 mg, 0.13 mmol). IR (hexane): 2044 cm^{-1} ν(NN) (2011 cm^{-1} for $^{15}N_\alpha$ labeled complex); 1865 cm^{-1} ν(CO). ^1H NMR ($CDCl_3$): δ 1.57 (d, 9H, PMe_3, J_{H-P} = 8.7 Hz), 2.00 (d, 15H, Cp*, J_{H-P} = 0.7 Hz). $^{13}C\{^1H\}$ NMR ($CDCl_3$): δ 10.76 (s, $C_5\underline{Me}_5$), 20.67 (d, PMe_3, J_{C-P} = 33 Hz), 93.29 (s, $\underline{C}_5Me_5$), 207.18 (d, CO, J_{C-P} = 7 Hz). $^{31}P\{^1H\}$ NMR ($CDCl_3$): δ -29.86 (s, PMe_3). ^{15}N NMR (acetone-d_6): δ -91.3 (s, $^{15}N_\alpha$). ^{15}N NMR (CD_3CN): δ -93.2 (s, $^{15}N_\alpha$). ^{14}N NMR (acetone-d_6): δ -91 (s, $^{14}N_\alpha$), -30 (s, $^{14}N_\beta$). M.S. (EI): m/z 454 (M^+), 426 ($M^+ - N_2$). Anal. Calcd: C, 37.08; H, 5.30; N, 6.16. Found: C, 36.92; H, 5.42; N, 6.28.

Preparation of Cp*Re(CO){P(OMe)$_3$}(N$_2$) (4.4) and (4.4-$^{15}N_\alpha$). A procedure similar to that described for the preparation of **4.2** was used. The carbonyl phosphite dinitrogen complex **4.4** or **4.4-$^{15}N_\alpha$** was obtained in 79% yield as a pale yellow microcrystalline solid (57 mg, 0.11 mmol). IR (hexane): 2078, 2066 cm^{-1} ν(NN) (2045, 2033 cm^{-1} for $^{15}N_\alpha$ labeled complex); 1877 cm^{-1} ν(CO). ^{1}H NMR ($CDCl_3$): δ 2.04 (d, 15H, Cp*, J_{H-P} = 0.8 Hz), 3.52 (d, 9H, P(OMe)$_3$, J_{H-P} = 12.1 Hz). $^{13}C\{^1H\}$ NMR ($CDCl_3$): δ 10.31 (s, $C_5\underline{Me}_5$), 51.27 (s, P(OMe)$_3$), 94.15 (s, $\underline{C}_5Me_5$), 204.96 (d, CO, J_{C-P} = 12 Hz). $^{31}P\{^1H\}$ NMR ($CDCl_3$): δ 139.12 (s, P(OMe)$_3$). ^{15}N NMR (acetone-d_6): δ -99.4 (s, $^{15}N_\alpha$). ^{15}N NMR (CD_3CN): δ -100.8 (s, $^{15}N_\alpha$). ^{14}N NMR (acetone-d_6): δ -99 (s, $^{14}N_\alpha$), -29 (s, $^{14}N_\beta$). M.S. (EI): m/z 502 (M$^+$), 474 (M$^+$ - N$_2$). Anal. Calcd: C, 33.46; H, 4.78; N, 5.57. Found: C, 33.37; H, 4.89; N, 5.69.

Preparation of Cp*Re(PMe$_3$)$_2$(N$_2$) (4.5), (4.5-$^{15}N_\alpha$), and (4.5-$^{15}N_\beta$). A procedure similar to that described for the preparation of **4.3** was used. The bis-trimethylphosphine dinitrogen complex **4.5**, **4.5-$^{15}N_\alpha$**, or **4.5-$^{15}N_\beta$** (synthesized from **2.17-$^{15}N_\beta$**) was obtained in 74% yield as a pale yellow microcrystalline solid (53 mg, 0.11 mmol). IR (hexane): 1975 cm^{-1} ν(NN) (1943 cm^{-1} for $^{15}N_\alpha$ or $^{15}N_\beta$ labeled complex). ^{1}H NMR (acetone-d_6): δ 1.48 (virtual doublet, 18H, PMe_3, J_{app} = 7.4 Hz), 1.88 (t, 15H, Cp*, J_{H-P} = 0.7 Hz). $^{31}P\{^1H\}$ NMR (acetone-d_6): δ -35.31 (s, PMe_3). ^{15}N NMR (acetone-d_6): δ -82.1 (s, $^{15}N_\alpha$), -51.7 (s, $^{15}N_\beta$). ^{14}N NMR (acetone-d_6): δ -82 (s, $^{14}N_\alpha$), -49 (s, $^{14}N_\beta$). M.S. (EI): m/z 502 (M$^+$), 474 (M$^+$ - N$_2$). Anal. Calcd: C, 38.31; H, 6.58; N, 5.59. Found: C, 38.01; H, 6.92; N, 5.87.

Preparation of Cp*Re(dmpe)(N$_2$) (4.6). A procedure similar to that described for the preparation of **4.3** was used. The bidentate phosphine dinitrogen complex **4.6** was obtained in 79% yield as a pale yellow microcrystalline solid (57 mg, 0.11 mmol). IR (hexane): 1977 cm^{-1} ν(NN). ^{1}H NMR (acetone-d_6): δ 1.33 (d, 6H, $P\underline{Me}_2CH_2CH_2\underline{Me}_2P$, J_{H-P} = 7.9 Hz), 1.35 (m, 4H, $PMe_2C\underline{H}_2C\underline{H}_2Me_2P$), 1.42 (d, 6H, $P\underline{Me}_2CH_2CH_2\underline{Me}_2P$, J_{H-P} =

7.8 Hz), 1.92 (s, 15H, Cp*). $^{31}P\{^1H\}$ NMR (acetone-d_6): δ -16.88 (s, dmpe). M.S. (EI): m/z 500 (M^+), 472 ($M^+ - N_2$). Anal. Calcd: C, 38.46; H, 6.21; N, 5.61. Found: C, 38.22; H, 6.37; N, 5.81.

Preparation of $Cp^*Re\{P(OMe)_3\}_2(N_2)$ (4.7). A procedure similar to that described for the preparation of **4.3** was used. The bis-trimethylphosphite dinitrogen complex **4.7** was obtained in 71% yield as a pale yellow microcrystalline solid (54 mg, 0.090 mmol). IR (hexane): 2014 cm^{-1} ν(NN). ^1H NMR (acetone-d_6): δ 1.87 (t, 15H, Cp*, J_{H-P} = 0.8 Hz), 3.45 (virtual doublet, 18H, $P(OMe)_3$, J_{app} = 11.5 Hz). $^{31}P\{^1H\}$ NMR (acetone-d_6): δ 138.80 (s, $P(OMe)_3$). M.S. (EI): m/z 598 (M^+), 570 ($M^+ - N_2$). Anal. Calcd: C, 32.15; H, 5.53; N, 4.69. Found: C, 31.79; H, 5.78; N, 4.93.

Reaction of $[Cp^*Re(CO)_2(p\text{-}N_2C_6H_4OMe)][BF_4]$ (2.2) with $LiAlH_4$. A 2-fold stoichiometric excess of $LiAlH_4$ was added as a solid to a solution of the cationic dicarbonyl complex **2.2** (50 mg, 0.083 mmol) in methanol (10 mL) at room temperature. Upon addition, an immediate reaction occurred, with considerable gas evolution, and the color of the solution changed from red-brown to yellow. The solution was then filtered through a short column of Celite. Removal of the solvent under vacuum and subsequent extraction with hexane (3 x 20 mL) gave the methoxycarbonyl complex $Cp^*Re(CO)(COOMe)(p\text{-}N_2C_6H_4OMe)$ (**4.9**) as a yellow solid in 89% yield (40 mg, 0.074 mmol). The dinitrogen complex **4.2** was not formed in this reaction. IR (MeOH): 1937 cm^{-1} ν(CO); 1632 cm^{-1} ν(NN); 1614 ν(COOMe). ^1H NMR ($CDCl_3$): δ 2.10 (s, 15H, Cp*), 3.66 (s, 3H, COOMe), 3.82 (s, 3H, OMe), 6.93 (d, 2H, C_6H_4), 7.45 (d, 2H, C_6H_4).

Reaction of $[Cp^*Re(CO)_2(p\text{-}N_2C_6H_4OMe)][BF_4]$ (2.2) with $NaBH_4$. A 2-fold stoichiometric excess of $NaBH_4$ was added as a solid to a solution of the cationic dicarbonyl complex **2.2** (50 mg, 0.083 mmol) in acetone (10 mL) at room temperature. An instantaneous reaction took place and the color of the solution changed from red-

brown to deep red. An IR spectrum of this solution demonstrated the total disappearance of **2.2** and the presence of minor absorptions corresponding to the dinitrogen complex **4.2** which were also accompanied by major absorptions at 1917 and 1852 cm^{-1}. The solution was stirred for 1 h during which time the color of the solution changed from red to yellow. An IR spectrum then obtained showed only the presence of **4.2**; the absorptions due to the unknown complex had disappeared. The solvent was removed under vacuum to give a yellow oil. The oil was then absorbed by a small amount of neutral alumina, dried under vacuum, and the mixture was then added to the top of a neutral alumina column and then chromatographed. Elution with hexane afforded **4.2** in 47% yield (16 mg, 0.039 mmol).

Low Temperature ^1H, $^{13}C\{^1H\}$, and ^{15}N NMR Experiments: Reaction of $[Cp^*Re(CO)_2(p\text{-}N_2C_6H_4OMe)][BF_4]$ (2.2) or (2.2-$^{15}N_\alpha$) with $NaBH_4$. A solution of the cationic dicarbonyl complex **2.2** or **2.2-$^{15}N_\alpha$** in acetone-d_6 was transferred to an NMR tube (5 mm tube for ^1H and $^{13}C\{^1H\}$; 10 mm tube for ^{15}N) which was kept in a Schlenk tube under a positive pressure of argon. The Schlenk tube containing the NMR solution was then cooled to 195 K in a dry ice-acetone bath. With a strong purge of argon, addition of a 2-fold stoichiometric excess of solid $NaBH_4$ directly to the NMR tube then lead to the formation of a deep red solution. The NMR tube was then quickly removed from the cold temperature bath and placed into the Bruker AMX 400 spectrometer whose cooling unit had been previously set to 233 K. The NMR sample was allowed to equilibrate for 30 min at this temperature before spectral acquisition. An identical procedure was used for obtaining spectra for each of the NMR active nuclei. The species responsible for the red colored solution was assigned as the neutral aryldiazene complex $Cp^*Re(CO)_2(p\text{-}NHNC_6H_4OMe)$ (**4.10**) or (**4.10-$^{15}N_\alpha$**). IR (acetone): 1917, 1852 cm^{-1} ν(CO). ^1H NMR (acetone-d_6, 233 K): δ 2.02 (s, 15H, Cp*), 3.83 (s, 3H, OMe), 6.97 (d, 2H, C_6H_4), 7.60 (d, 2H, C_6H_4), 15.68 (broad singlet, 1H, NH) (d, 1H, $^{15}N_\alpha H$, $J_{H\text{-}N} = 69$

Hz). $^{13}C\{^1H\}$ NMR (acetone-d_6, 233 K): δ 10.15 (s, $C_5\underline{Me}_5$), 55.58 (s, OMe), 99.35 (s, $\underline{C}_5Me_5$), 115.13, 120.99, 149.80, 160.03 (s, C_6H_4), 208.32 (s, CO). $^{13}C\{^1H\}$ NMR (methanol-d_4, 233 K): δ 10.19 (s, $C_5\underline{Me}_5$), 55.61 (s, OMe), 99.41 (s, $\underline{C}_5Me_5$), 115.32, 121.22, 149.97, 160.65 (s, C_6H_4), 208.79 (s, CO). ^{15}N NMR (acetone-d_6, 233 K): δ -46.7 (d, $^{15}N_\alpha H$, $J_{N\text{-}H}$ = 69 Hz).

Reaction of [Cp*Re(CO)$_2$(*p*-N$_2$C$_6$H$_4$OMe)][BF$_4$] (2.2) with HMPA. The cationic dicarbonyl complex **2.2** (50 mg, 0.083 mmol) was added directly to neat hexamethylphosphoramide (HMPA) (10 mL) at room temperature. An IR spectrum recorded immediately after the addition showed the presence of absorptions corresponding to the starting material **2.2** as well as the newly formed dinitrogen complex **4.2**. The solution was allowed to stir for 24 h. No apparent color change was noted. An IR spectrum obtained at this time displayed the complete disappearance of the cationic complex and only the presence of absorptions due to **4.2**. The dinitrogen complex was then extracted with diethyl ether (2 x 20 mL) and the extractions were then filtered through a column of Celite. The solvent was removed under vacuum to give a pale brown oil. The oil was then absorbed by a small amount of neutral alumina, dried under vacuum, and the mixture was then added to the top of a neutral alumina column and then chromatographed. Elution with hexane afforded **4.2** in 35% yield (12 mg, 0.029 mmol).

Reaction of [Cp*Re(CO)$_2$(*p*-N$_2$C$_6$H$_4$OMe)][BF$_4$] (2.2) with PMe$_3$. A 10-fold stoichiometric excess of neat PMe_3 was added *via* syringe to a solution of the cationic dicarbonyl complex **2.2** (50 mg, 0.083 mmol) in acetone (10 mL) at room temperature. The solution was allowed to stir for 30 min. No apparent color change was noted after this time. An IR spectrum of this solution showed the total disappearance of the cationic complex and only the presence of absorptions corresponding to the dinitrogen complex **4.2**. The solvent was then removed under vacuum and the remaining pale brown oil was

extracted with diethyl ether (2 x 20 mL). The ether extractions were then concentrated to *ca.* 2 mL under vacuum and chromatographed on a neutral alumina column. Elution with hexane produced **4.2** in 42% yield (14 mg, 0.035 mmol).

Reaction of [CpRe(CO)$_2$(*p*-N$_2$C$_6$H$_4$OMe)][BF$_4$] (2.1) with Ph$_3$C·. A solution of the triphenylmethyl radical (Ph$_3$C·) (commonly referred to as the trityl radical) was prepared by reduction of the corresponding chloride Ph$_3$CCl with zinc dust in THF. A 10-fold stoichiometric excess of the yellow colored triphenylmethyl radical solution was then added by cannula to an orange-brown solution of the cationic dicarbonyl complex **2.1** (50 mg, 0.095 mmol) in CH_2Cl_2 (10 mL) at room temperature. The resulting orange solution was allowed to stir for 30 min. An IR spectrum measured at this time showed the total disappearance of **2.1** and the presence of absorptions corresponding exclusively to the dinitrogen complex **4.1**. The solvent was then removed under vacuum and the remaining pale brown oil was extracted with diethyl ether (2 x 20 mL). The ether extractions were then concentrated to *ca.* 2 mL under vacuum and chromatographed on a neutral alumina column. Elution with hexane yielded **4.1** in 58% yield (18 mg, 0.055 mmol).

Reaction of [Cp*Re(CO)$_2$(*p*-N$_2$C$_6$H$_4$OMe)][BF$_4$] (2.2) with Ph$_3$C·. A procedure identical to that described for the Cp analog **2.1** was used. The dinitrogen complex **4.2** was obtained in 63% yield (21 mg, 0.052 mmol).

Reaction of [Cp*Re(CO)$_2$(*p*-N$_2$C$_6$H$_4$OMe)][BF$_4$] (2.2) with Na/THF. A stoichiometric amount of sodium metal was added in small pieces to a solution of the cationic dicarbonyl complex **2.2** (50 mg, 0.083 mmol) in THF (10 mL) at room temperature. The solution was then sonicated for 60 min. During this time period the red-brown solution of **2.2** became yellow-brown in color. An IR spectrum of this solution showed the complete disappearance of **2.2** and the presence of minor absorptions corresponding to the dinitrogen complex **4.2**. Major absorptions at 1929 and 1615 cm^{-1}

were present as well. Attempts to isolate this unknown neutral species were not successful due to its low stability to silica gel or neutral alumina columns. A partially purified sample obtained by extraction with hexane gave unsatisfactory ^{1}H NMR and mass spectra. Column chromatography using hexane as the elutant gave **4.2** in 17% yield (6 mg, 0.014 mmol).

Reaction of [Cp*Re(CO)$_2$(*p*-N$_2$C$_6$H$_4$OMe)][BF$_4$] (2.2) with Na/NH$_3$. A two-necked flask was equipped with a dry ice condenser containing a dry ice-acetone mixture. The flask was also fitted with an ammonia gas line, so as to provide the solvent for the reaction by condensation, and a gas line to maintain a nitrogen atmosphere. The cationic dicarbonyl complex **2.2** (50 mg, 0.083 mmol) was then added to the colorless liquid ammonia (100 mL). To this solution was added a minimum amount of THF (10 mL) to completely solubilize **2.2**. A stoichiometric amount of sodium metal, as monitored by the color of the mixture (blue color indicates excess sodium), was then added in small pieces to the reaction flask. The mixture was allowed to stir for 30 min. The ammonia was then allowed to escape and the remaining THF solution was filtered through a short column of Celite. Removal of the solvent under vacuum and subsequent extraction with hexane (3 x 20 mL) gave the neutral carbamoyl complex Cp*Re(CO)(CONH$_2$)(*p*-N$_2$C$_6$H$_4$OMe) **(4.11)** as a yellow solid in 78% yield (34 mg, 0.065 mmol). The dinitrogen complex **4.2** was not formed in this reaction. IR (CH_2Cl_2): 1931 cm^{-1} ν(CO); 1625 cm^{-1} ν(NN); 1586 ν(CONH$_2$). ^{1}H NMR ($CDCl_3$): δ 2.12 (s, 15H, Cp*), 3.83 (s, 3H, OMe), 6.95 (d, 2H, C_6H_4), 7.29 (d, 2H, C_6H_4); $\delta_{N\text{-}H}$ was not observed.

Reaction of [Cp*Re(PMe$_3$)$_2$(*p*-N$_2$C$_6$H$_4$OMe)][BF$_4$] (2.11) with Na/NH$_3$. A two-necked flask was equipped with a dry ice condenser containing a dry ice-acetone mixture. The flask was also fitted with an ammonia gas line, so as to provide the solvent for the reaction by condensation, and a gas line to maintain a nitrogen atmosphere. The

cationic bis-trimethylphosphine complex **2.11** (50 mg, 0.072 mmol) was taken up in THF (10 mL) and then added to the colorless liquid ammonia (100 mL). A stoichiometric amount of sodium metal, as monitored by the color of the mixture (blue color indicates excess sodium), was then added in small pieces to the reaction flask. The mixture was allowed to stir for 30 min. The ammonia was then allowed to escape and the remaining THF solution was filtered through a short column of Celite. The solvent was removed under vacuum and the remaining yellow-brown oil was then extracted with diethyl ether (2 x 20 mL). The ether extractions were then concentrated to *ca.* 2 mL under vacuum and chromatographed on a neutral alumina column. Elution with hexane gave the organic product *p*-anisidine ($NH_2C_6H_4OMe$). This product was verified by GC-MS and by comparison of its ^1H NMR spectrum to that of an authentic sample. Using diethyl ether as the elutant afforded the dihydrido complex *trans*-$Cp^*Re(PMe_3)_2H_2$ (***trans*-4.12**) as a yellow solid in 58% yield (20 mg, 0.042 mmol). The dinitrogen complex **4.2** was not formed in this reaction. ^1H NMR (benzene-d_6): δ 2.04 (s, 15H, Cp^*), 1.50 (virtual doublet, 18H, PMe_3, J_{app} = 7.5 Hz), -11.89 (t, 2H, ReH, J_{H-P} = 43.5 Hz). $^{31}P\{^1H\}$ NMR (benzene-d_6): δ -37.57 (s, PMe_3).

4.5.3. Electrochemical Methods

Acetonitrile was distilled from calcium hydride under a nitrogen atmosphere and used immediately. The supporting electrolyte was electrometric grade tetraethylammonium perchlorate (TEAP) (Anachemia Science Inc.) and was purified by recrystallization from distilled water (2 times) and then dried under vacuum for two days.

4.5.3.1. Cyclic Voltammetry

Experiments were performed in a single-compartment cell as shown in Figure 4.11.

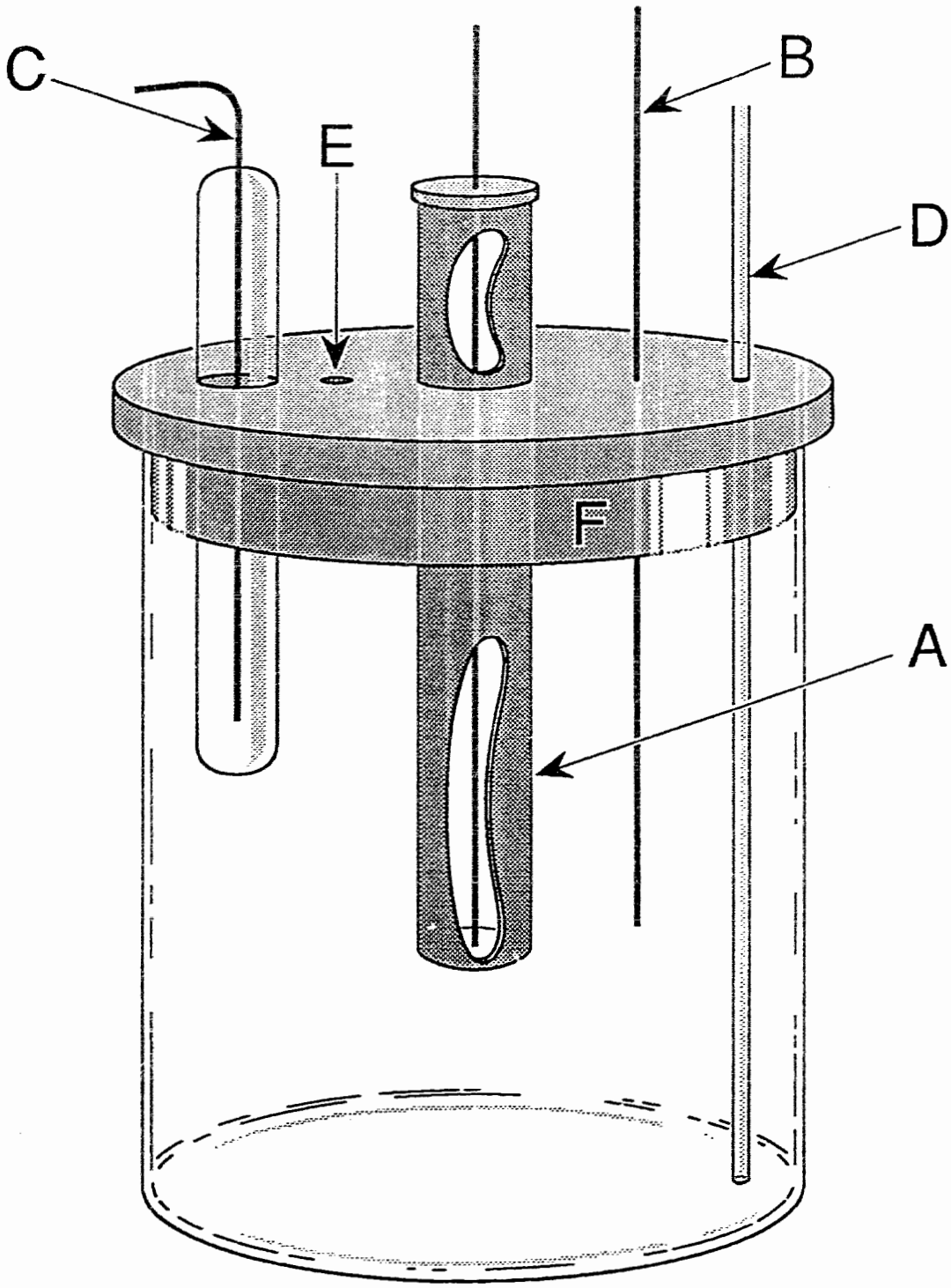

Figure 4.11. Electrochemical cell used for CV. (A) working electrode; (B) counter electrode; (C) reference electrode; (D) nitrogen inlet; (E) nitrogen outlet; (F) Teflon cap.

The working electrode was a stationary, mirror-polished, platinum (Pt) disk which measured 1 mm in diameter (Pine Instrument Co.). The Pt disk was surrounded by a cylindrical Teflon collar of 2.5 mm thickness. Before each experiment, the electrode was dipped sequentially in concentrated HNO_3, then saturated $FeSO_4$ in 2 M H_2SO_4, and finally rinsed thoroughly with distilled water; this procedure provided a consistent electrode surface.

A Pt wire was used as the counter electrode. The reference electrode was either a silver wire in a saturated solution of silver chloride (Ag/AgCl) or a standard calomel electrode (SCE). However, for convenience of comparison, the results are reported with respect to SCE.

The sample solutions were thoroughly deaerated with oxygen-free N_2, and an N_2 atmosphere was maintained throughout the voltammetric measurements. All experiments were carried out at room temperature. All experiments were performed using solutions of 0.2 M TEAP (as the supporting electrolyte) in MeCN. Concentrations of analytes were 1.0 mM for all experiments. The scan rate was 0.2 V/s unless stated otherwise.

The CV apparatus consisted of a Princeton Applied Research EG&G 175 programmer and an EG&G 170 potentiostat. Electrical responses were recorded on a Hewlett-Packard 7046A X-Y recorder.

CV measurements were carried out as follows. An acetonitrile solution containing the electrolyte was placed in the cell and then deaerated with a continuous stream of nitrogen gas until a cyclic voltammogram of the solution showed no fluctuations in the current. A solution of the particular cationic rhenium aryldiazenido complex in a minimum amount of degassed acetonitrile was then injected into the cell. A cyclic voltammogram of the solution using a potential range of +2.0 V to -2.0 V was then recorded.

4.5.3.2. Fast Scan Rate Cyclic Voltammetry and Scanning Electrochemical Microscopy

The fast scan rate cyclic voltammetry (CV) and scanning electrochemical microscopy (SECM) analyses of the cationic rhenium aryldiazenido complex $[Cp^*Re(CO)_2(p\text{-}N_2C_6H_4OMe)][BF_4]$ (**2.2**) reported in this chapter were conducted by Professor Allen J. Bard and Dr. Thomas C. Richards at the University of Texas at Austin. Detailed theory for the SECM and fast scan rate CV studies, a description of the apparatus used, and how these experiments were performed has been reported recently by Bard et al.[130-136] These analyses are not repeated here but instead the pertinent results obtained are used to elucidate mechanistic information for the conversion of the cationic aryldiazenido complex **2.2** to the corresponding neutral dinitrogen complex **4.2**.

4.5.3.3. Controlled Potential Electrolysis

A two-compartment cell as illustrated in Figure 4.12 was used. A sintered-glass disk of fine porosity separated the counter and working compartments. The working electrode was a Pt gauze. A Pt counter electrode was positioned above the working electrode to obtain a uniform potential distribution. An Ag/AgCl or SCE reference electrode was positioned close to the working electrode.

The CPE apparatus consisted of a Princeton Applied Research EG&G 175 programmer, an EG&G 170 potentiostat, and a EG&G 179 coulometer.

CPE measurements and analysis of the products were carried out as follows. The electrolyte solution was placed in the working electrode compartment of the cell. A small amount of the same solution was added to the counter electrode compartment until the solution levels were equalized. The solution in the working compartment was then deaerated with nitrogen gas while being stirred continuously. Pre-electrolysis was carried out until the background current became negligible.

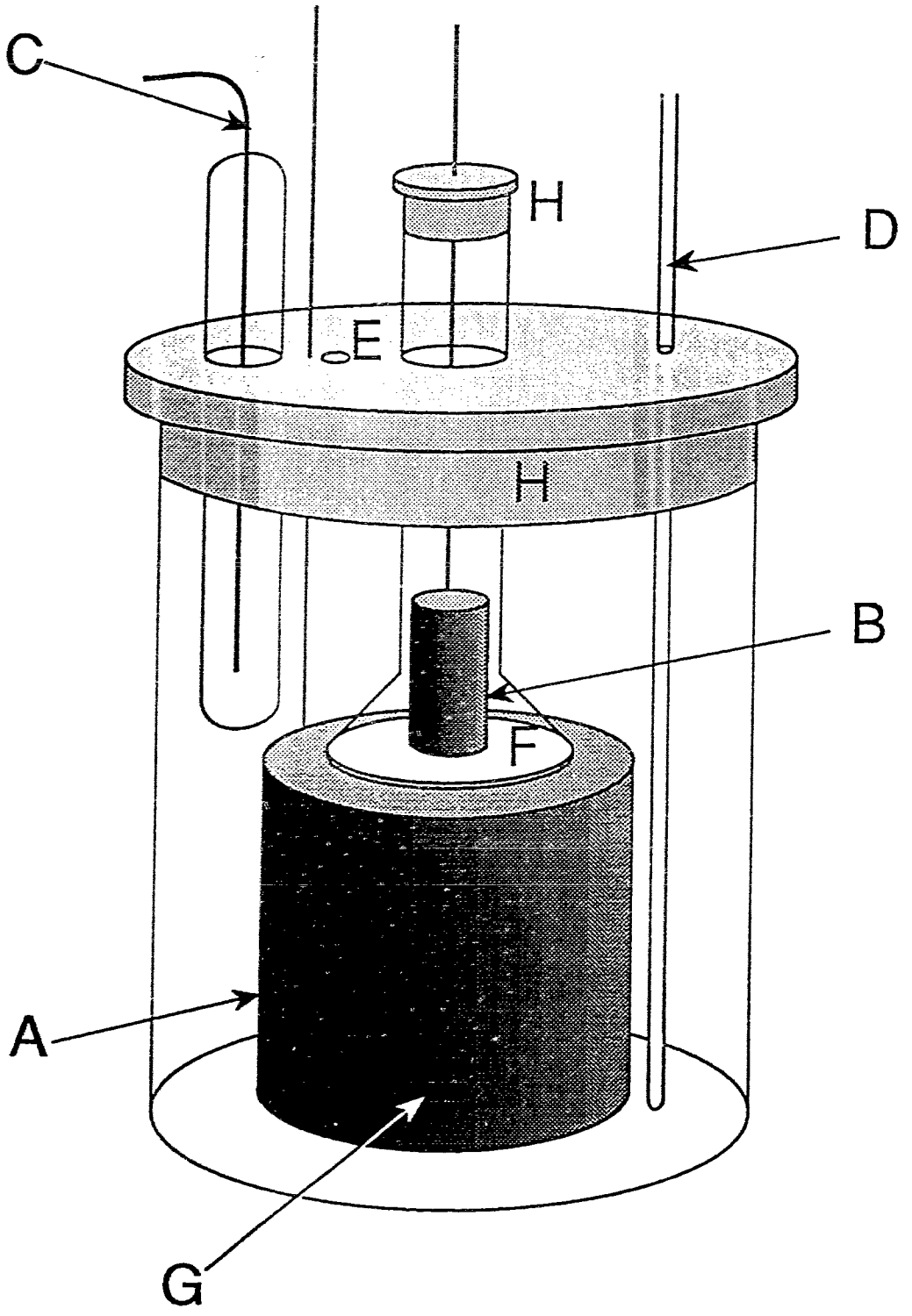

Figure 4.12 Electrochemical cell used for CPE. (A) working electrode; (B) counter electrode; (C) reference electrode; (D) nitrogen inlet; (E) nitrogen outlet; (F) fritted glass; (G) stir bar; (H) Teflon caps.

A 0.5 mL sample of the electrolyte solution was extracted by syringe and an IR spectrum was collected. The spectrum would serve as a background for subsequent IR spectra. A solution of the particular cationic rhenium aryldiazenido complex in a minimum amount of degassed acetonitrile was then injected into the working compartment. A sample of the electrolysis solution was withdrawn and an IR spectrum was recorded. The spectrum was then corrected by subtracting the background spectrum and was used as a reference from which to monitor the electrolysis. The electrolysis was then allowed to proceed at a given potential. At specific time intervals aliquots of the solution were withdrawn and subsequently analyzed by IR spectroscopy.

Preparation of the Dinitrogen Complexes 4.1-4.3 by CPE. Controlled potential electrolysis (CPE) was carried out on the cationic rhenium aryldiazenido complexes **2.1** (53 mg, 0.10 mmol), **2.2** (60 mg, 0.10 mmol), and **2.4** (65 mg, 0.10 mmol) using the procedure just described at the appropriate reduction potential (as determined by CV). An IR spectrum recorded after the bulk electrolysis was complete showed the total disappearance of the cationic complex and only the presence of absorptions corresponding to the respective dinitrogen complexes **4.1-4.3**. For **4.1**, IR (MeCN solution of TEAP): 2141 cm^{-1} ν(NN); 1956, 1894 cm^{-1} ν(CO). For **4.2**, IR (MeCN solution of TEAP): 2121 cm^{-1} ν(NN); 1939, 1879 cm^{-1} ν(CO). For **4.3**, IR (MeCN solution of TEAP): 2027 cm^{-1} ν(NN); 1834 cm^{-1} ν(CO). The solvent was then removed under vacuum and the remaining solid was extracted with diethyl ether (3 x 20 mL). The ether extractions were then concentrated to *ca.* 2 mL under vacuum and chromatographed on a neutral alumina column. Elution with hexane yielded **4.1** in 73% yield (24 mg, 0.073 mmol), **4.2** in 78% yield (32 mg, 0.078 mmol), and **4.3** in 74% yield (34 mg, 0.074 mmol).

CHAPTER 5

End-to-end Rotation of Rhenium-bound Dinitrogen

5.1. Introduction

The details of the coordination mode and dynamics of ligated dinitrogen are of fundamental interest with regard to its activation, reduction, or chemical transformation.[33] Dinitrogen typically binds to a mononuclear metal center in an end-on (η^1) fashion with a linear or near linear MNN skeleton (Figure 5.1).[153, 154] This particular bonding mode for the dinitrogen ligand has been spectroscopically and structurally characterized in many different transition metal complexes including the first ever reported dinitrogen complex $[Ru(NH_3)_5(N_2)]^{2+}$.[22] In stark contrast, the side-on (η^2) bonded form of the dinitrogen ligand has yet to be structurally determined for mononuclear metal complexes (Figure 5.1), whereas, it is well-established for polynuclear systems.[18, 28, 29]

end-on (η^1) side-on (η^2)

Figure 5.1. Bonding modes for the dinitrogen ligand in mononuclear metal complexes.

In fact, only one reasonably established example of the side-on bonded arrangement, illustrated in Figure 5.1, has been reported to date and it relies on spectroscopic evidence for its formulation. That is, the ESR spectrum of the 17-electron zirconium dinitrogen complex $Cp_2Zr\{(Me_3Si)_2CH\}(N_2)$ showed that the unpaired electron was coupled with

two equivalent nitrogen nuclei, which is supportive of an η^2-bound N_2 ligand.[32] The side-on bonded mode for the dinitrogen ligand was also suggested to occur in a matrix-isolated cobalt system;[155] unfortunately, the limited spectroscopic evidence available was also consistent with a binuclear complex.

As alluded to in the Introduction of this thesis, recent developments in the research area of nitrogen fixation have renewed interest into the accessibility of the side-on bonded form of dinitrogen, either in stable complexes or as a reactive intermediate. For example, it was demonstrated by Schrock et al. that dinitrogen can be converted to ammonia at a transition metal center and that an η^2-dinitrogen derivative lay on this mechanistic pathway.[46, 47, 48] Furthermore, evidence obtained from a crystallographic analysis of the N_2 "fixing" enzyme, nitrogenase, suggested that the active site of this enzyme, which contained several metals, was predisposed toward the binding of a dinitrogen molecule in a side-on fashion.[13, 17]

In this chapter, I report the results of a variable temperature and time-dependent solution ^{15}N NMR study of the rhenium dinitrogen complexes Cp'Re(CO)(L)($^{15}N^{14}N$) ((a) Cp' = Cp; L = CO (**4.1-$^{15}N_\alpha$**)[123, 124] and (b) Cp' = Cp*; L = CO (**4.2-$^{15}N_\alpha$**),[59] PMe_3 (**4.3-$^{15}N_\alpha$**),[59] or $P(OMe)_3$ (**4.4-$^{15}N_\alpha$**)[59]) which were specifically labeled at the rhenium-bound nitrogen atom (N_α) with ^{15}N (Scheme 5.1). The coordinated η^1-dinitrogen ligand in these complexes was shown to undergo a remarkable end-to-end rotation process *via* the elusive η^2-bonded dinitrogen species to the alternative η^1-dinitrogen complex where the ^{15}N label was now at the terminal nitrogen atom (N_β). The rates for the linkage isomerization of Cp'Re(CO)(L)($^{15}N^{14}N$) to Cp'Re(CO)(L)($^{14}N^{15}N$) were measured, and subsequently the barriers for this end-to-end rotation process were determined.

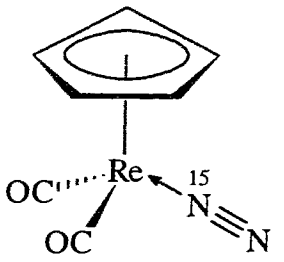

4.1-$^{15}N_{\alpha}$

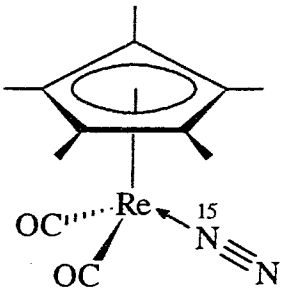

4.2-$^{15}N_{\alpha}$

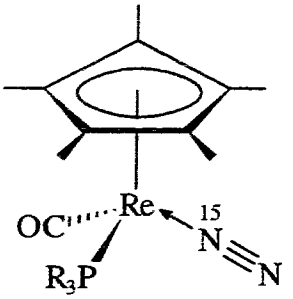

4.3-$^{15}N_{\alpha}$ and **4.4-$^{15}N_{\alpha}$**

	PR_3
4.3-$^{15}N_{\alpha}$	PMe_3
4.4-$^{15}N_{\alpha}$	$P(OMe)_3$

Scheme 5.1. Structures of **4.1-$^{15}N_{\alpha}$** to **4.4-$^{15}N_{\alpha}$**.

5.2. Results

5.2.1. Synthesis of the ^{15}N Linkage Isomers

The neutral carbonyl phosphine and phosphite dinitrogen complexes $Cp^*Re(CO)(PR_3)(^{15}N^{14}N)$ ($PR_3 = PMe_3$ (**4.3-$^{15}N_{\alpha}$**) or $P(OMe)_3$ (**4.4-$^{15}N_{\alpha}$**)) were prepared from their corresponding cationic aryldiazenido complexes, which were specifically labeled at the rhenium-bound nitrogen atom (N_{α}) with ^{15}N, by treatment with Na/Hg at room temperature. The ^{15}N NMR spectra obtained for these complexes in

acetone-d_6 at room temperature exhibited, in both cases, a single sharp resonance with no measurable coupling to phosphorus, at δ -91.3 and δ -99.4 respectively (Table 5.1).

Table 5.1. ^{15}N and ^{14}N NMR Data for the Dinitrogen Complexes

Complex	^{15}N NMR[a, b]		^{14}N NMR[a]	
	$\delta(^{15}N_\alpha)$	$\delta(^{15}N_\beta)$	$\delta(^{14}N_\alpha)$	$\delta(^{14}N_\beta)$
4.1[c]	-120.9	-27.3	-120	-26
4.2[c]	-110.8	-28.1	-110	-26
4.3	-91.3	-32.7[d]	-91	-30
4.4	-99.4	-32.5[d]	-99	-29

[a] In acetone-d_6; referenced to external $MeNO_2$; δ given in ppm.
[b] Samples enriched with ^{15}N (99%).
[c] Equimolar mixture of $^{15}N_\alpha$ and $^{15}N_\beta$ singly-enriched species.
[d] $^{15}N_\beta$ resonance was observed only after the corresponding $^{15}N_\alpha$ linkage isomer was maintained at an elevated temperature in CD_3CN for several hours.

The cationic dicarbonyl aryldiazenido complex [Cp*Re(CO)$_2$(*p*-$^{15}N^{14}NC_6H_4OMe$)][BF_4] (**2.2-$^{15}N_\alpha$**), which was specifically labeled at N_α with ^{15}N, was presumably converted to the neutral dinitrogen complex Cp*Re(CO)$_2$($^{15}N^{14}N$) (**4.2-$^{15}N_\alpha$**) at room temperature by treatment with Ph_3C·, Cp_2Co, or $NaBH_4$. However, a ^{15}N NMR spectrum acquired of the isolated dinitrogen complex in acetone-d_6 at room temperature exhibited two resonances of equal intensity at δ -110.8 and δ -28.1 (Table 5.1) (Figure 5.2).

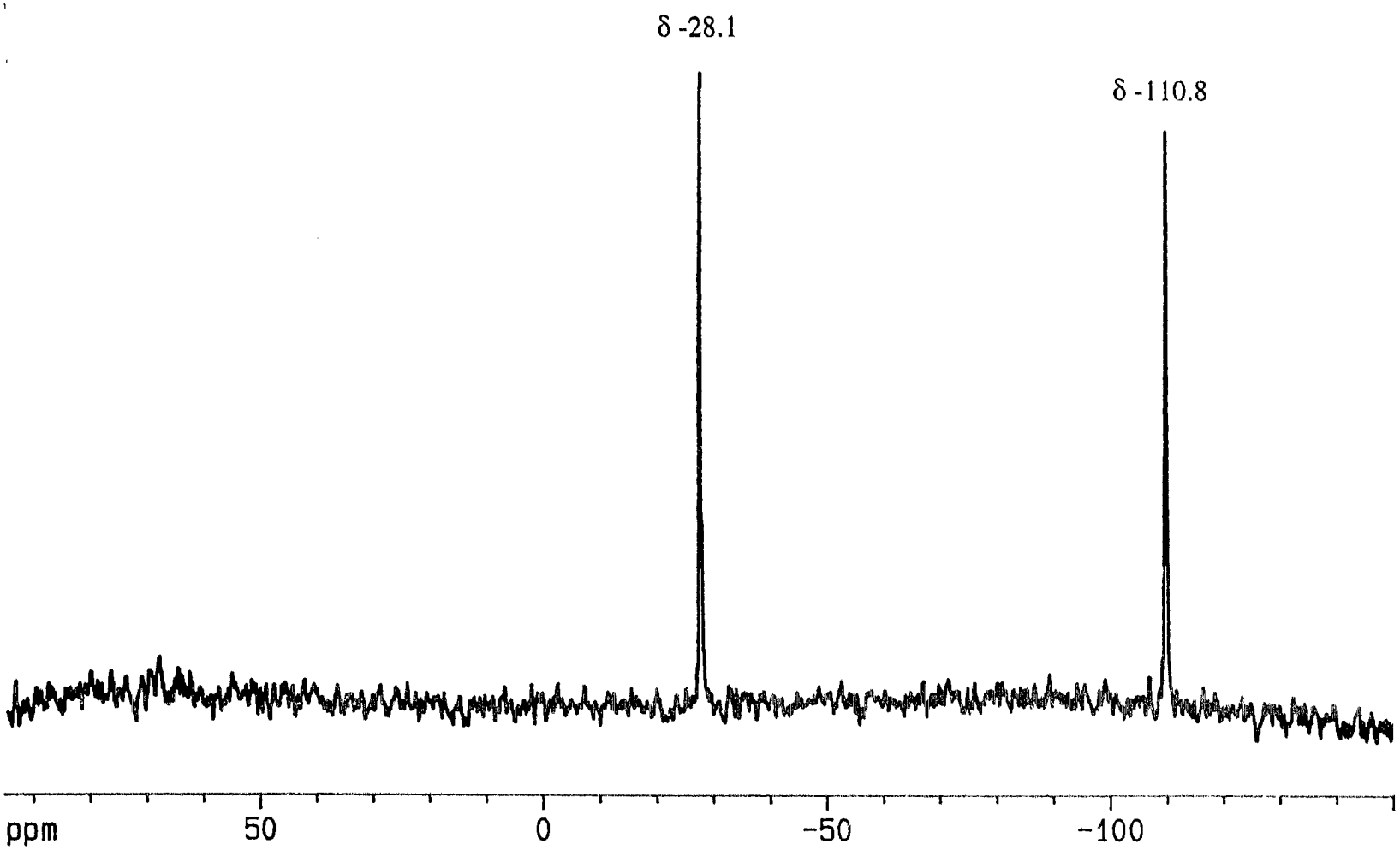

Figure 5.2. ^{15}N NMR spectrum (40.6 MHz) of presumably $Cp^*Re(CO)_2(^{15}N^{14}N)$ (**4.2-$^{15}N_\alpha$**) in acetone-d_6 at room temperature.

Similar results were obtained for the analogous Cp dinitrogen complex $CpRe(CO)_2(^{15}N^{14}N)$ (**4.1-$^{15}N_\alpha$**) after it was synthesized from the corresponding $^{15}N_\alpha$ labeled aryldiazenido complex $[CpRe(CO)_2(p\text{-}^{15}N^{14}NC_6H_4OMe)][BF_4]$ (**2.1-$^{15}N_\alpha$**) by reaction with Cp_2Co. The room temperature ^{15}N NMR spectrum of the isolated product in acetone-d_6 showed two resonances of equal intensity at δ -120.9 and δ -27.3 (Table 5.1).

GC analysis of the solvent removed from either the Cp or Cp* dicarbonyl dinitrogen reaction mixtures prior to purification indicated that anisole (C_6H_5OMe) was formed as the only other observable reaction product. This result suggested that the dinitrogen complexes produced in these reactions were solely responsible for the two observed ^{15}N NMR resonances and not the formation of an additional ^{15}N labeled byproduct. Therefore, it was postulated that these findings reflected the presence of an equimolar mixture of the respective linkage isomers $Cp'Re(CO)_2(^{15}N^{14}N)$ (Cp' = Cp (**4.1-$^{15}N_\alpha$**) or Cp* (**4.2-$^{15}N_\alpha$**)) and $Cp'Re(CO)_2(^{14}N^{15}N)$ (Cp' = Cp (**4.1-$^{15}N_\beta$**) or Cp* (**4.2-$^{15}N_\beta$**)) even though the precursor aryldiazenido complexes were both specifically ^{15}N labeled at N_α only (Scheme 5.2).[59]

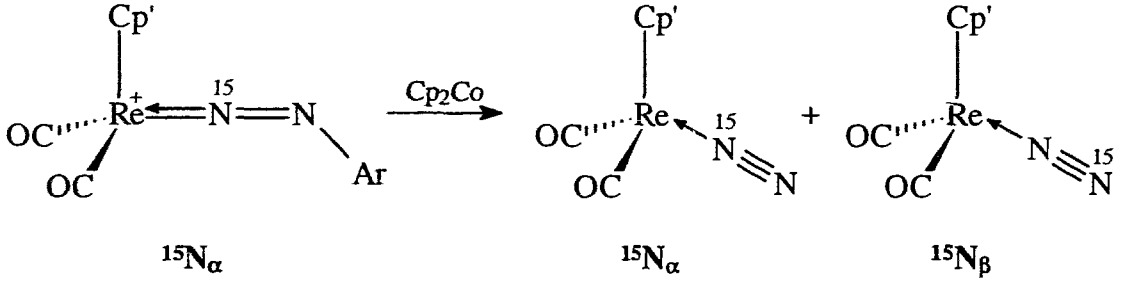

$^{15}N_\alpha$ **$^{15}N_\alpha$** **$^{15}N_\beta$**

Cp' = Cp or Cp*

Scheme 5.2. Production of the ^{15}N linkage isomers of rhenium-bound dinitrogen from the corresponding $^{15}N_\alpha$ labeled aryldiazenido complex.

5.2.2. Experiments to Examine the Distribution of the ^{15}N Label

5.2.2.1. Dynamic ^{15}N NMR Spectroscopy of $Cp^*Re(CO)_2(^{15}N^{14}N)$ (**4.2-$^{15}N_\alpha$**) Prepared Using $Ph_3C\cdot$

An excess of the triphenylmethyl radical ($Ph_3C\cdot$), prepared from the reduction of Ph_3CCl with zinc dust in THF, was added to a solution of the $^{15}N_\alpha$ labeled aryldiazenido complex $[Cp^*Re(CO)_2(p\text{-}^{15}N^{14}NC_6H_4OMe)][BF_4]$ (**2.2-$^{15}N_\alpha$**) in CD_2Cl_2 at room temperature. IR spectra of this solution recorded 15 and 33 min respectively after the addition of $Ph_3C\cdot$ showed the slow disappearance of **2.2-$^{15}N_\alpha$** and the concomitant formation of absorptions corresponding to the $^{15}N_\alpha$ labeled dinitrogen complex $Cp^*Re(CO)_2(^{15}N^{14}N)$ (**4.2-$^{15}N_\alpha$**) (Figure 5.3). A ^{15}N NMR spectrum of this solution recorded at 293 K, 27 min after the $Ph_3C\cdot$ addition, displayed resonances at δ -7.3, -110.6, and -66.2 corresponding to unreacted **2.2-$^{15}N_\alpha$**, to the concurrent production of the $^{15}N_\alpha$ linkage isomer $Cp^*Re(CO)_2(^{15}N^{14}N)$ (**4.2-$^{15}N_\alpha$**), and to an unknown product respectively (Figure 5.4). No resonance due to the $^{15}N_\beta$ linkage isomer $Cp^*Re(CO)_2(^{14}N^{15}N)$ (**4.2-$^{15}N_\beta$**) was observed. A sequence of ^{15}N NMR spectra acquired in the same manner over time showed the eventual disappearance of **2.2-$^{15}N_\alpha$** and the unknown species, along with the growth of a new resonance at δ -28.4 assigned to **4.2-$^{15}N_\beta$** (Figure 5.5). After 202 min, the ^{15}N NMR spectra showed two equally populated resonances attributable to the linkage isomers **4.2-$^{15}N_\alpha$** and **4.2-$^{15}N_\beta$** (Figure 5.5). An IR spectrum of this solution containing the linkage isomers **4.2-$^{15}N_\alpha$** and **4.2-$^{15}N_\beta$** exhibited a single absorption for ν(NN) coincident at 2092 cm^{-1}.

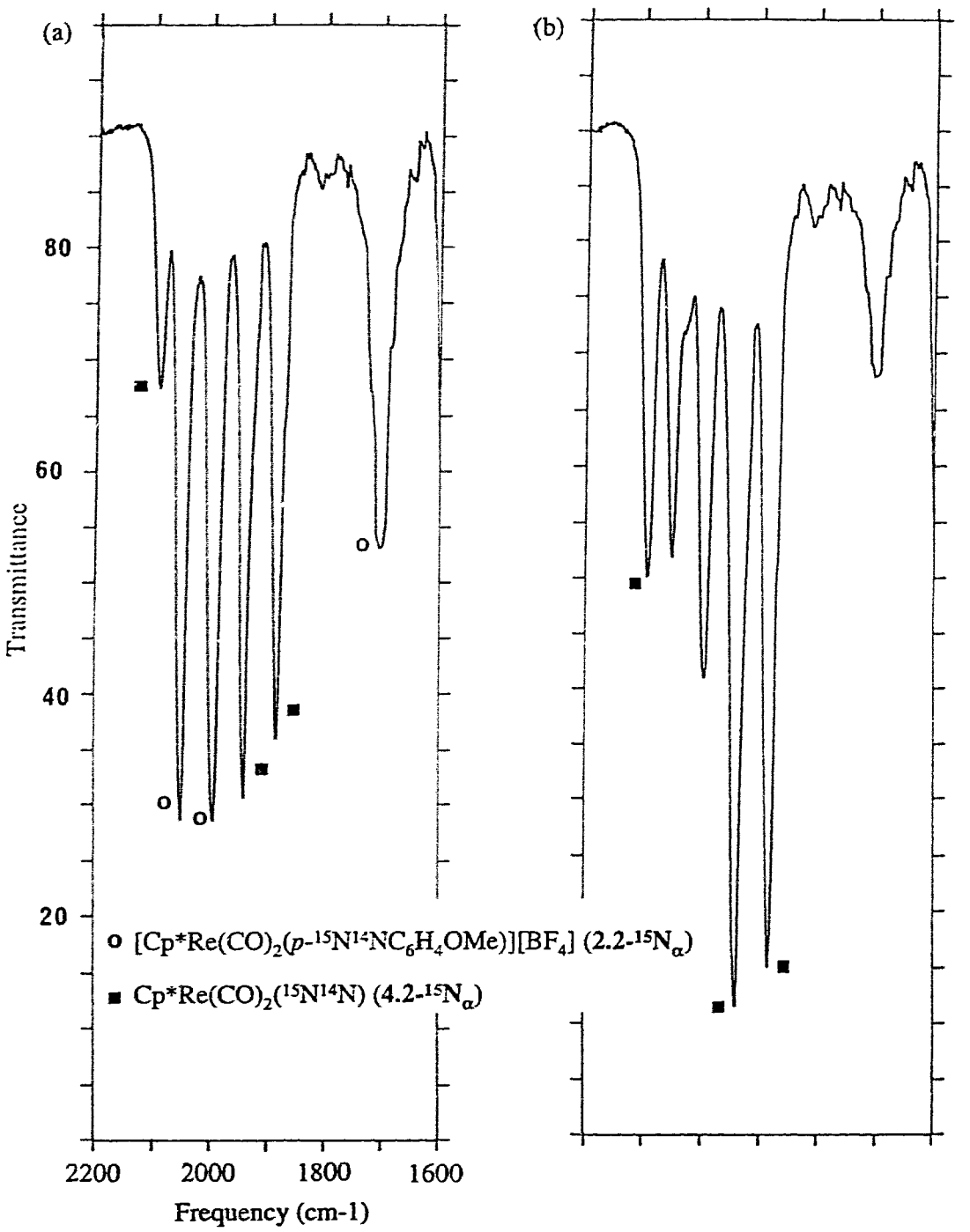

Figure 5.3. Time-dependent IR spectra of the reaction between (**2.2-$^{15}N_\alpha$**) and $Ph_3C\cdot$ in THF:CD_2Cl_2 (1:1) at room temperature. (a) 15 min. (b) 33 min. [Cp*Re(CO)$_2$(*p*-$^{15}N^{14}NC_6H_4OMe$)][BF_4] (**2.2-$^{15}N_\alpha$**): 2049, 1992 cm^{-1} ν(CO); 1703 cm^{-1} ν(NN). Cp*Re(CO)$_2$($^{15}N^{14}N$) (**4.2-$^{15}N_\alpha$**): 2090 cm^{-1} ν(NN); 1939, 1884 cm^{-1} ν(CO).

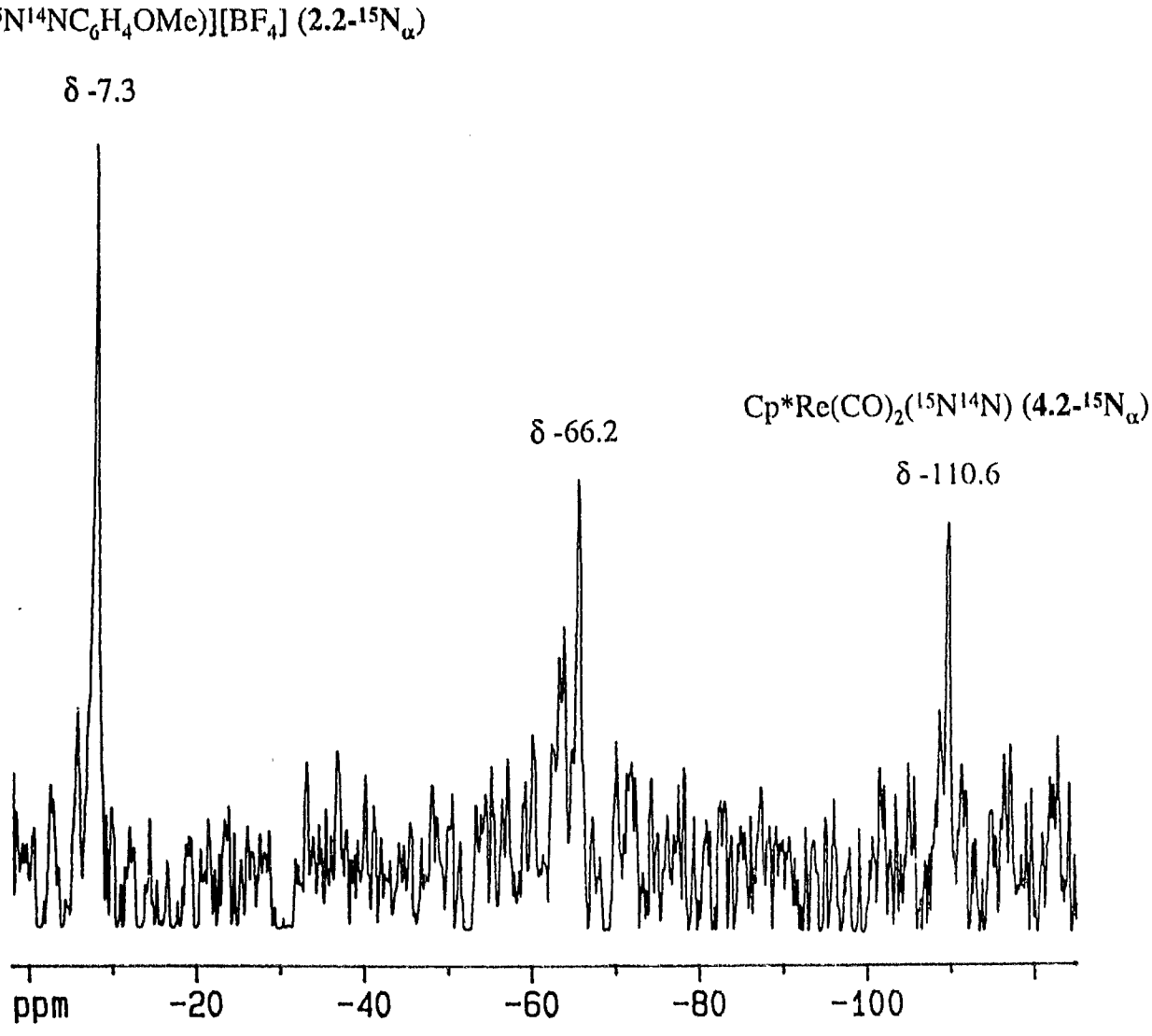

Figure 5.4. ^{15}N NMR spectrum (40.6 MHz) of the reaction between $[Cp^*Re(CO)_2(p\text{-}^{15}N^{14}NC_6H_4OMe)][BF_4]$ (**2.2-$^{15}N_\alpha$**) and Ph_3C^+ in $THF:CD_2Cl_2$ (1:1) at 293 K.

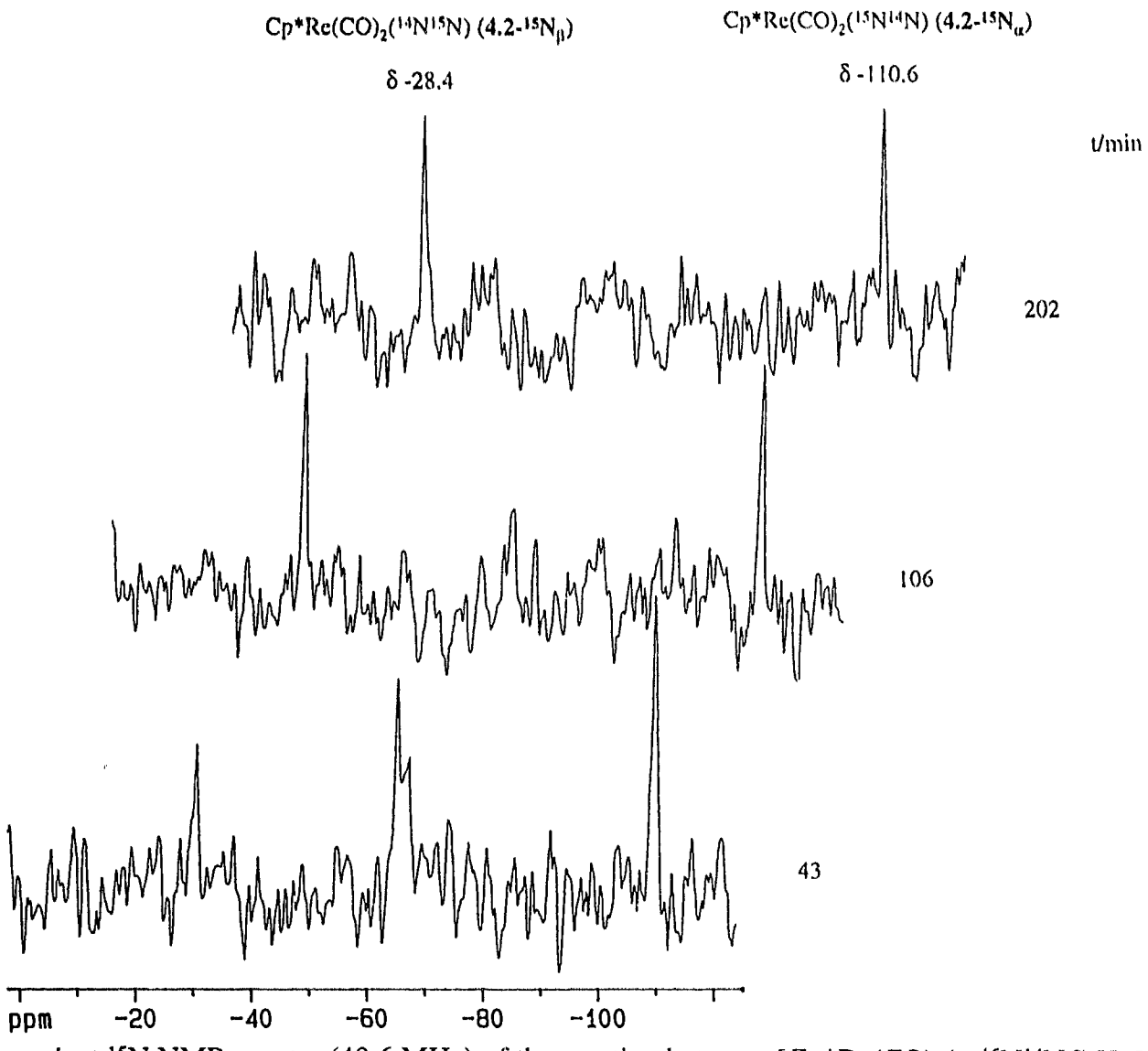

Figure 5.5. Time-dependent ^{15}N NMR spectra (40.6 MHz) of the reaction between $[Cp^*Re(CO)_2(p\text{-}^{15}N^{14}NC_6H_4OMe)][BF_4]$ (**2.2-$^{15}N_\alpha$**) and $Ph_3C\cdot$ in $THF:CD_2Cl_2$ (1:1) at 293 K.

5.2.2.2. Dynamic ^{15}N NMR Spectroscopy of $CpRe(CO)_2(^{15}N^{14}N)$ (**4.1-$^{15}N_\alpha$**) and $Cp^*Re(CO)_2(^{15}N^{14}N)$ (**4.2-$^{15}N_\alpha$**) Prepared Using Cp_2Co

The addition of excess cobaltocene (Cp_2Co) to a solution of the $^{15}N_\alpha$ labeled aryldiazenido complex $[Cp^*Re(CO)_2(p\text{-}^{15}N^{14}NC_6H_4OMe)][BF_4]$ (**2.2-$^{15}N_\alpha$**) in acetone-d_6 at room temperature proved to be a much more efficient route to the $^{15}N_\alpha$ labeled dinitrogen complex $Cp^*Re(CO)_2(^{15}N^{14}N)$ (**4.2-$^{15}N_\alpha$**). An IR spectrum of this solution obtained immediately after the Cp_2Co addition showed the total disappearance of **2.2-$^{15}N_\alpha$** and the presence of absorptions corresponding exclusively to the dinitrogen complex **4.2-$^{15}N_\alpha$**. A ^{15}N NMR spectrum of this solution acquired at 284 K, 25 min after the Cp_2Co addition, exhibited a single resonance at δ -110.8 assigned to the $^{15}N_\alpha$ linkage isomer $Cp^*Re(CO)_2(^{15}N^{14}N)$ (**4.2-$^{15}N_\alpha$**) (Figure 5.6). A sequence of ^{15}N NMR spectra then demonstrated the slow, gradual decay of this resonance and the concomitant growth of a second resonance at δ -28.1 due to the $^{15}N_\beta$ linkage isomer $Cp^*Re(CO)_2(^{14}N^{15}N)$ (**4.2-$^{15}N_\beta$**); equilibrium was established in *ca.* 7 h (Figure 5.6).

Similar results were obtained for the $^{15}N_\alpha$ labeled Cp analog $CpRe(CO)_2(^{15}N^{14}N)$ (**4.1-$^{15}N_\alpha$**) when it was synthesized from the corresponding $^{15}N_\alpha$ labeled aryldiazenido complex $[CpRe(CO)_2(p\text{-}^{15}N^{14}NC_6H_4OMe)][BF_4]$ (**2.1-$^{15}N_\alpha$**) by reaction with Cp_2Co in acetone-d_6 at room temperature. A sequence of ^{15}N NMR spectra of this solution recorded at 291 K showed that the ^{15}N label was once again scrambled from the $^{15}N_\alpha$ linkage isomer **4.1-$^{15}N_\alpha$** (δ -120.9) to the $^{15}N_\beta$ linkage isomer (**4.1-$^{15}N_\beta$**) (δ -27.3) until an equimolar mixture of the isomers was obtained (*ca.* 7 h) (Figure 5.7).

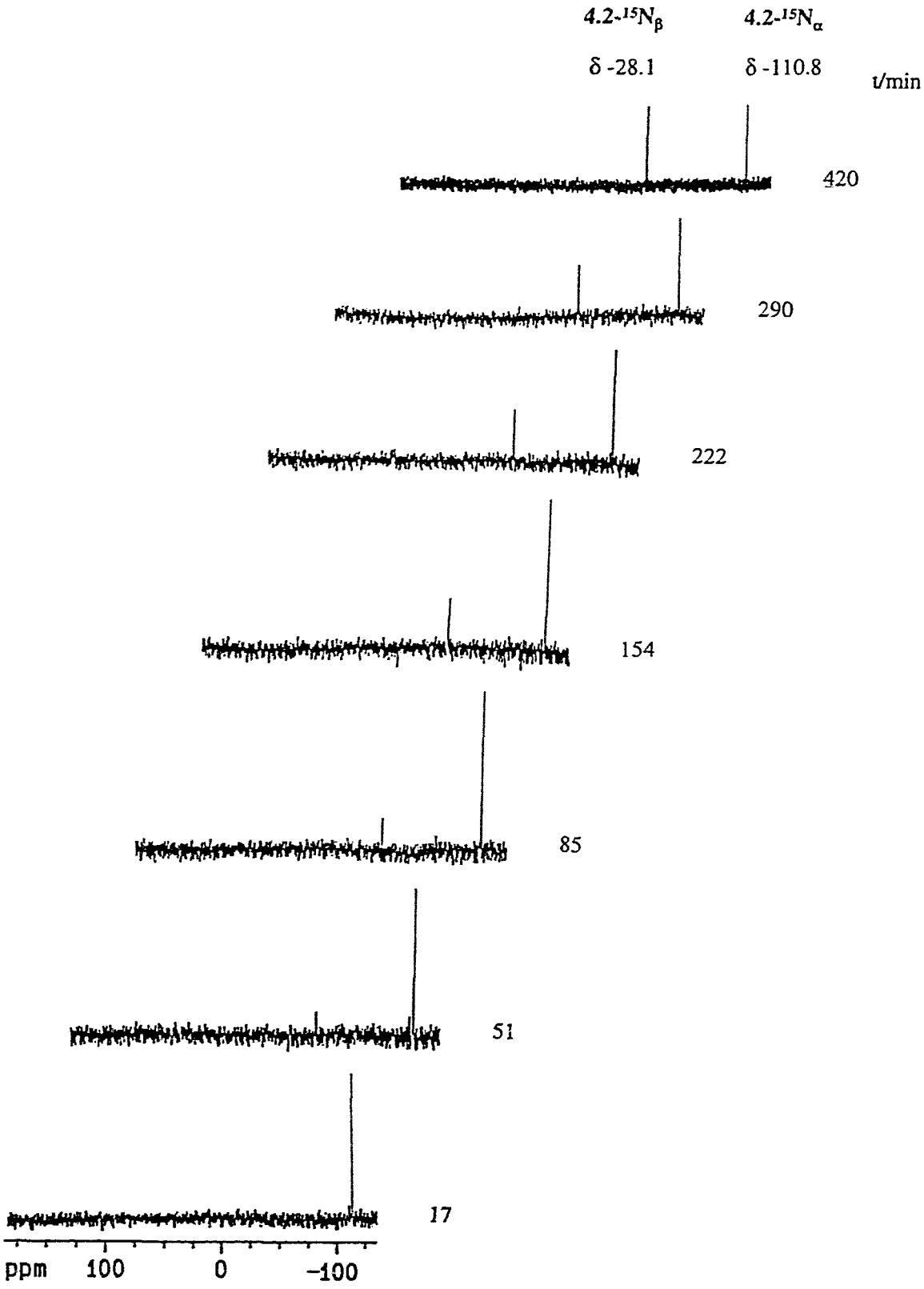

Figure 5.6. Time-dependent ^{15}N NMR spectra (40.6 MHz) of the $^{15}N_{\alpha}$ linkage isomer $Cp^*Re(CO)_2(^{15}N^{14}N)$ (**4.2-$^{15}N_{\alpha}$**) in acetone-d_6 at 284 K.

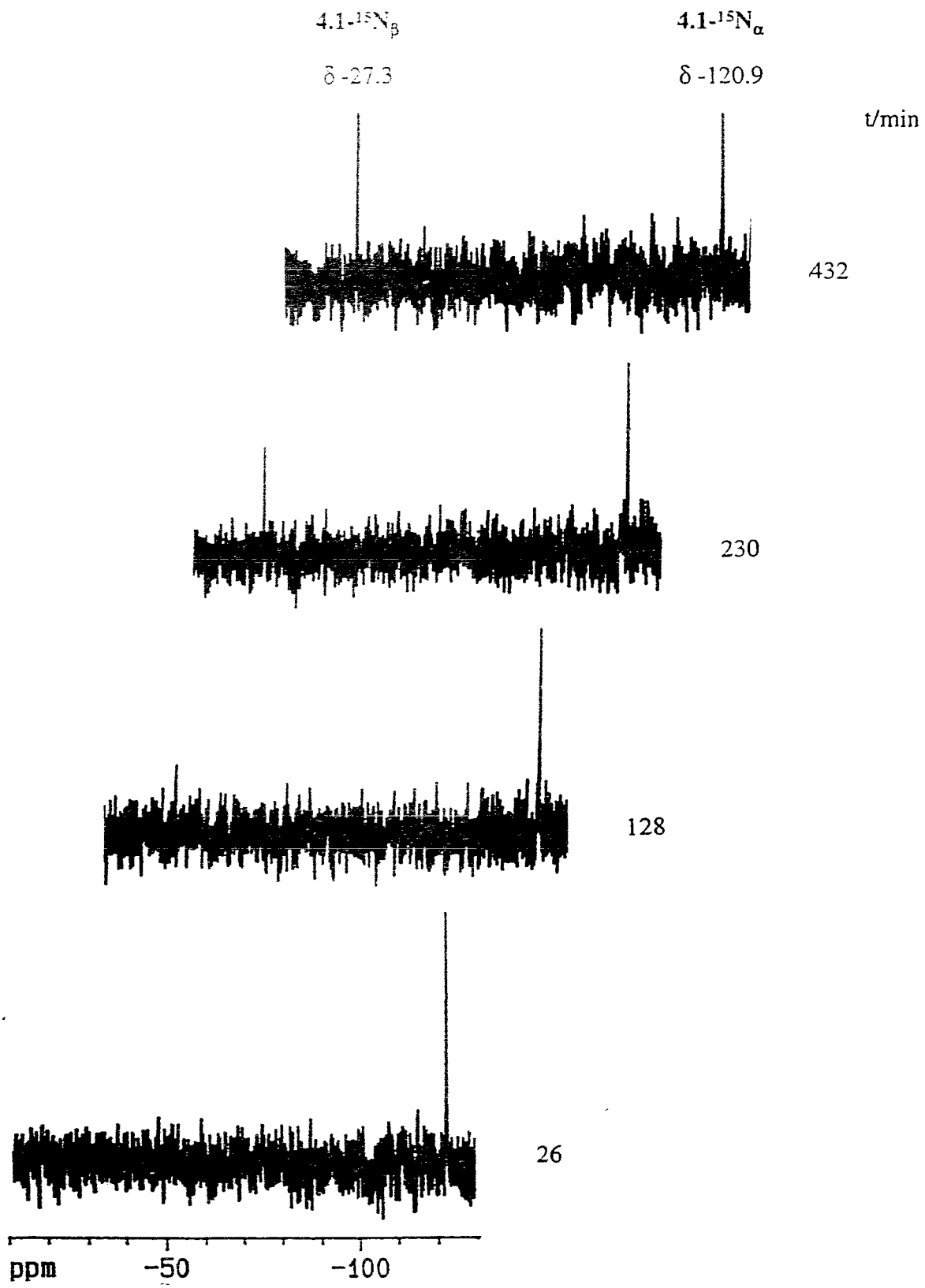

Figure 5.7. Time-dependent ^{15}N NMR spectra (40.6 MHz) of the $^{15}N_{\alpha}$ linkage isomer $CpRe(CO)_2(^{15}N^{14}N)$ (**4.1-$^{15}N_{\alpha}$**) in acetone-d_6 at 291 K.

5.2.2.3. Dynamic ^{15}N NMR Spectroscopy of $Cp^*Re(CO)_2(^{15}N^{14}N)$ (4.2-$^{15}N_\alpha$) Prepared Using $NaBH_4$

An excess of sodium borohydride ($NaBH_4$) was added to a solution of the $^{15}N_\alpha$ labeled aryldiazenido complex $[Cp^*Re(CO)_2(p\text{-}^{15}N^{14}NC_6H_4OMe)][BF_4]$ (**2.2-$^{15}N_\alpha$**) in acetone-d_6 at room temperature. An IR spectrum of this solution recorded immediately after the $NaBH_4$ addition demonstrated the total disappearance of **2.2-$^{15}N_\alpha$** and the presence of minor absorptions corresponding to the $^{15}N_\alpha$ labeled dinitrogen complex $Cp^*Re(CO)_2(^{15}N^{14}N)$ (**4.2-$^{15}N_\alpha$**) and major absorptions due to the aryldiazene complex $Cp^*Re(CO)_2(p\text{-}^{15}NH^{14}NC_6H_4OMe)$ (**4.10-$^{15}N_\alpha$**) (see Chapter 4). An IR spectrum obtained after 35 min showed only the presence of absorptions attributable to **4.2-$^{15}N_\alpha$**. A ^{15}N NMR spectrum of this solution acquired at 280 K, 40 min after the borohydride addition, exhibited a single resonance at δ -110.8 due to the $^{15}N_\alpha$ linkage isomer $Cp^*Re(CO)_2(^{15}N^{14}N)$ (**4.2-$^{15}N_\alpha$**) (Figure 5.8). The NMR solution was then warmed to 293 K. A ^{15}N NMR spectrum acquired after *ca.* 8 h showed an equimolar mixture of the linkage isomers **4.2-$^{15}N_\alpha$** and the newly formed $^{15}N_\beta$ isomer $Cp^*Re(CO)_2(^{14}N^{15}N)$ (**4.2-$^{15}N_\beta$**) (δ -28.1) (Figure 5.8).

5.2.2.4. Dynamic ^{15}N NMR Spectroscopy of $Cp^*Re(CO)(PMe_3)(^{15}N^{14}N)$ (4.3-$^{15}N_\alpha$) and $Cp^*Re(CO)\{P(OMe)_3\}(^{15}N^{14}N)$ (4.4-$^{15}N_\alpha$) Prepared Using Na/Hg

A solution of the $^{15}N_\alpha$ labeled aryldiazenido complex $[Cp^*Re(CO)\{P(OMe)_3\}(p\text{-}^{15}N^{14}NC_6H_4OMe)][BF_4]$ (**2.8-$^{15}N_\alpha$**) in THF was treated with Na/Hg at room temperature. An IR spectrum of this mixture obtained 30 min later showed the total disappearance of **2.8-$^{15}N_\alpha$** and the presence of absorptions corresponding to the $^{15}N_\alpha$ labeled dinitrogen complex $Cp^*Re(CO)\{P(OMe)_3\}(^{15}N^{14}N)$ (**4.4-$^{15}N_\alpha$**). A ^{15}N NMR spectrum of the purified dinitrogen complex in acetone-d_6, acquired at room temperature, exhibited a single resonance at δ -99.4 corresponding to **4.4-$^{15}N_\alpha$**.

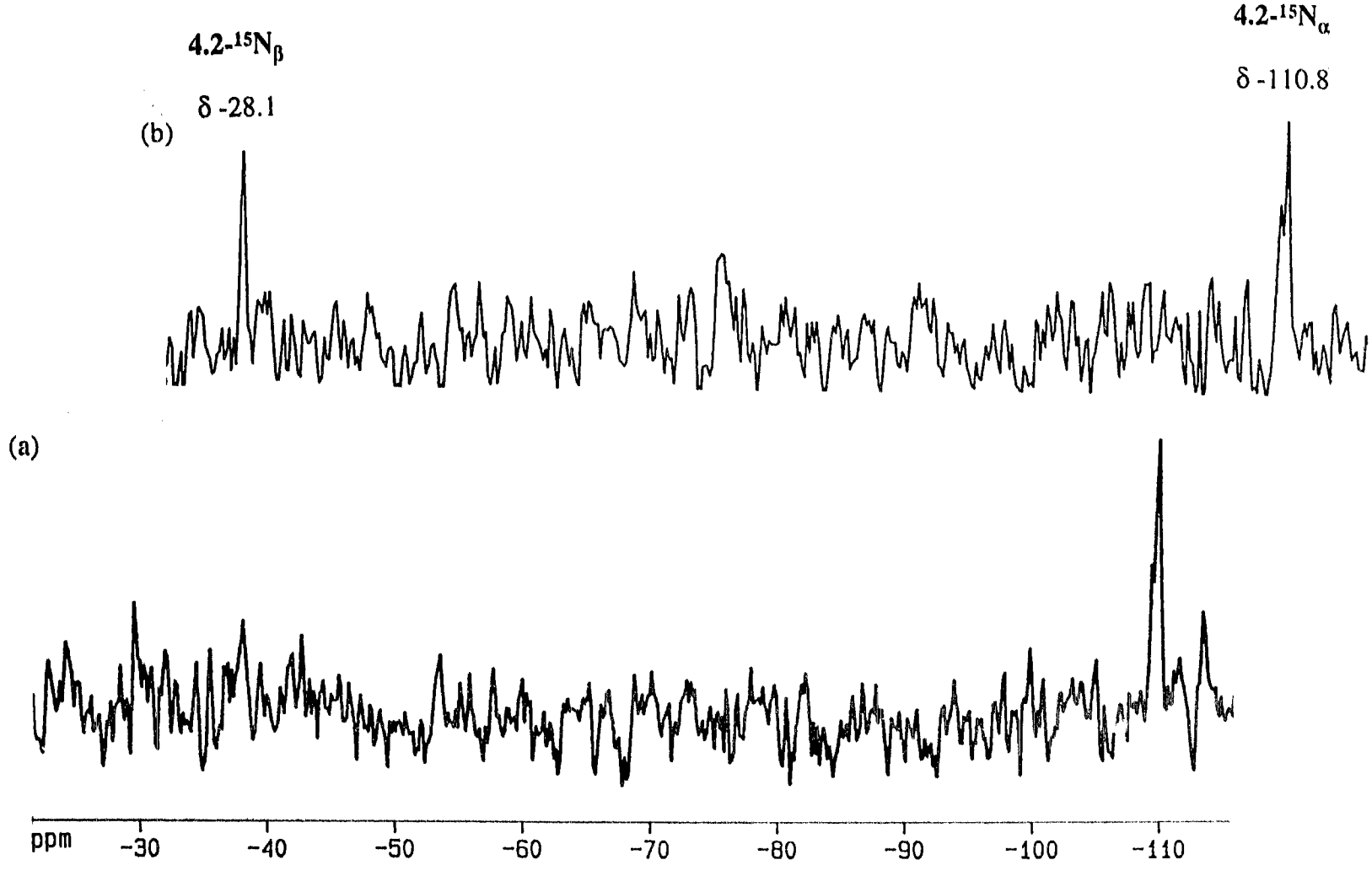

Figure 5.8. ^{15}N NMR spectra (40.6 MHz) of the reaction between $[Cp^*Re(CO)_2(p\text{-}^{15}N^{14}NC_6H_4OMe)][BF_4]$ (**2.2-$^{15}N_\alpha$**) and $NaBH_4$ in acetone-d_6 at (a) 280 K, 40 min after addition and (b) 293 K, 8 h later.

Notably, a ^{15}N NMR spectrum obtained of this sample after 24 h was unchanged; no ^{15}N resonance corresponding to the $^{15}N_\beta$ linkage isomer $Cp^*Re(CO)\{P(OMe)_3\}(^{14}N^{15}N)$ (**4.4-$^{15}N_\beta$**) was observed. The ^{15}N NMR experiment was then repeated at 320 K using CD_3CN as the NMR solvent. A sequence of ^{15}N NMR spectra obtained at this temperature showed initially a single resonance due to **4.4-$^{15}N_\alpha$** at δ -100.8, which then began to decay to produce a second resonance at δ -32.5 assigned to **4.4-$^{15}N_\beta$**; equilibrium was established in *ca.* 3 h (Figure 5.9).

The $^{15}N_\alpha$ labeled trimethylphosphine dinitrogen complex $Cp^*Re(CO)(PMe_3)(^{15}N^{14}N)$ (**4.3-$^{15}N_\alpha$**), which was synthesized in a similar manner to its $P(OMe)_3$ analog, also gave similar ^{15}N NMR results. Once again, a ^{15}N NMR spectrum of the purified dinitrogen complex, acquired at room temperature in acetone-d_6, showed a single resonance at δ -91.3 corresponding to **4.3-$^{15}N_\alpha$** and the spectrum remained the same after 24 h. Repeating the ^{15}N NMR experiment at 320 K in CD_3CN also failed to produce the $^{15}N_\beta$ linkage isomer $Cp^*Re(CO)(PMe_3)(^{14}N^{15}N)$ (**4.3-$^{15}N_\beta$**). However, a sequence of ^{15}N NMR spectra obtained at 333 K demonstrated the slow decay of the resonance due to **4.3-$^{15}N_\alpha$** (δ -93.2) and the concomitant growth of a second resonance at δ -32.7 corresponding to **4.3-$^{15}N_\beta$** until an equimolar mixture of these isomers was eventually obtained *ca.* 3 h (Figure 5.10).

5.2.3. Determination of Rate Constants and Activation Parameters

The rate constants (k_c) for the linkage isomerization of $Cp'Re(CO)_2(^{15}N^{14}N)$ (Cp' = Cp (**4.1-$^{15}N_\alpha$**) or Cp* (**4.2-$^{15}N_\alpha$**)) to give $Cp'Re(CO)_2(^{14}N^{15}N)$ (Cp' = Cp (**4.1-$^{15}N_\beta$**) or Cp* (**4.2-$^{15}N_\beta$**)) were determined from the sequence of ^{15}N NMR spectra obtained immediately following the formation of these complexes by reaction with Cp_2Co (Section 5.2.2.2.).

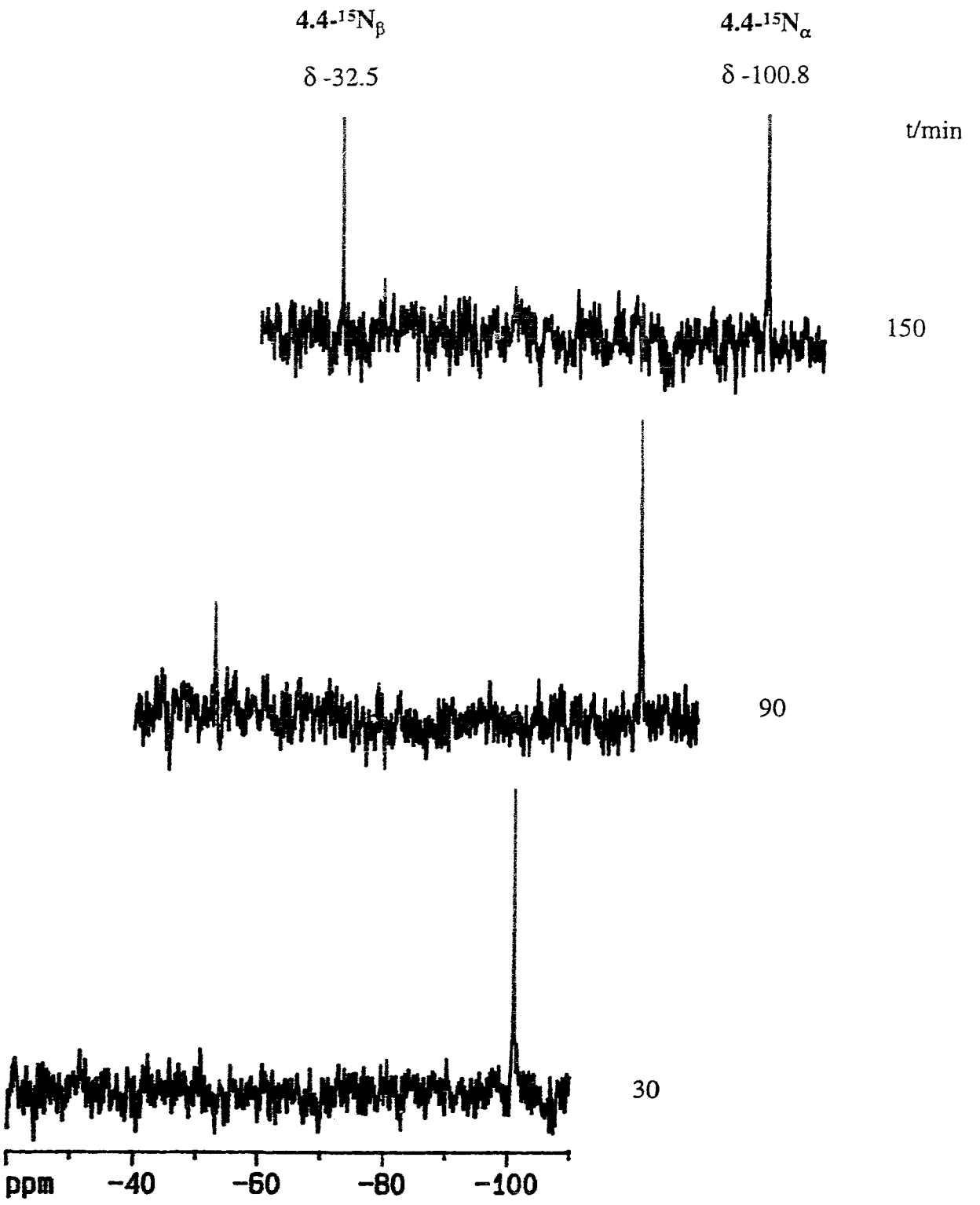

Figure 5.9. Time-dependent ^{15}N NMR spectra (40.6 MHz) of the $^{15}N_{\alpha}$ linkage isomer $Cp^*Re(CO)\{P(OMe)_3\}(^{15}N^{14}N)$ (**4.4-$^{15}N_{\alpha}$**) in CD_3CN at 320 K.

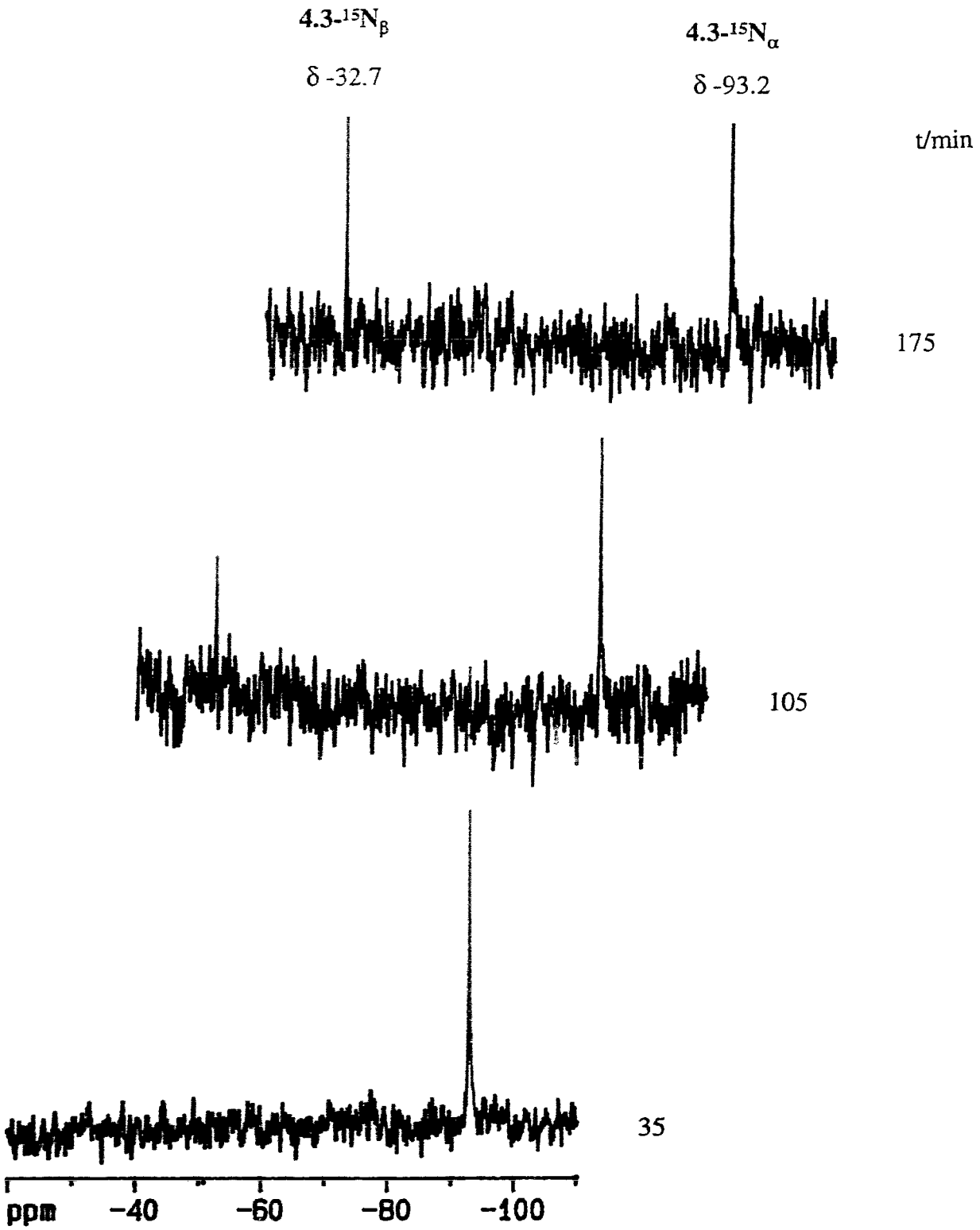

Figure 5.10. Time-dependent ^{15}N NMR spectra (40.6 MHz) of the $^{15}N_{\alpha}$ linkage isomer $Cp^*Re(CO)(PMe_3)(^{15}N^{14}N)$ (**4.3-$^{15}N_{\alpha}$**) in CD_3CN at 333 K.

Specifically, the k_c values were determined by monitoring the growth of the $^{15}N_\beta$ NMR resonance over time by integration relative to a $Na^{15}NO_2$ reference of known concentration which was sealed in a capillary and placed into the NMR tube containing the dinitrogen complex prior to the acquisition of the ^{15}N NMR spectra. Treatment of the observed interconversion between the $^{15}N_\alpha$ and $^{15}N_\beta$ linkage isomers as an "opposing reaction" and assuming first order kinetics (Equation 5.1a) lead to the rate constant expression depicted as Equation 5.1b.[156]

$$N_\alpha \underset{k_c}{\overset{k_c}{\rightleftharpoons}} N_\beta \qquad (5.1a)$$

$$(1/2)\ \ln\{N_{\beta\infty}/(N_{\beta\infty} - N_\beta)\} = k_c t \qquad (5.1b)$$

where $N_{\beta\infty}$ = the concentration of the $^{15}N_\beta$ isomer at equilibrium

N_β = the concentration of the $^{15}N_\beta$ isomer at a given time t

Values for k_c were then extracted from the slope of a straight line graph obtained by plotting $(1/2)\ \ln\{N_{\beta\infty}/(N_{\beta\infty} - N_\beta)\}$ vs t (Equation 5.1b) using a linear least-squares program[95] (Table 5.2). The errors in the rate constants were obtained from the standard deviations derived from the linear least-squares program.

^{15}N NMR spectroscopy was shown in the previous sections to be an extremely effective technique for probing the isomerization of the ^{15}N labeled dinitrogen ligand in complexes **4.1-$^{15}N_\alpha$** to **4.4-$^{15}N_\alpha$**. However, the inherent properties of the ^{15}N nucleus also hindered the extraction of the kinetic data. The ^{15}N nucleus (spin 1/2) has a natural abundance of 0.37%, a receptivity 1/100 times that of ^{13}C, and a very long spin lattice relaxation time (i.e. 9.8 s for **4.2-$^{15}N_\alpha$**).[59]

Table 5.2. Rate Constants (k_c) and Activation Parameters for the Isomerization of the ^{15}N Labeled Rhenium-bound Dinitrogen Ligand

Complex	Temperature (K)[a]	k_c (x 10^{-6} s^{-1})[b]	$\Delta G^{\neq}$ (kJ/mol)	$\Delta H^{\neq}$ (kJ/mol)	$\Delta S^{\neq}$ (J/mol·K)	E_a (kJ/mol)	A (x10^{15}) (s^{-1})
4.1[c]	291	48 ± 6	95.3 ± 0.5				
4.2[c]	274	9.5 ± 1.1					
	281	27 ± 3					
	284	47 ± 3					
	291	142 ± 11	92.6 ± 0.4	105.3 ± 6.0	43.5 ± 21.2	106.8 ± 5.4	2.1 ± 1.3

[a] All errors in temperature are ± 1 K.

[b] Calculated from the rate constant expression depicted as Equation 5.1.

[c] Equimolar mixture of $^{15}N_{\alpha}$ and $^{15}N_{\beta}$ singly-enriched species.

Despite the fact that highly concentrated 99% ^{15}N enriched samples were used for the ^{15}N NMR experiments, the acquisition of reliable spectra still required a lengthy period of time (*ca.* 40-60 min per spectra depending on the complex being investigated). As a result of this time-dependence, the temperature range over which meaningful ^{15}N NMR data could be acquired was limited. For example, the conversion of **4.2-$^{15}N_{\alpha}$** to **4.2-$^{15}N_{\beta}$** was too fast to be measured above 291 K, but yet no isomerization was detected below 274 K (Table 5.2). For the isomerization of **4.1-$^{15}N_{\alpha}$** to **4.1-$^{15}N_{\beta}$** the temperature range was even smaller and thus only a single reliable rate constant was obtained at 291 K (Table 5.2). Furthermore, a quantitative estimate of the rates of isomerization could not be obtained for the carbonyl phosphine and phosphite dinitrogen complexes **4.3-$^{15}N_{\alpha}$** and **4.4-$^{15}N_{\alpha}$** from measurements obtained by ^{15}N NMR spectroscopy for the reasons mentioned above.

From the rate constants (k_c), activation parameters were calculated for complexes **4.1-^{15}N** and **4.2-^{15}N** (Table 5.2). Values for the free energy of activation ($\Delta G^{\neq}$) were determined from the Eyring equation (Equation 5.2)[93] assuming a transmission coefficient of 1.

$$k_c = \kappa(K_B T/h)e^{(-\Delta G^{\neq})/RT} \qquad (5.2)$$

where κ = transmission coefficient

K_B = Boltzmann constant

h = Planck constant

R = Gas constant

T = Temperature

Errors in the $\Delta G^{\neq}$ values were obtained by use of Equation 5.3 for the linearized relative statistical error.[94]

$$(\sigma\Delta G^{\neq}/\Delta G^{\neq})^2 = [\ln(k_B T/hk)]^{-2}(\sigma_k/k)^2 + \{1 + [\ln(k_B T/hk)]^{-1}\}^2(\sigma_T/T)^2 \qquad (5.3)$$

For the dinitrogen complex $Cp^*Re(CO)_2(^{15}N^{14}N)$ (**4.2-$^{15}N_\alpha$**) rate constants were determined at 274, 281, 284, and 291 K and thus a value for the enthalpy of activation ($\Delta H^{\neq}$) and for the entropy of activation ($\Delta S^{\neq}$) was determined. These values were calculated from Equation 5.2 (substituting $\Delta H^{\neq} - T\Delta S^{\neq}$ for $\Delta G^{\neq}$), expressed as an equation of the form $y = a + bx$, by plotting a graph of $\ln(k_c/T)$ versus $1/T$ using a linear least-squares program.[95] Values for the activation energy (E_a) and the frequency factor (A) were determined from the Arrhenius equation (Equation 5.4)[93] by following the previous protocol and thus plotting a graph of $\ln k_c$ versus $1/T$ utilizing a linear least-squares program.[95]

$$k_c = A * e^{(-E_a)/RT} \qquad (5.4)$$

where R = Gas constant

T = Temperature

Errors in $\Delta H^{\neq}$, $\Delta S^{\neq}$, E_a, and A were obtained from the standard deviations derived from the Eyring and Arrhenius plots multiplied by the appropriate statistical factor.[94]

5.3. Discussion

5.3.1. Confirmation of the ^{15}N Linkage Isomers

The observation of a single resonance in the ^{15}N NMR spectrum of each of the singly ^{15}N labeled carbonyl phosphine (**4.3-$^{15}N_\alpha$**) and phosphite (**4.4-$^{15}N_\alpha$**) dinitrogen complexes (Table 5.1) can be accounted for by either a static end-on (η^1) coordinated dinitrogen ligand of the type Re—$^{15}N_\alpha \equiv {}^{14}N_\beta$ or by a rapid exchange of the dinitrogen ligands as illustrated in Equation 5.5 which would result in a ^{15}N signal at the average chemical shift for N_α and N_β.

$$\text{Re}—{}^{15}\underset{\alpha}{\text{N}}\equiv{}^{14}\text{N}_\beta \rightleftharpoons \text{Re}—{}^{14}\underset{\alpha}{\text{N}}\equiv{}^{15}\text{N}_\beta \qquad (5.5)$$

The ^{14}N NMR spectra obtained for the corresponding unlabeled dinitrogen complexes **4.3** and **4.4**, which had been synthesized in an analogous fashion to the ^{15}N labeled complexes, exhibited in each case two broad resonances at δ -91, -30 and δ -99, -29 respectively (Table 5.1). More importantly, the single resonance present in the ^{15}N NMR spectra of **4.3-$^{15}N_\alpha$** and **4.4-$^{15}N_\alpha$** was observed in exactly the same position as one of the corresponding ^{14}N NMR resonances allowing it to be assigned unequivocally to the rhenium-bound nitrogen atom (N_α). Based on these results an end-on static coordination for the dinitrogen ligand in these complexes was confirmed and furthermore, the ^{14}N NMR resonances at δ -91, -99 and δ -30, -29 were assigned to N_α and the terminal nitrogen atom (N_β) respectively.

To confirm that the two ^{15}N NMR resonances observed for each of the dicarbonyl dinitrogen complexes **4.1-$^{15}N_\alpha$** and **4.2-$^{15}N_\alpha$** were due to their respective linkage isomers, ^{14}N NMR spectra were recorded for the unlabeled dicarbonyl dinitrogen complexes **4.1** and **4.2** which had been prepared in an identical manner to the ^{15}N labeled complexes.

The ^{14}N spectra showed in each case two broad resonances at δ -120, -26 and δ -110, -26 respectively, in approximately the same positions as their respective ^{15}N resonances which unequivocally confirmed the presence of two linkage isomers (Table 5.1). The assignment of the N_α and N_β NMR resonances in these complexes was made by comparison with the ^{15}N NMR spectra obtained for the phosphorus-ligand dinitrogen complexes **4.3-$^{15}N_\alpha$** and **4.4-$^{15}N_\alpha$**. The positions of the N_α and N_β resonances for complexes **4.1-$^{15}N_\alpha$** to **4.4-$^{15}N_\alpha$** are also in the region observed in other studies of dinitrogen complexes by ^{15}N NMR.[37b, 69, 157-159]

To verify that the reducing agent was not responsible for the observed differences between the ^{15}N NMR spectra of the dicarbonyl dinitrogen complexes and those of the carbonyl phosphorus-ligand complexes, the carbonyl phosphite dinitrogen complex **4.4-$^{15}N_\alpha$** was prepared again using Cp_2Co (same reagent used for the preparation of **4.1-$^{15}N_\alpha$** and **4.2-$^{15}N_\alpha$**) instead of Na/Hg; a ^{15}N NMR spectrum acquired of this complex reproduced the spectrum obtained previously.

The ^{15}N NMR spectra of Cp'Re(CO)$_2$($^{15}N^{14}N$) (Cp' = Cp (**4.1-$^{15}N_\alpha$**) or Cp* (**4.2-$^{15}N_\alpha$**)) are also accountable if the dinitrogen ligand in each complex is instead doubly-labeled, i.e., Cp'Re(CO)$_2$($^{15}N^{15}N$). This was disproved by mass spectroscopy and is not in accord with the method of synthesis (from the singly $^{15}N_\alpha$ labeled aryldiazenido complex), or the absence of $^{15}N^{15}N$ coupling.

The IR spectra of the singly ^{15}N labeled Cp'Re(CO)$_2$($^{15}N^{14}N$) (Cp' = Cp (**4.1-$^{15}N_\alpha$**) or Cp* (**4.2-$^{15}N_\alpha$**)) exhibited in each case a single sharp absorption at 2110 and 2092 cm^{-1} respectively (2 cm^{-1} resolution, hexane solution) for ν(NN) (see Chapter 4). However, from the ^{15}N NMR evidence just presented, which supports scrambling of the label, it is theoretically feasible that two absorptions corresponding to ν(NN) for Re—$^{15}N\equiv^{14}N$ and Re—$^{14}N\equiv^{15}N$ should have been observed. It is concluded that these absorptions are coincident at this resolution. A similar result was reported for *trans-*

$RhCl(N_2)(PEt_3)_2$, where the $^{15}N_\alpha$ and $^{15}N_\beta$ labeled complexes synthesized from $^{15}N^{14}N$ both exhibited ν(NN) at the same position at 2 cm^{-1} resolution.[127]

From the ^{14}N and ^{15}N NMR spectra of complexes **4.1-4.4**, it was observed that the chemical shift for the N_α resonance of the dinitrogen ligand follow the order of the co-ligands $Cp^*(CO)(PMe_3) > Cp^*(CO)\{P(OMe)_3\} > Cp^*(CO)_2 > Cp(CO)_2$ (from less shielded to more shielded) which correlates with increasing electron donating ability of the co-ligands. A similar trend was found for δ(CO) for these complexes. By contrast, the resonance for N_β remained essentially unchanged. Varying the electron density on the metal evidently produces smaller changes in $\delta(N_\beta)$ than those observed in $\delta(N_\alpha)$, in agreement with previous results for a wide range of dinitrogen complexes.[158, 159] This effect, and the rationale for it, is similar to that mentioned previously in Chapter 2 for δ(CO) of the aryldiazenido derivatives.

5.3.2. Mechanistic Pathways for the Isomerization of the ^{15}N Labeled Rhenium-bound Dinitrogen Ligand

The scrambling of the ^{15}N label which gives rise to the linkage isomers **4.1-$^{15}N_\alpha$** to **4.4-$^{15}N_\alpha$** and **4.1-$^{15}N_\beta$** to **4.4-$^{15}N_\beta$** respectively, can, in principle, be visualized to occur through several different pathways (Scheme 5.3). In (i) the ^{15}N label is scrambled at some point in the synthesis, i.e., during the transformation of the $^{15}N_\alpha$ labeled aryldiazenido complex to the dinitrogen complex, eventually leading to the simultaneous formation of both linkage isomers. In (ii), the scrambling of the ^{15}N label results from a process in which the dinitrogen ligand first dissociates and then recombines with the metal center in a different orientation. The scrambling of the ^{15}N label may also arise from a four-center exchange of the ^{15}N labeled rhenium-bound dinitrogen ligand as illustrated in (iii). In this process two molecules of the $^{15}N_\alpha$ labeled dinitrogen complex combine to give two molecules of the $^{15}N_\beta$ labeled dinitrogen complex.

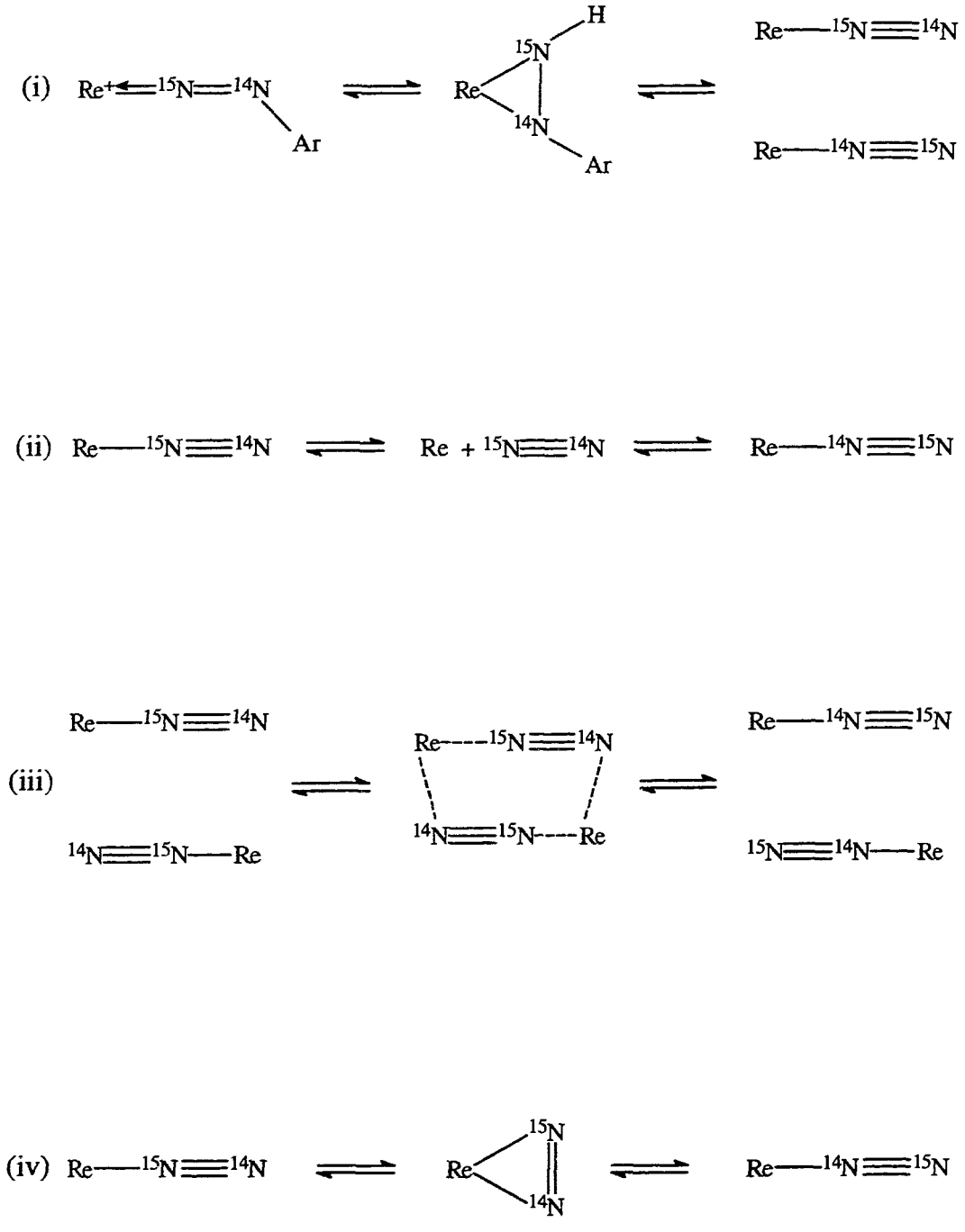

Scheme 5.3. Proposed possible mechanistic pathways for the isomerization of the ^{15}N labeled rhenium-bound dinitrogen ligand (Ar = *p*-C_6H_4OMe).

The final mechanistic pathway which may be responsible for the scrambling of the ^{15}N label (iv) involves the initial formation of the $^{15}N_{\alpha}$ labeled dinitrogen complex which then undergoes a rearrangement through a side-on (η^2) bonded dinitrogen species to produce the $^{15}N_{\beta}$ labeled dinitrogen complex.

5.3.2.1. Dicarbonyl Dinitrogen Complexes

Several methods were devised by which the ^{15}N labeled dicarbonyl dinitrogen complexes can be generated from the corresponding $^{15}N_{\alpha}$ labeled aryldiazenido complexes so that the process responsible for the scrambling of the ^{15}N label can be determined from ^{15}N NMR spectroscopy.

A ^{15}N NMR spectrum obtained immediately after the reaction of $[Cp^*Re(CO)_2(p\text{-}^{15}N^{14}NC_6H_4OMe)][BF_4]$ (**2.2-$^{15}N_{\alpha}$**) and $Ph_3C\cdot$ at 293 K exhibited resonances corresponding to unreacted **2.2-$^{15}N_{\alpha}$**, the newly formed dinitrogen complex $Cp^*Re(CO)_2(^{15}N^{14}N)$ (**4.2-$^{15}N_{\alpha}$**), and an unknown product at δ -66.2 (Figure 5.4). The unknown was identified as the free labeled diazonium salt $[p\text{-}^{15}N^{14}NC_6H_4OMe][BF_4]$ by comparison of its ^{15}N NMR spectra to that of an authentic sample (^{15}N NMR spectrum of $[p\text{-}^{15}N^{14}NC_6H_4OMe][BF_4]$ in $THF:CD_2Cl_2$ (1:1) exhibited a single resonance at δ -66). Notably, the free diazonium salt is most likely an impurity arising from the synthesis of **2.2-$^{15}N_{\alpha}$** (see Chapter 2) and not a product resulting from the reaction of **2.2-$^{15}N_{\alpha}$** and $Ph_3C\cdot$ (an IR spectrum of a sample of **2.2-$^{15}N_{\alpha}$** exhibited an absorption at 2224 cm^{-1} assigned to ν(NN) of $[p\text{-}^{15}N^{14}NC_6H_4OMe][BF_4]$). Monitoring this reaction mixture by ^{15}N NMR spectroscopy showed the eventual disappearance of **2.2-$^{15}N_{\alpha}$** and the free diazonium salt and the appearance of a new resonance assigned to $Cp^*Re(CO)_2(^{14}N^{15}N)$ (**4.2-$^{15}N_{\beta}$**) (Figure 5.5). Unfortunately, the unexpected presence of the free diazonium salt coupled with the poor signal to noise in the ^{15}N NMR spectra prevented the abstraction of reliable information which may have proved helpful in clarifying the

process responsible for the scrambling of the ^{15}N label.

To overcome the ^{15}N NMR complications associated with the $Ph_3C\cdot$ reaction, an alternative more efficient route to the ^{15}N labeled dinitrogen complex was developed. A ^{15}N NMR spectrum recorded immediately following the reaction of Cp_2Co and **2.2-$^{15}N_\alpha$** at 284 K showed a single ^{15}N resonance at δ -110.8, unambiguously demonstrating that **4.2-$^{15}N_\alpha$** is the initial product (Figure 5.6). Following this reaction mixture by ^{15}N NMR showed the slow, gradual conversion of **4.2-$^{15}N_\alpha$** to **4.2-$^{15}N_\beta$** until an equal molar mixture of these isomers was obtained (Figure 5.6); pathways (ii), (iii), and (iv) are consistent with these observations. Analogous results obtained for the dinitrogen complex $CpRe(CO)_2(^{15}N^{14}N)$ (**4.1-$^{15}N_\alpha$**) indicate that scrambling of the ^{15}N label occurs similarly in this complex when synthesized from the corresponding $^{15}N_\alpha$ labeled aryldiazenido complex **2.1-$^{15}N_\alpha$** by reaction with Cp_2Co (Figure 5.7).

As described in Chapter 4, the reaction of $[Cp^*Re(CO)_2(p\text{-}N_2C_6H_4OMe)][BF_4]$ (**2.2**) with $NaBH_4$ affords initially the aryldiazene complex $Cp^*Re(CO)_2(p\text{-}NHNC_6H_4OMe)$ (**4.10**) which then eliminates anisole to give the corresponding dinitrogen complex $Cp^*Re(CO)_2(N_2)$ (**4.2**). If the elimination of anisole from the aryldiazene complex is intramolecular, this introduces the possibility that the elimination occurs from an η^2-coordinated aryldiazene ligand as illustrated in pathway (i). The $NaBH_4$ reaction was repeated using **2.2-$^{15}N_\alpha$** at room temperature. A ^{15}N NMR spectrum collected at 280 K after the complete conversion of **2.2-$^{15}N_\alpha$** to the dinitrogen complex $Cp^*Re(CO)_2(^{15}N^{14}N)$ (**4.2-$^{15}N_\alpha$**) exhibited a single resonance at δ -110.8, unambiguously demonstrating that **4.2-$^{15}N_\alpha$** is, once again, the initial product (Figure 5.8). A ^{15}N NMR spectra obtained after the reaction mixture was warmed to 293 K and allowed to equilibrate for several hours showed two equally populated resonances corresponding to **4.2-$^{15}N_\alpha$** and $Cp^*Re(CO)_2(^{14}N^{15}N)$ (**4.2-$^{15}N_\beta$**) respectively (Figure 5.8). Therefore, regardless of the mechanism for elimination of anisole, it yields the $^{15}N_\alpha$

linkage isomer of the dinitrogen complex solely, and isomerization to the $^{15}N_{\beta}$ isomer again takes place in the dinitrogen complex itself, not during the conversion of the aryldiazene to the dinitrogen complex. These results are not consistent with pathway (i).

To differentiate between the remaining three pathways a sample of the equimolar mixture of $Cp^*Re(CO)_2(^{15}N^{14}N)$ (**4.2-$^{15}N_{\alpha}$**) and $Cp^*Re(CO)_2(^{14}N^{15}N)$ (**4.2-$^{15}N_{\beta}$**) in hexane was examined for dissociative exchange with $^{14}N_2$. After 24 h under 1500 psi of $^{14}N_2$, the IR spectrum of the ^{15}N labeled complex revealed negligible incorporation of $^{14}N_2$ as evidenced by the lack of a $\nu(^{14}N^{14}N)$ absorption. Furthermore, a hexane solution of $CpRe(CO)_2(^{15}N^{14}N)$ (**4.1-$^{15}N_{\alpha}$**) and $CpRe(CO)_2(^{14}N^{15}N)$ (**4.1-$^{15}N_{\beta}$**) also showed no observable IR absorption for $\nu(^{14}N^{14}N)$ when pressurized with $^{14}N_2$ at 1500 psi over 18 h. These results do not support a dissociation-recombination mechanism [pathway (ii)] as a viable route for the isomerization of the ^{15}N labeled rhenium-bound dinitrogen ligand.

The two remaining pathways [(iii) and (iv)] are both consistent with all the spectroscopic evidence obtained thus far. To discriminate between these pathways a mixture of unlabeled $CpRe(CO)_2(^{14}N^{14}N)$ [ν(NN) 2145 cm^{-1}] and ^{15}N labeled $Cp^*Re(CO)_2(N_2)$ [1:1 molar mixture of **4.2-$^{15}N_{\alpha}$** and **4.2-$^{15}N_{\beta}$**; ν(NN) coincident at 2092 cm^{-1}] in hexane was observed by IR spectroscopy at room temperature over a period of 3 weeks. The ν(NN) absorptions of the ^{15}N and ^{14}N isotopomers of these two complexes (Cp or Cp*) are characteristically sharp in hexane and would readily indicate if any cross products were formed. We observed no change; specifically, no absorptions attributable to ^{15}N labeled $CpRe(CO)_2(N_2)$ [$\nu(^{15}N^{14}N)$ and $\nu(^{14}N^{15}N)$ are coincident at 2110 cm^{-1}] or $Cp^*Re(CO)_2(^{14}N^{14}N)$ [ν(NN) 2125 cm^{-1}]. This result is not consistent with a four-center exchange mechanism [pathway (iii)]. Therefore, the mechanism which best describes the observed scrambling of the ^{15}N label is the intramolecular, non-dissociative process illustrated in pathway (iv).

5.3.2.2. Carbonyl Phosphine and Phosphite Dinitrogen Complexes

The process responsible for the scrambling of the ^{15}N label in the phosphine and phosphite dinitrogen complexes $Cp^*Re(CO)(PMe_3)(^{15}N^{14}N)$ (**4.3-$^{15}N_\alpha$**) and $Cp^*Re(CO)\{P(OMe)_3\}(^{15}N^{14}N)$ (**4.4-$^{15}N_\alpha$**) was also investigated. The room temperature ^{15}N NMR spectra of these complexes, recorded several days after their synthesis, exhibited in each case a single resonance ascribed to the respective $^{15}N_\alpha$ linkage isomers **4.3-$^{15}N_\alpha$** and **4.4-$^{15}N_\alpha$**. Elevating the temperature at which the ^{15}N NMR spectra were obtained, eventually resulted in the conversion of the $^{15}N_\alpha$ labeled dinitrogen complexes to the corresponding dinitrogen derivatives $Cp^*Re(CO)(PMe_3)(^{14}N^{15}N)$ (**4.3-$^{15}N_\beta$**) (320 K) and $Cp^*Re(CO)\{P(OMe)_3\}(^{14}N^{15}N)$ (**4.4-$^{15}N_\beta$**) (333 K) until an equimolar mixture of these isomers was obtained (Figures 5.9 and 5.10); pathways (ii), (iii), and (iv) are consistent with these observations. To accommodate the higher temperatures, CD_3CN was used as the NMR solvent instead of the lower boiling point acetone-d_6.

An equimolar mixture of **4.4-$^{15}N_\alpha$** and **4.4-$^{15}N_\beta$** in hexane was examined for dissociative exchange with $^{14}N_2$. After 4 h under 1000 psi of $^{14}N_2$, at a temperature of 320 K, the IR spectrum of the ^{15}N labeled complex exhibited negligible incorporation of $^{14}N_2$. A hexane solution of **4.3-$^{15}N_\alpha$** and **4.3-$^{15}N_\beta$** also showed no observable IR absorptions for $\nu(^{14}N^{14}N)$ when pressurized with $^{14}N_2$ at 1000 psi over 4 h at a temperature of 333 K. These results are not in agreement with a dissociation-recombination mechanism [pathway (ii)].

A cross-over experiment involving the unlabeled complex $Cp^*Re(CO)\{P(OMe)_3\}(^{14}N^{14}N)$ and the ^{15}N labeled complex $Cp^*Re(CO)(PMe_3)(N_2)$ [1:1 molar mixture of **4.3-$^{15}N_\alpha$** and **4.3-$^{15}N_\beta$**] in hexane was carried out at 333 K and the results were monitored by IR spectroscopy. After 4 h, no cross products were formed. Attempts to monitor the reaction for a longer time were not successful since both these dinitrogen complexes began to decompose at this temperature as indicated by the loss in

intensity of the corresponding ν(NN) absorptions. As was the case for the dicarbonyl dinitrogen complexes, these results are also supportive of an intramolecular, non-dissociative process [pathway (iv)] for the observed scrambling of the ^{15}N label in these carbonyl phosphine and phosphite dinitrogen complexes.

5.3.3. Rate Constants and Activation Parameters for Isomerization of the ^{15}N Labeled Dinitrogen Ligand

From the dynamic ^{15}N NMR investigation, the rate constants and subsequently the activation parameters for the end-to-end rotation of the ^{15}N labeled dinitrogen ligand in complexes **4.1-$^{15}N_\alpha$** and **4.2-$^{15}N_\alpha$** were determined, and are summarized in Table 5.2. For the Cp* dicarbonyl dinitrogen complex **4.2-$^{15}N_\alpha$**, the rate constant (k_c) was calculated to be $(1.4 \pm 0.1) \times 10^{-4}$ s^{-1} at 291 K, providing a $\Delta G^{\neq}$ value of 92.6 ± 0.4 kJ/mole for the energy of activation to rotation at this temperature. For the Cp analog **4.1-$^{15}N_\alpha$**, a k_c value of $(4.8 \pm 0.6) \times 10^{-5}$ s^{-1} was obtained at the same temperature, giving rise to a $\Delta G^{\neq}$ value of 95.3 ± 0.5 kJ/mole for the energy of activation. These results indicate that the energy of activation for the isomerization of the ^{15}N labeled dinitrogen ligand is lowered when the Cp ligand is replaced by its methylated analog Cp*.

These $\Delta G^{\neq}$ values are similar to the energy of activation estimated from IR spectroscopy by Taube et al. for $[Ru(NH_3)_5(N_2)]^{2+}$ (*ca.* 88 kJ/mole), which is the only other example that we are aware of for which the energy of activation for linkage isomerization of metal-bound dinitrogen has been estimated.[160] From measurements of the rate of aquation of $[Ru(NH_3)_5(N_2)]^{2+}$, Taube et al. also obtained a value of *ca.* 117 kJ/mole for the enthalpy of activation for the dissociation of the N_2 ligand.[161] For **4.2-$^{15}N_\alpha$**, $\Delta H^{\neq}$ was calculated to be 105.3 ± 6.0 kJ/mole; this value is significantly smaller than the one obtained by Taube for N_2 dissociation and thus lends further support to an intramolecular, non-dissociative process for the observed isomerization of the rhenium-

bound N_2 ligand. The isomerization of N_2 was also reported to have been detected in other related ruthenium complexes.[162]

The observed, relatively slow, rate of exchange in **4.1-$^{15}N_\alpha$** and **4.2-$^{15}N_\alpha$** and the large chemical shift separation between the N_α and N_β resonances in the ^{14}N and ^{15}N NMR spectra of these dinitrogen complexes made it impossible to use an NMR lineshape analysis to calculate the kinetic parameters for this interconversion. Therefore, the only viable method that we could devise to monitor this isomerization process involved the rapid synthesis of the $^{15}N_\alpha$ linkage isomer and the subsequent measurement of its rate of decay to the $^{15}N_\beta$ isomer by ^{15}N NMR spectroscopy. Employing this method generated quantitative data (i.e., rate constants and activation parameters) for the dicarbonyl dinitrogen complexes **4.1-$^{15}N_\alpha$** and **4.2-$^{15}N_\alpha$**. However, a quantitative estimate of the rates of isomerization could not be obtained for the carbonyl phosphine and phosphite dinitrogen complexes **4.3-$^{15}N_\alpha$** and **4.4-$^{15}N_\alpha$** respectively (see Results section 5.2.3). The isomerization between **4.4-$^{15}N_\alpha$** and **4.4-$^{15}N_\beta$** was detected at an elevated temperature of 320 K, whereas a temperature of 333 K was required to interconvert the linkage isomers **4.3-$^{15}N_\alpha$** and **4.3-$^{15}N_\beta$**. From these qualitative findings it appears that the barrier to isomerization for the rhenium-bound ^{15}N labeled dinitrogen ligand is raised by replacing a CO group in $Cp^*Re(CO)_2(^{15}N^{14}N)$ (**4.2-$^{15}N_\alpha$**) by $P(OMe)_3$, and raised further when CO is substituted by PMe_3.

5.4. Conclusion

In this chapter we have demonstrated that the scrambling of the ^{15}N label equally between the N_α and N_β sites occurs at room temperature in the case of $Cp'Re(CO)_2(^{15}N^{14}N)$ (Cp' = Cp (**4.1-$^{15}N_\alpha$**) or Cp* (**4.2-$^{15}N_\alpha$**)), or at elevated temperatures in the case of $Cp^*Re(CO)(PR_3)(^{15}N^{14}N)$ (PR_3 = PMe_3 (**4.3-$^{15}N_\alpha$**) or $P(OMe)_3$ (**4.4-$^{15}N_\alpha$**)) so that equimolar amounts of the $^{15}N_\alpha$ and $^{15}N_\beta$ labeled molecules result. All these

complexes were prepared from the corresponding aryldiazenido complexes, which were specifically labeled at the rhenium-bound nitrogen atom (N_α) with ^{15}N. For all the complexes examined, the scrambling of the ^{15}N label was shown to proceed by an intramolecular, non dissociative process involving an end-to-end rotation of the rhenium-bound dinitrogen ligand *via* the elusive side-on (η^2) bonded dinitrogen species. The barriers for this linkage isomerization were also measured.

5.5. Experimental

5.5.1. General Methods and Syntheses

Manipulations, solvent purification, and routine spectroscopic measurements were carried out as described in Chapter 2. High pressure reactions were carried out in a Parr bomb, at room temperature or at elevated temperatures, using oxygen free nitrogen (Linde Union Carbide). The complexes which were investigated in this chapter were prepared and purified following the procedures detailed in Chapter 4.

The deuterated solvents used for NMR spectroscopy were degassed prior to use to remove any residual oxygen. ^{14}N and ^{15}N NMR chemical shifts (downfield positive) are referenced to external nitromethane ($MeNO_2$).

5.5.2. Variable Temperature and Time-dependent NMR Spectroscopy

The variable temperature and time-dependent ^{15}N and ^{14}N NMR spectra of complexes **4.1-$^{15}N_\alpha$** to **4.4-$^{15}N_\alpha$** were recorded at 40.6 and 28.9 MHz respectively on a Bruker AMX 400 instrument equipped with a B-VT 1000 variable temperature unit. A cooling unit containing liquid nitrogen and a heater coil was attached to the NMR probe and was used to attain the desired temperature. A 5 mm NMR tube was used to acquire the ^{14}N spectra whereas a 10 mm NMR tube was used to obtain the ^{15}N spectra. A

Bruker single frequency probe was used to acquire the ^{14}N spectra, while a Bruker tunable broad band probe was used to acquire the ^{15}N spectra. Acetone-d_6 (Isotec Inc.), and in some cases CD_2Cl_2 (Isotec) or CD_3CN (Isotec), were used as solvents for the variable temperature and time-dependent NMR work.

Temperatures, which were obtained directly from the VT unit, were checked by measuring peak separations for a standard Bruker sealed sample of methanol and converting these into temperature values using the quadratic equation of Van Geet[119] for methanol. Temperature gradients within the sample region of the AMX 400 spectrometer are considered to be negligible because of the large distance between the cooling unit and the probe; temperatures are accurate to ±1 K.

Time-dependent ^{15}N NMR Spectroscopy of Cp*Re(CO)$_2$($^{15}N^{14}N$) (4.2-$^{15}N_\alpha$) Prepared Using Ph_3C·. A solution containing the triphenylmethyl radical (Ph_3C·) was prepared by reduction of the corresponding chloride Ph_3CCl with zinc dust in THF. A 10-fold stoichiometric excess of the Ph_3C· solution was then added by cannula to a solution of the $^{15}N_\alpha$ labeled aryldiazenido complex [Cp*Re(CO)$_2$(*p*-$^{15}N^{14}NC_6H_4OMe$)][BF_4] (**2.2-$^{15}N_\alpha$**) in CD_2Cl_2 at room temperature. An IR spectrum recorded 15 min after the Ph_3C· addition showed the presence of both the starting aryldiazenido complex **2.2-$^{15}N_\alpha$** and the newly formed $^{15}N_\alpha$ labeled dinitrogen complex Cp*Re(CO)$_2$($^{15}N^{14}N$) (**4.2-$^{15}N_\alpha$**). The solution was then immediately transferred to an NMR tube which was kept in a Schlenk tube under a positive pressure of argon at a temperature of 273 K in an ice bath. The NMR tube was then quickly removed from the cold temperature bath and placed into the Bruker AMX 400 spectrometer whose temperature unit had been previously set to 293 K. A sequence of ^{15}N NMR spectra were then acquired over a measured period of time.

Variable Temperature and Time-dependent ^{15}N NMR Spectroscopy of $CpRe(CO)_2(^{15}N^{14}N)$ (4.1-$^{15}N_\alpha$) and $Cp^*Re(CO)_2(^{15}N^{14}N)$ (4.2-$^{15}N_\alpha$) Prepared Using Cp_2Co. A 5-fold stoichiometric excess of Cp_2Co was dissolved in a minimum amount of acetone-d_6 and then added *via* syringe to a solution of the $^{15}N_\alpha$ labeled aryldiazenido complexes $[CpRe(CO)_2(p\text{-}^{15}N^{14}NC_6H_4OMe)][BF_4]$ (**2.1-$^{15}N_\alpha$**) or $[Cp^*Re(CO)_2(p\text{-}^{15}N^{14}NC_6H_4OMe)][BF_4]$ (**2.2-$^{15}N_\alpha$**) in acetone-d_6 at room temperature. An IR spectrum, obtained immediately after the Cp_2Co addition, showed in both cases the complete disappearance of the aryldiazenido complexes and the presence of the respective $^{15}N_\alpha$ labeled dinitrogen complexes $CpRe(CO)_2(^{15}N^{14}N)$ (**4.1-$^{15}N_\alpha$**) and $Cp^*Re(CO)_2(^{15}N^{14}N)$ (**4.2-$^{15}N_\alpha$**). In both cases, the solution was then immediately transferred to an NMR tube which was kept in a Schlenk tube under a positive pressure of argon at a temperature of 273 K in an ice bath. The NMR tube was then quickly removed from the cold temperature bath and placed into the Bruker AMX 400 spectrometer whose temperature unit had been previously set to the desired temperature (i.e., 291 K for **4.1-$^{15}N_\alpha$**; 274, 281, 284, and 291 K for **4.2-$^{15}N_\alpha$**). A sequence of ^{15}N NMR spectra were then acquired over a measured period of time.

Time-dependent ^{15}N NMR Spectroscopy of $Cp^*Re(CO)_2(^{15}N^{14}N)$ (4.2-$^{15}N_\alpha$) Prepared Using $NaBH_4$. A 2-fold stoichiometric excess of $NaBH_4$ was added as a solid to a solution of the $^{15}N_\alpha$ labeled aryldiazenido complex $[Cp^*Re(CO)_2(p\text{-}^{15}N^{14}NC_6H_4OMe)][BF_4]$ (**2.2-$^{15}N_\alpha$**) in acetone-d_6 at room temperature. An IR spectrum of this solution recorded immediately after the $NaBH_4$ addition demonstrated the total disappearance of **2.2-$^{15}N_\alpha$** and the presence of minor absorptions corresponding to the $^{15}N_\alpha$ labeled dinitrogen complex $Cp^*Re(CO)_2(^{15}N^{14}N)$ (**4.2-$^{15}N_\alpha$**) and major absorptions due to the aryldiazene complex $Cp^*Re(CO)_2(p\text{-}NHNC_6H_4OMe)$ (**4.10-$^{15}N_\alpha$**) (see Chapter 4). An IR spectrum obtained after 35 min showed only the presence of absorptions attributable to **4.2-$^{15}N_\alpha$**. The solution was then immediately transferred to an NMR tube

which was kept in a Schlenk tube under a positive pressure of argon at a temperature of 273 K in an ice bath. The NMR tube was then quickly removed from the cold temperature bath and placed into the Bruker AMX 400 spectrometer whose temperature unit had been previously set to 280 K. A sequence of ^{15}N NMR spectra were then acquired over a measured period of time.

Variable Temperature and Time-dependent ^{15}N NMR Spectroscopy of Cp*Re(CO){P(OMe)$_3$}($^{15}N^{14}N$) (4.4-$^{15}N_\alpha$) Prepared Using Na/Hg. A sodium amalgam was prepared by adding small, freshly cut pieces of sodium metal (5-fold stoichiometric excess) to a pool of mercury under argon; with gentle stirring the sodium pieces were taken up by the mercury. A solution of the $^{15}N_\alpha$ labeled aryldiazenido complex [Cp*Re(CO){P(OMe)$_3$}(*p*-$^{15}N^{14}NC_6H_4OMe$)][BF_4] (**2.8-$^{15}N_\alpha$**) in THF was then added *via* syringe to the sodium amalgam at room temperature and the mixture was vigorously stirred for 30 min. An IR spectrum recorded at this time showed the complete disappearance of **2.8-$^{15}N_\alpha$** and the presence of the respective $^{15}N_\alpha$ labeled dinitrogen complex Cp*Re(CO){P(OMe)$_3$}($^{15}N^{14}N$) (**4.4-$^{15}N_\alpha$**). Complex **4.4-$^{15}N_\alpha$** was then purified following the procedure described in Chapter 4 and subsequently taken up in CD_3CN. The solution was then transferred to an NMR tube which was kept in a Schlenk tube under a positive pressure of argon at room temperature. The NMR tube was then placed into the Bruker AMX 400 spectrometer whose temperature unit had been previously set to 293 K. A sequence of ^{15}N NMR spectra acquired over 24 h exhibited no change in the ^{15}N resonance of **4.4-$^{15}N_\alpha$**. A change in intensity of the ^{15}N resonance corresponding to **4.4-$^{15}N_\alpha$** was achieved by elevating the temperature to 320 K. A sequence of ^{15}N NMR spectra were then acquired over a measured period of time at this temperature.

Variable Temperature and Time-dependent ^{15}N NMR Spectroscopy of Cp*Re(CO)(PMe$_3$)($^{15}N^{14}N$) (4.3-$^{15}N_\alpha$) Prepared Using Na/Hg. The $^{15}N_\alpha$ labeled

trimethylphosphine dinitrogen complex Cp*Re(CO)(PMe_3)($^{15}N^{14}N$) (**4.3-$^{15}N_\alpha$**) was synthesized from the corresponding aryldiazenido complex [Cp*Re(CO)(PMe_3)(*p*-$^{15}N^{14}NC_6H_4OMe$)][BF_4] (**2.4-$^{15}N_\alpha$**) and subsequently purified following a similar procedure to that described previously for the $P(OMe)_3$ analog. A CD_3CN solution of **4.3-$^{15}N_\alpha$** was then transferred to an NMR tube which was kept in a Schlenk tube under a positive pressure of argon at room temperature. The NMR tube was then placed into the Bruker AMX 400 spectrometer whose temperature unit had been previously set to 293 K. A sequence of ^{15}N NMR spectra acquired over 24 h exhibited no change in the ^{15}N resonance of **4.3-$^{15}N_\alpha$**. A similar result was obtained at 320 K. A change in intensity of the ^{15}N resonance corresponding to **4.3-$^{15}N_\alpha$** was finally achieved by elevating the temperature to 333 K. A sequence of ^{15}N NMR spectra were then acquired over a measured period of time at this temperature.

CHAPTER 6

Protonation Reactions of Rhenium-bound Dinitrogen

6.1. Introduction

The discovery of the first dinitrogen complex $[Ru(NH_3)_5(N_2)]^{2+}$ in 1965,[22] together with the announcement of some less well-characterized systems for fixing nitrogen uncovered by Vol'pin and his co-workers,[21] encouraged a large amount of research into transition metal dinitrogen complexes and their reactions. Despite the steady stream of new dinitrogen complexes,[23] it was not until 1972 that the first reaction of coordinated dinitrogen to give a well-defined product was announced (Equation 6.1).[163]

$$W(N_2)_2(dppe)_2 + CH_3COCl \longrightarrow WCl(N_2COCH_3)(dppe)_2 + N_2 \qquad (6.1)$$

This reaction was interpreted as being essentially an oxidative addition to a WN≡N fragment, with the principal step being nucleophilic attack of the coordinated N_2 on the carbon of the acetyl group. As a result, this work was successfully extended to protonation reactions, as evidenced by the initial discovery by Chatt et al. of the protonation of coordinated dinitrogen to give hydrazido complexes and the subsequent conversion of these intermediate species to ammonia (Equation 6.2).[164]

$$M(N_2)_2(PMe_2Ph)_4 + H_2SO_4 \longrightarrow [M(SO_4H)(NNH_2)(PMe_2Ph)_4][SO_4H] \longrightarrow 2NH_3 + N_2 + \text{other products} \qquad (6.2)$$

M = Mo or W

The chemistry developed from the protonation of these low oxidation state complexes of molybdenum and tungsten formed the basis for a general understanding of the reactivity displayed by metal-bound dinitrogen. According to Chatt et al.,[33] the activation of the dinitrogen ligand, at least as far as the initial step of the protonation reaction is concerned (i.e., the delivery of the first proton to the metal complex), was suggested to be dependent on the ease of release of electrons from the metal center into the coordinated dinitrogen ligand. That is, if one is dealing with nucleophilic attack by coordinated dinitrogen on protons, those dinitrogens with the higher negative charge, provided by the metal d-π*(NN) donation into the N_2 antibonding orbitals, should be the more effective. Therefore, it was generally concluded that the protonation of ligated dinitrogen required a low oxidation state complex composed of a metal center with a low first ionization potential, and ancillary ligands which were good σ-donors but poor π-acceptors of electron density.

Based on the criteria just presented, combined with the knowledge I had acquired of the chemistry exhibited by rhenium-bound dinitrogen derivatives, a protonation study of the low oxidation state dinitrogen complex $Cp^*Re(PMe_3)_2(N_2)$ **(4.5)** (Figure 6.1) was undertaken, the results of which are described in this chapter.

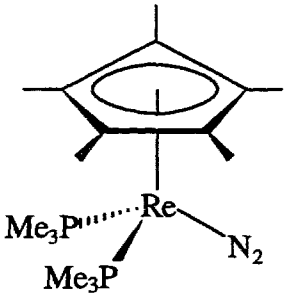

4.5

Figure 6.1. Structure of **4.5**.

6.2. Results

6.2.1. Examination of $Cp^*Re(PMe_3)_2(N_2)$ (4.5), (4.5-$^{15}N_\alpha$), or (4.5-$^{15}N_\beta$)

The bis-trimethylphosphine dinitrogen complex $Cp^*Re(PMe_3)_2(N_2)$ (**4.5**) was prepared from the corresponding aryldiazenido complex **2.11** by treatment with Na/Hg at room temperature (see Chapter 4). The ^{14}N NMR spectrum of **4.5** exhibited two broad resonances at δ -82 and δ -49 assigned to the rhenium-bound nitrogen atom (N_α) and the terminal nitrogen atom (N_β) respectively (Table 6.1). Confirmation of these assignments was obtained by recording the ^{15}N NMR spectra of the specifically ^{15}N labeled dinitrogen complexes $Cp^*Re(PMe_3)_2(^{15}N^{14}N)$ (**4.5-$^{15}N_\alpha$**) and $Cp^*Re(PMe_3)_2(^{14}N^{15}N)$ (**4.5-$^{15}N_\beta$**) which had been synthesized in an analogous manner to the corresponding unlabeled complex. In both cases a single sharp resonance (i.e., δ -82.1 for **4.5-$^{15}N_\alpha$** and δ -51.7 for **4.5-$^{15}N_\beta$**), with no measurable coupling to phosphorus was observed in approximately the same positions as the two ^{14}N resonances, allowing the unequivocal assignment of N_α and N_β (Table 6.1).

Of equal importance, the single $^{15}N_\alpha$ resonance observed in the ^{15}N NMR spectrum of **4.5-$^{15}N_\alpha$** in acetone-d_6 at room temperature was unchanged even after 24 h. The absence of a signal in the position expected for N_β in the ^{15}N NMR spectrum of the singly-labeled complex after this time shows that there is negligible incorporation of ^{15}N at the β-position and no detectable isomerization of the dinitrogen ligand (see Chapter 5) under these experimental conditions for this complex. Analogous results were obtained for the $^{15}N_\beta$ labeled dinitrogen complex **4.5-$^{15}N_\beta$** when it was examined by ^{15}N NMR spectroscopy. The fact that the N_2 ligand in **4.5** can be specifically ^{15}N labeled and does not interconvert was an essential requirememt in order to utilize ^1H, $^{31}P\{^1H\}$, and ^{15}N NMR spectroscopy as a reliable probe to determine which particular site on this dinitrogen complex was attacked upon protonation, in the event of this occurring.

Table 6.1. IR, ^{15}N, and ^{14}N NMR Data for Selected Dinitrogen Complexes

Complex	^{15}N NMR[a]		^{14}N NMR[a]		IR $\nu(^{14}N_2)$[b]	Reference
	$\delta(^{15}N_\alpha)$	$\delta(^{15}N_\beta)$	$\delta(^{14}N_\alpha)$	$\delta(^{14}N_\beta)$		
$CpRe(CO)_2(N_2)$ **(4.1)**[c]	-120.9	-27.3	-120	-26	2145	This work
$Cp^*Re(CO)_2(N_2)$ **(4.2)**[c]	-110.8	-28.1	-110	-26	2125	This work
$Cp^*Re(CO)(PMe_3)(N_2)$ **(4.3)**[c]	-91.3	-32.7	-91	-30	2044	This work
$Cp^*Re(CO)\{P(OMe)_3\}(N_2)$ **(4.4)**[c]	-99.4	-32.5	-99	-29	2078, 2066	This work
$Cp^*Re(PMe_3)_2(N_2)$ **(4.5)**[c]	-82.1	-51.7	-82	-49	1975	This work
trans-$Mo(N_2)_2(dppe)_2$[d]	-43.1	-42.8			1976	158
trans-$W(N_2)_2(dppe)_2$[d]	-60.1	-48.6			1946	158
$Fe(N_2)(dmpe)_2$[e]					1975	166

[a] Referenced to external $MeNO_2$; δ given in ppm.

[b] $\nu(^{14}N_2)$ given in cm^{-1}.

[c] Acetone-d_6 used as the NMR solvent; hexane used as the IR solvent.

[d] THF used as the NMR solvent; IR recorded in Nujol.

[e] THF used as the IR solvent.

6.2.2. Room Temperature Reactions of $Cp^*Re(PMe_3)_2(N_2)$ (4.5) with $HBF_4 \cdot OEt_2$, CF_3SO_3H, or CF_3COOH

A 5-fold stoichiometric excess of tetrafluoroboric acid diethyl ether complex ($HBF_4 \cdot OEt_2$) was added *via* syringe to a pale yellow solution of $Cp^*Re(PMe_3)_2(N_2)$ (**4.5**) in acetone-d_6 at room temperature. An instantaneous reaction took place as the color of the solution turned dark orange immediately after the acid was added. An IR spectrum obtained of this solution showed the complete disappearance of **4.5** with no concomitant growth of absorptions in the 2400-1400 cm^{-1} region, consistent with protic attack of the dinitrogen complex. However, the lack of an NH band in the 4000-3500 cm^{-1} region suggested that the ligated dinitrogen was not protonated.

A room temperature ^1H NMR spectrum, acquired *ca.* 60 min after the acid addition, did not exhibit a downfield signal assignable to an NH resonance nor an upfield signal suggestive of a metal hydride resonance. These results infer that protic attack did not occur at the nitrogen ligand nor at the metal center respectively. Purification of the NMR solution confirmed the presence of trace amounts of the trioxo complex Cp^*ReO_3 (**4.8**)[138] and trimethylphosphine oxide ($POMe_3$) by comparison to the NMR spectra of the authentic samples. No other rhenium containing products were identified. The oxidation products were presumably formed by exposure of the NMR solution to improperly degassed NMR solvent or to residual oxygen which may have entered the non flame-sealed NMR tube.

Analogous results were obtained when the protonation of **4.5** was repeated using trifluoromethanesulfonic acid (CF_3SO_3H). Surprisingly, this was not the case for the protonation reaction involving trifluoroacetic acid (CF_3COOH). The pale yellow solution of **4.5** in acetone-d_6 turned orange in color upon addition of a 5-fold stoichiometric excess of CF_3COOH *via* syringe at room temperature. An IR spectrum recorded immediately after the acid was added showed the complete disappearance of **4.5**

and the presence of a weak broad absorption at 2080 cm^{-1}. An examination of the 4000-3500 cm^{-1} region revealed no absorptions which could be assigned to an NH vibration, and thus inferred that the coordinated dinitrogen ligand was not protonated.

A room temperature ^1H NMR spectrum, obtained *ca.* 60 min after the acid addition, exhibited a singlet at δ 2.05 integrating to 15 protons assigned to a Cp* group (Figure 6.2). The ^1H resonance at δ 1.75 assigned to the PMe_3 ligands was observed to be a virtual doublet integrating to 18 protons with a coupling constant ($^2J_{H-P} + {}^4J_{H-P}$) of 9.5 Hz (Figure 6.2). Most importantly, although a downfield signal which may be attributable to an NH resonance was not observed, a high field triplet (J = 49.6 Hz) at δ -10.58 integrating to 1 proton was present (Figure 6.2). This result is consistent with protic attack at the metal center resulting in a rhenium hydrido species and the triplet indicates that the metal hydride ligand is coupled to two symmetry-equivalent PMe_3 ligands. Interestingly, a ^1H NMR spectrum recorded *ca.* 12 h later of the same NMR sample showed the total disappearance of all resonances corresponding to the newly formed rhenium hydrido complex. Purification of the NMR solution gave residual amounts of the trioxo complex **4.8**[138] and $POMe_3$; the same products which had been identified previously for the reactions where $HBF_4 \cdot OEt_2$ and CF_3SO_3H were used as the proton source.

The protonation of **4.5** with CF_3COOH was repeated in acetone at room temperature. The product(s) of this reaction were found to be insoluble in hexane or diethyl ether but very soluble in acetone. A diagnostic mass spectrum for this metal hydrido complex was not obtained despite numerous attempts using electon impact (EI), low voltage electron impact, or chemical ionization (CI) mass spectroscopy, presumably as a result of its thermal instability.

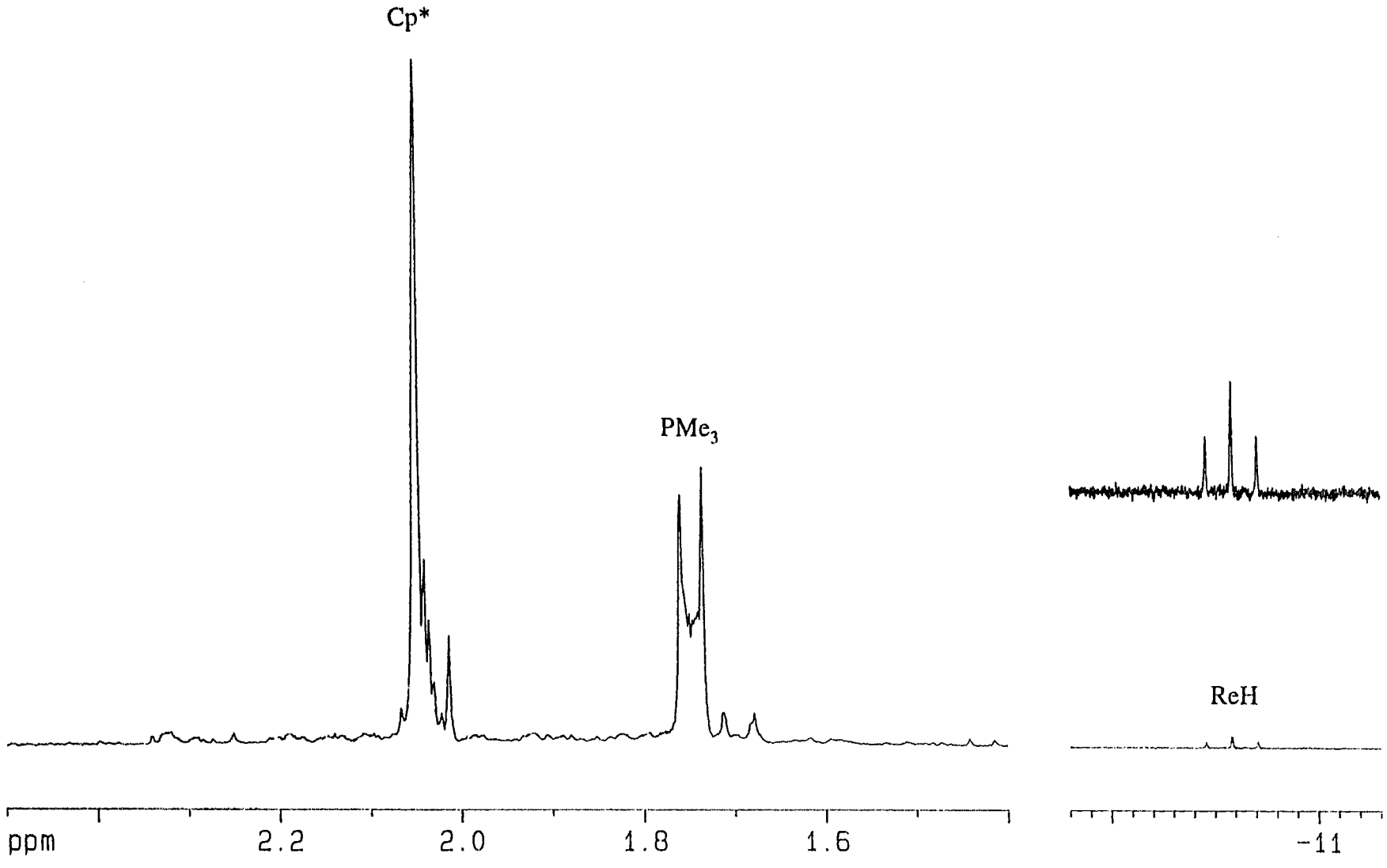

Figure 6.2. ^{1}H NMR spectrum (400 MHz) of the reaction between Cp*Re(PMe_3)$_2$(N_2) (**4.5**) and CF_3COOH in acetone-d_6 at room temperature. Upfield triplet has been expanded for clarity.

6.2.3. Low Temperature Reactions of $Cp^*Re(PMe_3)_2(N_2)$ (4.5), (4.5-$^{15}N_\alpha$), or (4.5-$^{15}N_\beta$) with CF_3COOH

A 5-fold stoichiometric excess of CF_3COOH was added *via* syringe to a solution of $Cp^*Re(PMe_3)_2(N_2)$ (**4.5**) in acetone-d_6 at 195 K. A ^1H NMR spectrum, obtained *ca.* 60 min after the acid addition at 213 K, showed the total disappearance of **4.5** and the apparent formation of a single rhenium product which exhibited a singlet at δ 2.08 integrating to 15 protons assigned to a Cp* group (Figure 6.3a). The ^1H resonance at δ 1.76 assigned to the PMe_3 ligands was observed to be an apparent broad triplet integrating to 18 protons with a coupling constant of 8.8 Hz (Figure 6.3a). The ^1H NMR spectrum also exhibited a doublet at δ -10.96 integrating to 1 proton with a coupling constant of 64.2 Hz (Figure 6.3a); no signal corresponding to an NH resonance was found. These results are consistent with protic attack at the metal center giving a rhenium hydrido complex.

A $^{31}P\{^1H\}$ NMR spectrum recorded for the same NMR sample at 213 K showed two resonances at δ -42.16 and δ -38.67 indicative of two symmetry-inequivalent PMe_3 ligands (Figure 6.4). The ^{31}P resonances were assigned as a typical AB quartet with a $J_{P\text{-}P}$ coupling of 48.6 Hz. These results suggest that the apparent PMe_3 triplet observed in the ^1H NMR spectrum may best be interpreted as two overlapping doublets; each doublet corresponding to one inequivalent PMe_3 group. Furthermore, by irradiating the PMe_3 methyl resonance but not the resonance due to the metal hydride, the ^{31}P resonance at δ -42.16 appeared as a doublet of doublets arising from coupling to both the other phosphine and the metal hydride ($J_{P\text{-}H}$ = 64.4 Hz; $J_{P\text{-}P}$ = 48.6 Hz). Notably, the ^{31}P resonance at δ -38.67 remained a doublet. These results are consistent with the previous ^1H NMR spectrum which showed that the rhenium hydride resonance was observably coupled to only one PMe_3 ligand.

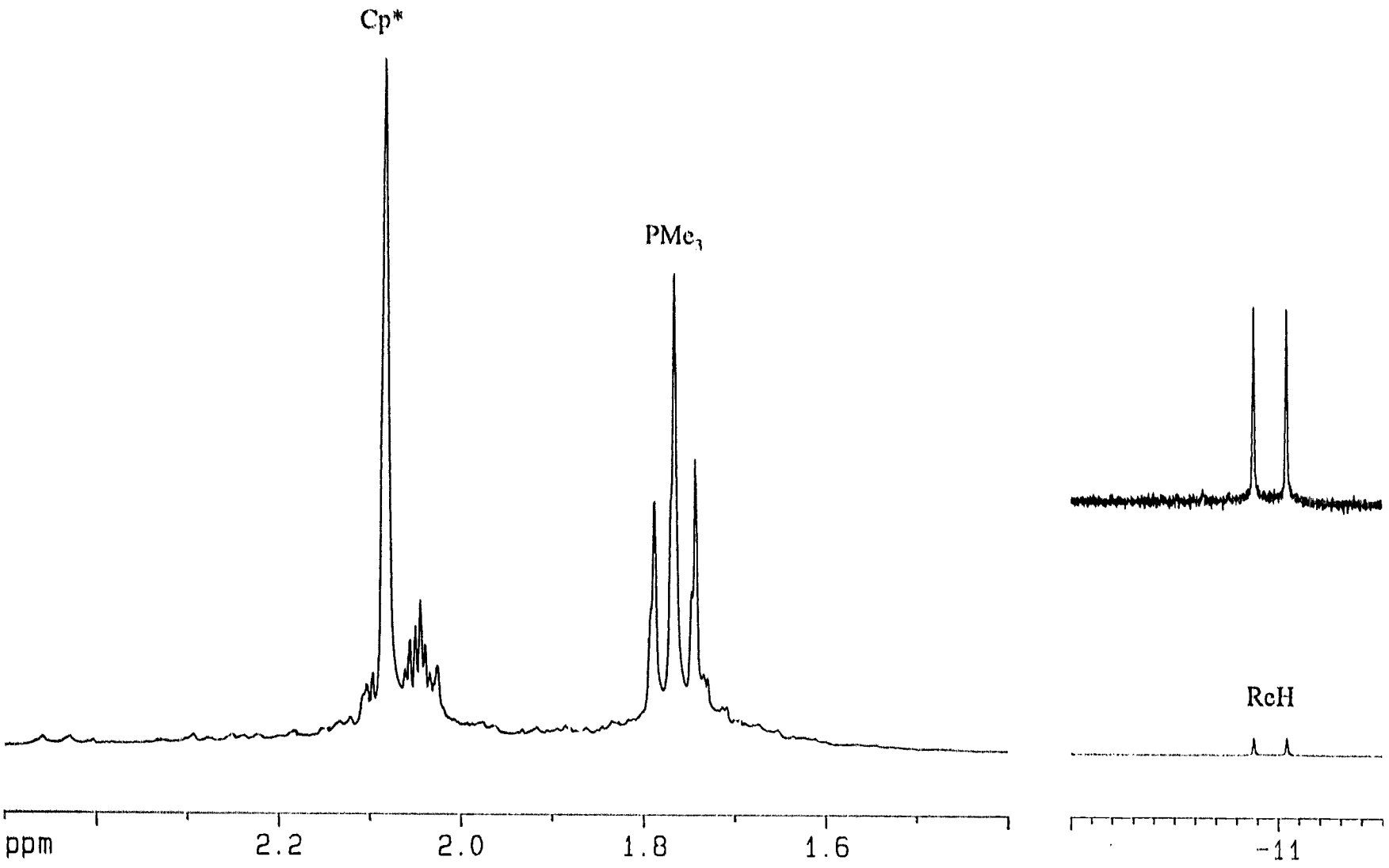

Figure 6.3a. ^1H NMR spectrum (400 MHz) of the reaction between $Cp^*Re(PMe_3)_2(N_2)$ (**4.5**) and CF_3COOH in acetone-d_6 at 213 K. Upfield doublet has been expanded for clarity.

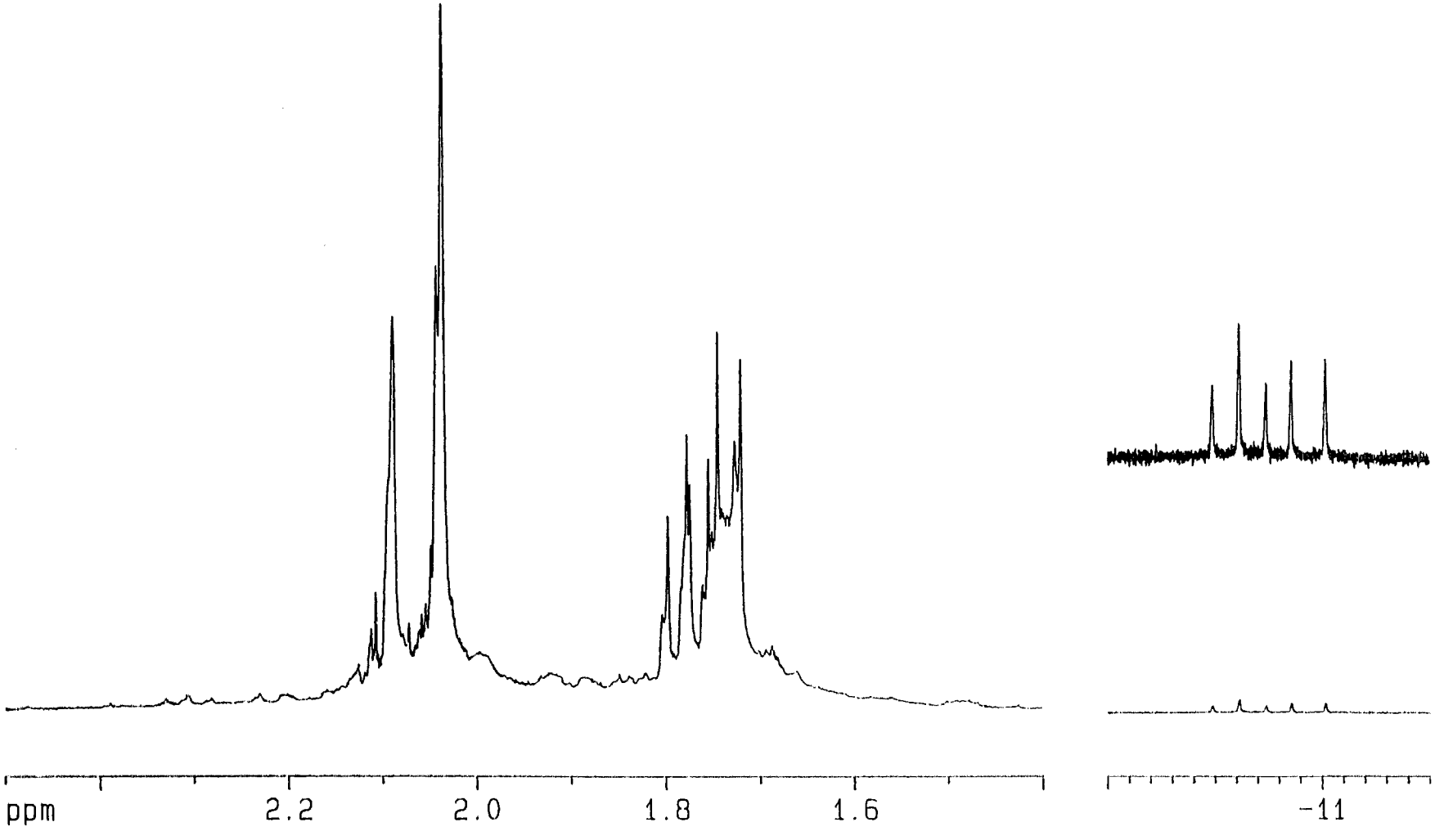

Figure 6.3b. ^{1}H NMR spectrum (400 MHz) of the reaction between Cp*Re(PMe_3)$_2$(N_2) (**4.5**) and CF_3COOH in acetone-d_6 at 253 K. Upfield resonances have been expanded for clarity.

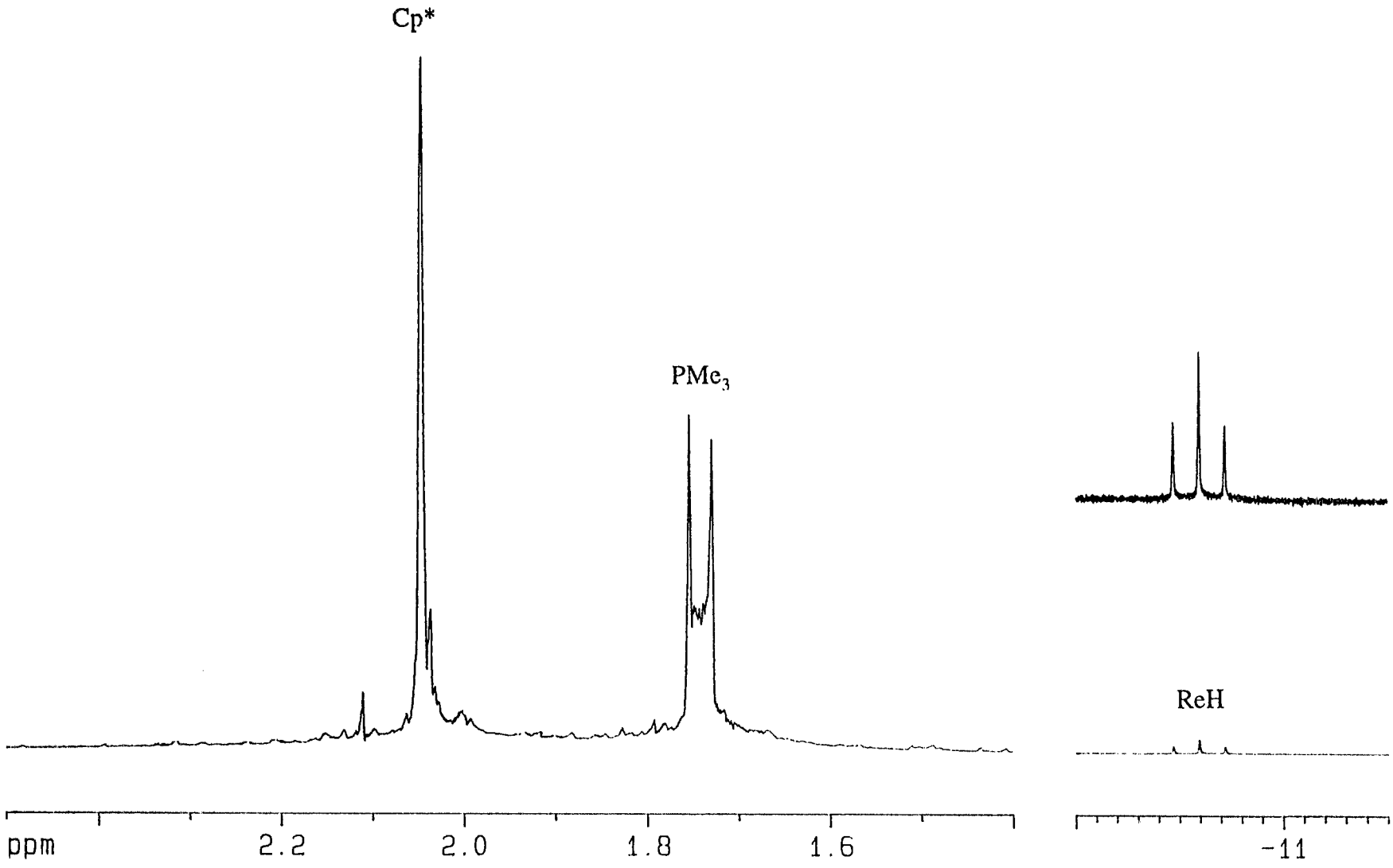

Figure 6.3c. ^{1}H NMR spectrum (400 MHz) of the reaction between Cp*Re(PMe_3)$_2$(N_2) (**4.5**) and CF_3COOH in acetone-d_6 at 273 K. Upfield triplet has been expanded for clarity.

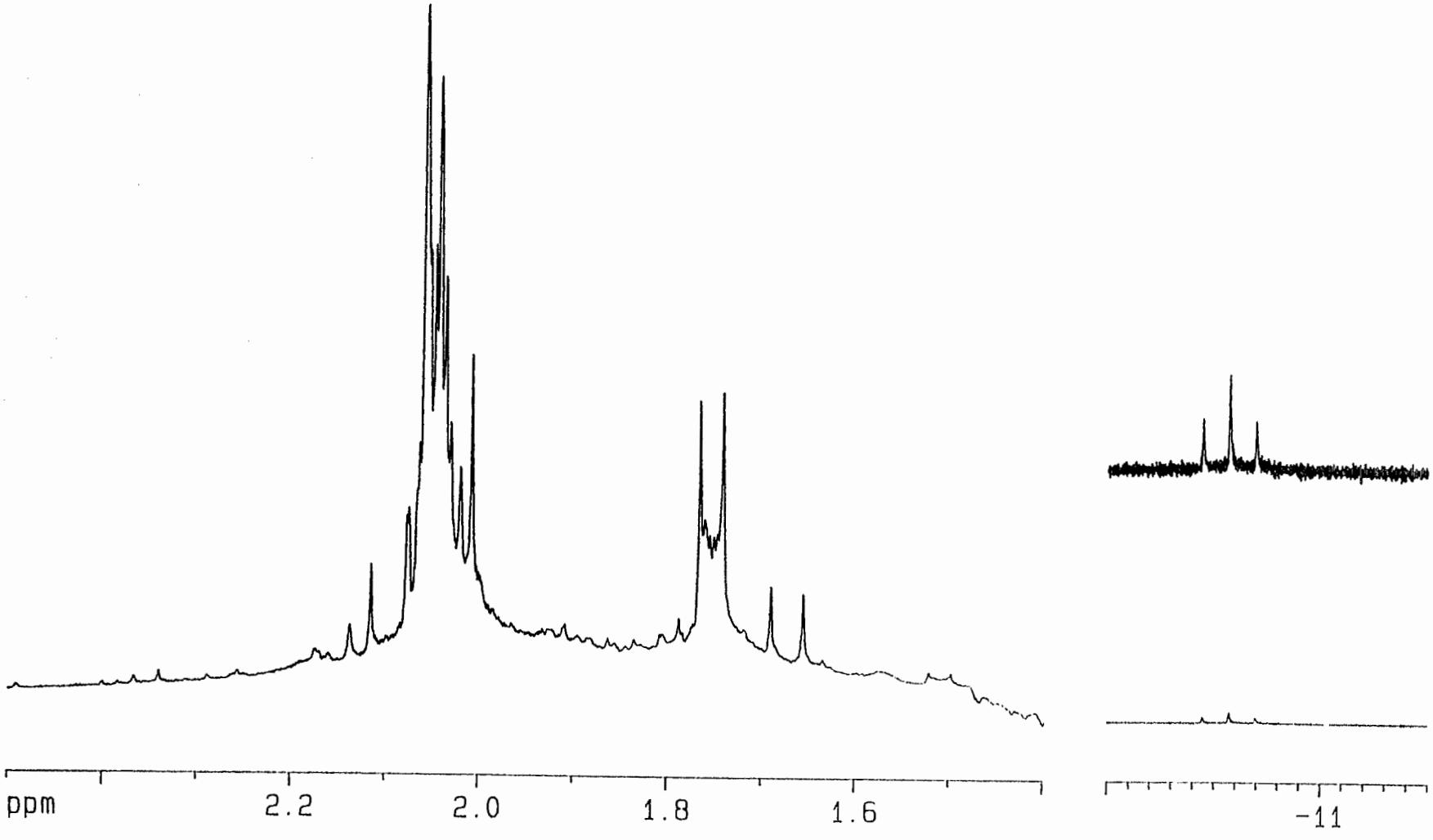

Figure 6.3d. ^{1}H NMR spectrum (400 MHz) of the reaction between $Cp^*Rc(PMe_3)_2(N_2)$ (**4.5**) and CF_3COOH in acetone-d_6 after 3 h at room temperature. Upfield triplet has been expanded for clarity.

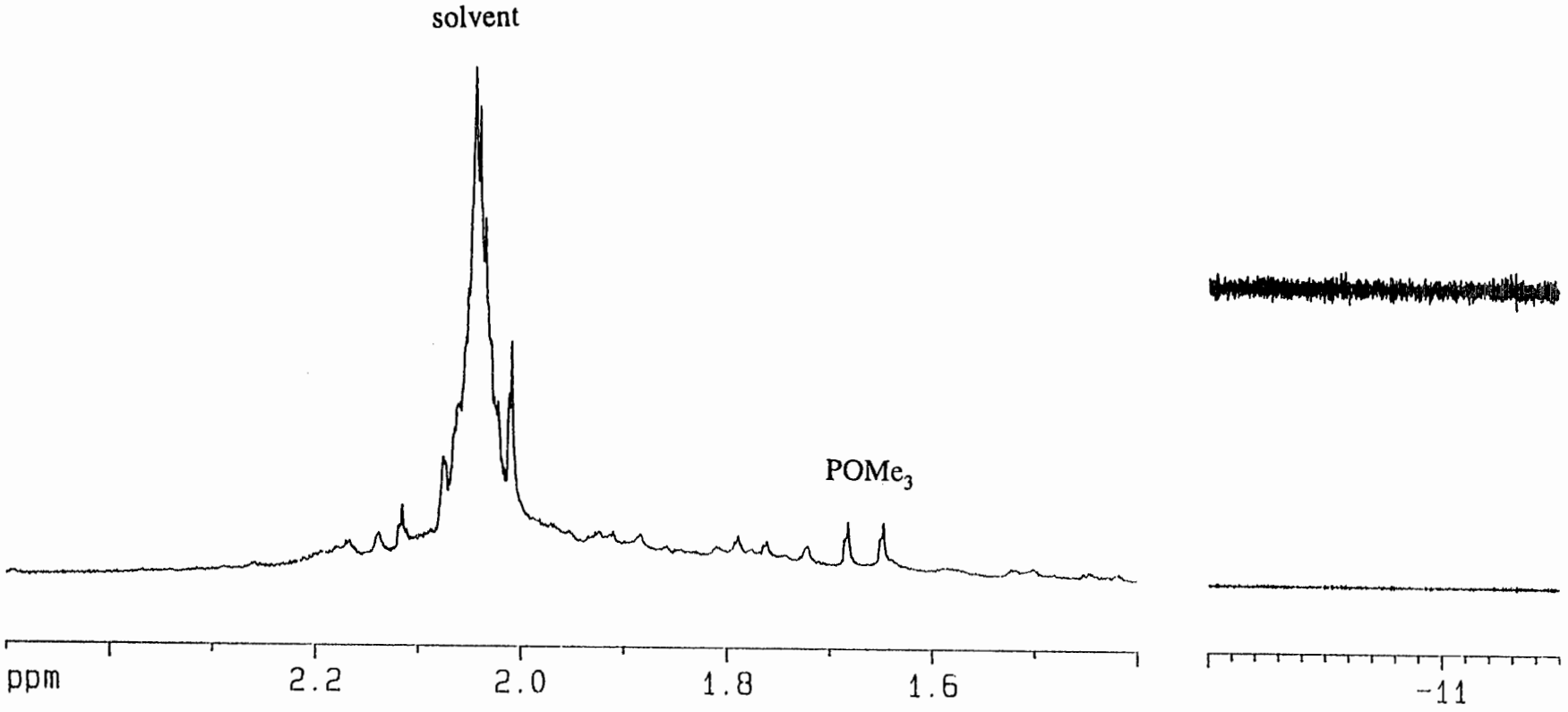

Figure 6.3e. ^{1}H NMR spectrum (400 MHz) of the reaction between Cp*Re(PMe_3)$_2$(N_2) (**4.5**) and CF_3COOH in acetone-d_6 after 15 h at room temperature.

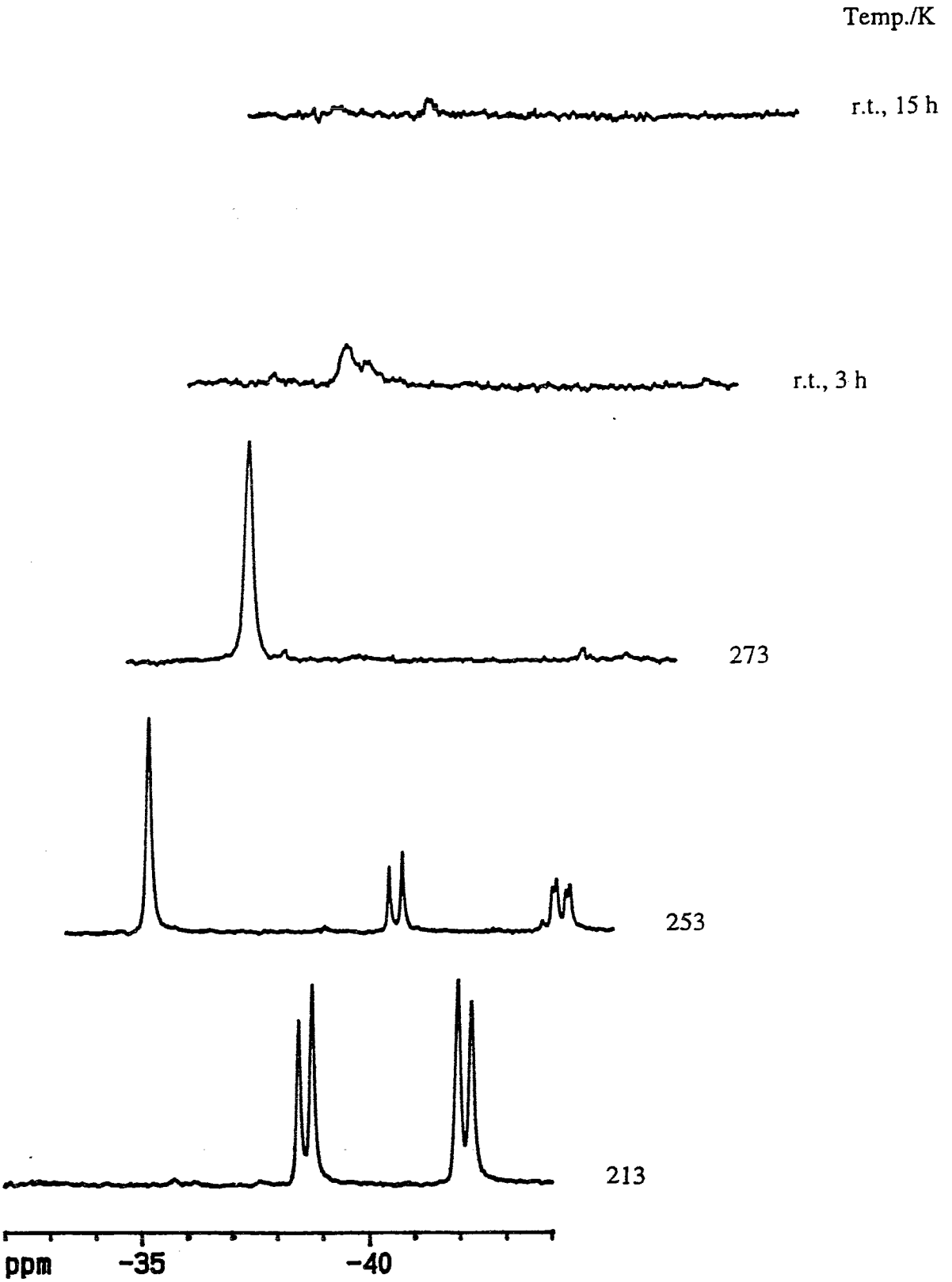

Figure 6.4. Variable temperature $^{31}P\{^{1}H\}$ NMR spectra (162 MHz) of the reaction between $Cp^*Re(PMe_3)_2(N_2)$ (**4.5**) and CF_3COOH in acetone-d_6.

As the temperature was raised, a sequence of ^1H and $^{31}P\{^1H\}$ NMR spectra demonstrated the decay of the product and the concomitant growth of resonances corresponding to a second rhenium hydrido product (Figures 6.3b and 6.4). At 273 K the conversion of the original product to the second product was complete. The ^1H NMR spectrum obtained of this solution at 273 K exhibited a singlet at δ 2.05 and a virtual doublet at δ 1.75 assigned to Cp* and the PMe_3 ligands respectively (Figure 6.3c). A coupling constant ($^2J_{H-P} + {}^4J_{H-P}$) of 9.8 Hz was extracted from the ^1H resonance corresponding to the PMe_3 groups. The ^1H NMR spectrum also exhibited a triplet in the metal hydride region at δ -10.60 integrating to 1 proton with a coupling constant of 50.3 Hz (Figure 6.3c); no signal due to an NH resonance was observed. The $^{31}P\{^1H\}$ NMR spectrum acquired at 273 K exhibited a singlet at δ -34.71 suggesting that the PMe_3 ligands were equivalent by symmetry (Figure 6.4). Once again, by selectively decoupling only the PMe_3 methyl resonance, this ^{31}P resonance appeared as a doublet indicating that it was coupled to the metal hydride (J_{P-H} = 50.1 Hz). These results are in agreement with the triplet observed for the rhenium hydride ^1H resonance.

The NMR sample was then warmed to room temperature. A ^1H NMR spectrum recorded after 3 h showed a significant loss in intensity of the resonances corresponding to Cp*, PMe_3, and the metal hydride (Figure 6.3d). Interestingly, a ^1H NMR spectrum recorded 12 h later showed the total disappearance of all resonances corresponding to the rhenium hydrido complex (Figure 6.3e). Analogous results were observed from $^{31}P\{^1H\}$ NMR spectra recorded at these times (Figure 6.4). As evidenced from the last set of spectra, except for resonances attributable to the NMR solvent (acetone-d_6) and residual $POMe_3$ (Figure 6.3e), no other resonances were observed. An examination of the NMR tube once it was removed from the probe showed no precipitate. Purification of the NMR solution confirmed the presence of residual amounts of the trioxo complex Cp^*ReO_3 **(4.8)**[138] (δ 2.09 in acetone-d_6) and $POMe_3$ (δ 1.67 in acetone-d_6,

J_{H-P} = 13.7 Hz).

The elapsed time for the variable temperature ^1H and $^{31}P\{^1H\}$ NMR experiments just described was *ca.* 19 h from the initial reaction to the point where the products apparently decomposed. The protonation of **4.5** with CF_3COOH was repeated in acetone-d_6 at 195 K. The resulting solution was then transferred to an NMR tube and kept at 195 K for *ca.* 32 h using a dry ice-acetone bath. A room temperature ^1H NMR spectrum of this solution at the end of this time was identical to the variable temperature ^1H NMR spectrum obtained previously at 273 K. This result suggests that (i) the rhenium hydrido product observed previously by treatment of **4.5** with CF_3COOH at room temperature and the product observed during the variable temperature NMR experiment at 273 K are identical, and (ii) that temperature rather than oxygen is responsible for the observed decay of the product(s) formed from the protonation reactions at room temperature. However, the fact that oxidation products (**4.8**[138] and $POMe_3$) are produced in these reactions suggests that the rhenium hydrido product is also extremely oxygen sensitive.

A 5-fold stoichiometric excess of CF_3COOH was added *via* syringe to a solution of the $^{15}N_\alpha$ labeled bis-trimethylphosphine dinitrogen complex $Cp^*Re(PMe_3)_2(^{15}N^{14}N)$ (**4.5-$^{15}N_\alpha$**) in acetone-d_6 at 195 K. A ^{15}N NMR spectrum, obtained *ca.* 120 min after the acid addition at 213 K, showed the total disappearance of **4.5-$^{15}N_\alpha$** and the formation of a product which exhibited a singlet at δ -108.3 (Figure 6.5). Although this result clearly demonstrates that the coordinated dinitrogen was not protonated at N_α, since this would have yielded a doublet for the observed ^{15}N resonance, it does show that a new species containing at least one nitrogen atom was produced by protonation. A ^{15}N NMR spectrum of free N_2, under the same protic conditions, exhibited a resonance at δ -73.7 confirming that free dinitrogen was not responsible for the observed ^{15}N resonance.

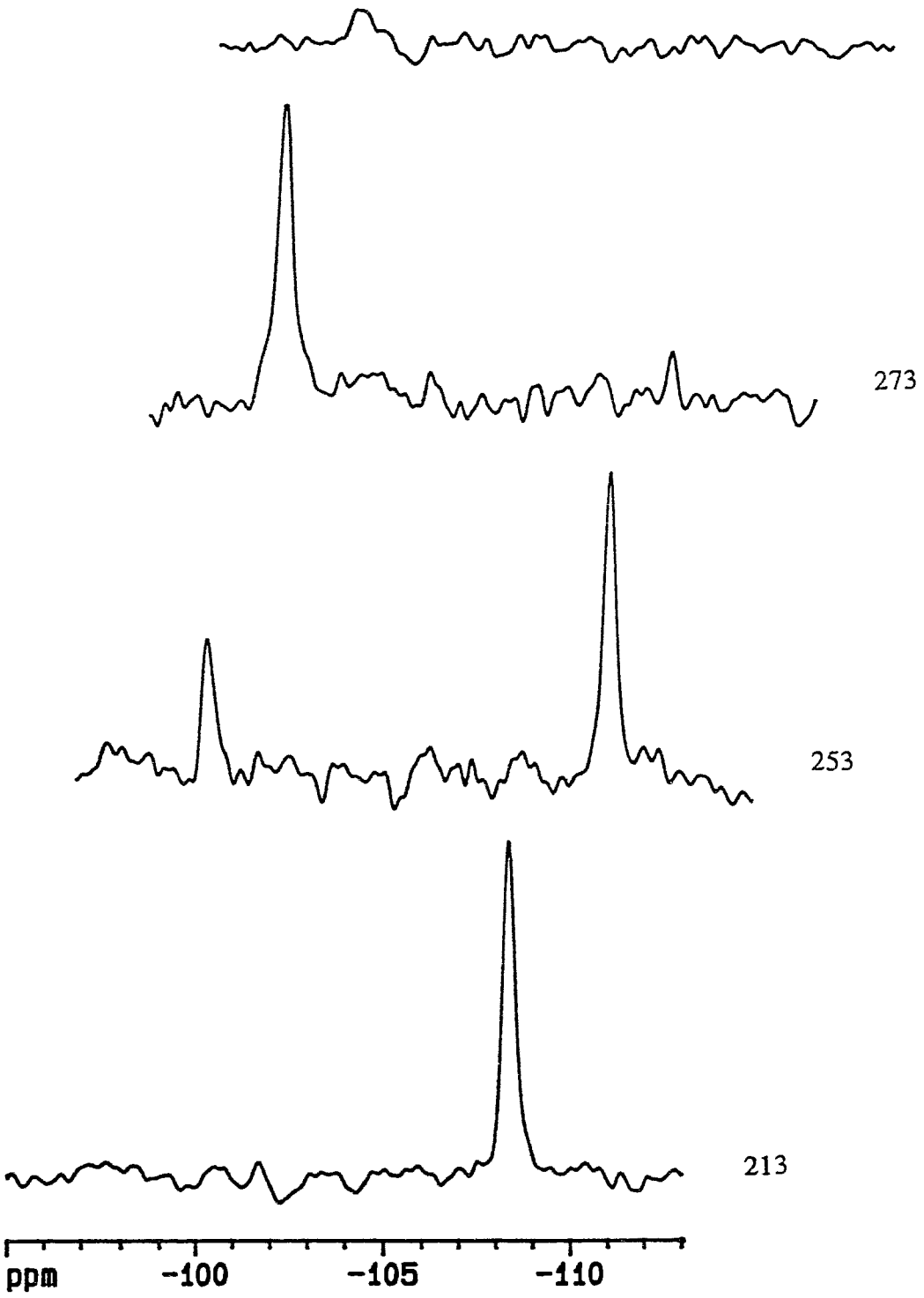

Figure 6.5. Variable temperature ^{15}N NMR spectra (40.6 MHz) of the reaction between $Cp^*Re(PMe_3)_2(^{15}N^{14}N)$ (**4.5-$^{15}N_\alpha$**) and CF_3COOH in acetone-d_6.

(Note: A ^{1}H NMR spectrum obtained of the same solution reproduced the results obtained previously; no $H^{15}N$ coupling for the metal hydride ^{1}H NMR resonance was observed). A sequence of ^{15}N NMR spectra acquired as the temperature was raised showed the gradual decay of this resonance and the concomitant growth of a second singlet at δ -98.6 until at 273 K only the resonance corresponding to the second product was present (Figure 6.5). As the temperature of the NMR sample was raised to room temperature, the ^{15}N resonance due to the second product disappeared (Figure 6.5) without the concomitant growth of resonances assignable to nitrogen containing products such as $[NH_4][CF_3COO]$.

Similar results were obtained when a solution of the $^{15}N_{\beta}$ labeled bis-trimethylphosphine dinitrogen complex $Cp^*Re(PMe_3)_2(^{14}N^{15}N)$ (**4.5-$^{15}N_{\beta}$**) in acetone-d_6 was reacted with a 5-fold stoichiometric excess of CF_3COOH at 195 K. A ^{15}N NMR spectrum of this solution, recorded *ca.* 120 min after the acid addition at 213 K, demonstrated the complete disappearance of **4.5-$^{15}N_{\beta}$** and the presence of a singlet at δ -26.0 (Figure 6.6). This result indicates that the coordinated dinitrogen was not protonated at N_{β}. However, the presence of a ^{15}N signal after protonation further substantiates the suggestion made previously that a new nitrogen containing species was produced. (Note: A ^{1}H NMR spectrum obtained of the same solution reproduced the results obtained previously; no $H^{15}N$ coupling for the metal hydride ^{1}H NMR resonance was observed). Once again, a sequence of ^{15}N NMR spectra acquired as the temperature was raised showed the gradual decay of this resonance and the concomitant growth of a second singlet at δ -6.2 (Figure 6.6). At 273 K the conversion of the original product to the second product was complete. As the temperature of the NMR sample was raised to room temperature, the ^{15}N resonance due to the second product disappeared (Figure 6.6) with no concomitant growth of resonances assignable to nitrogen containing derivatives.

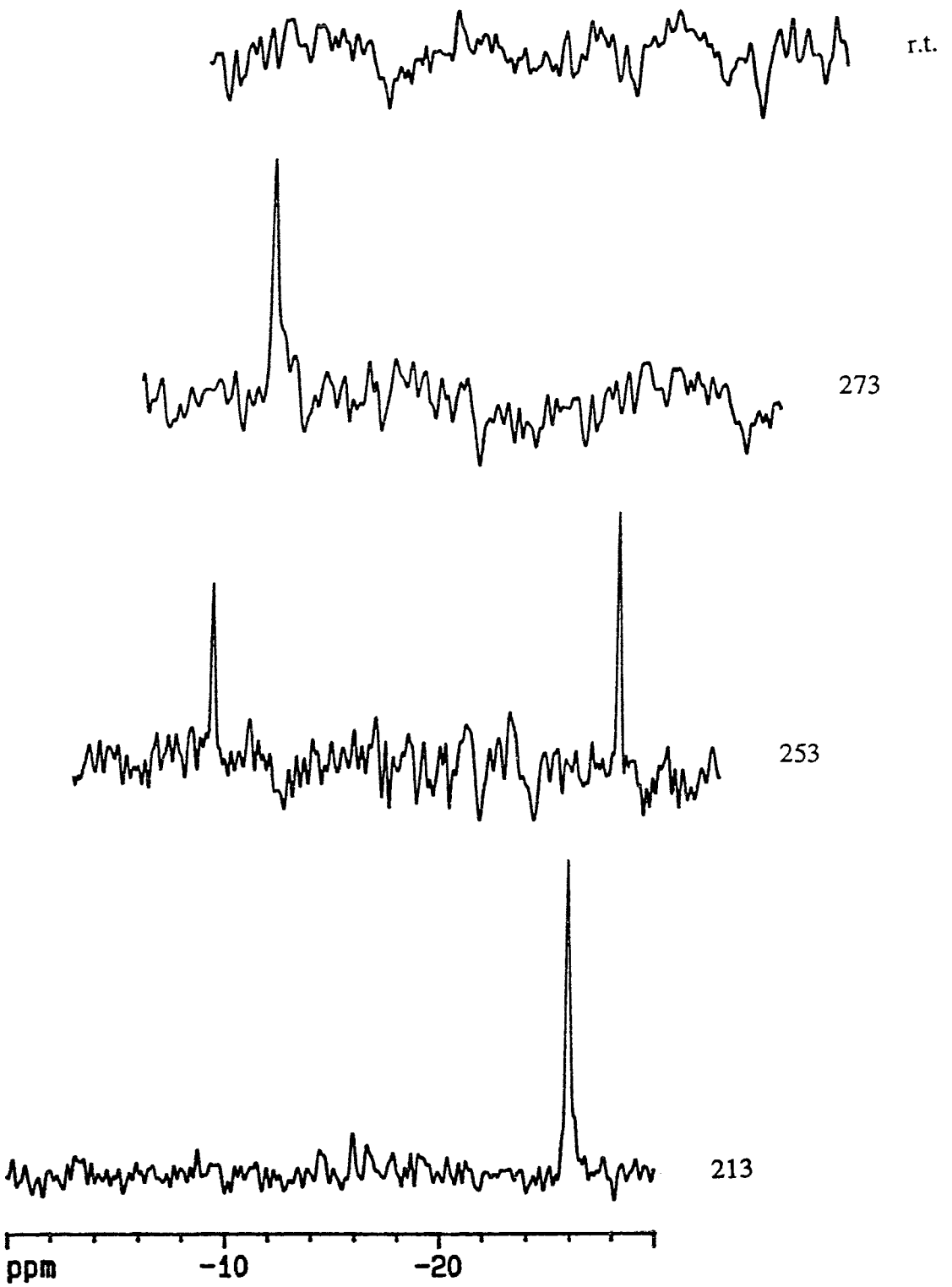

Figure 6.6. Variable temperature ^{15}N NMR spectra (40.6 MHz) of the reaction between $Cp^*Re(PMe_3)_2(^{14}N^{15}N)$ (**4.5-$^{15}N_\beta$**) and CF_3COOH in acetone-d_6.

The protonation of the unlabeled dinitrogen complex **4.5** with CF_3COOH was repeated in acetone at 273 K. An IR spectrum obtained of this solution at 273 K exhibited a broad, moderately intense absorption at 2079 cm^{-1} assigned to ν(NN). The assignment of ν(NN) to the protonation product was confirmed by repeating the protonation reaction using the $^{15}N_\alpha$ labeled dinitrogen complex **4.5-$^{15}N_\alpha$**. An isotopic shift in ν(NN) of 32 cm^{-1} was observed. This observation is in agreement with the results obtained from the ^{15}N NMR experiments and taken together these results confirm the presence of a dinitrogen ligand in the protonation product(s).

6.2.4. Low Temperature Reactions of Cp*Re(PMe_3)$_2$(N_2) (4.5) with HBF_4·OEt_2 or CF_3SO_3H

A 5-fold stoichiometric excess of HBF_4·OEt_2 was added *via* syringe to a solution of Cp*Re(PMe_3)$_2$(N_2) (**4.5**) in acetone-d_6 at 195 K. A ^1H NMR spectrum of the resulting solution, acquired *ca.* 60 min after the addition of the acid at 213 K, showed the total disappearance of **4.5** and the presence of a singlet at δ 2.05 assigned to a Cp* group. The ^1H resonance at δ 1.73 assigned to the PMe_3 ligands was observed to be an apparent broad triplet integrating to 18 protons with a coupling constant of 9.8 Hz. The ^1H NMR spectrum also exhibited a doublet at δ -10.99 integrating to 1 proton with a coupling constant of 64.1 Hz; no signal correspondong to an NH resonance was found. These results are consistent with protic attack at the metal center giving a rhenium hydrido complex.

Raising the temperature of the NMR solution resulted in the decay of the ^1H resonances assigned to the rhenium hydrido complex and the concomitant growth of resonances corresponding to a second rhenium hydrido product; the conversion was complete at 273 K. The ^1H NMR spectrum obtained of this solution at 273 K exhibited a singlet at δ 2.03 and a virtual doublet at δ 1.72 assigned to Cp* and the PMe_3 ligands

respectively. A coupling constant ($^2J_{H-P} + {}^4J_{H-P}$) of 9.7 Hz was extracted from the ^1H resonance corresponding to the PMe_3 groups. The ^1H NMR spectrum also exhibited a triplet in the metal hydride region at δ -10.63 integrating to 1 proton with a coupling constant of 50.4 Hz; no signal due to an NH resonance was observed. As the temperature of the NMR sample was raised to room temperature, the ^1H resonances due to the second product disappeared.

Analogous results were obtained for the reaction between $Cp^*Re(PMe_3)_2(N_2)$ **(4.5)** and CF_3SO_3H.

6.3. Discussion

6.3.1. Predisposition of $Cp^*Re(PMe_3)_2(N_2)$ (4.5) Toward Protonation

All the dinitrogen complexes reported in this thesis, including $Cp^*Re(PMe_3)_2(N_2)$ (**4.5**), have ground state structures in which the dinitrogen ligand is bound end-on to the metal center. It has been assumed that ν(NN), which is infrared active in these complexes, will be a measure of the strength of metal dinitrogen binding because a low value of ν(NN) suggests metal d-π^*(NN) donation into the N_2 antibonding system. Therefore, a low value of ν(NN) may also be indicative of activation of the N_2 ligand to protonation since it may imply negative charge buildup on the dinitrogen (Figure 6.7). Consequently, activation and strong metal dinitrogen binding might be expected to go together and both be indicated by low values of ν(NN).

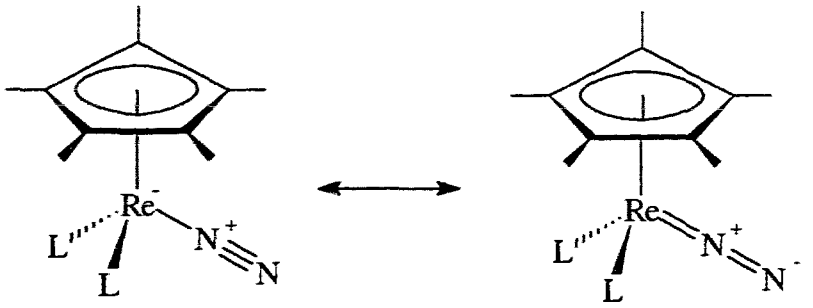

(I) (II)

Weak metal d-π*(NN) donation Strong metal d-π*(NN) donation

Figure 6.7. Canonical structures illustrating the effect of weak and strong d-π*(NN) donation on the dinitrogen ligand.

With respect to the rhenium dinitrogen complexes **4.1-4.5**, it is clear that replacing a CO ligand (poor σ-donor, good π-acceptor) by PMe_3 (good σ-donor, poor π-acceptor) increases the metal d-π*(NN) donation and thus lowers ν(NN) (Table 6.1). This effect is even more pronounced when both CO groups are substituted by PMe_3 and thus indicates that complex **4.5** may be the most susceptible to protonation at the dinitrogen ligand. Furthermore, ν(NN) obtained for **4.5** [ν(NN) 1975 cm^{-1}] is similar to values obtained for other dinitrogen complexes such as *trans*-$Mo(N_2)_2(dppe)_2$ [ν(NN) 1976 cm^{-1}], *trans*-$W(N_2)_2(dppe)_2$ [ν(NN) 1946 cm^{-1}], and $Fe(N_2)(dmpe)_2$ [ν(NN) 1975 cm^{-1}] which are prone to protic attack at the terminal nitrogen atom (N_β) (Table 6.1).[158, 165, 166]

Nitrogen NMR spectroscopy can also provide information about the chemical environment of the coordinated dinitrogen ligand. From the ^{14}N and ^{15}N NMR spectra of complexes **4.1-4.4**, it was observed that the chemical shift for the N_α resonance of the dinitrogen ligand follow the order of σ-ligands $Cp^*(CO)(PMe_3)$ > $Cp^*(CO)\{P(OMe)_3\}$ > $Cp^*(CO)_2$ > $Cp(CO)_2$ (from less shielded to more shielded) which correlates with

increasing electron donating ability of the co-ligands (Table 6.1). By contrast, the resonance for N_β remains essentially unaffected; varying the electron density on the metal evidently produces smaller changes in $\delta(N_\beta)$ than those observed in $\delta(N_\alpha)$ for these complexes. However, for the bis-trimethylphosphine dinitrogen complex **4.5** a significant change in chemical shift was observed for both the N_α and the N_β resonances clearly indicating that the ancillary ligands have a prominent effect on the electronic environment of the ligated dinitrogen with respect to both N_α and N_β (Table 6.1). It is also worth mentioning that the N_β resonance for **4.5** [$\delta(N_\beta)$ -51.7] is comparable to those reported for other dinitrogen complexes such as *trans*-$Mo(N_2)_2(dppe)_2$ [$\delta(N_\beta)$ -42.8] and *trans*-$W(N_2)_2(dppe)_2$ [$\delta(N_\beta)$ -48.6] which have been previously shown to undergo protic attack at the terminal nitrogen atom (N_β) (Table 6.1).[158, 165] Therefore, **4.5** is considered a good target complex to investigate protonation reactions, in anticipation of being able to protonate the N_2 ligand.

6.3.2. Protonation of $Cp^*Re(PMe_3)_2(N_2)$ (4.5)

Protic attack of $Cp^*Re(PMe_3)_2(N_2)$ **(4.5)** can, in principle, be visualized to occur at different sites on the metal complex as is illustrated in Scheme 6.1. In (i), attack at the coordinated dinitrogen ligand, presumably at the terminal nitrogen atom (N_β), produces a rhenium diazenido complex. Alternatively, attack at the metal center forms either the *cis*-rhenium hydrido dinitrogen complex (ii), or the *trans*-rhenium hydrido dinitrogen complex (iii). In view of the existence of the aryldiazenido complex $[Cp^*Re(PMe_3)_2(p\text{-}N_2C_6H_4OMe)][BF_4]$ **(2.11)**, formation of the rhenium diazenido complex as in (i) seems a distinct possibility.

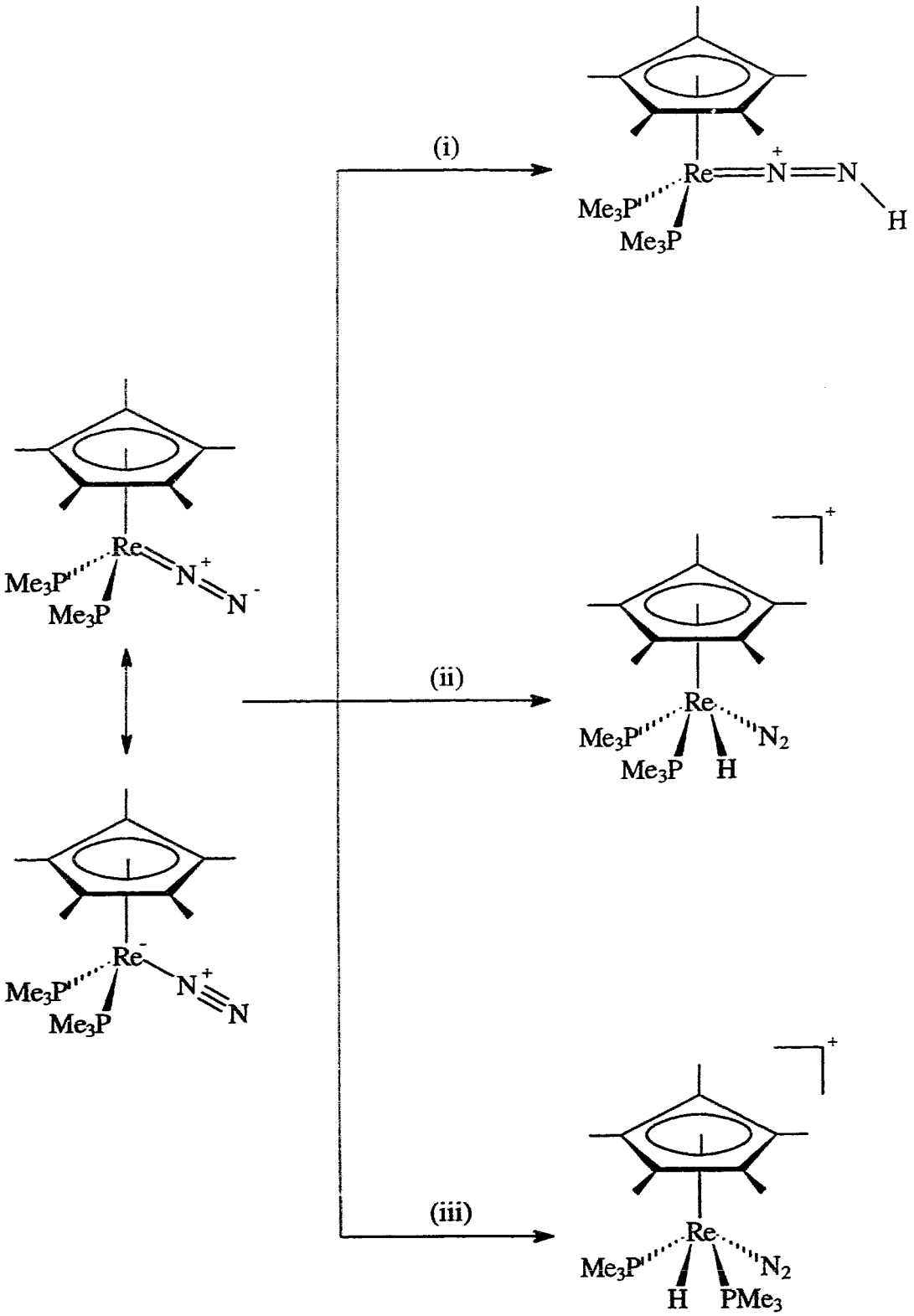

Scheme 6.1. Proposed products arising from protic attack at different sites on the dinitrogen complex $Cp^*Re(PMe_3)_2(N_2)$ **(4.5)**.

Room temperature IR and ^1H NMR experiments failed to produce conclusive information concerning whether or not the bis-trimethylphosphine dinitrogen complex $Cp^*Re(PMe_3)_2(N_2)$ **(4.5)** was protonated, and if so at which site, because of the apparent thermal instability of the products. To overcome this problem, variable temperature ^1H, $^{31}P\{^1H\}$, and ^{15}N NMR experiments were devised to examine the protonation of **4.5**, **4.5-$^{15}N_\alpha$**, or **4.5-$^{15}N_\beta$** and the results obtained are summarized in Table 6.2.

The ^{15}N NMR spectra, obtained at 213 K for the reaction between $Cp^*Re(PMe_3)_2(^{15}N^{14}N)$ **(4.5-$^{15}N_\alpha$)** or $Cp^*Re(PMe_3)_2(^{14}N^{15}N)$ **(4.5-$^{15}N_\beta$)** and CF_3COOH, exhibited a singlet in each case (Table 6.2) in the region expected for a typical metal-bound dinitrogen ligand.[69, 158] Notably, the $^{15}N_\beta$ resonance corresponding to a metal-bound dinitrogen ligand [i.e., *trans*-$W(N_2)_2(dppe)_2$: $\delta(^{15}N_\alpha)$ -60.1, $\delta(^{15}N_\beta)$ -48.6][158] undergoes a dramatic change in chemical shift if it is protonated to give a diazenido complex [i.e., *trans*-$WBr(N_2H)(dppe)_2$: $\delta(^{15}N_\alpha)$ -25.9, $\delta(^{15}N_\beta)$ -187.1]; a smaller change in chemical shift is observed for the $^{15}N_\alpha$ resonance.[167] These ^{15}N NMR results clearly demonstrate that the coordinated dinitrogen was not attacked by the proton [pathway (i)] and that it remained bound to the rhenium center.

The ^1H NMR spectrum, recorded at 213 K after **4.5** was treated with CF_3COOH, exhibited a metal hydride resonance which was observably coupled to only one PMe_3 group (Table 6.2). A $^{31}P\{^1H\}$ NMR spectrum of the same sample acquired at the same temperature showed the presence of two symmetry-inequivalent PMe_3 ligands and only one of the PMe_3 ligands was coupled to the rhenium hydride substituent, corroborating the previous ^1H NMR observation (Table 6.2). Taken together, the spectroscopic results are consistent with protic attack at the metal center giving the cationic rhenium hydrido dinitrogen complex *cis*-$[Cp^*ReH(N_2)(PMe_3)_2][CF_3COO]$ **(*cis*-6.1)** [pathway (ii)] but **not** *trans*-$[Cp^*ReH(N_2)(PMe_3)_2][CF_3COO]$ **(*trans*-6.1)** [pathway (iii)].

Table 6.2. Variable Temperature (T) IR, $^{31}P\{^1H\}$, and ^{15}N NMR Data for the Protonation of $Cp^*Re(PMe_3)_2(N_2)$ (4.5), (4.5-$^{15}N_\alpha$), or (4.5-$^{15}N_\beta$)

T (K)	4.5, 4.5-$^{15}N_\alpha$, or 4.5-$^{15}N_\beta$ + CF_3COOH					4.5 + $HBF_4{\cdot}OEt_2$	4.5 + CF_3SO_3H
	^1H NMR[a] (δ)	$^{31}P\{^1H\}$ NMR[b] (δ)	$^{15}N_\alpha$ NMR[c] (δ)	$^{15}N_\beta$ NMR[d] (δ)	IR ν($^{14}N_2$)[e]	^1H NMR[a] (δ)	^1H NMR[a] (δ)
213	2.08 (s, Cp*) 1.76 (at, PMe_3, J=8.8) -10.96 (d, ReH, J=64.2)	-38.67 (d, PMe_3, J=48.6) -42.16 (d, PMe_3, J=48.6)	-108.3 (s, $^{15}N_\alpha$)	-26.0 (s, $^{15}N_\beta$)		2.05 (s, Cp*) 1.73 (at, PMe_3, J=9.8) -10.99 (d, ReH, J=64.1)	1.97 (s, Cp*) 1.64 (at, PMe_3, J=9.9) -11.06 (d, ReH, J=64.3)
273	2.05 (s, Cp*) 1.75 (vd, PMe_3, J=9.8) -10.60 (t, ReH, J=50.3)	-34.71 (s, PMe_3)	-98.6 (s, $^{15}N_\alpha$)	-6.2 (s, $^{15}N_\beta$)	2079	2.03 (s, Cp*) 1.72 (vd, PMe_3, J=9.7) -10.63 (t, ReH, J=50.4)	1.94 (s, Cp*) 1.63 (vd, PMe_3, J=9.6) -10.65 (t, ReH, J=50.7)
r.t., 3 h[f]	same as 273 K[g]	same as 273 K[g]	no resonances	no resonances	no band	no resonances	no resonances
r.t., 15 h[f]	no resonances	no resonances					

[a] In acetone-d_6; referenced to TMS; δ given in ppm; at represents apparent triplet; vd represents virtual doublet; J given in Hz.

[b] In acetone-d_6; referenced to 85% H_3PO_4; δ given in ppm; J given in Hz.

[c] In acetone-d_6; specifically ^{15}N labeled at N_α; referenced to $MeNO_2$; δ given in ppm.

[d] In acetone-d_6; specifically ^{15}N labeled at N_β; referenced to $MeNO_2$; δ given in ppm.

[e] In acetone; ν($^{14}N_2$) given in cm^{-1}.

[f] r.t. denotes room temperature.

[g] Resonances are significantly decreased in intensity.

Notably, precedents in the literature suggests that in four-legged piano-stool type complexes with phosphorus and hydrogen co-ligands, the magnitude of the *cis* J_{H-P} coupling is generally large whereas that of the *trans* J_{H-P} coupling is small and sometimes unobservable. For example, in the cyclometalated complex $Cp^*Re(CO)(\eta^2\text{-}CH_2PMe_2)H$ where P and H (hydride) are *cis*, the *cis* J_{H-P} coupling was reported to be 38.2 Hz.[168, 169] However, in the cyclometalated tricyclohexylphosphine derivative $Cp^*Re(CO)\{\eta^2\text{-}C_6H_{10}P(C_6H_{11})_2\}H$ where P is *trans* to H, the metal hydride ligand was reported to exhibit no observable coupling to the phosphine group.[169] Thus, the observed J_{H-P} coupling in the rhenium hydrido dinitrogen complex ***cis*-6.1** is assigned to the PMe_3 group *cis* to the metal hydride ligand. Analogous results were obtained from the ^1H NMR spectra obtained at 213 K for the reaction between **4.5** and $HBF_4{\cdot}OEt_2$ or CF_3SO_3H (Table 6.2) and thus the protonation products arising from these reactions were also assigned to the respective cationic rhenium hydrido dinitrogen complexes *cis*-$[Cp^*ReH(N_2)(PMe_3)_2][BF_4]$ (***cis*-6.2**) and *cis*-$[Cp^*ReH(N_2)(PMe_3)_2][CF_3SO_3]$ (***cis*-6.3**).

The ^{15}N NMR spectra, obtained at 273 K for the reaction between **4.5-$^{15}N_\alpha$** or **4.5-$^{15}N_\beta$** and CF_3COOH, exhibited a singlet in each case (Table 6.2) in the region expected for a typical coordinated N_2.[69, 158] An IR spectrum of this solution at 273 K also displayed an absorption unequivocally assigned to ν(NN) of a metal-bound dinitrogen ligand (Table 6.2). The ^1H NMR spectrum, recorded at this temperature after **4.5** was treated with CF_3COOH, exhibited a triplet for the metal hydride resonance indicating that it was coupled to two symmetry-equivalent PMe_3 groups (Table 6.2). A $^{31}P\{^1H\}$ NMR spectrum also acquired at 273 K corroborated the presence of two symmetry-equivalent PMe_3 ligands (Table 6.2). These results are not in agreement with the products resulting from pathways (i) and (ii) but are consistent with protic attack at the metal center yielding the cationic rhenium hydrido dinitrogen complex *trans*-$[Cp^*ReH(N_2)(PMe_3)_2][CF_3COO]$ (***trans*-6.1**) [pathway (iii)]. Once again, similar results

were obtained from the ^1H NMR spectra obtained at 273 K for the reaction between **4.5** and $HBF_4 \cdot OEt_2$ or CF_3SO_3H (Table 6.2). Consequently, the protonation products arising from these reactions were assigned to the cationic rhenium hydrido dinitrogen complexes *trans*-[Cp*ReH(N_2)(PMe_3)$_2$][BF_4] (***trans*-6.2**) and *trans*-[Cp*ReH(N_2)(PMe_3)$_2$][CF_3SO_3] (***trans*-6.3**) respectively.

Interestingly, ^1H, $^{31}P\{^1H\}$, and ^{15}N NMR spectra recorded 3 h after room temperature had been attained, demonstrated the decay of ***trans*-6.1** and the total disappearance of ***trans*-6.2** and ***trans*-6.3**, with no concomitant growth of resonances attributable to rhenium containing complexes (Table 6.2) except for trace amounts of Cp^*ReO_3 (**4.8**)[138] obtained after purification.

To summarize, the bis-trimethylphosphine dinitrogen complex Cp*Re(PMe_3)$_2$(N_2) (**4.5**) is susceptible to protonation at the metal center but not at the coordinated dinitrogen ligand. Furthermore, the protonation reaction appears to be independent of the acid used since treatment of **4.5** with CF_3COOH, $HBF_4 \cdot OEt_2$, or CF_3SO_3H, in all cases, lead to the formation of the respective rhenium hydrido dinitrogen complexes *cis*-[Cp*ReH(N_2)(PMe_3)$_2$][CF_3COO] (***cis*-6.1**), *cis*-[Cp*ReH(N_2)(PMe_3)$_2$][BF_4] (***cis*-6.2**), and *cis*-[Cp*ReH(N_2)(PMe_3)$_2$][CF_3SO_3] (***cis*-6.3**) at 213 K. In all cases, these complexes were found to isomerize to ***trans*-6.1**, ***trans*-6.2**, and ***trans*-6.3** respectively and the isomerization was complete at 273 K. Interestingly, the three *trans* complexes were found to be thermally unstable at room temperature, and their decomposition, presumably *via* loss of the dinitrogen ligand although no evidence for N_2 loss was obtained, was found to be complete after 15 h. However, ***trans*-6.1** was found to be more stable than its analogs ***trans*-6.2** and ***trans*-6.3** inferring that the counter anion may play a role in stabilizing these cationic rhenium hydrido dinitrogen complexes.

The activation of metal-bound dinitrogen by protic attack was suggested by Chatt et al.[33] to be favored by low oxidation state complexes composed of a metal center with a low first ionization potential, and ancillary ligands which were good σ-donors but poor π-acceptors of electron density. It was rationalized that increasing the electron density on the metal center would increase the metal d-π*(NN) donation into the N_2 antibonding orbitals resulting in a negatively charged dinitrogen ligand which may be prone to protonation. Unfortunately, the protonation reactions involving $Cp^*Re(PMe_3)_2(N_2)$ (**4.5**) have revealed that the metal center rather than the ligated dinitrogen was attacked by the proton. Furthermore, these results show that (i) the criteria established by Chatt et al.[33] from investigations conducted on dinitrogen complexes of the type $M(N_2)_2(PR_3)_4$ (M = Mo or W) are not sufficient to ensure the protonation of the dinitrogen ligand in **4.5** and subsequently (ii) that the activation of coordinated dinitrogen may be dependent on the geometry of the dinitrogen complex but not neccessarily on the acid used as the protic source, although the counter anion of the acid may influence the stability of the protonated product.

6.3.3. *Cis*- and *Trans*-$[Cp^*ReH(N_2)(PMe_3)_2][X]$ (X = CF_3COO^- (6.1), BF_4^- (6.2), or $CF_3SO_3^-$ (6.3))

Although a substantial number of dinitrogen complexes have been characterized, only a small number of these also contain hydrogen bonded to the metal atom.[158, 167] The majority of these metal hydrido dinitrogen complexes have been reported for the group VIII transition metals (Fe, Ru, and Os) as well as for cobalt and tungsten. Examples include the cationic tungsten and iron complexes *trans*-$[WH(N_2)_2(dppe)_2][HCl_2]$[158] and $[FeH(N_2)(dmpe)_2][BPh_4]$[166] respectively. In contrast, hydrido dinitrogen complexes of rhenium are not common. Notable documented examples include the first synthesized rhenium hydrido dinitrogen complex *trans*-$ReH(N_2)(dppe)_2$[122] and the

tetrakis(dimethylphenyl)phosphine complex *cis*-$ReH(N_2)(PMe_2Ph)_4$ whose spectroscopic and structural determinations show that the metal hydride and dinitrogen groups adopt a *cis* orientation rather than the expected *trans* arrangement reported for most octahedral metal hydrido dinitrogen complexes.[170] The former complex was synthesized by reaction of $[Et_4N]_2[ReH_9]$ with two equivalents of dppe in 2-propanol solution under a nitrogen atmosphere at 298 K.[122] Interestingly, treatment of a benzene solution of this complex with a stoichiometric amount of HBF_4 protonates the metal center and affords the cationic rhenium dihydrido dinitrogen complex $[ReH_2(N_2)(dppe)_2][BF_4]$.[122] The tetrakis(dimethylphenyl)phosphine complex *cis*-$ReH(N_2)(PMe_2Ph)_4$ was prepared by treatment of *mer*-$ReCl_3(PMe_2Ph)_3$ with propyl lithium again under a nitrogen atmosphere.[170]

As described in the previous Results and Discussion sections, the *cis* and *trans* cationic rhenium hydrido dinitrogen complexes of the type $[Cp^*ReH(N_2)(PMe_3)_2][X]$ ($X = CF_3COO^-$ **(6.1)**, BF_4^- **(6.2)**, or $CF_3SO_3^-$ **(6.3)**) were synthesized by reaction of the bis-trimethylphosphine dinitrogen complex $Cp^*Re(PMe_3)_2(N_2)$ **(4.5)** with the appropriate acid. Unlike the rhenium complexes mentioned above which are moderately air-stable at room temperature, complexes **6.1-6.3** are thermally unstable and very oxygen sensitive, decomposing under ambient temperatures to give only residual amounts of the oxidized products Cp^*ReO_3 **(4.8)**[138] and $POMe_3$. However, the spectroscopic parameters ($^{15}N_\alpha$, $^{15}N_\beta$ NMR chemical shifts and ν(NN) IR absorptions) obtained for complexes **6.1-6.3** are comparable to those reported for similar cationic metal hydrido dinitrogen complexes such as the examples described previously (Table 6.3).

Table 6.3. IR and ^{15}N NMR Data for Selected Hydrido Dinitrogen and Dinitrogen Complexes

Complex	^{15}N NMR[a]		IR $\nu(^{14}N_2)$[b]	Reference
	$\delta(^{15}N_\alpha)$	$\delta(^{15}N_\beta)$		
$Cp^*Re(PMe_3)_2(N_2)$ (**4.5**)[c, d]	-82.1	-51.7	1975	This work
trans-$W(N_2)_2(dppe)_2$[e, f]	-60.1	-48.6	1946	158
$Fe(N_2)(dmpe)_2$[g]			1975	166
cis-$[Cp^*ReH(N_2)(PMe_3)_2][CF_3COO]$ (*cis*-**6.1**)[c]	-108.3	-26.0		This work
trans-$[Cp^*ReH(N_2)(PMe_3)_2][CF_3COO]$ (*trans*-**6.1**)[c, h]	-98.6	-6.2	2079	This work
trans-$[WH(N_2)_2(dppe)_2][HCl_2]$[e]	-75.3	-48.6		158
$[FeH(N_2)(dmpe)_2][BPh_4]$[g]			2094	166
trans-$ReH(N_2)(dppe)_2$[i]			2006	122
$[ReH_2(N_2)(dppe)_2][BF_4]$[i]			2118	122
cis-$ReH(N_2)(PMe_2Ph)_4$[j]			2000	170

[a] Referenced to external $MeNO_2$; δ given in ppm.
[b] $\nu(^{14}N_2)$ given in cm^{-1}.
[c] Acetone-d_6 used as the NMR solvent.
[d] Hexane used as the IR solvent.
[e] THF used as the NMR solvent.
[f] IR measured in Nujol.
[g] THF used as the IR solvent.
[h] Acetone used as the IR solvent.
[i] IR measured on pressed CsI disks.
[j] Diethyl ether used as the IR solvent.

It is worth noting that the dinitrogen complexes, *trans*-$W(N_2)_2(dppe)_2$ and $Fe(N_2)(dmpe)_2$, which afforded the corresponding metal hydrido dinitrogen complexes *trans*-$[WH(N_2)_2(dppe)_2][HCl_2]$ and $[FeH(N_2)(dmpe)_2][BPh_4]$ respectively, were also shown to undergo protic attack at the terminal nitrogen atom under the right chemical conditions.[166, 171] Therefore, although protic attack at the coordinated dinitrogen ligand was not observed for $Cp^*Re(PMe_3)_2(N_2)$ **(4.5)**, the results obtained for the rhenium system are encouraging.

6.4. Conclusion

In this chapter I have shown that the bis-trimethylphosphine dinitrogen complex $Cp^*Re(PMe_3)_2(N_2)$ **(4.5)** is prone to protonation at the metal center but not at the rhenium-bound dinitrogen ligand. Furthermore, the protonation reaction appears to be independent of the acid used since treatment of **4.5** with CF_3COOH, $HBF_4{\cdot}OEt_2$, or CF_3SO_3H afforded the respective rhenium hydrido dinitrogen complexes *cis*-$[Cp^*ReH(N_2)(PMe_3)_2][CF_3COO]$ (***cis*-6.1**), *cis*-$[Cp^*ReH(N_2)(PMe_3)_2][BF_4]$ (***cis*-6.2**), and *cis*-$[Cp^*ReH(N_2)(PMe_3)_2][CF_3SO_3]$ (***cis*-6.3**) at 213 K and these complexes isomerized to their corresponding *trans* isomers as the temperature was raised to 273 K. Interestingly, the *trans* isomers were found to be thermally unstable at room temperature, although ***trans*-6.1** was observed to be significantly more stable than its analogs ***trans*-6.2** and ***trans*-6.3** inferring that the counter anion may play a role in stabilizing these cationic rhenium hydrido dinitrogen complexes. These results demonstrate that tailoring a dinitrogen complex so as to promote the release of electrons from the metal center into the coordinated dinitrogen ligand is not sufficient to ensure the protonation of the dinitrogen ligand in **4.5** and that other factors such as the geometry of the dinitrogen complex and the steric properties of the ancillary ligands must also be considered.

6.5. Experimental

6.5.1. General Methods and Syntheses

Manipulations, solvent purification, and routine spectroscopic measurements were carried out as described in Chapter 2.

Low temperature IR spectra were measured by using a Bomem Michelson model 120 FT-IR instrument. The spectra were recorded as solutions using acetone as the solvent in a variable temperature Research and Industrial Instruments model VLT-2 cell modified with attached cannulae and equipped with CaF_2 windows (0.5 mm). The low temperature IR spectrum of the ^{15}N labeled complex was obtained for a 99% ^{15}N isotopically enriched sample. The cell was flushed with argon and dry acetone prior to transfer of the solution *via* cannula to the cell. All spectra were recorded at 273 K unless stated otherwise.

The dinitrogen complex $Cp^*Re(PMe_3)_2(N_2)$ (**4.5**), and its ^{15}N derivatives **4.5-$^{15}N_\alpha$** and **4.5-$^{15}N_\beta$**, investigated in this chapter were prepared and purified following the procedures detailed in Chapter 4. Tetrafluoroboric acid diethyl ether complex ($HBF_4 \cdot OEt_2$) (Aldrich Chemical Co.), trifluoromethanesulfonic acid (CF_3SO_3H) (Aldrich), and trifluoroacetic acid (CF_3COOH) (Aldrich) were used as purchased and were stored under nitrogen.

The deuterated solvent used for NMR spectroscopy (acetone-d_6) was degassed prior to use to remove any residual oxygen. ^1H NMR chemical shifts are reported in ppm downfield (positive) of tetramethylsilane. ^{31}P NMR chemical shifts are referenced to external 85% H_3PO_4. ^{14}N and ^{15}N NMR chemical shifts are referenced to external nitromethane ($MeNO_2$). The term "virtual doublet" refers to the non-first-order multiplet which is seen in some of the ^1H NMR spectra; the apparent coupling constant is given by the separation between the two outside peaks.

Room Temperature ^{1}H NMR Experiments: Reaction of Cp*Re(PMe$_3$)$_2$(N$_2$) (4.5) with HBF$_4$·OEt$_2$, CF$_3$SO$_3$H, or CF$_3$COOH. A 5-fold stoichiometric excess of HBF$_4$·OEt$_2$, CF$_3$SO$_3$H, or CF$_3$COOH was added *via* syringe to a pale yellow solution of the neutral bis-trimethylphosphine dinitrogen complex **4.5** (50 mg, 0.10 mmol) in acetone-d$_6$ at room temperature. In all cases, the solution changed from yellow to orange immediately after the acid was added. An IR spectrum recorded of the solution after the addition of CF$_3$COOH demonstated the total disappearance of **4.5** and the presence of a weak broad absorption at 2080 cm^{-1}. IR spectra of the solutions following the HBF$_4$·OEt$_2$ or CF$_3$SO$_3$H additions also showed the complete disappearance of **4.5** but no concomitant formation of any other observable bands. The respective solutions were then transferred to a 5 mm NMR tube which was kept in a Schlenk tube under a positive pressure of argon. Room temperature ^{1}H NMR spectra, acquired *ca.* 60 min after the additions of HBF$_4$·OEt$_2$ or CF$_3$SO$_3$H, exhibited in each case a singlet at δ 2.09 and a doublet at δ 1.67 ($J_{H\text{-}P}$ = 13.7 Hz) assigned to Cp*ReO$_3$ (**4.8**) and POMe$_3$ respectively. In both cases, removal of the solvent under vacuum gave a yellow-brown oil. Diethyl ether extractions of the oil gave trace amounts of **4.8** and POMe$_3$. The remaining yellow-brown oil exhibited no ^{1}H NMR resonances and no diagnostic IR absorptions. A room temperature ^{1}H NMR spectrum, recorded *ca.* 60 min after the addition of CF$_3$COOH, was assigned to the cationic rhenium hydrido dinitrogen complex *trans*-[Cp*ReH(N$_2$)(PMe$_3$)$_2$][CF$_3$COO] (***trans*-6.1**). IR (acetone-d$_6$): 2080 cm^{-1} ν(NN). ^{1}H NMR (acetone-d$_6$): δ -10.58 (t, 1H, ReH, $J_{H\text{-}P}$ = 49.6 Hz), 1.75 (virtual doublet, 18H, PMe$_3$, J_{app} = 9.5 Hz), 2.05 (s, 15H, Cp*). A room temperature ^{1}H NMR spectrum recorded 12 h later showed the total disappearance of ***trans*-6.1** and the presence of resonances due to **4.8** and POMe$_3$. Subsequent removal of the solvent under vacuum gave a yellow-brown oil. Diethyl ether extractions of the oil gave residual

amounts of **4.8** (4.4 mg, 0.012 mmol) and $POMe_3$ and the remaining yellow-brown oil exhibited no ^1H NMR resonances and no diagnostic IR absorptions.

6.5.2. Variable Temperature NMR Spectroscopy

The variable temperature ^1H, $^{31}P\{^1H\}$, and ^{15}N NMR spectra of the products resulting from the protonation of complexes **4.5**, **4.5-$^{15}N_\alpha$**, or **4.5-$^{15}N_\beta$** were recorded at 400, 162, and 40.6 MHz respectively on a Bruker AMX 400 instrument equipped with a B-VT 1000 variable temperature unit. A cooling unit containing liquid nitrogen and a heater coil was attached to the NMR probe and was used to attain the desired temperature. A Bruker single frequency probe was used to acquire the ^1H spectra. A Bruker tunable broad band probe was used to acquire the $^{31}P\{^1H\}$ and ^{15}N spectra. Acetone-d_6 (Isotec Inc.) was used as the solvent for all the variable temperature NMR work.

Variable Temperature ^1H, $^{31}P\{^1H\}$, and ^{15}N NMR Experiments: Reaction of $Cp^*Re(PMe_3)_2(N_2)$ (4.5), (4.5-$^{15}N_\alpha$), or (4.5-$^{15}N_\beta$) with CF_3COOH. A pale yellow solution of the neutral bis-trimethylphosphine dinitrogen complex **4.5** (50 mg, 0.10 mmol), **4.5-$^{15}N_\alpha$**, or **4.5-$^{15}N_\beta$** in acetone-d_6 was transferred to an NMR tube (5 mm tube for ^1H and ^{31}P; 10 mm tube for ^{15}N) which was kept in a Schlenk tube under a positive pressure of argon. The Schlenk tube containing the NMR solution was then cooled to 195 K in a dry ice-acetone bath. With a strong purge of argon, addition of a 5-fold stoichiometric excess of CF_3COOH directly to the NMR tube, *via* syringe, resulted in the formation of an orange colored solution. The NMR tube was then quickly removed from the cold temperature bath and placed into the Bruker AMX 400 spectrometer whose cooling unit had been previously set to 213 K. An NMR spectrum was then acquired *ca.* 60 min after the acid addition. An identical procedure was used for obtaining spectra for all the NMR active nuclei. The protonation product formed at 213 K was assigned as the

cationic rhenium hydrido dinitrogen complex *cis*-[Cp*ReH(N_2)(PMe_3)$_2$][CF_3COO] (***cis*-6.1**), (***cis*-6.1-$^{15}N_\alpha$**), or (***cis*-6.1-$^{15}N_\beta$**). ^{1}H NMR (acetone-d_6, 213 K): δ -10.96 (broad doublet, 1H, ReH, J_{H-P} = 64.2 Hz), 1.76 (apparent triplet, 18H, PMe_3, J_{H-P} = 8.8 Hz), 2.08 (s, 15H, Cp*). $^{31}P\{^1H\}$ NMR (not metal hydride decoupled, acetone-d_6, 213 K): δ -42.16 (dd, PMe_3, J_{P-H} = 64.4 Hz, J_{P-P} = 48.6 Hz), -38.67 (d, PMe_3, J_{P-P} = 48.6 Hz). ^{15}N NMR (acetone-d_6, 213 K): δ -108.3 (s, $^{15}N_\alpha$), -26.0 (s, $^{15}N_\beta$). As the temperature of the NMR solution was raised to 273 K the cationic *cis* complex isomerized to give *trans*-[Cp*ReH(N_2)(PMe_3)$_2$][CF_3COO] (***trans*-6.1**), (***trans*-6.1-$^{15}N_\alpha$**), or (***trans*-6.1-$^{15}N_\beta$**) respectively. IR (acetone, 273 K): 2079 cm^{-1} ν(NN) (2047 cm^{-1} for $^{15}N_\alpha$ labeled complex). ^{1}H NMR (acetone-d_6, 273 K): δ -10.60 (t, 1H, ReH, J_{H-P} = 50.3 Hz), 1.75 (virtual doublet, 18H, PMe_3, J_{app} = 9.8 Hz), 2.05 (s, 15H, Cp*). $^{31}P\{^1H\}$ NMR (not metal hydride decoupled, acetone-d_6, 273 K): δ -34.71 (d, PMe_3, J_{P-H} = 50.1 Hz). ^{15}N NMR (acetone-d_6, 273 K): δ -98.6 (s, $^{15}N_\alpha$), -6.2 (s, $^{15}N_\beta$). The temperature of the NMR sample was then raised to room temperature. The room temperature ^{1}H, $^{31}P\{^1H\}$, and ^{15}N NMR spectra recorded 3 h later demonstrated the decay of ***trans*-6.1**, ***trans*-6.1-$^{15}N_\alpha$**, or ***trans*-6.1-$^{15}N_\beta$**; after 15 h the *trans* rhenium hydrido dinitrogen complex had completely disappeared. Removal of the solvent under vacuum gave a yellow-brown oil. Diethyl ether extractions of the oil gave residual amounts of **4.8** (5.5 mg, 0.015 mmol) and $POMe_3$. The remaining yellow-brown oil exhibited no ^{1}H NMR resonances and no diagnostic IR absorptions.

Variable Temperature ^{1}H NMR Experiments: Reaction of Cp*Re(PMe_3)$_2$(N_2) (4.5) with HBF_4·OEt_2 or CF_3SO_3H. A procedure similar to that described for the low temperature NMR experiments involving CF_3COOH was used. The product formed at 213 K using HBF_4·OEt_2 was assigned as the cationic rhenium hydrido dinitrogen complex *cis*-[Cp*ReH(N_2)(PMe_3)$_2$][BF_4] (***cis*-6.2**). ^{1}H NMR (acetone-d_6, 213 K): δ -10.99 (broad doublet, 1H, ReH, J_{H-P} = 64.1 Hz), 1.73 (apparent

triplet, 18H, PMe_3, J_{H-P} = 9.8 Hz), 2.05 (s, 15H, Cp*). The product formed at 213 K using CF_3SO_3H was assigned as the cationic rhenium hydrido dinitrogen complex *cis*-[Cp*ReH(N_2)(PMe_3)$_2$][CF_3SO_3] (***cis*-6.3**). ^{1}H NMR (acetone-d_6, 213 K): δ -11.06 (broad doublet, 1H, ReH, J_{H-P} = 64.3 Hz), 1.64 (apparent triplet, 18H, PMe_3, J_{H-P} = 9.9 Hz), 1.97 (s, 15H, Cp*). As the temperature of the NMR solutions was raised to 273 K the cationic *cis* complexes isomerized to give *trans*-[Cp*ReH(N_2)(PMe_3)$_2$][BF_4] (***trans*-6.2**) [^{1}H NMR (acetone-d_6, 273 K): δ -10.63 (t, 1H, ReH, J_{H-P} = 50.4 Hz), 1.72 (virtual doublet, 18H, PMe_3, J_{app} = 9.7 Hz), 2.03 (s, 15H, Cp*)] and *trans*-[Cp*ReH(N_2)(PMe_3)$_2$][CF_3SO_3] (***trans*-6.3**) [^{1}H NMR (acetone-d_6, 273 K): δ -10.65 (t, 1H, ReH, J_{H-P} = 50.7 Hz), 1.63 (virtual doublet, 18H, PMe_3, J_{app} = 9.6 Hz), 1.94 (s, 15H, Cp*)] respectively. As the temperature of the NMR samples was raised to room temperature, the ^{1}H resonances corresponding to ***trans*-6.2** and ***trans*-6.3** slowly disappeared. Removal of the solvent under vacuum gave a yellow-brown oil. Diethyl ether extractions of the oil gave residual amounts of **4.8** and $POMe_3$ and the remaining yellow-brown oil exhibited no ^{1}H NMR resonances and no diagnostic IR absorptions.

CHAPTER 7

Oxidative Addition of Hydrocarbon C-H Bonds to Rhenium

7.1. Introduction

The photoextrusion of N_2 from dinitrogen complexes was first reported in 1972 by Darensbourg et al., who showed that N_2 substitution by CO in Fe, Mo, Re, and Os complexes was facilitated by UV irradiation.[172] Subsequently, numerous reports were published involving photochemical reactions of dinitrogen complexes to promote substitution[173] or addition reactions[174] at the metal center. In most of these reactions, notably carried out in aromatic solvents such as benzene, the unsaturated metal fragment formed by photoextrusion of N_2 apparently does not react with the solvent.[175]

An intriguing goal of homogeneous organo-transition-metal chemistry is the possibility of carrying out selective chemical transformations on, or functionalizing, very unreactive materials such as saturated hydrocarbons.[176, 177] To this end, transition metal complexes of iridium and rhodium capable of intermolecular oxidative addition to single C-H bonds in saturated hydrocarbons, leading to stable hydrido-alkyl metal complexes (Equation 7.1) were first reported in the early 1980's.[178-181]

$$M + R{-}H \longrightarrow M(R)(H) \qquad (7.1)$$

These systems function under ambient conditions and generally employ photolysis to create the reactive intermediate (M) responsible for the activation of the hydrocarbon.

In 1985, Bergman et al. reported the first examples of the reaction of hydrocarbon C-H bonds with rhenium intermediates photogenerated from *inter alia* $Cp^*Re(CO)_2(PMe_3)$ (Scheme 7.1).[73, 182]

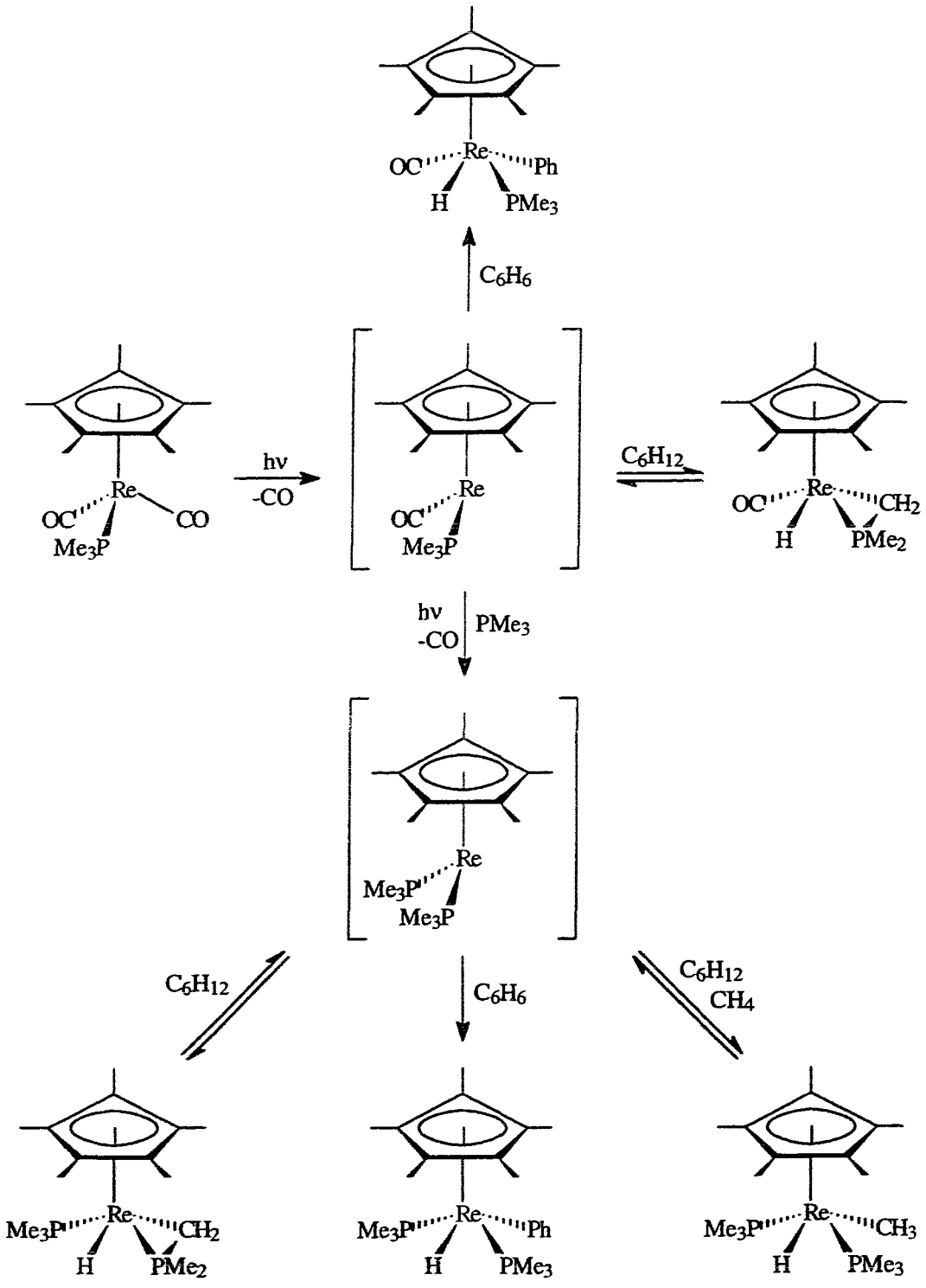

Scheme 7.1. Intra- and intermolecular C-H activation products formed from specific rhenium intermediates photogenerated from *inter alia* $Cp^*Re(CO)_2(PMe_3)$.

The coordinatively unsaturated bis-trimethylphosphine intermediate was observed to be more effective in the intermolecular activation of hydrocarbons than its carbonyl trimethylphosphine analog as evidenced by its ability to activate methane. Unfortunately, the synthetic route to this useful bis-PMe_3 species was not an efficient one since it involved exhaustive photolysis of the precursor $Cp^*Re(CO)_2(PMe_3)$ in the presence of added PMe_3.

In this chapter, the demonstrated propensity of dinitrogen complexes to extrude the N_2 ligand is utilized in C-H bond activation as demonstrated by reactions of the rhenium dinitrogen complexes $Cp^*Re(PMe_3)_2(N_2)$ (**4.5**) and $Cp^*Re(dmpe)(N_2)$ (**4.6**) (Figure 7.1) in saturated and unsaturated hydrocarbons. Under photochemical or *thermal* conditions complex **4.5** readily loses the N_2 ligand, and the 16-electron intermediate then produced reacts with C-H bonds both in an intra- and intermolecular fashion. The effectiveness of **4.5** in intra- and intermolecular C-H activation by comparison with the Bergman precursor $Cp^*Re(CO)_2(PMe_3)$ will also be addressed since both precursors generate the same unsaturated bis-PMe_3 intermediate. Furthermore, preliminary results obtained from the photochemical reaction of **4.6** in benzene are also presented in this chapter.

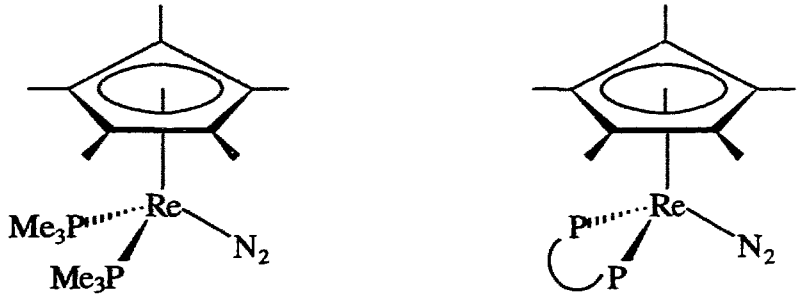

4.5 **4.6**

Figure 7.1. Structures of **4.5** and **4.6**.

7.2. Results

7.2.1. Photo- or Thermal Extrusion of N_2 from $Cp^*Re(PMe_3)_2(N_2)$ (4.5) or $Cp^*Re(dmpe)(N_2)$ (4.6) in Benzene

Irradiation of a benzene solution of $Cp^*Re(PMe_3)_2(N_2)$ (**4.5**) in a quartz vessel for only 10 min liberated dinitrogen and cleanly provided the intermolecular C-H activation product *trans*-$Cp^*Re(PMe_3)_2(Ph)H$ (***trans*-7.1**) (Figure 7.2).

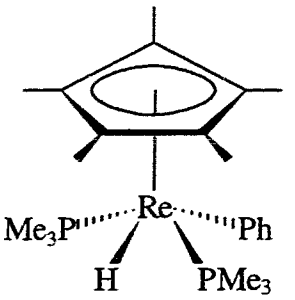

***trans*-7.1**

Figure 7.2. Structure of ***trans*-7.1**.

By comparison, irradiation of the Bergman precursor $Cp^*Re(CO)_2(PMe_3)$,[73] which required exhaustive photolysis (*ca.* several hours) in the presence of added PMe_3, resulted in a lower yield of ***trans*-7.1**. Furthermore, the hydrido phenyl complex ***trans*-7.1** was also prepared *thermally* by refluxing a benzene solution of the dinitrogen complex **4.5** for 2 h.

The hydrido phenyl complex ***trans*-7.1** was isolated by recrystallization from hexane at 195 K as a pale yellow solid and was spectroscopically and analytically characterized. Complex ***trans*-7.1** is very air-sensitive and reacts with trace amounts of oxygen to give the trioxo complex Cp^*ReO_3 (**4.8**).[138] However, ***trans*-7.1** is thermally

stable as a solid at room temperature under inert conditions and is soluble in benzene, hexane, and cyclohexane.

The IR spectrum of ***trans*-7.1** showed no detectable absorptions corresponding to a metal hydride vibration. The ^1H NMR spectrum obtained for ***trans*-7.1** in benzene-d_6 exhibited the typical resonances expected for the Cp* and phenyl ligands. However, the ^1H resonance at δ 1.37 assigned to the PMe_3 ligands was observed to be a virtual doublet integrating to 18 protons with a coupling constant ($^2J_{H-P} + {}^4J_{H-P}$) of 6.9 Hz. The ^1H NMR spectrum also exhibited a triplet in the metal hydride region at δ -11.00 integrating to 1 proton with a coupling constant of 53.4 Hz. The $^{31}P\{^1H\}$ NMR spectrum of ***trans*-7.1** in benzene-d_6 exhibited a single resonance at δ -44.93 suggesting that the PMe_3 ligands were equivalent by symmetry. Furthermore, by decoupling only the PMe_3 methyl resonance but not the resonance due to the metal hydride, the ^{31}P resonance appeared as a doublet indicating that it was coupled to the metal hydride (J_{P-H} = 52.9 Hz). These results are in agreement with the triplet observed for the rhenium hydride ^1H resonance, and taken together the NMR results suggest that the PMe_3 ligands are located *trans* to one another in ***trans*-7.1**.

Low voltage electron impact (EI) mass spectroscopy at 12 eV further corroborates the formulation of ***trans*-7.1**. It showed the molecular ion at m/z 552, and a base peak at m/z 474 resulting from loss of benzene.

Interestingly, a complete regeneration of the parent dinitrogen complex $Cp^*Re(PMe_3)_2(N_2)$ **(4.5)** was observed by IR and ^1H NMR spectroscopy when a cyclohexane solution of ***trans*-7.1** was pressurized to 1500 psi with N_2 for 12 h. The formation of **4.5** was also accompanied by the production of free benzene, as confirmed by GC analysis of the solvent remains. Furthermore, treatment of ***trans*-7.1** with chloroform lead to the formation of a yellow-orange solution which was assigned by ^1H NMR and mass spectroscopy, *not* to the corresponding chloro phenyl complex

$Cp^*Re(PMe_3)_2(Ph)Cl$, but to the dichloro complex *trans*-$Cp^*Re(PMe_3)_2Cl_2$ (***trans*-7.5**). The reaction was repeated using $CDCl_3$. A ^1H NMR spectrum acquired after 2 h showed the quantitative conversion of ***trans*-7.1** to ***trans*-7.5** and the concomitant production of free benzene (identified by comparison to a ^1H NMR spectrum of the authentic sample in $CDCl_3$). A ^1H NMR spectrum of ***trans*-7.5** in $CDCl_3$ exhibited a singlet at δ 1.65 and a virtual doublet at δ 1.45 assigned to Cp* and the PMe_3 ligands respectively. A coupling constant ($^2J_{H-P} + {}^4J_{H-P}$) of 8.8 Hz was extracted from the ^1H resonance corresponding to the PMe_3 groups. As was the case for the hydrido phenyl complex *trans*-$Cp^*Re(PMe_3)_2(Ph)H$ (***trans*-7.1**), the virtual doublet observed for the PMe_3 methyl resonance is consistent with a *trans* arrangement of the PMe_3 ligands in ***trans*-7.5**.

A benzene solution of the bidentate phosphine complex $Cp^*Re(dmpe)(N_2)$ (**4.6**) in a Pyrex vessel was irradiated for only 10 min. A ^1H NMR spectrum of the crude sample recorded immediately after the irradiation in benzene-d_6 showed the complete disappearance of **4.6** and the apparent formation of a C-H activation product(s) (Figure 7.3). The ^1H resonances at δ 1.86 (singlet) and δ 1.55-1.27 (multiplet) integrating to 30 and 32 protons respectively were assigned to the presence of *two* Cp* and *two* dmpe groups (Figure 7.3). Similarly, the aromatic region displayed two sets of resonances, each of which was composed of two multiplets integrating to 2 and 3 protons respectively, and thus were assigned to the presence of *two* metal-bound phenyl groups (Figure 7.3). More importantly, the ^1H NMR spectrum also exhibited two resonances in the metal hydride region, each integrating to 1 proton (Figure 7.3). The ^1H resonance at δ -12.91 was observed to be a triplet with a coupling constant of 54.7 Hz, while the signal at δ -11.00 was a broad doublet with a coupling constant of 51.7 Hz.

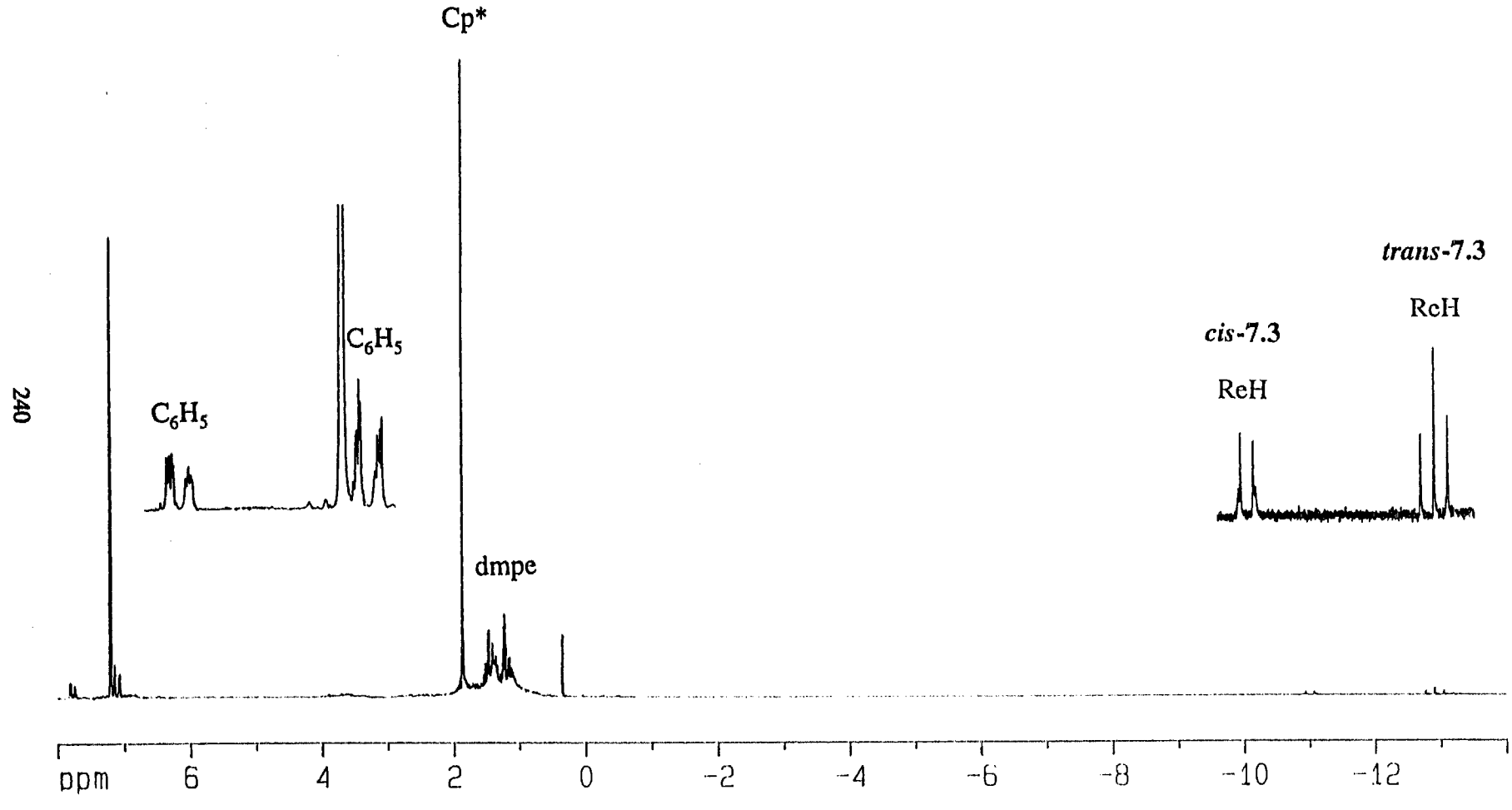

Figure 7.3. ^{1}H NMR spectrum (400 MHz, benzene-d_6) of the crude product formed after a benzene solution of Cp*Re(dmpe)(N_2) **(4.6)** in a Pyrex vessel was irradiated for 10 min. Upfield and aromatic resonances have been expanded for clarity.

The large coupling constants exhibited by these rhenium hydride resonances are consistent with a *cis*-J_{H-P} coupling between the hydride and an adjacent phosphine as reported previously for ***trans*-7.1**; the *trans*-J_{P-H} couplings in these half-sandwich piano-stool type complexes are usually small or unobservable.[169] Furthermore, the rhenium hydride triplet indicates that it is coupled to two symmetry-equivalent phosphorus atoms whereas the rhenium hydride doublet is suggestive of a complex in which the phosphorus atoms are not equivalent by symmetry. The intermolecular activation products *trans*-Cp*Re(dmpe)(Ph)H (***trans*-7.3**) and *cis*-Cp*Re(dmpe)(Ph)H (***cis*-7.3**) are consistent with the limited spectroscopic evidence presented above (Figure 7.4) .

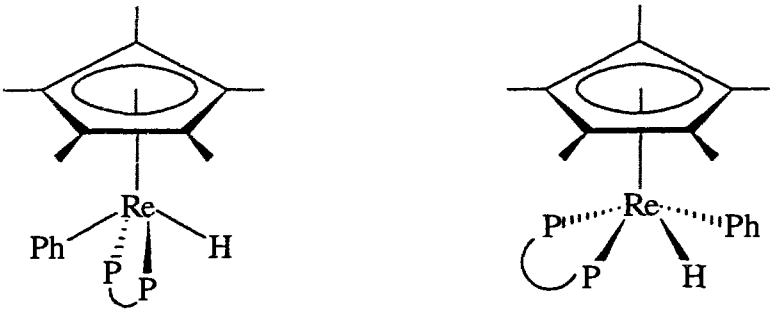

***trans*-7.3** ***cis*-7.3**

Figure 7.4. Structures of ***trans*-7.3** and ***cis*-7.3**.

Further spectroscopic or analytical evidence is required before complexes ***trans*-7.3** and ***cis*-7.3** can be unequivocally identified as the C-H activation products arising from the photochemical reaction of Cp*Re(dmpe)(N_2) (**4.6**) in benzene. Unfortunately, these complexes proved difficult to characterize analytically or spectroscopically owing to their thermal instability at room temperature. Specifically, the C-H activation products were found to have a lifetime of less than 30 min, reductively eliminating benzene in solution at room temperature as observed by ^{1}H NMR spectroscopy.

7.2.2. Photoextrusion of N_2 from $Cp^*Re(PMe_3)_2(N_2)$ (4.5) in Cyclohexane or Hexane

Photolysis of a cyclohexane solution of $Cp^*Re(PMe_3)_2(N_2)$ (**4.5**) in a quartz vessel for 10 min afforded exclusively the cyclometalated complex *trans*-$Cp^*Re(PMe_3)(\eta^2\text{-}CH_2PMe_2)H$ (***trans*-7.2**) (61% yield after purification) resulting from intramolecular C-H activation of a methyl group of one of the bound PMe_3 ligands (Figure 7.5).

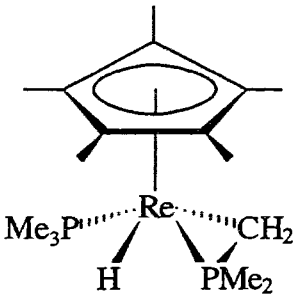

***trans*-7.2**

Figure 7.5. Structure of ***trans*-7.2**.

Similar results were obtained by Bergman et al. from exhaustive photolysis of $Cp^*Re(CO)_2(PMe_3)$[73] in cyclohexane in the presence of added PMe_3, although their yield of ***trans*-7.2** (*ca.* 20% yield by NMR spectroscopy) was much lower despite the longer irradiation time.

The cyclometalated complex ***trans*-7.2** was isolated by recrystallization from hexane at 195 K as a pale yellow solid. Although thermally stable as a solid at room temperature, this material proved difficult to purify to analytical standards; it was spectroscopically characterized by ^1H, $^{31}P\{^1H\}$ NMR, and MS. Complex ***trans*-7.2** is very air-sensitive and immediately reacts with residual oxygen to give the trioxo complex Cp^*ReO_3 (**4.8**).[138] However, ***trans*-7.2** is very soluble in hexane and cyclohexane, and reasonably stable under N_2 or Ar at room temperature in these solvents.

The IR spectrum of ***trans*-7.2** showed no absorptions corresponding to a metal hydride vibration. However, the assigned structure was fully supported by NMR spectroscopic evidence. The $^{31}P\{^1H\}$ NMR spectrum of ***trans*-7.2** in benzene-d_6 exhibited an AX quartet at δ -39.23 and δ -76.54 with a $J_{P\text{-}P}$ coupling of *ca.* 20 Hz assigned to the PMe_3 and η^2-CH_2PMe_2 groups respectively. The presence of the η^2-CH_2PMe_2 moiety is convincingly demonstrated by the large upfield shift of the ring phosphorus in the $^{31}P\{^1H\}$ NMR spectrum, an observation that is well-precedented for such structures.[183] The ^1H NMR spectrum of ***trans*-7.2** in benzene-d_6 exhibited a singlet at δ 1.95 and a doublet at δ 1.28 ($J_{H\text{-}P}$ = 7.1 Hz) integrating to 15 and 9 protons respectively which were assigned to the Cp* and PMe_3 ligands. The two doublets at δ 1.31 ($J_{H\text{-}P}$ = 9.8 Hz) and δ 1.38 ($J_{H\text{-}P}$ = 9.8 Hz), each integrating to 3 protons, were assigned to the two non-equivalent methyl groups of the η^2-CH_2PMe_2 moiety. The ^1H resonance at δ -0.24 assigned to one of the non-equivalent methylene protons was observed to be an apparent quartet with a coupling constant of 13.6 Hz indicating that the coupling between the other methylene proton and the two phosphorus groups were of the same magnitude. In contrast, the resonance for the other methylene proton appeared as a doublet of doublets of doublets ($J_{H\text{-}H}$ = 14.0 Hz, $J_{H\text{-}P}$ = 7.2, 1.9 Hz) at δ 0.09. The ^1H NMR spectrum of ***trans*-7.2** also exhibited a doublet of doublets at δ -12.04 ($J_{H\text{-}P}$ = 39.3, 32.1 Hz) clearly supportive of a rhenium hydride resonance, and more importantly, on the basis of these large, nearly identical NMR couplings to the hydride ligand, a *trans* relationship between the phosphorus atoms was inferred (i.e., a *cis*-$J_{H\text{-}P}$ coupling).

The formulation of ***trans*-7.2** was further corroborated by low voltage electron impact (EI) mass spectroscopy at 12 eV, which showed the molecular ion at m/z 474 as the highest mass peak. No fragments were observed.

Interestingly, the cyclometalated complex ***trans*-7.2** slowly reacted with benzene (*ca.* 48 h) at room temperature to give the hydrido phenyl complex ***trans*-7.1** (90% yield

as monitored by ^{1}H NMR spectroscopy). Furthermore, treatment of ***trans*-7.2** with either high pressure N_2 or chloroform produced results analogous to those reported previously for the hydrido phenyl complex ***trans*-7.1**. Specifically, pressurizing a cyclohexane solution of ***trans*-7.2** to 1500 psi with N_2 for 8 h resulted in the quantitative conversion to the parent dinitrogen complex Cp*Re(PMe_3)$_2$(N_2) (**4.5**) and treatment of ***trans*-7.2** with $CHCl_3$ or $CDCl_3$ lead to the production of the dichloro complex *trans*-Cp*Re(PMe_3)$_2$$Cl_2$ (***trans*-7.5**).

A hexane solution of Cp*Re(PMe_3)$_2$(N_2) (**4.5**) in a quartz vessel was irradiated for only 10 min. A ^{1}H NMR spectrum of the crude sample in acetone-d_6 recorded immediately after the irradiation showed the cyclometalated complex ***trans*-7.2** to be present as the major product (Figure 7.6). However, the spectrum also exhibited a broad triplet in the metal hydride region (δ -10.89, J = 50 Hz), presumably corresponding to a second C-H activation product (Figure 7.6). The unknown C-H activation product was found to have a lifetime of *ca.* 30 min in solution at room temperature as monitored by ^{1}H NMR spectroscopy. By comparison, similar results were not reported by Bergman et al. during their investigation into the C-H activation chemistry displayed by the rhenium precursor Cp*Re(CO)$_2$(PMe_3).[73] However, they were able to show that photolysis of the Cp complex CpRe(PMe_3)$_3$ in hexane at 243 K produced a C-H activation product identifiable by ^{1}H NMR spectroscopy (metal hydride resonance appears as a triplet of triplets, $J_{H\text{-}H}$ = 3.6 Hz, $J_{H\text{-}P}$ = 50.1 Hz) as the primary C-H insertion product *trans*-CpRe(PMe_3)$_2$(*n*-C_6H_{13})H.[182] Furthermore, the hydrido *n*-hexyl complex was reported to be extremely unstable, reductively eliminating *n*-hexane at room temperature with a half-life of *ca.* 12 min.[182] The similarities between our results and those reported for the Cp rhenium system suggested that the unknown Cp* C-H activation product was the hydrido *n*-hexyl complex *trans*-Cp*Re(PMe_3)$_2$(*n*-C_6H_{13})H (***trans*-7.4**) (Figure 7.7).

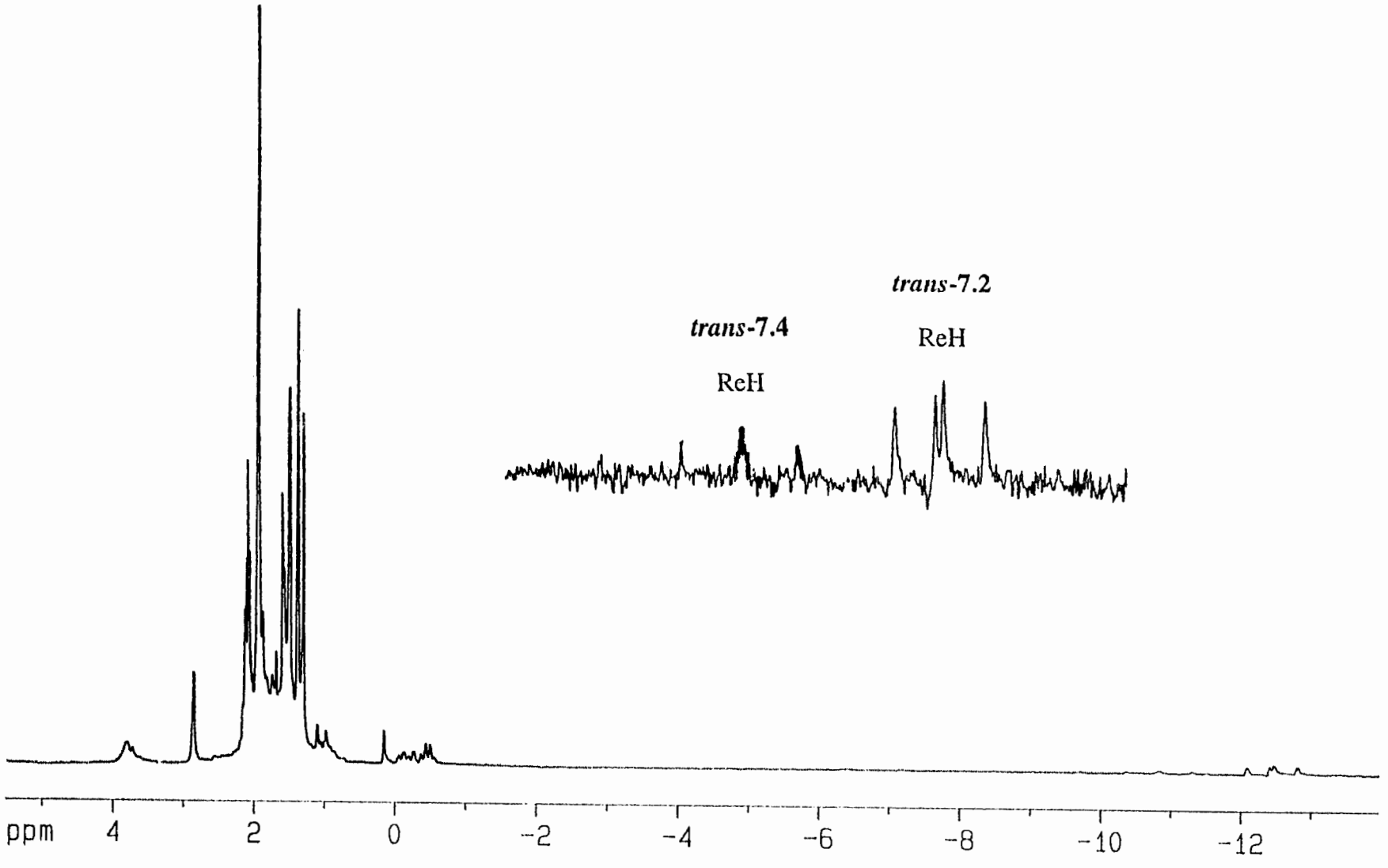

Figure 7.6. ^{1}H NMR spectrum (100 MHz, acetone-d_6) of the crude product formed after a hexane solution of Cp*Re(PMe_3)$_2$(N_2) **(4.5)** in a quartz vessel was irradiated for 10 min. Upfield resonances have been expanded for clarity.

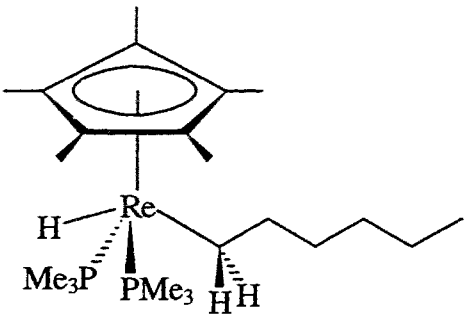

***trans*-7.4**

Figure 7.7. Structure of ***trans*-7.4**.

Complex ***trans*-7.4** proved difficult to characterize analytically or spectroscopically owing to its thermal instability.

7.3. Discussion

7.3.1. Mechanism of Rhenium C-H Insertions

The simplest mechanistic hypothesis for both the thermal and the photochemical C-H insertion reactions of the rhenium dinitrogen precursor $Cp^*Re(PMe_3)_2(N_2)$ (**4.5**) involves the unsaturated intermediate "$Cp^*Re(PMe_3)_2$" (Scheme 7.2). A similar scheme was proposed by Bergman et al. using $Cp^*Re(CO)_2(PMe_3)$ or $CpRe(PMe_3)_3$ as the precursors for the C-H activation reactions.[73, 182] Alternatively, the creation of the required coordination site could proceed *via* an η^5 to η^3 isomerization of the pentamethylcyclopentadienyl ring. However, given the propensity for these dinitrogen complexes to extrude N_2,[172-175] the former mechanism involving the coordinatively unsaturated intermediate seems the more likely pathway for C-H activation rather than the latter mechanism which involves a preference for ring slippage over loss of N_2.

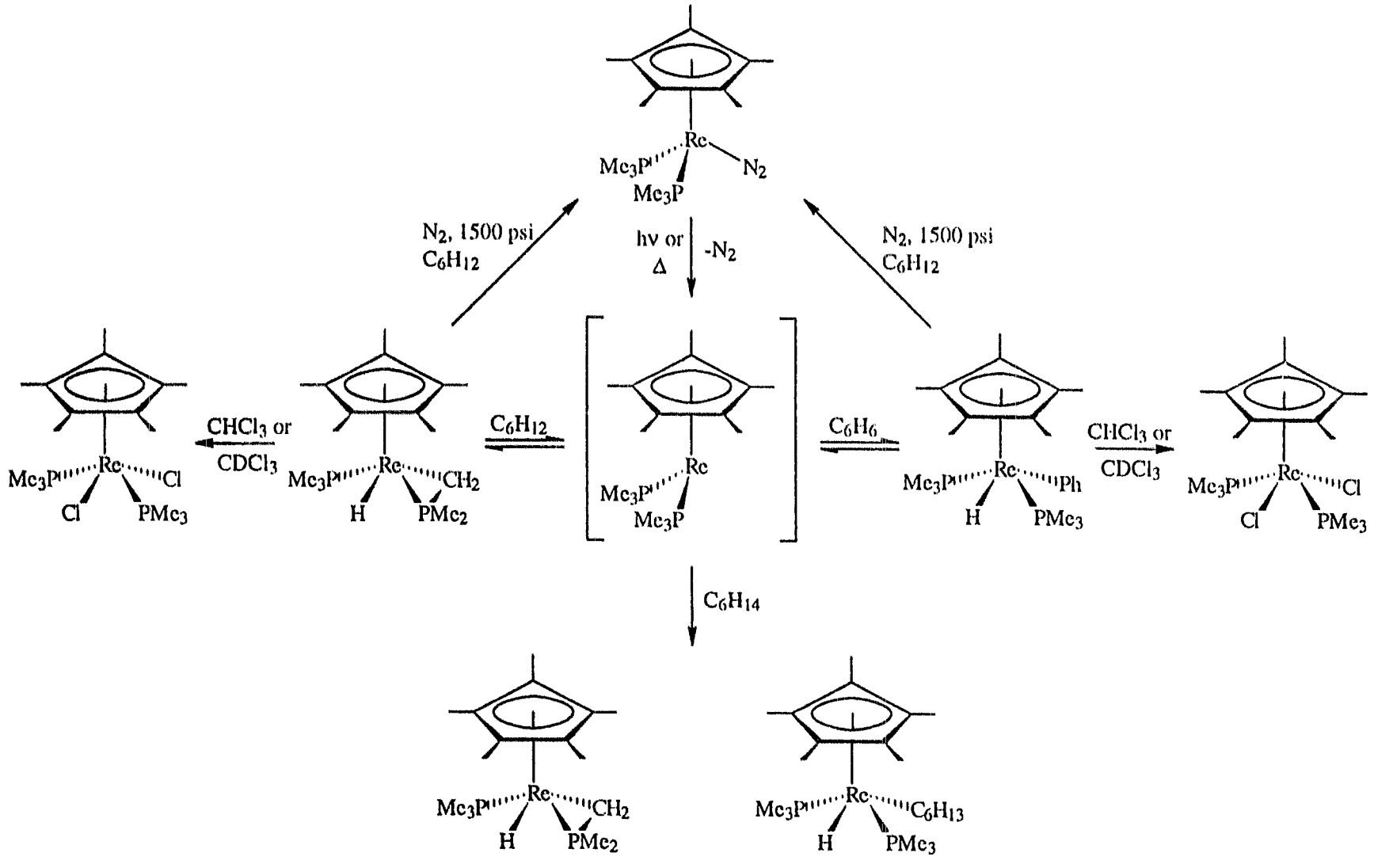

Scheme 7.2. Intra- and intermolecular C-H activation products photo- or thermally generated from $Cp^*Re(PMe_3)_2(N_2)$ (**4.5**).

Once photochemically or thermally produced, the reactive 16-electron metal center inserts into the C-H bond of a benzene molecule to give presumably the *cis* hydrido phenyl complex *cis*-Cp*Re(PMe_3)$_2$(Ph)H (***cis*-7.1**) which then isomerizes to the observed *trans* isomer (Scheme 7.2). Despite the assumption that a *cis* geometry is required for reductive elimation[184] and its microscopic reverse, C-H insertion, no evidence to support such a geometry was obtained from our investigations of the bis-PMe_3 rhenium system. Generating the unsaturated fragment "Cp*Re(PMe_3)$_2$" in a solvent such as cyclohexane, which contains only secondary C-H bonds, leads to internal activation of one of the PMe_3 ligands to give exclusively the cyclometalated complex *trans*-Cp*Re(PMe_3)(η^2-CH_2PMe_2)H (***trans*-7.2**). As was the case for the hydrido phenyl complex no evidence to support ***cis*-7.2** was found. In contrast to these results, the production of the 16-electron species in hexane affords both the intramolecular activation product ***trans*-7.2** and apparently the intermolecular primary C-H insertion product *trans*-Cp*Re(PMe_3)$_2$(*n*-C_6H_{13})H (***trans*-7.4**).

The *trans* stereochemistry observed for these insertion products was not surprising given the steric bulk of the two PMe_3 ligands. However, the *trans* geometry is also prevalent for insertion products containing ligands which are not sterically demanding. For example, it was reported by Graham et al that irradiation of Cp*Re(CO)$_3$ in the presence of H_2 yielded the rhenium hydrido complex *trans*-Cp*Re(CO)$_2H_2$.[185] Furthermore, it was proposed by Graham et al. that the reaction proceeded *via* photodissociation of CO and subsequent oxidative addition of H_2, presumably to give a *cis* insertion product.[185] However, since no comment was offered concerning possible *cis-trans* isomerization at the rhenium center, it must be concluded that a metal dihydride product with *cis* geometry was not detected.

The cyclometalated complex *trans*-Cp*Re(PMe_3)(η^2-CH_2PMe_2)H (***trans*-7.2**) was observed to react slowly (*ca.* 48 h) with benzene at room temperature to form the hydrido

phenyl complex *trans*-Cp*Re(PMe_3)$_2$(Ph)H (***trans*-7.1**) in approximately 90% yield as monitored by ^{1}H NMR spectroscopy. This suggests that reversible formation of "Cp*Re(PMe_3)$_2$" from ***trans*-7.2** occurs[73] and that ***trans*-7.1** results from the thermal reaction of this intermediate with benzene (Scheme 7.2). However, this reactive intermediate was not present in sufficient concentration to be observed directly in the ^{1}H NMR spectra of ***trans*-7.2**. Furthermore, ***trans*-7.2** was characterized by ^{1}H NMR spectroscopy using benzene-d_6 as the solvent (^{1}H NMR spectra generally recorded within 1 h of sample preparation) with no apparent activation of the deuterated solvent to give *trans*-Cp*Re(PMe_3)$_2$(C_6D_5)D, suggesting that the equilibration with "Cp*Re(PMe_3)$_2$" was not sufficiently rapid to interfere. The reversible formation of "Cp*Re(PMe_3)$_2$" from ***trans*-7.2** was further indicated by (i) the quantitative regeneration of the dinitrogen complex **4.5** when ***trans*-7.2** was pressurized with N_2 and by (ii) the production of the dichloro complex *trans*-Cp*Re(PMe_3)$_2$$Cl_2$ (***trans*-7.5**) when ***trans*-7.2** was taken up in $CHCl_3$ or $CDCl_3$ (Scheme 7.2).

More surprising is the observation that the dinitrogen complex **4.5** was also formed quantitatively (but more slowly) from the hydrido phenyl complex ***trans*-7.1** under N_2 pressure (Scheme 7.2). Furthermore, treatment of ***trans*-7.1** with $CHCl_3$ or $CDCl_3$ also afforded the dichloro complex ***trans*-7.5** (Scheme 7.2). These results infer that, in solution, ***trans*-7.1** is partly dissociated into benzene and the unsaturated fragment "Cp*Re(PMe_3)$_2$", and this in turn suggests that there is an undetectable amount of the hydrido phenyl species *cis*-Cp*Re(PMe_3)$_2$(Ph)H (***cis*-7.1**) in equilibrium with ***trans*-7.1**. (Scheme 7.2).

7.3.2. Effect of the Ancillary Ligands on Rhenium C-H Insertions

It was reported by Pasman et al. that irradiation of Cp*Re(CO)$_3$ in benzene lead to the formation of the η^2-benzene complex Cp*Re(CO)$_2$(η^2-C_6H_6), indicating that the

photolysis of the tricarbonyl complex gives the reactive fragment "$Cp^*Re(CO)_2$".[186] More importantly, no products arising from insertion into benzene C-H bonds were observed. Similar results were obtained when the dicarbonyl dinitrogen complex $Cp^*Re(CO)_2(N_2)$ (**4.2**) was irradiated in benzene.[168] Furthermore, photolysis of $Cp^*Re(CO)_3$[67, 185] or **4.2**[168] in hexane did not yield C-H activation products, but instead gave the rhenium dimers $Cp^*_2Re_2(\mu\text{-}CO)_3$ and $Cp^*_2Re_2(CO)_4(\mu\text{-}CO)$ apparently formed from attack of "$Cp^*Re(CO)_2$" upon the starting rhenium tricarbonyl complex. The differences in reactivity between the unsaturated fragments "$Cp^*Re(CO)_2$" and "$Cp^*Re(PMe_3)_2$" suggests that the presence of the more electron donating PMe_3 ligands promotes the insertion of the rhenium center into hydrocarbon C-H bonds.

It was pointed out by Bergman et al., from work conducted on the photoprecursor $CpRe(PMe_3)_3$,[182] that the rhenium fragment "$CpRe(PMe_3)_2$" exhibited a high selectivity with respect to intermolecular C-H bond insertion, while also undergoing competitive cyclometalation. Other reported C-H activating systems containing the PMe_3 ligand which generate the "$Cp^*Re(CO)(PMe_3)$" fragment give isolable products formed from cyclometalation or intermolecular C-H insertion but not both.[73, 169] Furthermore, Bergman et al. concluded that the intermolecular selectivities for the rhenium system (i.e., "$CpRe(PMe_3)_2$") parallel the thermodynamic stabilities of the products: aryl > primary alkyl >> secondary alkyl.[182] Our results with the dinitrogen complex $Cp^*Re(PMe_3)_2(N_2)$ (**4.5**) are generally in agreement with and extend those of Bergman. For example, irradiation of **4.5** in hexane gives the primary C-H insertion product *trans*-$Cp^*Re(PMe_3)_2(n\text{-}C_6H_{13})H$ (***trans*-7.4**) as well as the cyclometalated complex ***trans*-7.2**, whereas photolysis of **4.5** in cyclohexane produces exclusively ***trans*-7.2**. It is not clear yet whether these selectivities are governed by thermodynamics or kinetics. In either case, I believe that the sterically demanding metal center may be responsible for the high selectivity demonstrated by the unsaturated rhenium fragment "$Cp^*Re(PMe_3)_2$"; the

bulky PMe_3 ligands preventing the metal center from inserting into the secondary C-H bonds. Unfortunately, the steric crowding may also be responsible for the propensity of "$Cp^*Re(PMe_3)_2$" to cyclometalate.[187]

The results obtained from the investigations of the bis-trimethylphosphine system suggested that the ideal rhenium-bound dinitrogen precursor for intermolecular activation of hydrocarbons was one in which the ancillary ligands were (i) sterically demanding, (ii) electron donating (good σ-donor, poor π-acceptor), and (iii) not susceptible to cyclometalation. These requirements were satisfied by the 1,2-bis(dimethylphosphino)ethane dinitrogen complex $Cp^*Re(dmpe)(N_2)$ (**4.6**). Of equal importance, complex **4.6** was also chosen because it was believed that the bidentate phosphine ligand may prevent the conversion of the *cis* C-H activation product, presumably required for C-H insertion, to the more stable *trans* arrangement observed previously for the bis-PMe_3 system. The preliminary results obtained from the photochemical reaction of **4.6** in benzene were provided previously in the Results section 7.2.1. The ^1H NMR spectrum of the resultant products demonstrated the formation of apparently two intermolecular C-H activation species speculatively assigned as the hydrido phenyl complexes *trans*-$Cp^*Re(dmpe)(Ph)H$ (***trans*-7.3**) and the corresponding isomer *cis*-$Cp^*Re(dmpe)(Ph)H$ (***cis*-7.3**) (Figure 7.4). These results if corroborated provide detectable evidence to support the presence of the elusive *cis* C-H activation product which up to now has not been observed in our laboratory. The results provided by the $Cp^*Re(dmpe)(N_2)$ (**4.6**) system are encouraging and warrant further investigation.

7.4. Conlusion

In this chapter we have shown the dinitrogen complex $Cp^*Re(PMe_3)_2(N_2)$ (**4.5**) to be a very useful alternative to the rhenium complexes $Cp^*Re(CO)_2(PMe_3)$ or $CpRe(PMe_3)_3$ in promoting the C-H activation of hydrocarbons.[73, 182] The reason

manifests itself in the short irradiation time (*ca.* 10 min) required for virtually quantitative reaction as a result of the facile photoextrusion of N_2 compared with CO or PMe_3. Irradiation or refluxing **4.5** in benzene forms exclusively the intermolecular C-H activation product *trans*-Cp*Re(PMe_3)$_2$(Ph)H (***trans*-7.1**) whereas photolysis of a cyclohexane solution of **4.5** gives only the cyclometalated product *trans*-Cp*Re(PMe_3)(η^2-CH_2PMe_2)H (***trans*-7.2**). Both activation products were also shown to be in equilibrium with the unsaturated fragment "Cp*Re(PMe_3)$_2$". Furthermore, irradiation of **4.5** in hexane produces the primary C-H insertion product *trans*-Cp*Re(PMe_3)$_2$(*n*-C_6H_{13})H (***trans*-7.4**) as well as the cyclometalated complex ***trans*-7.2**. These results demonstrate that the rhenium system, despite lowered inter/intra selectivity, is more selective to intermolecular activation of hydrocarbons; aromatic and primary C-H bonds are intermolecularly activated, secondary C-H bonds are not. The sterically demanding rhenium center is believed to be responsible for the observed selectivity. Furthermore, the preliminary results obtained from the photochemical reaction of the 1,2-bis(dimethylphosphino)ethane dinitrogen complex Cp*Re(dmpe)(N_2) (**4.6**) in benzene appear to provide detectable evidence to support the presence of the elusive *cis* C-H activation product, presumably required for C-H insertion or reductive elimination.

7.5. Experimental

7.5.1. General Methods

Manipulations, solvent purification, and routine spectroscopic measurements were carried out as described in Chapter 2. Some of the room temperature ^{1}H NMR spectra were recorded at an operating frequency of 100 MHz by using a Bruker SY100 instrument. High pressure reactions were carried out in a Parr bomb, at room temperature using oxygen free nitrogen (Linde Union Carbide).

Photochemical reactions were carried out at atmospheric pressure and a temperature of 273 K with a water-jacketed 200 watt Hanovia high pressure mercury lamp as the UV source. The radiation was otherwise unfiltered. The photochemical reactions were conducted in quartz or Pyrex tubes which were placed adjacent to the lamp. Nitrogen was passed through the reaction tubes prior to the introduction of the solvent and starting materials; the tubes were then sealed. All solutions were subjected to a freeze-pump-thaw cycle (2 times) prior to photolysis. Benzene, cyclohexane, and hexane, which were used as the solvents for the C-H activation reactions, were distilled over sodium and transferred directly into the reaction quartz or Pyrex tubes under oxygen free nitrogen (Linde).

The complexes which were investigated in this chapter were prepared and purified following the procedures detailed in Chapter 4.

The deuterated solvents (benzene-d_6, acetone-d_6, or $CDCl_3$) used for NMR spectroscopy were degassed prior to use to remove any residual oxygen. ^1H NMR chemical shifts are reported in ppm downfield (positive) of tetramethylsilane. ^{31}P NMR chemical shifts are referenced to external 85% H_3PO_4. The term "virtual doublet" refers to the non-first-order multiplet which is seen in some of the ^1H NMR spectra; the apparent coupling constant is given by the separation between the two outside peaks.

7.5.2. Syntheses

Photochemical preparation of *trans*-Cp*Re(PMe$_3$)$_2$(Ph)H (*trans*-7.1). A solution of the bis-trimethylphosphine dinitrogen complex **4.5** (50 mg, 0.10 mmol) in benzene (10 mL) was irradiated in a quartz tube for 10 min. An IR spectrum of the resulting yellow solution showed the total disappearance of the dinitrogen complex. After removal of the volatile materials under vacuum at room temperature, the remaining oily residue was redissolved in *ca.* 2 mL of benzene and carefully transferred to an air-

free neutral alumina column and eluted with benzene-hexane (2:1). Removal of the solvent under vacuum gave a yellow solid which was recrystallized from hexane at 195 K to provide ***trans*-7.1** as a pale yellow microcrystalline solid in 69% yield (38 mg, 0.069 mmol). ^{1}H NMR (benzene-d_6): δ -11.00 (t, 1H, ReH, J_{H-P} = 53.4 Hz), 1.37 (virtual doublet, 18H, PMe_3, J_{app} = 6.9 Hz), 1.70 (s, 15H, Cp*), 7.09 (m, 3H, C_6H_5), 7.71 (m, 2H, C_6H_5). ^{31}P{^{1}H} NMR (not metal hydride decoupled, benzene-d_6): δ -44.93 (d, PMe_3, J_{P-H} = 52.9 Hz). M.S. (EI, 12 eV): m/z 552 (M^+), 474 (M^+ - C_6H_6). Anal. Calcd: C, 47.90; H, 7.08. Found: C, 47.52; H, 7.37.

Thermal preparation of *trans*-Cp*Re(PMe_3)$_2$(Ph)H (*trans*-7.1). A solution of the bis-trimethylphosphine dinitrogen complex **4.5** (50 mg, 0.10 mmol) in benzene (10 mL) was refluxed for 2 h. An IR spectrum of the resulting yellow solution showed the total disappearance of the dinitrogen complex. The volatile materials were removed under vacuum at room temperature and the resulting oily residue was purified following the procedure described for the photochemical preparation of ***trans*-7.1**. Recrystallization from hexane at 195 K afforded ***trans*-7.1** as a pale yellow microcrystalline solid in 27% yield (15 mg, 0.027 mmol).

Photochemical preparation of *trans*-Cp*Re(PMe_3)(η^2-CH_2PMe_2)H (*trans*-7.2). A solution of the bis-trimethylphosphine dinitrogen complex **4.5** (50 mg, 0.10 mmol) in cyclohexane (10 mL) was irradiated in a quartz tube for 10 min. An IR spectrum of the resulting yellow solution showed the total disappearance of the dinitrogen complex. After removal of the volatile materials under vacuum at room temperature, the remaining oily residue was redissolved in *ca.* 5 mL of cyclohexane and filtered through a short neutral alumina column. Removal of the solvent under vacuum gave a pale yellow solid which was recrystallized from hexane at 195 K to provide ***trans*-7.2** in 61% yield (29 mg, 0.061 mmol). ^{1}H NMR (benzene-d_6): δ -12.04 (dd, 1H, ReH, J_{H-P} = 39.3, 32.1 Hz), -0.24 (apparent quartet, 1H, CH_2, J = 13.6 Hz), 0.09 (ddd, 1H,

CH_2, J_{H-H} = 14.0, J_{H-P} = 7.2, 1.9 Hz), 1.28 (d, 9H, PMe_3, J_{H-P} = 7.1 Hz), 1.31 (d, 3H, PMe_2, J_{H-P} = 9.8 Hz), 1.38 (d, 3H, PMe_2, J_{H-P} = 9.8 Hz), 1.95 (s, 15H, Cp*). $^{31}P\{^1H\}$ NMR (benzene-d_6): δ -39.23 (d, PMe_3, J_{P-P} = 19.6 Hz), -76.54 (d, η^2-CH_2PMe_2, J_{P-P} = 19.9 Hz). M.S. (EI, 12 eV): m/z 474 (M^+).

Reaction of *trans*-Cp*Re(PMe$_3$)(η^2-CH$_2$PMe$_2$)H (*trans*-7.2) with benzene. The cyclometalated complex ***trans*-7.2** was dissolved in benzene (5 mL) at room temperature under nitrogen and the solution was allowed to stir for 48 h. A ^1H NMR spectrum (benzene-d_6) of the solution acquired at the end of this time showed a mixture of the cyclometalated complex ***trans*-7.2** and the newly formed hydrido phenyl complex ***trans*-7.1**. Conversion from ***trans*-7.2** to ***trans*-7.1** was estimated to be *ca.* 90% by ^1H NMR spectroscopy.

Photochemical reaction of Cp*Re(dmpe)(N$_2$) in benzene. A solution of the bidentate phosphine dinitrogen complex **4.6** (50 mg, 0.10 mmol) in benzene (10 mL) was irradiated in a Pyrex tube for 10 min. An IR spectrum of the resulting yellow solution showed the total disappearance of the dinitrogen complex. Immediately after the irradiation, the volatile materials were removed under vacuum at room temperature and the resulting oily residue was taken up in benzene-d_6 without purification. Notably, a ^1H NMR spectrum of this solution exhibited two resonances in the metal hydride region. ^1H NMR (benzene-d_6): δ -12.91 (t, 1H, ReH, J_{H-P} = 54.7 Hz), -11.00 (broad doublet, 1H, ReH, J_{H-P} = 51.7 Hz), 1.55-1.27 (m, 32H, dmpe), 1.86 (s, 30H, Cp*), 7.07 (m, 3H, C_6H_5), 7.15 (m, 3H, C_6H_5), 7.74 (m, 2H, C_6H_5), 7.81 (m, 2H, C_6H_5). The limited spectroscopic evidence was assigned to the intermolecular activation products of benzene *trans*-Cp*Re(dmpe)(Ph)H (***trans*-7.3**) and the corresponding isomer *cis*-Cp*Re(dmpe)(Ph)H (***cis*-7.3**). Interestingly, a ^1H NMR spectrum acquired of the same solution less than 30 min later showed the total disappearance of the metal hydride resonances with the concomitant growth of resonances corresponding to free benzene.

Purification of the NMR solution by either solvent extraction or column chromatography failed to produce identifiable products.

Photochemical reaction of Cp*Re(PMe_3)$_2$(N_2) in hexane. A solution of the bis-trimethylphosphine dinitrogen complex **4.5** (50 mg, 0.10 mmol) in hexane (10 mL) was irradiated in a quartz tube for 10 min. An IR spectrum of the resulting yellow solution showed the total disappearance of the dinitrogen complex. Immediately after the irradiation, the volatile materials were removed under vacuum at room temperature and the resulting oily residue was taken up in acetone-d_6 without purification. A ^{1}H NMR spectrum of this solution showed the intramolecular C-H activation complex ***trans*-7.2** to be present as the major product from this reaction. However, the spectrum also exhibited a broad triplet in the metal hydride region (δ -10.89, J = 50 Hz) speculatively assigned to the primary C-H insertion product *trans*-Cp*Re(PMe_3)$_2$(*n*-C_6H_{13})H (***trans*-7.4**). Interestingly, a ^{1}H NMR spectrum acquired for the same solution 30 min later showed the total disappearance of the metal hydride triplet and only the presence of resonances due to ***trans*-7.2**. The solvent was then removed under vacuum at room temperature and the remaining oily residue was redissolved in *ca.* 5 mL of cyclohexane and filtered through a short neutral alumina column. Recrystallization from hexane at 195 K provided exclusively ***trans*-7.2** in 27% yield (13 mg, 0.027 mmol).

High pressure N_2 reaction of *trans*-Cp*Re(PMe_3)$_2$(Ph)H (*trans*-7.1). The intermolecular C-H activation product ***trans*-7.1** was dissolved in cyclohexane (10 mL) at room temperature under nitrogen. This solution was carefully transferred to a Parr bomb under nitrogen and pressurized to 1500 psi with oxygen-free nitrogen for 12 h at room temperature. An IR spectrum of the resulting solution showed the formation of the dinitrogen complex **4.5**. The solvent was then removed under vacuum and the remaining pale yellow solid was taken up in acetone-d_6. A GC analysis of the solvent remains

confirmed the presence of benzene. A ^{1}H NMR spectrum of the acetone-d_6 solution confirmed the quantitative conversion of ***trans*-7.1** to **4.5**.

High pressure N_2 reaction of *trans*-Cp*Re(PMe$_3$)(η^2-CH$_2$PMe$_2$)H (*trans*-7.2). This reaction was carried out following the same procedure described for the high pressure reaction of ***trans*-7.1**. Once again, an IR spectrum obtained after 8 h showed the presence of **4.5** and a ^{1}H NMR spectrum of the solution confirmed the quantitative conversion of ***trans*-7.2** to the dinitrogen complex **4.5**.

Reaction of *trans*-Cp*Re(PMe$_3$)$_2$(Ph)H (*trans*-7.1) with CHCl$_3$ or CDCl$_3$. The intermolecular C-H activation product ***trans*-7.1** (25 mg, 0.045 mmol) was dissolved in $CHCl_3$ or $CDCl_3$ (2 mL) at room temperature under nitrogen and the solution was allowed to stir for 2 h. A ^{1}H NMR spectrum ($CDCl_3$) of the solution showed the complete disappearance of ***trans*-7.1** and the presence of the dichloro complex *trans*-Cp*Re(PMe$_3$)$_2$Cl$_2$ (***trans*-7.5**) and benzene. The formation of benzene was verified by comparison to a ^{1}H NMR spectrum recorded for an authentic sample in $CDCl_3$. Removal of the solvent under vacuum and subsequent extraction with diethyl ether (3 x 20 mL) gave ***trans*-7.5** as a yellow-orange solid in 77% yield (19 mg, 0.035 mmol). ^{1}H NMR ($CDCl_3$): δ 1.45 (virtual doublet, 18H, PMe_3, J_{app} = 8.8 Hz), 1.65 (s, 15H, Cp*). M.S. (EI): m/z 546 (M^+, ^{35}Cl and ^{37}Cl), 544 (M^+, ^{35}Cl and ^{35}Cl).

Reaction of *trans*-Cp*Re(PMe$_3$)(η^2-CH$_2$PMe$_2$)H (*trans*-7.2) with CHCl$_3$ or CDCl$_3$. The cyclometalated complex ***trans*-7.2** (25 mg, 0.053 mmol) was dissolved in $CHCl_3$ or $CDCl_3$ (2 mL) at room temperature under nitrogen and the solution was allowed to stir for 2 h. A ^{1}H NMR ($CDCl_3$) of the solution showed the total disappearance of ***trans*-7.2** and presence of the dichloro complex *trans*-Cp*Re(PMe$_3$)$_2$Cl$_2$ (***trans*-7.5**). Removal of the solvent under vacuum and subsequent extraction with diethyl ether (3 x 20 mL) gave ***trans*-7.5** as a yellow-orange solid in 68% yield (20 mg, 0.036 mmol).

CHAPTER 8

Conclusion to the Thesis

8.1. Concluding Remarks and Thesis Summary

Although I cannot make the lofty claim of having solved the problem of chemical nitrogen fixation, the work described in this thesis has made significant inroads towards understanding the chemistry associated with metal-bound dinitrogen (MNN), the metal diazenido complex (MNNH) as modeled by its aryldiazenido analog (MNNAr), and their interconversion. The fruits of my graduate student labors are summarized below.

A general route to a series of cationic aryldiazenido complexes of general formula $[Cp^*Re(L_1)(L_2)(N_2Ar)][BF_4]$ ((a) Ar = *p*-C_6H_4OMe; L_1 = CO; L_2 = PMe_3 (**2.4**), PEt_3 (**2.5**), PPh_3 (**2.6**), PCy_3 (**2.7**), $P(OMe)_3$ (**2.8**), or PCage (**2.9**), (b) Ar = *p*-C_6H_4OMe; L_1 = L_2 = CO (**2.2**), PMe_3 (**2.11**), PEt_3 (**2.12**), or $P(OMe)_3$ (**2.14**), and (c) Ar = C_6H_5; L_1 = L_2 = CO (**2.15**) or PMe_3 (**2.17**)) and to the cationic bidentate aryldiazenido complex $[Cp^*Re(dmpe)(p\text{-}N_2C_6H_4OMe)][BF_4]$ (**2.13**) was developed. This route was of utmost importance since it (i) allowed the synthesis of complexes whose ancillary ligands could be tuned electronically as well as sterically and (ii) it also provided a means of introducing a ^{15}N label specifically at the rhenium-bound nitrogen atom (N_α) or the terminal nitrogen atom (N_β) so that the chemistry exhibited by these aryldiazenido complexes or their derivatives could be investigated by ^{15}N NMR spectroscopy.

An X-ray structural and variable temperature solution ^1H, $^{31}P\{^1H\}$, and $^{13}C\{^1H\}$ NMR study of complexes **2.2**, **2.4-2.9**, **2.11**, and **2.14** provided the first unambiguous examples of stereochemical non-rigidity of a singly-bent aryldiazenido ligand. These complexes were shown to have ground state structures in the solid state and in solution in which the aryl ring of the singly-bent aryldiazenido ligand orients with its molecular

plane orthogonal to the plane bisecting the L_1ReL_2 angle. Furthermore, the aryldiazenido ligand was shown to undergo a conformational isomerization which interconverted the conformer in which the aryl group is oriented towards L_1 with its partner in which it is oriented towards L_2. The relative populations of the two conformers were influenced by the steric bulk of the co-ligands; the major conformer arising from the aryldiazenido group adopting a position adjacent to the less sterically demanding ligand. The barriers to isomerization of the aryldiazenido group were also demonstrated to be dependent on the electronic properties of the co-ligands; the better electron donating ligands raising the activation barrier.

A series of neutral dinitrogen complexes of the type $Cp'Re(L_1)(L_2)(N_2)$ ((a) Cp' = Cp; $L_1 = L_2 = CO$ (**4.1**), (b) Cp' = Cp*; $L_1 = CO$; $L_2 = PMe_3$ (**4.3**) or $P(OMe)_3$ (**4.4**), and (c) Cp' = Cp*; $L_1 = L_2 = CO$ (**4.2**), PMe_3 (**4.5**), dmpe (**4.6**), or $P(OMe)_3$ (**4.7**)) were synthesized from the corresponding cationic aryldiazenido complexes. This conversion, which I believe is unique to rhenium systems, was shown to be consistent with two different mechanisms. First, reaction of the cationic dicarbonyl aryldiazenido complex **2.2** with $NaBH_4$ results in initial H^- attack at the rhenium-bound nitrogen atom to give the neutral aryldiazene complex $Cp^*Re(CO)_2(p\text{-}NHNC_6H_4OMe)$ (**4.10**), which then eliminates anisole to form the respective neutral dinitrogen complex **4.2**. Second, treatment of any of the cationic aryldiazenido complexes **2.1**, **2.2**, **2.4**, **2.8**, **2.11**, **2.13**, and **2.14** with a suitable reducing agent leads tc the initial transfer of one-electron from the reducing agent to the cationic aryldiazenido complex to give a neutral 19-electron intermediate. Once formed this unstable intermediate then decomposes to produce the desired dinitrogen complex and the *p*-methoxyphenyl radical which then abstracts a hydrogen from the solvent to give anisole. This one-electron reduction mechanism was corroborated by cyclic voltammetry (CV), scanning electrochemical microscopy (SECM), and controlled potential electrolysis (CPE).

Evidence to support the occurrence of a side-on (η^2) bonded dinitrogen species was obtained from a variable temperature and time-dependent ^{15}N NMR study of the dinitrogen complexes Cp'Re(CO)(L)($^{15}N^{14}N$) ((a) Cp' = Cp; L = CO (**4.1-$^{15}N_\alpha$**) and (b) Cp' = Cp*; L = CO (**4.2-$^{15}N_\alpha$**), PMe_3 (**4.3-$^{15}N_\alpha$**), or $P(OMe)_3$ (**4.4-$^{15}N_\alpha$**)) which were specifically labeled at the rhenium-bound nitrogen atom (N_α) with ^{15}N. Scrambling of the ^{15}N label equally between the N_α and N_β sites was shown to occur at room temperature in the case of **4.1-$^{15}N_\alpha$** and **4.2-$^{15}N_\alpha$** or at elevated temperatures in the case of **4.3-$^{15}N_\alpha$** and **4.4-$^{15}N_\alpha$** so that equimolar amounts of the $^{15}N_\alpha$ and $^{15}N_\beta$ labeled molecules result. For all the complexes examined, the scrambling of the ^{15}N label was shown to proceed by a remarkable intramolecular, non dissociative process involving an end-to-end rotation of the rhenium-bound dinitrogen ligand *via* the elusive side-on (η^2) bonded dinitrogen species. The barrier for this linkage isomerization, which was measured for **4.1-$^{15}N_\alpha$** and **4.2-$^{15}N_\alpha$**, was found to be lowered significantly when the Cp ligand was replaced by its methylated analog Cp*.

The reactivity of rhenium dinitrogen complexes toward protonation was also explored. The bis-trimethylphosphine dinitrogen complex $Cp^*Re(PMe_3)_2(N_2)$ (**4.5**) was prone to protonation at the metal center but not at the desired rhenium-bound dinitrogen ligand. The protonation reaction appeared to be independent of the acid used since treatment of **4.5** with CF_3COOH, $HBF_4{\cdot}OEt_2$, or CF_3SO_3H afforded the respective rhenium hydrido dinitrogen complexes *cis*-$[Cp^*ReH(N_2)(PMe_3)_2][CF_3COO]$ (***cis*-6.1**), *cis*-$[Cp^*ReH(N_2)(PMe_3)_2][BF_4]$ (***cis*-6.2**), and *cis*-$[Cp^*ReH(N_2)(PMe_3)_2][CF_3SO_3]$ (***cis*-6.3**) at 213 K and these complexes isomerized to their corresponding *trans* isomers as the temperature was raised to 273 K. Interestingly, the *trans* isomers were found to be thermally unstable at room temperature, although ***trans*-6.1** was observed to be significantly more stable than its analogs ***trans*-6.2** and ***trans*-6.3** inferring that the

counter anion may play a role in stabilizing these cationic rhenium hydrido dinitrogen complexes.

In addition to investigating the rhenium dinitrogen complexes for their susceptibility to protonation, the demonstrated propensity of these dinitrogen complexes to extrude the N_2 ligand was utilized to activate C-H bonds as demonstrated by reactions of the rhenium dinitrogen complexes $Cp^*Re(PMe_3)_2(N_2)$ (**4.5**) and $Cp^*Re(dmpe)(N_2)$ (**4.6**) in saturated and unsaturated hydrocarbons. Under photochemical or *thermal* conditions complex **4.5** readily loses the N_2 ligand, and the 16-electron intermediate then produced reacts with C-H bonds; intermolecularly in benzene to give the hydrido phenyl complex *trans*-$Cp^*Re(PMe_3)_2(Ph)H$ (***trans*-7.1**) or intramolecularly in cyclohexane to form the cyclometalated product *trans*-$Cp^*Re(PMe_3)(\eta^2\text{-}CH_2PMe_2)H$ (***trans*-7.2**). Interestingly, irradiation of **4.5** in hexane produces the primary C-H insertion product *trans*-$Cp^*Re(PMe_3)_2(n\text{-}C_6H_{13})H$ (***trans*-7.4**) as well as the cyclometalated complex ***trans*-7.2**. These results demonstrate that the rhenium system, despite lowered inter/intra selectivity, is more selective to intermolecular activation of hydrocarbons; aromatic and primary C-H bonds are intermolecularly activated, secondary C-H bonds are not. The sterically demanding rhenium center is believed to be responsible for the observed selectivity.

References

1. Raoel, S. R.; Navidi, M. H. In *Chemistry*; West: New York, 1990; Chapt. 9, p. 363.
2. Cotton, F. A.; Wilkinson, G. In *Advanced Inorganic Chemistry*; Wiley: New York, 1980; Chapt. 13.
3. Leigh, J. *New Scientist* **1990**, *10*, 55.
4. Bortels, H. *Arch. Mikrobiol.* **1930**, *1*, 333.
5. Carnahan, J. E.; Mortenson, L. E.; Mower, H. F.; Castle, J. E. *Biochim. Biophys. Acta*, **1960**, *44*, 520.
6. In *Molybdenum Enzymes*; Spiro, T. G., Ed.;Wiley: New York, 1985.
7. (a) Bishop, P. E.; Jarlenski, D. M. L.; Hetherington, D. R. Proc. *Natl. Acad. Sci. USA* **1980**, *77*, 7342. (b) Bishop, P. E. *Trends Biol. Sci.* **1986**, *11*, 225.
8. Chisnell, J. R.; Premakumar, R.; Bishop, P. E. *J. Bacteriol.* **1988**, *170*, 27.
9. Sellmann, D. *Angew. Chem. Int. Ed. Engl.* **1993**, *32*, 64.
10. Shah, V. K.; Brill, W. J. Proc. *Natl. Acad. Sci. USA* **1977**, *74*, 3249.
11. Müller, A.; Knüttel, K.; Krickemayer, E.; Hildebrand, A.; Bögge, M.; Schneider, K.; Armatage, A. *Naturwissenschaften* **1991**, *78*, 460, and references therein.
12. Bolin, J. T.; Ronco, A. E.; Mortenson, L. E.; Morgan, T. V.; Williamson, M.; Xuong, N.-H. In *Nitrogen Fixation: Achievements and Objectives, Proc. 8th Int. Congr. Nitrogen Fixation*; Grashoff, P. M., Roth, L. E., Stacey, G., Newton, W. E., Eds.; Chapman and Hall: New York, 1990; p. 117-124.
13. (a) Georgiadis, M. M.; Komiya, H.; Chakrabarti, P.; Woo, D.; Kornuc, J. J.; Rees, D. C. *Science* **1992**, *257*, 1653. (b) Kim, J.; Rees, D. C. *Science* **1992**, *257*, 1677. (c) Kim, J.; Rees, D. C. *Nature* **1992**, *360*, 553.
14. Burgess, B. K. *Chem. Rev.* **1990**, *90*, 1377.

15. (a) Averill, B. A. *Struct. Bond.* **1983**, *53*, 59. (b) Coucouvanis, D. *Acc. Chem. Res.* **1991**, *24*, 1. (c) Ciurli, S.; Holm, R. H. *Inorg. Chem.* **1989**, *28*, 1685.

16. Richards, R. L. In *Biology and Biochemistry of Nitrogen Fixation*; Dilworth, M. J. and Glenn, A. R., Eds.; Elsevier: New York, 1991; Chapt. 4.

17. Orme-Johnson, W. H. *Science* **1992**, *257*, 1639.

18. (a) Evans, W. J.; Ulibarri, T. A.; Ziller, J. W. *J. Am. Chem. Soc.* **1988**, *110*, 6877. (b) Fryzuk, M. D.; Haddad, T. S.; Rettig, S. J. *J. Am. Chem. Soc.* **1990**, *112*, 8185.

19. Orgel, L. E. In *An Introduction to Transition Metal Chemistry*; Methuen: London, 1960; p. 137.

20. Leigh, G. J. *Sci. Prog.* **1989**, *73*, 389.

21. Vol'pin, M. E.; Shur, V. B. *Doklady Akad. Nauk S.S.S.R.* **1964**, *156*, 1102.

22. Allen, A. D.; Senoff, C. V. *J. Chem. Soc., Chem. Commun.* **1965**, 621.

23. Henderson, R. A.; Leigh, G. J.; Pickett, C. J. *Adv. Inorg. Chem. Radiochem.* **1983**, *27*, 197.

24. (a) Barclay, J. E.; Hills, A.; Hughes, D. L.; Leigh, G. J.; MacDonald, C. J. *J. Chem. Soc., Dalton Trans.* **1990**, 2503. (b) Chatt, J.; Heath, G. A.; Richards, R. L. *J. Chem. Soc., Dalton Trans.* **1974**, 2074.

25. Anderson, S. N.; Hughes, D. L.; Richards, R. L. *J. Chem. Soc., Dalton Trans.* **1986**, 1591.

26. (a) Richards, R. L. *Chemistry in Britain* **1988**, 133. (b) Adachi, T.; Nabyoshi, S.; Tatsuo, U.; Manabu, K.; Yoshida, T. *J. Chem. Soc., Chem. Commun.* **1989**, 1320.

27. Yoshida, T; Adachi, T.; Kaminaka, M; Ueda, T. *J. Am. Chem. Soc.* **1988**, *110*, 4872.

28. Anderson, S. N.; Hughes, D. L.; Richards, R. L. *J. Chem. Soc., Dalton Trans.* **1986**, 245.

29. Rocklage, S. M.; Turner, H. W.; Fellmann, J. D.; Schrock, R. R. *Organometallics* **1982**, *1*, 703.

30. Mazio, R.; Sgamellotti, A.; Tarantelli, F.; Floriani, C.; Cederbaum, L. S. *J. Chem. Soc., Dalton Trans.* **1989**, 33.

31. (a) Robinson, P. R.; Moorehead, E. L.; Weathers, B. J.; Ufkes, E. A.; Vickrey, T. M.; Schrauzer, G. N. *J. Am. Chem. Soc.* **1977**, *99*, 3657. (b) Weathers, B. J.; Grate, J. H.; Strampach, N. A.; Schrauzer, G. N. *J. Am. Chem. Soc.* **1979**, *101*, 925. (c) Zones, S. I.; Vickrey, T. M.; Palmer, J. G.; Schrauzer, G. N. *J. Am. Chem. Soc.* **1976**, *98*, 7289.

32. (a) Jeffery, J.; Lappert, M. F.; Riley, P. I. *J. Organomet. Chem.* **1979**, *151*, 25. (b) Gynane, M. J. S.; Jeffery, J.; Lappert, M. F. *J. Chem. Soc., Chem. Commun.* **1978**, 34.

33. Chatt, J.; Dilworth, J. R.; Richards, R. L. *Chem. Rev.* **1978**, *78*, 589.

34. Chatt, J.; Leigh, G. J. *Quart. Rev. Chem. Soc.* **1972**, *1*, 121.

35. (a) Dilworth, J. R.; Richards, R. L. In *Comprehensive Organometallic Chemistry*; Wilkinson, G., Stone, F. G. A., Abel. E. W., Eds.; Pergamon Press: Oxford, 1982; Vol. 5, p. 1073. (b) Pickett, C. J.; Cate, K.; McDonald, C. J.; Mohammed, M. Y.; Ryder, K. S.; Talarmin, J. In *Nitrogen Fixation: Hundred Years After*; Bothe, H., de Bruijn, F. J., Newton, W. E., Eds.; G. Fisher: New York, 1988; p. 51.

36. (a) Anderson, S. N.; Chatt, J.; Fakley, M. E.; Richards, R. L. *J. Chem. Soc., Dalton Trans.* **1981**, 1973. (b) George, T. A.; Kocson, C. M.; Tisdale, R. C.; Gebrayes, K.; Zubieta, J. *Inorg. Chem.* **1986**, *25*, 405. (c) Galindo, A.; Hills, A.; Hughes, D. L.; Richards, R. L. *J. Chem. Soc., Chem. Commun.* **1987**, 1815.

37. (a) Henderson, R. A. *J. Chem. Soc., Chem. Commun.* **1987**, 1670. (b) Dilworth, J. R.; Donovan-Mtunzi, S. D.; Kan, C. T.; Richards, R. L.; Mason, J. *Inorg. Chim. Acta.* **1981**, *53*, L161,

38. (a) Chatt, J.; Pearman, A. J.; Richards, R. L. *J. Chem. Soc., Dalton Trans.* **1976**, 1520. (b) Chatt, J.; Kan, C. T.; Leigh, G. H.; Pickett, C. J.; Stanley, D. R. *J. Chem. Soc., Dalton Trans.* **1980**, 2032.

39. Takahashi, T.; Mizobe, Y.; Sato, M.; Uchida, Y.; Hidai, M. *J. Am. Chem. Soc.* **1980**, *102*, 7461.

40. Dobinson, G. C.; Mason, R.; Robertson, G. B.; Ugo, R.; Conti, F.; Morelli, D.; Cenini, S.; Bonati, F. *J. Chem. Soc., Chem. Commun.* **1967**, 739.

41. Glassman, T. E.; Liu, A. H.; Schrock, R. R. *Inorg. Chem.* **1991**, 30, 4723.

42. Baumann, J. A.; Bossard, G. E.; George, T. A.; Howell, D. B.; Koczon, L. M.; Lester, R. K.; Noddings, C. M. *Inorg. Chem.* **1985**, *24*, 3568.

43. Thorneley, R. N. F.; Lowe, D. J. In *Molybdenum Enzymes*; Spiro, T. G., Ed.; Wiley: London, 1985; p. 221.

44. Sellmann, D.; Soglowek, W.; Knock, F.; Moll, M. *Angew. Chem. Int. Ed. Engl.* **1989**, *28*, 1271.

45. Schrauzer, G. N. In *New Trends in the Chemistry of Nitrogen Fixation*; Chatt, J., Pina, L., Richards, R. L., Eds.; Academic Press: London, 1980; p. 103.

46. Schrock, R. R.; Glassman, T. E.; Vale, M. G. *J. Am. Chem. Soc.* **1991**, *113*, 725.

47. Glassman, T. E.; Vale, M. G.; Schrock, R. R. *J. Am. Chem. Soc.* **1992**, *114*, 8098.

48. Schrock, R. R.; Glassman, T. E.; Vale, M. G.; Kol, M. *J. Am. Chem. Soc.* **1993**, *115*, 1760.

49. (a) Sutton, D. *Chem. Soc. Rev.* **1975**, *4*, 443. (b) Sutton, D. *Chem. Rev.* **1993**, *93*, 995.

50. (a) Rayner-Canham, G. W.; Sutton, D. *Can. J. Chem.* **1971**, *49*, 3994. (b) Einstein, F. W. B.; Gilchrist, A. B.; Rayner-Canham, G. W.; Sutton, D. *J. Am. Chem. Soc.* **1972**, *94*, 645. (c) Gilchrist, A. B.; Rayner-Canham, G. W.; Sutton, D. *Nature* **1972**, *235*, 42.

51. Barrientos-Penna, C. F.; Campana, C. F.; Einstein, F. W. B; Jones, T.; Sutton, D.; Tracey, A. S. *Inorg. Chem.* **1984**, *23*, 363.

52. Johnson, B. F. G.; Haymore, B. L.; Dilworth, J. R. In *Comprehensive Coordination Chemistry*; Wilkinson, G., Gillard, R.D., McCleverty, J. A., Eds.; Pergamon Press: Oxford, U.K., 1987; Vol. 2, p. 130.

53. King, R. B.; Bisnette, M. B. *J. Am. Chem. Soc.* **1964**, *86*, 5694.

54. Parshall, G. W. *J. Am. Chem. Soc.* **1965**, *87*, 2133.

55. For reviews of organodiazenido complexes see:
(a) Dilworth, J. R. *Coord. Chem. Rev.* **1976**, *21*, 29. (b) Bruce, M. I.; Goodall, B. L. In *The Chemistry of Hydrazo, Azo and Azoxy Groups*; Patai, S., Ed.; Wiley: London, 1975; Part 1, Chapt. 9.

56. Barrientos-Penna, C. F.; Einstein, F. W. B.; Jones, T.; Sutton, D. *Inorg. Chem.* **1982**, *21*, 2578.

57. Barrientos-Penna, C. F.; Klahn-Oliva, A. H.; Sutton, D. *Organometallics* **1985**, *4*, 367.

58. Barrientos-Penna, C. F.; Gilchrist, A. B.; Klahn-Oliva, A. H.; Hanlan, A. J. L.; Sutton, D. *Organometallics* **1985**, *4*, 478.

59. Klahn-Oliva, A. H.; Sutton, D. *Organometallics* **1989**, *8*, 198.

60. (a) Patton. A. T.; Strouse, C. E.; Knobler, C. B.; Gladysz, J. A. *J. Am. Chem. Soc.* **1983**, *105*, 5804. (b) Tam, W.; Lin, G. Y.; Wong, W. K.; Kiel, W. A.; Wong, V. K.; Gladysz, J. A. *J. Am. Chem. Soc.* **1982**, *104*, 141.

61. Klahn-Oliva, A. H. Ph.D. Thesis, Simon Fraser University, 1986.

62. Koelle, U. *J. Organomet. Chem.* **1978**, *155*, 53.

63. Webb, M. J.; Graham, W. A. G. *J. Organomet. Chem.* **1975**, *93*, 119.

64. Casey, C. P.; Marder, S. R.; Colbron, R. E.; Goodson, P. A. *Organometallics* **1986**, *5*, 199.

65. Catheline, D.; Astruc, D. *J. Organomet. Chem.* **1984**, *272*, 417.

66. (a) Rouschias, G.; Wilkinson, G. *J. Chem. Soc. A* **1967**, 993. (b) Butcher, A. V.; Chatt, J.; Leigh, G. J.; Richards, P. L. *J. Chem. Soc., Dalton Trans.* **1972**, 1064.

67. Hoyano, J. K.; Graham, W. A. G. *J. Chem. Soc., Chem. Commun.* **1982**, 27.

68. Tolman, C. A. *Chem. Rev.* **1977**, *77*, 313.

69. Mason, J. *Chem. Rev.* **1981**, *81*, 205.

70. Bodner, G. M.; May, M. P.; McKinney, L. E. *Inorg. Chem.* **1980**, *19*, 1951.

71. Muetterties, E. A. In *Transition Metal Hydrides*; M. Dekker: New York, 1971; p. 85.

72. (a) Tilley, T. D.; Grubbs, R. H.; Bercaw, J. E. *Organometallics* **1984**, *3*, 274. (b) Straus, D. A.; Grumbine, S. D.; Tilley, T. D. *J. Am. Chem. Soc.* **1990**, *112*, 7801.

73. Bergman, R. G.; Seidler, P. F.; Wenzel, T. T. *J. Am. Chem. Soc.* **1985**, *107*, 4358.

74. Musher, J. I.; Corey, E. J. *Tetrahedron* **1962**, *18*, 791.

75. Jenkins, J. M.; Shaw, B. L. *J. Chem. Soc. A* **1966**, 1407.

76. Garrou, P. E. *Chem. Rev.* **1981**, *81*, 229.

77. Heitsch, C. W.; Verkade, J. G. *Inorg. Chem.* **1962**, *1*, 392.

78. Saltzman, H.; Sharefkin, J. G. In *Organic Syntheses*; Wiley: New York, 1973; Collect. Vol. V, p. 658.

79. King, R. B.; Reimann, R. H. *Inorg. Chem.* **1976**, *15*, 179.

80. Roe, A. In *Organic Reactions*; Adams, R., Ed.; Wiley: New York, 1949; Vol. V, p. 193.

81. Klahn-Oliva, A. H. unpublished results.

82. Krogsrud, S.; Ibers, J. A. *Inorg. Chem.* **1975**, *14*, 2298.

83. Cobbledick, R. E.; Einstein, F. W. B.; Farrell, N.; Gilchrist, A. B.; Sutton, D. *J. Chem. Soc., Dalton Trans.* **1977**, 373.

84. Gaughan, A. P.; Haymore, B. L.; Ibers, J. A.; Myers, W. H.; Nappier, T. E.; Meek, D. W. *J. Am. Chem. Soc.* **1973**, *95*, 6859.

85. (a) Dilworth, J. R.; Latham, I. A.; Leigh, G. J.; Huttner, G.; Jibril, I. *J. Chem. Soc., Chem. Commun.* **1983**, 1368. (b) Latham, I. A.; Leigh, G. J.; Huttner, G.; Jibril, I. *J. Chem. Soc., Dalton Trans.* **1986**, 377.

86. (a) Mason, R.; Thomas, K. M.; Zubieta, J. A.; Douglas, P. G.; Galbraith, A. R.; Shaw, B. L. *J. Am. Chem. Soc.* **1974**, *96*, 260. (b) Dilworth, J. R.; Harrison, S. A.; Walton, D. R. M.; Schweda, E. *Inorg. Chem.* **1985**, *24*, 2594. (c) Chatt, J.; Fakley, M. E.; Hitchcock, P. B.; Richards, R. L.; Luong-Thi, N. T. *J. Chem. Soc., Dalton Trans.* **1982**, 345. (d) Nicholson, T.; Zubieta, J. *Inorg. Chim. Acta.* **1985**, *100*, L35. (e) Nicholson, T.; Lombardi, P.; Zubieta, J. *Polyhedron* **1987**, *6*, 1577.

87. Barrientos-Penna, C. F.; Einstein, F. W. B.; Jones, T.; Sutton, D. *Inorg. Chem.* **1985**, *24*, 632.

88. Hubbard, J. L.; Kimball, K. L.; Burns, R. M.; Sum, V. *Inorg. Chem.* **1992**, *31*, 4224.

89. Consiglio, G.; Bangerter, F.; Darpin, C. *Organometallics* **1984**, *3*, 1446.

90. Harris, R. K. In *Nuclear Magnetic Resonance Spectroscopy*; Pitman: Massachusetts, 1983; p. 185.

91. Kost, D.; Carlson, E. H.; Raban, M. *J. Chem. Soc., Chem. Commun.* **1971**, 656.

92. Klier, D. A.; Binsch, G. *DNMR3*: A computer program for the calculation of complex exchange-broadened NMR spectra. Modified version for spin systems exhibiting magnetic equivalence or symmetry. Quantum Chemistry Program Exchange, Program 165, Indiana University (1970).

93. Sandstrom, J. *Dynamic NMR Spectroscopy*; Academic Press: London, 1982; Chapt. 7.

94. (a) Binsch, G. In *Dynamic Nuclear Magnetic Resonance Spectroscopy*; Jackman, L. M.; Cotton, F. A., Eds.; Academic Press: New York, 1975; Chapt. 3. (b) Davies, O. L.; Goldsmith, P. L. *Statistical Methods in Research and Production*; Longman: London, 1976; p.438.

95. Gay, I. D. *LSP*: A computer program which plots linear least-squares polynomials. Simon Fraser University.

96. For a comprehensive list of structures to 1986 see: ref. 52.

97. (a) Ferguson, G.; Ruhl, B. L.; Parvez, M.; Lalor, F. J.; Deane, M. E. *J. Organomet. Chem.* **1990**, *381*, 357. (b) Deane, M. E.; Lalor, F. J.; Ferguson, G.; Ruhl, B. L.; Parvez, M. *J. Organomet. Chem.* **1990**, *381*, 213.

98. (a) Barrientos-Penna, C. F.; Einstein, F. W. B.; Sutton, D.; Willis, A. C *Inorg. Chem.* **1980**, *19*, 2740. (b) Barrientos-Penna, C. F.; Sutton, D. *J. Chem. Soc., Chem. Commun.* **1980**, 111.

99. Avitabile, G.; Ganis, P.; Nemiroff, M. *Acta. Crystallogr., Sect. B* **1971**, *27*, 725.

100. (a) Einstein, F. W. B.; Yan, X.; Sutton, D. *J. Chem. Soc., Chem. Commun.* **1990**, 1466. (b) Yan, X and Sutton, D. manuscript in preparation.

101. *PCMODEL* is available from Serena Software, Bloomington, IN. See: Gajewski, J. J.; Gilbert, K. E.; McKelvey, I. In *Advances in Molecular Modelling*; Liotta, D., Ed.; JAI Press: Greenwich, CT, 1990; Vol. 2, p.65.

102. (a) Luck, L. A.; Elcesser, W. L.; Hubbard, J. L.; Bushweller, C. H. *Magn. Reson. Chem.* **1989**, *27*, 488. (b) Bushweller, C. H. *J. Am. Chem. Soc.* **1969**, *91*, 1968. (c) Jensen, F. R.; Bushweller, C. H. *J. Am. Chem. Soc.* **1969**, *91*, 3223. (d) Bushweller, C. H.; Golini, J.; Rao, G. U.; O'Neil, J. W. *J. Am. Chem. Soc.* **1970**, *92*, 3055. (e) Bushweller, C. H.; O'Neil, J. W.; Halford, M. H.; Bissett, F. H. *J. Am. Chem. Soc.* **1971**, *93*, 1471.

103. Senn, D. R.; Wong, A.; Patton, A. T.; Marsi, M.; Strouse, C. E.; Gladysz, J. A. *J. Am. Chem. Soc.* **1988**, *10*, 6096.

104. (a) Herrmann, W. A.; Biersack, H. *Chem. Ber.* **1977**, *110*, 896. (b) Hillhouse, G. L.; Haymore, B. L.; Herrmann, W. A. *Inorg. Chem.* **1979**, *18*, 2423.

105. (a) Lindner, E.; Mockel, A.; Mayer, H. A.; Kuhbauch, H.; Fawzi, R.; Steimann, M. *Inorg. Chem.* **1993**, *32*, 1266. (b) Koe, J. R.; Tobita, H.; Suzuki, T.; Ogino, H. *Organometallics* **1992**, *11*, 150.

106. (a) Howe, J. J.; Pinnavaia, T. J. *J. Am. Chem. Soc.* **1970**, *92*, 7342. (b) Pinnavaia, T. J.; Lott, A. L. *Inorg. Chem.* **1971**, *10*, 1388. (c) Hutchison, J. R.; Gordon, J. G.; Holm, R. H. *Inorg. Chem.* **1971**, *10*, 1004. (d) Case, D. A.; Pinnavaia, T. J. *Inorg. Chem.* **1971**, *10*, 482.

107. Berg, U.; Sjöstrand, U. *Org. Magnet. Res.* **1978**, *11*, 555.

108. (a) Harris, R. K. In *Nuclear Magnetic Resonance Spectroscopy*; Pitman: Massachusetts, 1983; p. 201. (b) Sandström, J. *Dynamic NMR Spectroscopy*; Academic Press: London, 1982; Chapt. 6. (c) Berg, U.; Sandström, J.; Jennings, W. B.; Randall, D. *J. Chem. Soc., Perkin II* **1980**, 949; *Tetrahedron Lett.* **1976**, 3197.

109. Carillo, D.; Gouzerh, P; Jeannin, Y. *Nouv. J. Chim.* **1985**, *9*, 749.

110. See ref. 97(a) and references cited therein.

111. Bank, S.; Liu, S.; Shaikh, S. N.; Sun, X.; Zubieta, J.; Ellis, P.D. *Inorg. Chem.* **1988**, *27*, 3535.

112. Bishop, E. O.; Butler, G.; Chatt, J.; Dilworth, J. R.; Leigh, G. J.; Orchard, D.; Bishop, M. W. *J. Chem. Soc., Dalton Trans.* **1978**, 1654.

113. Jackman, L. M. In *Dynamic Nuclear Magnetic Resonance Spectroscopy*; Jackman, L. M., Cotton, F. A., Eds.; Academic Press: New York, 1975; p. 244.

114. (a) Curtin, D. Y.; Grubbs, E. J.; McCarty, C. G. *J. Am. Chem. Soc.* **1966**, *88*, 2775. (b) Marullo, N. P.; Wagener, E. H. *Tetrahedron Lett.* **1969**, 2555.

115. (a) Raban, *J. Chem. Soc., Chem. Commun.* **1970**, 1415. (b) Lehn, J. M.; Munsch, B.; Millie, P. *Theor. Chim. Acta* **1970**, *16*, 351.

116. Powell, K. R.; Perez, P. J.; Luan, L.; Feng, S. G.; White, P. S.; Brookhart, M.; Templeton, J. L. *Organometallics* **1994**, *13*, 1851.

117. Erker, G.; Fromberg, W.; Kruger, C.; Raabe, E. *J. Am. Chem. Soc.* **1988**, *110*, 2400.

118. Dormond, A.; Aaliti, A.; Elbouadili, A.; Moise, C. *J. Organomet. Chem.* **1987**, *329*, 187.

119. Van Geet, A. L. *Anal. Chem.* **1970**, *42*, 679.

120. Chatt, J.; Dilworth, J. R.; Leigh, G. L. *J. Chem. Soc., Chem. Commun.* **1969**, 687.

121. Chatt, J.; Dilworth, J. R.; Leigh, G. L. *J. Chem. Soc., Dalton Trans.* **1973**, 612.

122. Tully, M. E.; Ginsberg, A. D. *J. Am. Chem. Soc.* **1973**, *95*, 2042.

123. Sellmann, D. *J. Organomet. Chem.* **1972**, *36*, C27.

124. Sellmann, D.; Kleinschmidt, E. *Z. Naturforsch., B: Anorg. Chem., Org. Chem.* **1977**, *32B*, 795.

125. Dong, D. F.; Hoyano, J. K.; Graham, W. A. G. *Can. J. Chem.* **1981**, *59*, 1455.

126. Nesmeyanov, A. N.; Kolobova, N. E.; Makarov, Y. V.; Animisov, K. N. *Bull. Acad. Sci. USSR. Div. Chem. Sci.* **1969**, 1687.

127 Thorn, D. L.; Tulip, T. H.; Ibers, J. A. *J. Chem. Soc., Dalton Trans.* **1979**, 2022.

128 Richards, T. C.; Bard, A. J.; Cusanelli, A.; Sutton, D. *Organometallics* **1994**, *13*, 757.

129 Rudolph, M.; Reddy, D. P.; Feldberg, S. W. *Anal. Chem.* submitted for publication; DigiSim, Bioanalytical Systems, Inc., West Lafayette, IN.

130. (a) Bard, A. J.; Fan, F.-R. F.; Pierce, D. T.; Unwin, P. R.; Wipf, D. O.; Zhou, F. *Science* **1991**, *254*, 68. (b) Bard, A. J.; Fan, F.-R. F.; Mirkin, M. V. In *Electroanalytical Chemistry*; Bard, A. J., Ed.; Marcel Dekker: New York, 1993; Vol. 18, p. 243.

131. Zhou, F.; Unwin, P. R.; Bard, A. J. *J. Phys. Chem.* **1992**, *96*, 4917.

132. Unwin, P. R.; Bard, A. J. *J. Phys. Chem.* **1991**, *95*, 7814.

133. (a) Wightman, R. M. *Science* **1988**, *240*, 415. (b) Wightman, R. M.; Wipf, D. O. In *Electroanalytical Chemistry*; Bard, A. J., Ed.; Marcel Dekker: New York, 1988; Vol. 15, p 267.

134. Wipf, D. O.; Bard, A. J. *J. Electrochem. Soc.* **1991**, *138*, 469.

135. Kwak, J.; Bard, A. J. *Anal. Chem.* **1989**, *61*, 1794.

136. Bard, A. J.; Fan, F. R. F.; Kwak, J.; Lev, O. *Anal. Chem.* **1989**, *61*, 132.

137. Southampton Electrochemistry Group In *Instrumental Methods in Electrochemistry*; Kemp, T. J., Ed.; Wiley: New York, 1985, p 44.

138. (a) Klahn-Oliva, A. H.; Sutton, D. *Organometallics* **1984**, *3*, 1313. (b) Herrmann, W. A.; Serrano, R; Bock, H. *Angew. Chem. Int. Ed. Engl.* **1984**, *23*, 383.

139. Sellmann, D.; Maisel, G. *Z. Naturforsch.* **1972**, 425.

140. Gladysz, J. A. *Adv. Organomet. Chem.* **1982**, *20*, 1.

141. Parshall, G. W. *J. Am. Chem. Soc.* **1967**, *89*, 1822.

142. Haymore, B. L.; Ibers, J. A. *J. Am. Chem. Soc.* **1975**, *97*, 5369.

143. Smith, M. R.; Hillhouse, G. L. *J. Am. Chem. Soc.* **1988**, *110*, 4066.

144. Einstein, F. W. B.; Sutton, D.; Tyers, K. G. *Inorg. Chem.* **1987**, *26*, 111.

145. (a) Sweet, J. R.; Graham, W. A. G. *J. Organomet. Chem.* **1979**, *173*, C9. (b) Sweet, J. R.; Graham, W. A. G. *J. Am. Chem. Soc.* **1982**, *104*, 2811.

146. Haymore, B. L.; Ibers, J. A. *Inorg. Chem.* **1975**, *14*, 2784.

147. Connelly, N. G.; Demidowicz, Z. *J. Organomet. Chem.* **1974**, *73*, C31.

148. Herrmann, W. A.; Albach, R. W.; Behm, J. *J. Chem. Soc., Chem. Commun.* **1991**, 367.

149. Bard, A. J.; Faulkner, L. R. In *Electrochemical Methods*; Wiley: New York, 1980.

150. Sabacky, M. J.; Johnson, C. S.; Smith, R. G.; Gutowsky, H. S.; Martin, J. C. *J. Am. Chem. Soc.* **1967**, *89*, 2054.

151. Bachmann, W. E. *Org. Syntheses* **1943**, *23*, 100.

152. Wilkinson, G.; Cotton, F. A.; Birmingham, J. M. *J. Inorg. Nucl. Chem.* **1956**, *2*, 95.

153. Bottomley, F.; Nyburg, S. C. *Acta Cryst.* **1968**, *B24*, 1289.

154. Davis, B. R.; Payne, N. C.; Ibers, J. A. *Inorg. Chem.* **1969**, *8*, 2719.

155. Ozin, G. A.; Vander Voet, A. *Can. J. Chem.* **1973**, *51*, 637.

156. Laidler, K. J. In *Chemical Kinetics*; McGraw Hill: New York, 1950; p. 18-22.

157. Dilworth, J. R.; Kan, C.-T.; Richards, R. L.; Mason, J.; Stenhouse, I. A. *J. Organomet. Chem.* **1980**, *20*, C24.

158. Donovan-Mtunzi, S.; Richards, R. L.; Mason, J. *J. Chem. Soc., Dalton, Trans.* **1984**, 469.

159. Donovan-Mtunzi, S.; Richards, R. L.; Mason, J. *J. Chem. Soc., Dalton, Trans.* **1984**, 2729.

160. Armor, J. N.; Taube, H. *J. Am. Chem. Soc.* **1970**, *92*, 2560.

161. Armor, J. N.; Taube, H. *J. Am. Chem. Soc.* **1970**, *92*, 6170.

162. Quinby, M. S.; Feltham, R. D. *Inorg. Chem.* **1972**, *11*, 2468.

163. Chatt, J.; Heath, G. A.; Leigh, G. J.; *J. Chem. Soc., Chem. Commun.* **1972**, 444.

164. Chatt, J.; Pearman, A. J.; Richards, R. L. *Nature* **1975**, *253*, 39.

165. Chatt, J.; Fakley, M. E.; Mason, J.; Richards, R. L.; Stenhouse, I. A. *J. Chem. Res.* **1979**, *44*, 873.

166. Leigh, G. J.; Jimenez-Tenorio, M. *J. Am. Chem. Soc.* **1991**, *113*, 5862.

167. Haymore, B. L.; Hughes, M.; Mason, J.; Richards, R. L. *J. Chem. Soc., Dalton Trans.* **1988**, 2935.

168. Klahn-Oliva, A. H.; Singer, R. D.; Sutton, D. *J. Am. Chem. Soc.* **1986**, *108*, 3107.

169. Aramini, J. M.; Einstein, F. W. B.; Jones, R. H.; Klahn-Oliva, A. H.; Sutton, D *J. Organomet. Chem.* **1990**, *385*, 73.

170. Komiya, S.; Baba, A. *Organometallics* **1991**, *10*, 3105.

171. Pickett, C. J.; Ryder, K. S.; Talarmin, J. *J. Chem. Soc., Dalton Trans.* **1986**, 1453.

172. Darensbourg, D. J. *Inorg. Nucl. Chem. Lett.* **1972**, *8*, 529.

173. Archer, L. J.; George, T. A. *Inorg. Chim. Acta* **1980**, *44*, L129.

174. Chatt, J.; Head, R. A.; Leigh, G. J.; Pickett, C. J. *J. Chem. Soc., Dalton Trans.* **1978**, 1638.

175. Hughes, D. L.; Pombeiro, A. J. L.; Pickett, C. J.; Richards, R. L. *J. Organomet. Chem.* **1983**, *248*, C26.

176. Parshall, G. W. *Catalysis* **1977**, *1*, 335.

177. Shilov, A. E.; Shteinman, A. A. *Coord. Chem. Rev.* **1977**, *24*, 97.

178. (a) Janowicz, A. H.; Bergman, R. G. *J. Am. Chem. Soc.* **1982**, *104*, 352. (b) Janowicz, A. H.; Bergman, R. G. *J. Am. Chem. Soc.* **1983**, *105*, 3929.

179. Hoyano, J. K.; Graham, W. A. G. *J. Am. Chem. Soc.* **1982**, *104*, 3723.

180. (a) Jones, W. D.; Feher, F. J. *Organometallics* **1983**, *2*, 562. (b) Jones, W. D.; Feher, F. J. *J. Am. Chem. Soc.* **1984**, *106*, 1650.

181. (a) Periana, R. A.; Bergman, R. G. *Organometallics* **1984**, *3*, 508. (b) Periana, R. A.; Bergman, R. G. *J. Am. Chem. Soc.* **1984**, *106*, 7272.

182. Wenzel, T. T.; Bergman, R. G. *J. Am. Chem. Soc.* **1986**, *108*, 4856.

183. Anderson, R. A.; Mainz, V. V. *Organometallics* **1984**, *3*, 675 and references cited therein.

184. Abis, L.; Sen, A.; Halpern, J. *J. Am. Chem. Soc.* **1978**, *100*, 2915.

185. Hoyano, J. K.; Graham, W. A. G. *J. Am. Chem. Soc.* **1982**, *104*, 3722.

186. Van der Heijden, H.; Orpen, A. G.; Pasman, P. *J. Chem. Soc., Chem. Commun.* **1985**, 1576.

187. Halpern, J. *Inorg. Chim. Acta* **1985**, *100*, 41.